

University of Denver

Digital Commons @ DU

Electronic Theses and Dissertations

Graduate Studies

2022

Antioxidant Biomarkers and Nutraceutical Therapeutics in Neurodegeneration and Neurotrauma

Lilia A. Koza
University of Denver

Follow this and additional works at: <https://digitalcommons.du.edu/etd>



Part of the [Cell Biology Commons](#), [Molecular Biology Commons](#), and the [Neurology Commons](#)

Recommended Citation

Koza, Lilia A., "Antioxidant Biomarkers and Nutraceutical Therapeutics in Neurodegeneration and Neurotrauma" (2022). *Electronic Theses and Dissertations*. 2133.
<https://digitalcommons.du.edu/etd/2133>

This Dissertation is brought to you for free and open access by the Graduate Studies at Digital Commons @ DU. It has been accepted for inclusion in Electronic Theses and Dissertations by an authorized administrator of Digital Commons @ DU. For more information, please contact jennifer.cox@du.edu, dig-commons@du.edu.

Antioxidant Biomarkers and Nutraceutical Therapeutics in Neurodegeneration and Neurotrauma

Abstract

Mild traumatic brain injury (mTBI), yielding a Glasgow Coma Scale of 13-15, is the most commonly occurring severity of TBI. Pathology from mTBI consists of blood brain barrier disruption, neuroinflammation, oxidative stress, excitotoxicity, mitochondrial dysfunction, protein aggregation, axonal degeneration, and resulting neuronal death. These processes deplete the body's endogenous antioxidant system. We report a retrospective analysis of antioxidant blood biomarkers in patients with a history of mTBI from a local sports medicine clinic, Resilience Code. We found persistent sex-specific antioxidant depletions in mTBI patients associated with worsened symptomology.

Certain populations, such as athletes, are at high risk for repetitive mTBI (rmTBI). There are currently no FDA approved treatments for rmTBI for high-risk populations. We propose Immunocal®, a glutathione precursor supplement, as a preventative and restorative treatment for rmTBI. We show that Immunocal® significantly reduces astrogliosis at 2 weeks and 2 months in mice post-rmTBI and microgliosis at 72 hours following more severe repetitive mild-moderate TBI.

Persistent pathology from rmTBI has been linked to an increased risk for developing neurodegenerative disease like amyotrophic lateral sclerosis (ALS). This devastating disease is characterized by motor neuron death and a prognosis of 2-5 years following diagnosis. Pathology mirrors that of mTBI and consists of oxidative stress, neuroinflammation, mitochondrial dysfunction, excitotoxicity, protein aggregation, and changes to axonal transport and structure. We explored protocatechuic acid (PCA), a phenolic anthocyanin metabolite, as a treatment in the hSOD1G93A mouse model of ALS. PCA has been well studied for its antioxidant properties in other models of neurodegeneration. When administered at symptom onset, PCA prolonged survival, improved motor function, reduced gliosis, and offered significant neuroprotection in hSOD1G93A mice.

It is hypothesized that rmTBI results in an increased oxidative stress burden and subsequent antioxidant depletion. These persist when left untreated and may contribute to the development of neurodegenerative diseases like ALS. The connection between rmTBI and ALS should be further studied using preclinical models such as the hSOD1G93A mouse model of ALS. Treatment with nutraceutical therapeutics, such as glutathione precursors (Immunocal®) or anthocyanin metabolites (PCA), could restore antioxidant reserves and reduce rmTBI pathology, ultimately reducing the risk for developing neurodegenerative disease.

Document Type

Dissertation

Degree Name

Ph.D.

Department

Biological Sciences

First Advisor

Daniel A. Linseman

Second Advisor

Scott A. Barbee

Third Advisor

Yan Qin

Keywords

Amyotrophic lateral sclerosis, Anti-inflammatory, Antioxidants, Biomarkers, Nutraceutical, Traumatic brain injury

Subject Categories

Cell and Developmental Biology | Cell Biology | Life Sciences | Molecular Biology | Neurology

Publication Statement

Copyright is held by the author. User is responsible for all copyright compliance.

Antioxidant Biomarkers and Nutraceutical Therapeutics in Neurodegeneration and
Neurotrauma.

A Dissertation

Presented to

the Faculty of the College of Natural Sciences and Mathematics

University of Denver

In Partial Fulfillment

of the Requirements for the Degree

Doctor of Philosophy

by

Lilia A. Koza

August 2022

Advisor: Dr. Daniel Linseman

©Copyright by Lilia A. Koza 2022
All Rights Reserved

Author: Lilia A. Koza

Title: Antioxidant Biomarkers and Nutraceutical Therapeutics in Neurodegeneration and Neurotrauma

Advisor: Dr. Daniel Linseman

Degree Date: August 2022

ABSTRACT

Mild traumatic brain injury (mTBI), yielding a Glasgow Coma Scale of 13-15, is the most commonly occurring severity of TBI. Pathology from mTBI consists of blood brain barrier disruption, neuroinflammation, oxidative stress, excitotoxicity, mitochondrial dysfunction, protein aggregation, axonal degeneration, and resulting neuronal death. These processes deplete the body's endogenous antioxidant system. We report a retrospective analysis of antioxidant blood biomarkers in patients with a history of mTBI from a local sports medicine clinic, Resilience Code. We found persistent sex-specific antioxidant depletions in mTBI patients associated with worsened symptomology.

Certain populations, such as athletes, are at high risk for repetitive mTBI (rmTBI). There are currently no FDA approved treatments for rmTBI for high-risk populations. We propose Immunocal®, a glutathione precursor supplement, as a preventative and restorative treatment for rmTBI. We show that Immunocal® significantly reduces astrogliosis at 2 weeks and 2 months in mice post-rmTBI and microgliosis at 72 hours following more severe repetitive mild-moderate TBI.

Persistent pathology from rmTBI has been linked to an increased risk for developing neurodegenerative disease like amyotrophic lateral sclerosis (ALS). This devastating disease is characterized by motor neuron death and a prognosis of 2-5 years following diagnosis. Pathology mirrors that of mTBI and consists of oxidative stress,

neuroinflammation, mitochondrial dysfunction, excitotoxicity, protein aggregation, and changes to axonal transport and structure. We explored protocatechuic acid (PCA), a phenolic anthocyanin metabolite, as a treatment in the hSOD1^{G93A} mouse model of ALS. PCA has been well studied for its antioxidant properties in other models of neurodegeneration. When administered at symptom onset, PCA prolonged survival, improved motor function, reduced gliosis, and offered significant neuroprotection in hSOD1^{G93A} mice.

It is hypothesized that rmTBI results in an increased oxidative stress burden and subsequent antioxidant depletion. These persist when left untreated and may contribute to the development of neurodegenerative diseases like ALS. The connection between rmTBI and ALS should be further studied using preclinical models such as the hSOD1^{G93A} mouse model of ALS. Treatment with nutraceutical therapeutics, such as glutathione precursors (Immunocal®) or anthocyanin metabolites (PCA), could restore antioxidant reserves and reduce rmTBI pathology, ultimately reducing the risk for developing neurodegenerative disease.

ACKNOWLEDGEMENTS

First, I would like to thank my advisor, Dr. Daniel Linseman, for helping me develop enthusiasm for research as an undergraduate. I am grateful for the opportunity to pursue graduate school with him as my mentor. I sincerely thank him for his intelligence, patience, and support which have allowed me to grow immensely as a researcher and an individual. I also want to thank my committee, including Dr. Scott Barbee, Dr. Yan Qin, Dr. Lotta Granholm-Bentley, and Dr. Karen Krukowski for their continued assistance, time, and input. I appreciate the patience and advice of past lab members, Dr. Aimee Winter, Dr. Randall Mazzarino, Dr. Nathan Duval, and Elizabeth Ignowski who've trained me. I want to thank current/recent members and affiliated faculty including Dr. Daniel Paredes, Claudia Pena, Allison Grossberg, and Dr. Alex Sandberg for their friendship. I also thank Dr. Chad Prusmack, Sally Crawford, and others at Resilience Code for guiding my clinical research. Lastly, I want to thank undergraduate mentees including Jessica Holsopple, Angela Baybayon-Grandgeorge, Alec Smith, McKensey Bishop, Maeve Devine, and also, Madison Russell, who is greatly missed.

Personally, I want to thank my mom, Cecelia Koza, for her advice and encouragement to be a strong woman, and my dad, Ken Koza, for help with everything from arithmetic to car troubles, and for taking an interest in my research. Finally, I would like to thank my fiancé, Alex Chapin-Koppel, for supporting me and for helping me become a more confident and communicative individual. I look forward to continuing growing together. I could not have completed this without the kindness, companionship, and support of these individuals.

TABLE OF CONTENTS

CHAPTER ONE: INTRODUCTION	1
1.1 Background and Statement of the Problem	1
1.2 Secondary Injury Mechanisms and Pathology of Mild TBI	8
1.2.1 Blood Brain Barrier Disruption and Neuroinflammation	10
1.2.2 Excessive Glutamate Release and Excitotoxicity	14
1.2.3 Oxidative Stress and Mitochondrial Damage	17
1.2.4 Observed Changes to Autophagy and Protein Aggregation Following Mild TBI	20
1.2.5 Axonal Injury and Pathology Following Mild TBI	22
1.2.6 Mild TBI Secondary Injury Pathology Symptom Presentation	23
1.3 Endogenous Antioxidant Depletion Following Mild TBI	24
1.3.1 Enzymatic Endogenous Antioxidant Depletion Following Mild TBI	25
1.3.2 Nonenzymatic Antioxidant Depletion Following Mild TBI.....	26
1.3.3 Glutathione, GSH Precursor, and GSH Enzymatic Antioxidant Depletion Following Mild TBI.....	27
1.3.4 Evaluation of Antioxidant Biomarker Depletion in a Patient Cohort with a History of Mild TBI.....	30
1.4 Glutathione Precursor Supplementation to Treat Mild TBI	32
1.4.1 Glutathione Precursors as Treatment Options for Mild TBI	34
1.4.2 Immunocal® as a Potential GSH Precursor Supplement for Mild TBI.....	36
1.5 Preclinical Murine Models of Repetitive Mild and Repetitive Mild-Moderate TBI Induced by CCI to Assess the Therapeutic Benefit of Immunocal®.....	38
1.5.1 Controlled Cortical Impact as a Standardized and Highly Reproducible Model of TBI.....	40
1.5.2 Models of Repetitive Mild and Mild-Moderate TBI Induced by CCI Used to Assess the Therapeutic Benefit of Immunocal®	43
1.6 Pathology of ALS Results in Motor Neuron Cell Death, Skeletal Muscle Denervation, and Muscle Atrophy	45
1.6.1 Oxidative Stress and Mitochondrial Dysfunction in ALS	47
1.6.2 Neuroinflammation in ALS	50
1.6.3 Excitotoxicity in ALS	52
1.6.4 Observed Protein Aggregation Contributes to ALS Pathology	53
1.6.5 Dysfunctional Axonal Transport, Synaptic Failure, Motor Neuron Death, NMJ Deterioration, and Muscle Atrophy in ALS.....	55
1.6.6 Endogenous Antioxidant Depletion Underlies ALS Pathology.....	56
1.7 Berry Anthocyanin Nutraceutical Compounds and Their Phenolic Acid Metabolites as Potential Treatments for Neurodegenerative Diseases Like ALS	61
1.7.1 Nutraceutical Berry Anthocyanins and Their Antioxidant Properties	62
1.7.2 The Berry Anthocyanin, Cyanidin-3- <i>O</i> -Glucoside, and its Phenolic Acid Metabolites Including Protocatechuic Acid (PCA)	64
1.7.2 Evidence of Antioxidant, Anti-Inflammatory, and Neuroprotective Properties of PCA in Support of Its Use as a Therapeutic Treatment for ALS	69

1.8 The hSOD1 ^{G93A} Transgenic Mouse: A Preclinical Model of ALS to Explore the Potential Treatment Efficacy of PCA	73
1.8.1 Phenotype and Pathology of the hSOD1 ^{G93A} Mouse Model of ALS.....	73
1.8.2 Neuroinflammation in the hSOD1 ^{G93A} Mouse Model of ALS	77
1.8.3 Preclinical Study of PCA in the hSOD1 ^{G93A} Mouse Model of ALS	77

CHAPTER TWO: SIGNIFICANT AND SEX-SPECIFIC ANTIOXIDANT BIOMARKER DEPLETION IN HISTORY OF MILD TRAUMATIC BRAIN INJURY PATIENTS

CHAPTER TWO: SIGNIFICANT AND SEX-SPECIFIC ANTIOXIDANT BIOMARKER DEPLETION IN HISTORY OF MILD TRAUMATIC BRAIN INJURY PATIENTS	78
2.1 Abstract.....	78
2.2 Introduction.....	79
2.3 Methods.....	82
2.3.1 Participant Population.....	82
2.3.3 Blood collection, Processing, and Analysis.....	83
2.3.4 Medical Symptom Questionnaire	83
2.3.5 Statistics.....	84
2.3.6 Study Approval	88
2.4 Results.....	88
2.4.1 Patient population	88
2.4.2 Sex-Specific Antioxidant Depletion in Patients with Versus Without a History of mTBI.....	92
2.4.3 Sex-Specific Differences in Emotional, Energy, Head, and Cognitive Symptom Symptomology in Patients with Versus Without a History of mTBI.	101
2.4.4 Multiple mTBI Patients Seemed to Have Worsened and More Frequent Symptomology Compared to Patients Who Sustained a Single mTBI.....	112
2.4.5 Chronic mTBI Patients Seemed to Have Worsened and More Frequent Emotional, Energy, and Cognitive, but Not Head Symptoms, When Compared to Acute-Subchronic mTBI Patients.	113
2.4.6 History of mTBI Patients with Lower Levels of PUFA Biomarkers Have Significantly Worsened and Increased Frequency of Symptoms When Compared to mTBI Patients with Higher Levels of PUFA Biomarkers.	115
2.5 Discussion.....	118

CHAPTER THREE: IMMUNOCAL® LIMITS GLIOSIS IN MOUSE MODELS OF REPETITIVE MILD-MODERATE TRAUMATIC BRAIN INJURY

CHAPTER THREE: IMMUNOCAL® LIMITS GLIOSIS IN MOUSE MODELS OF REPETITIVE MILD-MODERATE TRAUMATIC BRAIN INJURY	126
3.1 Abstract.....	126
3.1.1 Objective.....	126
3.1.2 Methods.....	126
3.1.3 Results.....	126
3.1.4 Interpretation.....	127
3.2 Introduction.....	127
3.3 Methods.....	129

3.3.1 Animal Care and Treatment.....	129
3.3.2 Mice Subjected to rmTBI for Analysis at 2 Weeks, 2 Months, and 6 Months Post-TBI.....	130
3.3.3 Repetitive mTBI Procedure	130
3.3.4 Mice Subjected to rmmTBI and Analysis at 72 Hours Post-TBI	131
3.3.5 Repetitive mmTBI Procedure	132
3.3.6 MRI Analysis of BBB Disruption/Edema and Activated Macrophages	132
3.3.7 Euthanasia and Sample Collection	133
3.3.8 Immunohistochemical Staining of GFAP and Iba-1 in Cortex.....	134
3.3.9 Immunofluorescence Microscopy of GFAP and Iba-1-Stained Cortex.....	134
3.3.10 Quantification of Astrocyte and Microglia Number in Cortex	135
3.3.11 Measurement of Serum NfL by Enzyme-Linked Immunosorbent Assay (ELISA).....	135
3.3.12 Colorimetric Detection of Brain GSH and GSSG	136
3.3.13 Statistical analysis	136
3.4 Results.....	137
3.4.1 Immunocal®-Treatment Effects on Body Weight and Righting Reflex Times After rmTBI	137
3.4.2 MRI Analysis of Immunocal®-Treatment Effects on Macrophage Activation After rmTBI	139
3.4.3 Immunocal®-Treatment Significantly Reduces Astrogliosis at 2 Weeks and 2 Months After rmTBI.....	142
3.4.4 Immunocal®-Treatment Effects on Body Weight, Apnea, and Righting Reflex Times After rmmTBI	147
3.4.5 Analysis of Immunocal®-Treatment Effects on Increases in Serum NfL Induced by rmmTBI.....	150
3.4.6 Analysis of Immunocal®-Treatment Effects on Changes in Brain GSH and GSSG Induced by rmmTBI	152
3.4.7 Immunocal®-Treatment Significantly Reduces Microgliosis at 72 Hours After rmmTBI.....	155
3.5 Discussion.....	160

CHAPTER FOUR: PROTOCATECHUIC ACID EXTENDS SURVIVAL, IMPROVES MOTOR FUNCTION, DIMINISHES GLIOSIS, AND SUSTAINS NEUROMUSCULAR JUNCTIONS IN THE hSOD1^{G93A} MOUSE MODEL OF AMYOTROPHIC LATERAL SCLEROSIS	165
4.1 Abstract.....	165
4.2 Introduction.....	166
4.3 Materials and Methods.....	170
4.3.1 The hSOD1 ^{G93A} Mouse Model of ALS.....	170
4.3.2 Survival Data	171
4.3.3 Paw Grip Endurance and Rotarod Testing.....	171

4.3.4 Analysis of Mice at End Stage of the Untreated hSOD1 ^{G93A} Littermate Mouse	172
4.3.5 Analysis of Mice at 105 Days of Age	173
4.3.6 Tissue Preparation and Cryosectioning	173
4.3.7 Immunohistochemistry of Spinal Cord Sections	174
4.3.8 Imaging and Quantification of Spinal Cord Sections Stained for Iba-1 and GFAP at End Stage of the Untreated hSOD1 ^{G93A} Littermate Mouse	176
4.3.9 Nissl Staining of Spinal Cord Sections	177
4.3.10 Imaging and Quantification of Nissl-Stained Spinal Cord Sections at End Stage of the Untreated hSOD1 ^{G93A} Littermate	177
4.3.11 Alpha-Bungarotoxin and VAcHT Staining of Gastrocnemius Sections.....	178
4.3.12 Imaging and Area, Perimeter, and Sholl Analysis Quantification of Gastrocnemius Sections Stained with Alpha-Bungarotoxin at End Stage of the Untreated hSOD1 ^{G93A} Littermate Mouse.....	179
4.3.13 Analysis of Gastrocnemius Muscle Wet Weight at 105 Days of Age.....	180
4.3.14 Imaging of Gastrocnemius Sections Stained with Alpha-BTx and VAcHT at 105 Days of Age	181
4.3.15 Imaging of Quantification of 4-HNE-Stained Spinal Cord Sections at 105 Days of Age	181
4.3.16 Statistical Analysis.....	182
4.4 Results.....	183
4.4.1 PCA Orally Administered Beginning at Disease Onset Results in a Significant Extension of Survival but Does Not Preserve Body Weight in the hSOD1 ^{G93A} Mouse Model of ALS	183
4.4.2 PCA Treatment Improves Grip Strength and Motor Performance in the hSOD1 ^{G93A} Mouse Model of ALS.....	185
4.4.3 PCA Treatment Preserves Gastrocnemius Muscle Wet Weight, Protects NMJ Innervation, and Reduces Oxidative Stress in the hSOD1 ^{G93A} Mouse Model of ALS at 105 Days of Age	190
4.4.4 PCA Treatment Significantly Preserves Motor Neurons in the Ventral Horn of the Spinal Cord in the hSOD1 ^{G93A} Mouse Model of ALS.....	194
4.4.5 PCA Treatment Significantly Reduces Astrogliosis and Microgliosis in the Ventral Horn of the Spinal Cord in the hSOD1 ^{G93A} Mouse Model of ALS	197
4.4.6 PCA Treatment Significantly Preserves Neuromuscular Junctions of the Gastrocnemius Muscle in the hSOD1 ^{G93A} Mouse Model of ALS	202
4.5 Discussion.....	205
4.6 Conclusion	212

CHAPTER FIVE: CONCLUSIONS AND FUTURE DIRECTIONS	214
5.1 Summary of Major Findings.....	214
5.2 Evidence for, Potential Benefits, and Limitations of Supplementing the Endogenous Antioxidant System with Exogenous Nutraceutical Antioxidants to Treat Mild Single and Repetitive TBI.....	216

5.2.1. Evidence for Antioxidant Nutraceutical Compound Supplementation to Treat Antioxidant Depletion Resulting from Mild Single and Repetitive TBI.....	217
5.2.2 Benefits and Limitations to Immunocal® Supplementation for Mild TBI....	220
5.3 Prolonged Antioxidant Depletion in Mild TBI May Contribute to the Development of Neurodegenerative Diseases such as ALS.....	222
5.4 Future Directions to Explore the Connection Between Repetitive Mild TBI and ALS	224
5.5 Timing, Bioavailability, and Impact of External Factors with PCA Treatment ...	228
5.6 Conclusion	231

REFERENCES..... 233

APPENDICES.....	320
Appendix A: Abbreviations	320
Appendix B: Supplementary Figures.....	325
Appendix C: Supplementary Tables	330
Appendix D: List of Published Manuscripts and Abstracts.....	333
Manuscripts.....	333
Abstracts	334

LIST OF FIGURES

CHAPTER ONE

Figure 1.1 Secondary Injury Mechanisms in the Pathology of Mild TBI.	9
Figure 1.2 Blood Brain Barrier Disruption in Mild TBI.....	13
Figure 1.3 Excitotoxicity in Mild TBI.	16
Figure 1.4 Mitochondrial Dysfunction in Mild TBI.	19
Figure 1.5 Endogenous Antioxidant Depletion from Mild TBI and Treatment with Nutraceutical Antioxidant Supplementation.....	33
Figure 1.6 Controlled Cortical Impact Device to Induce Mild TBI.	42
Figure 1.7 Pathology of ALS.....	46
Figure 1.8 Antioxidant Depletion and ALS.....	60
Figure 1.9 Structures of Cyanidin 3-O-glucoside and its Metabolite Protocatechuic Acid.....	68
Figure 1.10 Antioxidant and Anti-Inflammatory Properties of Protocatechuic Acid in Models of Neurodegeneration.	72
Figure 1.11 The hSOD1 ^{G93A} Mouse Model of ALS Disease Phenotype.....	76

CHAPTER TWO

Figure 2.1 Significantly or Trending Significantly Reduced Levels of Serum Antioxidant Biomarkers in Total, Male, and Female Patients Without Versus with a History of mTBI.....	95
Figure 2.2 Significantly or Trending Significantly Reduced Levels of Plasma Antioxidant Biomarkers in Total, Male, and Female Patients Without Versus with a History of mTBI.....	97
Figure 2.3 Significantly or Trending Significantly Reduced Levels of RBC Antioxidant Biomarkers in Total, Male, and Female Patients Without Versus with a History of mTBI.	99
Figure 2.4 Significantly or Trending Significantly Worsened Symptoms Pertaining to Emotional State in Total, Male, and Female Patients with Versus Without a History of mTBI.	105
Figure 2.5 Significantly or Trending Significantly Worsened Symptoms Pertaining to Energy in Total, Male, and Female Patients with Versus Without a History of mTBI	107
Figure 2.6 Significantly or Trending Significantly Worsened Head Symptoms in Total, Male, and Female Patients with Versus Without a History of mTBI.	109
Figure 2.7 Trending Significantly Worsened Symptoms Pertaining to Cognition in Total, Male, and Female Patients with Versus Without a History of mTBI.....	111
Figure 2.8 Qualitative Differences in Emotional, Energy, Head, and Cognitive Symptom Severity and Frequency Between Patients with No History of mTBI Versus Patients with a Past Single mTBI or with a History of Multiple mTBI and Between Patients with No History of mTBI Versus Patients with Acute-Subchronic mTBI or Chronic mTBI.	114

Figure 2.9 Significantly Worsened Symptoms Pertaining to Emotional State, Energy, Head Symptoms, or Cognition in Total History of mTBI Patients with PUFA Biomarker Depletion When Compared to History of mTBI Patients with Higher Levels of PUFA Biomarkers.. 117

CHAPTER THREE

Figure 3.1 Percent of Peak Body Weight and Righting Reflex Times of Mice Subjected to Sham Surgery (Sham) or Untreated (TBI) and Immunocal®-Treated (TBI + ICAL) Mice Subjected to Repetitive Mild TBI (rmTBI). 138

Figure 3.2 Repetitive Mild Traumatic Brain Injury (rmTBI) Did Not Result in Blood Brain Barrier (BBB) Disruption/Edema but Did Cause an Increase in Inflammation as Analyzed by Magnetic Resonance Imaging (MRI). 141

Figure 3.3 Immunocal®-Treatment Pre- and Post-Repetitive Mild Traumatic Brain Injury (rmTBI) Significantly Reduced Astrogliosis in the Cortex of Mice Subjected to rmTBI When Analyzed at 2 Weeks and 2 Months, but Not at 6 Months Post-Last rmTBI..... 144

Figure 3.4. Microgliosis Was Not Observed in the Cortex of Mice Subjected to Repetitive Mild Traumatic Brain Injury (rmTBI) When Analyzed at 2 Weeks, 2 Months, or 6 Months Post-Last mTBI. 146

Figure 3.5 Percent of Peak Bodyweight, Apnea, and Righting Reflex Times of Mice Subjected to Sham Surgery (Sham) or Untreated (TBI) and Immunocal®-Treated (TBI + ICAL) Mice Subjected to Repetitive Mild-Moderate Traumatic Brain Injury (rmmTBI) Analyzed at 72 Hours Post-Last TBI. 149

Figure 3.6 Repetitive Mild-Moderate Traumatic Brain Injury (rmmTBI) Results in Acute Neuronal Damage in Mice Analyzed at 72 Hours Post-Last mmTBI..... 152

Figure 3.7. Repetitive Mild-Moderate Traumatic Brain Injury (rmmTBI) Reduced Glutathione (GSH) and Significantly Increased Glutathione Disulfide (GSSG) in Brain of Mice Analyzed at 72 hours Post-Last mmTBI. 154

Figure 3.8. Significant Astrogliosis Present in the Cortex of Mice Subjected to Repetitive Mild-Moderate-Traumatic Brain Injury (rmmTBI) When Analyzed at 72 Hours Post-ast mmTBI. 157

Figure 3.9 Immunocal®-Treatment Pre- and Post-Repetitive Mild-Moderate TBI (rmmTBI) Significantly Reduced Microgliosis in the Cortex of Mice When Analyzed at 72 Hours Post-Last mmTBI. 159

CHAPTER FOUR

Figure 4.1 PCA Treatment Extends Survival in the hSOD1^{G93A} Mouse Model of ALS. 184

Figure 4.2 PCA Treatment Improves Grip Strength as Assessed by PaGE in the hSOD1^{G93A} Mouse Model of ALS..... 187

Figure 4.3 PCA Treatment Improves Motor Function as Assessed by Rotarod and Also Preserves Gastrocnemius Muscle Weight and Neuromuscular Junction (NMJ) Innervation at 105 Days of Age in the hSOD1 ^{G93A} Mouse Model of ALS.	189
Figure 4.4 PCA Treatment Significantly Reduces Lipid Peroxidation in the Ventral Horn of the Spinal Cord in the hSOD1 ^{G93A} Mouse Model of ALS.	193
Figure 4.5 PCA Treatment Significantly Preserves Motor Neurons in the Ventral Horn of the Spinal Cord in the hSOD1 ^{G93A} Mouse Model of ALS.	196
Figure 4.6 PCA Treatment Significantly Reduces Astrogliosis in the Ventral Horn of the Spinal Cord in the hSOD1 ^{G93A} Mouse Model of ALS.	199
Figure 4.7 PCA Treatment Significantly Reduces Microgliosis in the Ventral Horn of the Spinal Cord in the hSOD1 ^{G93A} Mouse Model of ALS.	201
Figure 4.8 PCA Treatment Significantly Preserves Neuromuscular Junctions (NMJ) in the Gastrocnemius Muscle in the hSOD1 ^{G93A} Mouse Model of ALS.	204

CHAPTER ONE: INTRODUCTION

1.1 Background and Statement of the Problem

An estimated 64-74 million new cases of traumatic brain injury (TBI) are predicted to occur globally each year (Dewan et al., 2018). TBI is the leading cause of death by injury, particularly for children and the elderly, in the United States (US; Pavlovic et al., 2019; Popescu et al., 2015; Rutland-Brown et al., 2006). Of those who survive a TBI, an estimated 2.5-6.5 million individuals live with a TBI-related disability and require long-term aid in the US alone (Popescu et al., 2015). As a result, TBI represents an estimated annual financial burden of \$60 billion (Dixon, 2017).

Traumatic brain injury is defined as an injury resulting from an impact to the head which can vary in mode and severity. Resulting injury can be characterized as diffuse, blunt, blast, or focal which can be further characterized as contusion, penetrating injury, or hematoma (Andriessen et al., 2010; Hill et al., 2016). Severity of injury may range anywhere from mild (i.e., concussion) to severe. The Glasgow Coma scale, along with information on loss of consciousness and neurological symptoms, are used by clinicians to assess visual, motor, and verbal responses following a TBI. This information gives insight into severity and neurological recovery (Pavlovic et al., 2019). However, individual circumstances resulting from TBI vary widely even within a particular

classified range of severity and mode of injury. Therefore, TBI is difficult to assess, treat, and predict outcomes for patients.

Traumatic brain injury of mild severity, the primary focus of this dissertation, is the most common occurring severity of TBI. With an incidence of 600 per 100,000 people, mild TBI accounts for approximately 84% of new cases that occur worldwide each year with the majority due to falls and motor vehicle accidents (Cassidy, J.D., et al., 2004; Gardner & Yaffe, 2015; McCrory et al., 2013). The definition of mild TBI varies widely and current research aims to further define this type of injury. The World Health Organization Collaborating Center Task Force and the Centers for Disease Control and Prevention consider a TBI to be of mild severity if an individual has either neurological symptoms, amnesia for less than 24 hours, or loss of consciousness for less than 30 minutes, and a Glasgow Coma Scale of 13-15 (Carroll et al., 2004).

Mild TBI, and especially *repetitive* mild TBI, has been studied as a risk factor for neurodegenerative diseases such as chronic traumatic encephalopathy (CTE) and Alzheimer's disease (AD; Gavett et al., 2011; Graham & Sharp, 2019; Mortimer et al., 1991). The pathology resulting from TBI seems to mirror that observed in neurodegenerative disease. Furthermore, nervous system trauma has been linked to the neurodegenerative disease, amyotrophic lateral sclerosis (ALS), which is the secondary focus of this dissertation (Chen, H., et al., 2007; Schmidt et al., 2010).

Amyotrophic lateral sclerosis, also known as Lou Gehrig's disease, is a devastating progressive neurodegenerative disease that results in the death of motor neurons and skeletal muscle atrophy. Although ALS is relatively rare, with a global incidence of 0.6-

3.8 per 100,000 person-years, 5,000 new cases arise each year in the US alone (Longinetti & Fang, 2019; Orsini et al., 2015). Furthermore, the number of patients diagnosed worldwide continues to increase over time (Longinetti & Fang, 2019). This may be due to increased longevity in populations as the median age of ALS onset is between 51-66 years of age (Longinetti & Fang, 2019). Pathology underlying ALS contributes to the retraction of motor neuron axons from neuromuscular junctions (NMJs), motor neuron cell death, and muscle atrophy. Patients with ALS become unable to move their muscles, may suffer cognitive and psychological impairments, and experience respiratory distress and failure (Chiò et al., 2009a). There is a rapid decline resulting in an average life expectancy of 2-5 years following diagnosis (Chiò et al., 2009a). Therefore, the economic cost to ALS patients is high, an estimated \$13,667 per year, with the annual US economic burden being between \$279-472 million (Gladman & Zinman, 2015). Approximately 10% of ALS cases are familial, with known genetic causes, such as mutations to genes like Cu, Zn-superoxide dismutase-1 (SOD-1) or TAR DNA-binding protein-43 (TDP-43), among others. Sporadic ALS accounts for 90% of cases that have no identified genetic cause (Kumar, V., et al., 2019). Sporadic cases have been linked to environmental factors such as heavy metals, toxins, pesticides, and physical activity. Populations that engage in high levels of physical activity, are exposed to chemicals, or sustain multiple mild TBIs, such as athletes and military personnel, have a higher risk of developing ALS (Bozzoni et al., 2016).

Shared pathology between mild TBI and ALS includes oxidative stress, neuroinflammation, mitochondrial dysfunction, excitotoxicity, protein aggregation, and

changes to axonal transport and structure. Neuronal cell death is both a result of, and contributor to, these processes in mild TBI and ALS. Due to injury and blood brain barrier (BBB) disruption, as with mild TBI, or to mutations affecting endogenous antioxidant function, such as in ALS, an increase in reactive oxygen or nitrogen species (ROS/RNS) occurs. The presence of ROS/RNS can cause neuroinflammation which is characterized by activation of glial cells, including astrocytes, microglia, and resident macrophages, along with infiltrating immune cells, in the central nervous system (CNS). These cells, particularly astrocytes and microglia, release pro-inflammatory cytokines, chemokines, and oxidative species which further damage neurons and add to the oxidative burden. As a result, mitochondria experience damage to the electron transport chain (ETC) and energy metabolism which result in apoptosis. Physical and chemical damage from increased ROS/RNS generation by these dysfunctional mitochondria and neuroinflammatory glial cells can further contribute to excitotoxicity in mild TBI and ALS.

Excitotoxicity is defined as the excessive production and reduced uptake of excitatory neurotransmitters, mainly glutamate. Ionotropic glutamate receptors on post-synaptic neurons, such as N-methyl-D-aspartic acid (NMDA) and α -amino-3-hydroxy-5-methyl-4-isoxazole propionic acid (AMPA) receptors become overactive. This is due to excessive glutamate release from pre-synaptic neurons and reduced uptake from the synapse by astrocytes. As a result, sodium and calcium ions flood into the neuron, which in turn, results in depolarization. Due to an imbalance of solutes in the cell, water also rushes in and the cell swells. Metabotropic glutamate receptors become activated

resulting in increased metabolism, further mitochondrial dysfunction, disrupted ion homeostasis, and increased generation of action potentials. These processes encourage the release of pro-apoptotic factors from mitochondria resulting in neuronal cell death which further increases the amount of glutamate released into the environment (Armada-Moreira et al., 2020; Van Den Bosch et al., 2006).

These processes, when prolonged, contribute to axonal damage, disrupted axonal transport, and alterations to the post-synaptic neuron (Baracaldo-Santamaría et al., 2022). Changes to autophagy, one of two main degradation systems used by the body and brain, have also been reported in mild TBI and ALS. Protein aggregates and organelles, such as mitochondria, are targeted for lysosomal degradation through a type of autophagy known as macroautophagy. Autophagosomes, containing proteins and organelles targeted for degradation, are transported along the axons via microtubules and allowed to fuse with lysosomes which degrade content (Lamark & Johansen, 2012). Deficits to this process can result in the buildup of protein aggregates which are observed in both mild TBI and ALS. Misfolded proteins have exposed hydrophobic structures which cause the protein to break into fibrils or oligomers. These constructs are nonfunctional and have the capacity to adopt toxic functions. The oligomers and fibrils can also aggregate, disrupt cellular functions, and trap other proteins (Malik & Wiedau, 2020). The accumulation of misfolded proteins has been observed in mild TBI and ALS and is a major contributing factor to the pathology described above.

Pathology has been shown to persist for weeks to years following mild TBI and can be exacerbated by subsequent mild TBIs (Donovan et al., 2014; Fehily & Fitzgerald,

2017; Mouzon et al., 2017; Webster et al., 2015). Certain individuals are at an elevated risk for sustaining mild TBI such as children, the elderly, contact sport athletes, and military personnel. These individuals may sustain multiple mild TBIs throughout their lifetime. In fact, the risk is increased for sustaining a subsequent TBI for individuals who have already suffered a single TBI (Guskiewicz et al., 2003). Prolonged pathology, particularly neuroinflammation and oxidative stress, may lead to depletion of the endogenous antioxidant system. Extended or exacerbated pathology can also present in a multitude of cognitive, emotional, and motor symptoms which can persist in individuals following mild TBI (Mott et al., 2012). However, there are currently no US Food and Drug Administration (FDA) approved treatments for TBI or mild TBI. Some studies have explored nutraceutical antioxidant compounds as potential treatments for mild TBI; however, additional rigorous research needs to be done. Therefore, there is a critical unmet need for both preventative and restorative treatments for mild TBI, particularly for high-risk populations.

As mentioned above, prior head trauma, particularly in athletes and military personnel, may be responsible for the increased ALS cases seen in these populations (Bozzoni et al., 2016). The pathology observed in ALS contributes to antioxidant depletion which has been measured and is well-studied in ALS patients (Carrera-Juliá et al., 2020). Only two FDA treatments for ALS have been approved. Riluzole, which acts on glutamate signaling and excitotoxicity, is the most widely administered and first drug to be approved for ALS in 1995. Edaravone was approved in 2017 and acts as a free radical scavenger (Mejzini et al., 2019). Unfortunately, these treatments extend life by

only a few months (Kumar, V., et al., 2019). Other antioxidant treatments, like naturally occurring nutraceutical compounds, such as anthocyanins and other phenolic compounds, have been explored as treatments for ALS in preclinical studies with promising results (Carrera-Juliá et al., 2020; Winter & Bickford, 2019).

This dissertation reports the pathology observed, to date, in both mild TBI and ALS. There is a focus on oxidative stress, neuroinflammation, and resulting antioxidant depletion in these conditions. It is hypothesized that treating this pathology with natural nutraceutical antioxidant compounds will help mitigate the adverse effects of mild TBI and ALS. Here, the use of a nutraceutical compound, Immunocal®, designed to increase brain glutathione (GSH) antioxidant levels, was analyzed for its ability to reduce neuroinflammation and BBB disruption in mouse models of repetitive mild and mild-moderate TBI. Antioxidant depletion and emotional, energy/activity, head, and cognitive symptoms were also analyzed in a patient cohort with a history of mild TBI. Finally, protocatechuic acid (PCA), a well-studied phenolic acid metabolite of the anthocyanin, cyanidin-3-*O*-glucoside, commonly found in berries, was studied for its antioxidant, anti-inflammatory, and neuroprotective properties in a mouse model ALS (Koza et al., 2020). This dissertation concludes by exploring the connection between mild TBI and ALS - mild TBI, especially of repetitive nature, may result in an increased oxidative stress burden and depletion of endogenous antioxidant reserves in the long-term which may in turn, increase the risk of developing ALS.

1.2 Secondary Injury Mechanisms and Pathology of Mild TBI

The pathology of TBI can be divided into primary and secondary injuries.

Primary injury results directly from the impact and can cause damage to the skull or compression, shearing, or contusion forces to the brain. Necrosis of neuronal and glial cells may occur directly as a result of the physical damage (Ng & Lee, 2019). Although primary injuries such as compression, shearing, and contusion may occur with mild TBI, typically, the damage is not very severe and the skull remains intact. Therefore, this dissertation will focus primarily on secondary injury mechanisms and pathology of mild TBI. Secondary injury includes neuroinflammation, BBB disruption, oxidative stress, excitotoxicity, mitochondrial dysfunction, protein aggregation, axonal damage, and ultimately, neuronal cell death (Figure 1.1; Ng & Lee, 2019; Prins et al., 2013). Although primary injury may not be severe in the case of mild TBI, secondary injury occurs later, may persist over time, and can be exacerbated by subsequent TBIs. Symptom severity and persistence resulting from mild TBI and repetitive mild TBI varies on an individual basis. Symptoms commonly resulting from mild TBI, termed post-concussion syndrome, include cognitive, psychological, motor function, and somatic symptoms (Ponsford et al., 2012). Many patients return to sport or work before symptoms have resolved and, in cases where symptoms have subsided, secondary injury pathology may continue. Furthermore, for a small number of patients, symptoms have been reported to persist for months following even a single mild TBI. Prolonged secondary injury, with the presence or absence of symptoms, can deplete the endogenous antioxidant system and may lead to an increased risk of developing neurodegenerative disease.

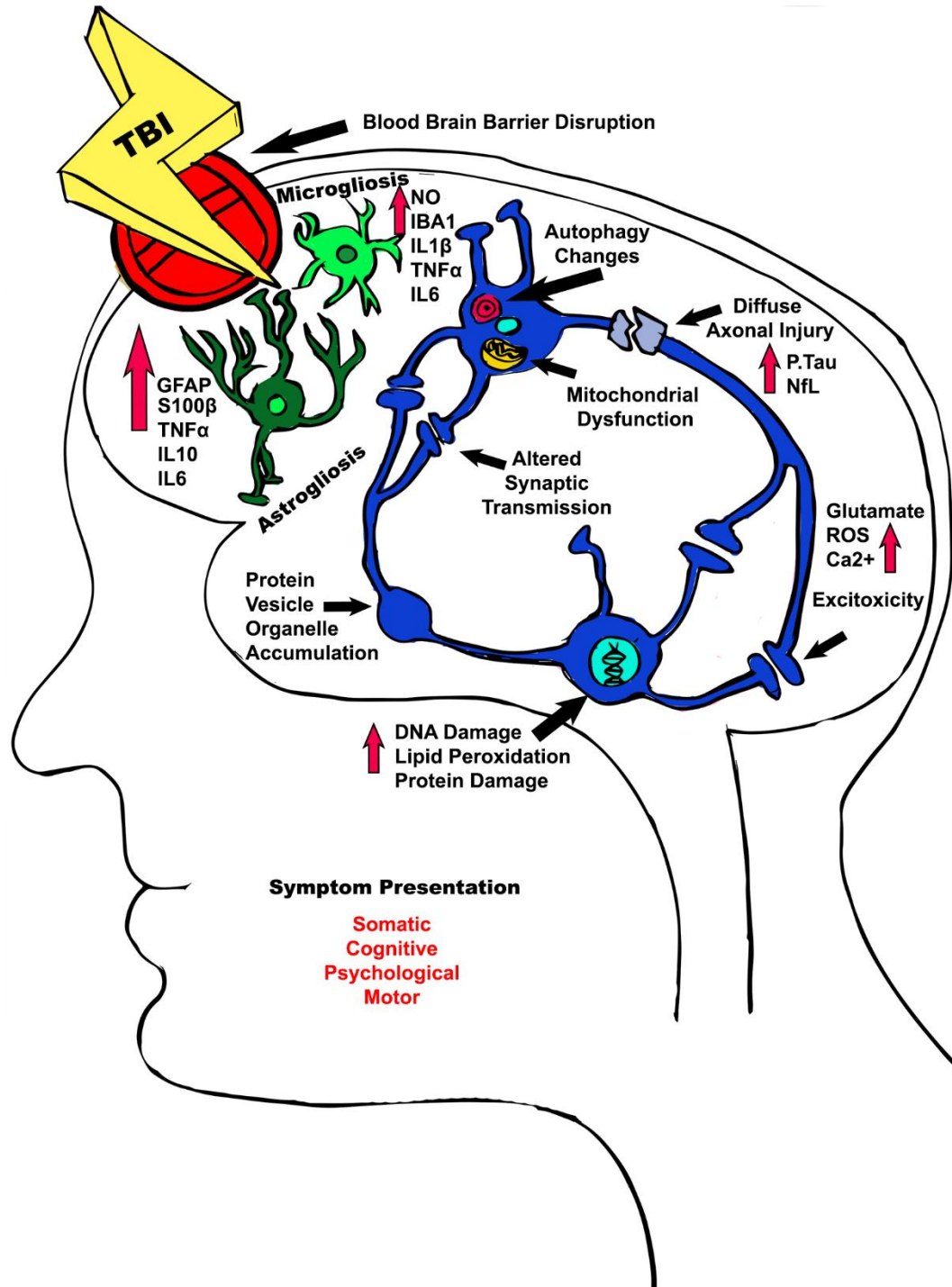


Figure 1.1 Secondary Injury Mechanisms in the Pathology of Mild TBI. Secondary injury from mild TBI includes neuroinflammation, blood brain barrier disruption, oxidative stress, excitotoxicity, mitochondrial dysfunction, protein aggregation, axonal damage, and ultimately, neuronal cell death. When the blood brain barrier loses its integrity, toxins can enter the CNS. Endothelial cells within the blood brain barrier, and cells from the periphery, release pro-inflammatory cytokines. These processes elicit a neuro-inflammatory response from resident astrocytes expressing glial fibrillary acidic protein (GFAP) and S100 calcium-binding protein β (S100 β) and microglia expressing ionized calcium-binding adapter molecule 1 (Iba-1). Both astrocytes and microglia release pro-inflammatory cytokines (interleukin-1 β (IL-1 β), IL-6, IL-10, tumor necrosis factor- α (TNF- α)) and reactive oxygen and nitrogen species ((ROS/RNS), nitric oxide (NO)). Astrocytes, which have homeostatic functions including maintaining neuronal synapses and clearing extracellular glutamate, contribute to excitotoxicity. Following mild TBI, extracellular glutamate increases and remains in synapses triggering increased calcium ion (Ca²⁺) build up in post-synaptic neurons. Excessive depolarization causes mitochondrial dysfunction and the release pro-apoptotic caspases. When taken together, these changes increase the oxidative burden in the brain and contribute to DNA damage, lipid peroxidation, and protein degradation. Diffuse axonal injury from mild TBI can contribute to aberrant accumulation of proteins, synaptic vesicles, and organelles along the axon which can result in axonal swelling and transport deficits. Proteins such as phosphorylated tau (P. Tau) and neurofilament light chain protein (NfL) can aggregate and further disrupt axonal transport and, along with the processes described previously, result in altered synaptic transmission. Ultimately, the pathology from mild TBI can present as somatic, cognitive, psychological, and motor symptoms.

1.2.1 Blood Brain Barrier Disruption and Neuroinflammation

Blood brain barrier disruption is well researched and has been observed in animal models of mild TBI (Figure 1.2; Sandsmark et al., 2019). Blood brain barrier disruption is an early event, occurring within hours to days following mild TBI. It can persist long-term following a TBI, although more research needs to be done in this area (O'Keefe et al., 2020; Shlosberg et al., 2010). The disruption can be a result of physical trauma and increased oxidative stress. The BBB maintains homeostasis in the brain and consists of a barrier of cells such as astrocytes, pericytes, and endothelial cells. When this barrier loses its integrity, toxins can enter the brain and, on the other hand, toxic protein aggregates are

unable to be removed. Furthermore, endothelial cells which construct the BBB can release pro-inflammatory cytokines such as interleukin-1 β (IL-1 β) and tumor necrosis factor- α (TNF- α ; Patterson & Holahan, 2012; Sandsmark et al., 2019). Peripheral immune cells may also infiltrate the brain and contribute to neuroinflammation. These processes illicit a neuroinflammatory response from astrocytes and microglia in the brain.

As a result of neuronal cell death and BBB disruption in response to mild TBI, the brain mounts an inflammatory response. Astrocytes and microglia are recruited to the BBB. Astrocytes help to maintain synapse function, neurotransmitter homeostasis, and provide neurotrophic factors (Singh et al., 2011). In mild TBI, astrocytes take on a pro-inflammatory phenotype which is characterized by a change in physical shape, expression of glial fibrillary acidic protein (GFAP) and S100 calcium-binding protein β , and secretion of pro-inflammatory cytokines such as IL-6, IL-10, and TNF- α (Metting et al., 2012; Singh et al., 2011). Morphological changes in astrocytes have also been observed in response to mild TBI which is coupled with a downregulation of homeostatic proteins. These changes have been observed in astrocytes months following injury (Clément et al., 2020; George et al., 2022; Shandra et al., 2019). Astrocytes also play roles in glutamate uptake from synapses and, when they adopt a pro-inflammatory phenotype, they lose this ability as evidenced by decreased expression of the glutamate transporter, excitatory amino acid transporter 2 (EAAT2; Dorsett et al., 2017; Shandra et al., 2019). Reduced glutamate reuptake contributes to excitotoxicity as further described below.

Blood brain barrier disruption, increased oxidative stress, and cytokine release from astrocytes can result in microglial activation. Microglia, resident immune cells of the

brain, also adopt a pro-inflammatory phenotype in response to increased ROS/RNS, toxins released from dying neurons, or foreign particles from the periphery. In response to mild TBI, microglia take on morphological changes and can cause damage to surrounding tissue through the secretion of pro-inflammatory cytokines such as IL-1 β , TNF α , IL-6, and nitric oxide (NO; Grovola et al., 2021; Robinson et al., 2017). In the case of mild TBI, and especially repetitive mild TBI, neuroinflammation has been observed to persist for months to years following injury (Chaban et al., 2020; Grovola et al., 2021; Mouzon et al., 2017).

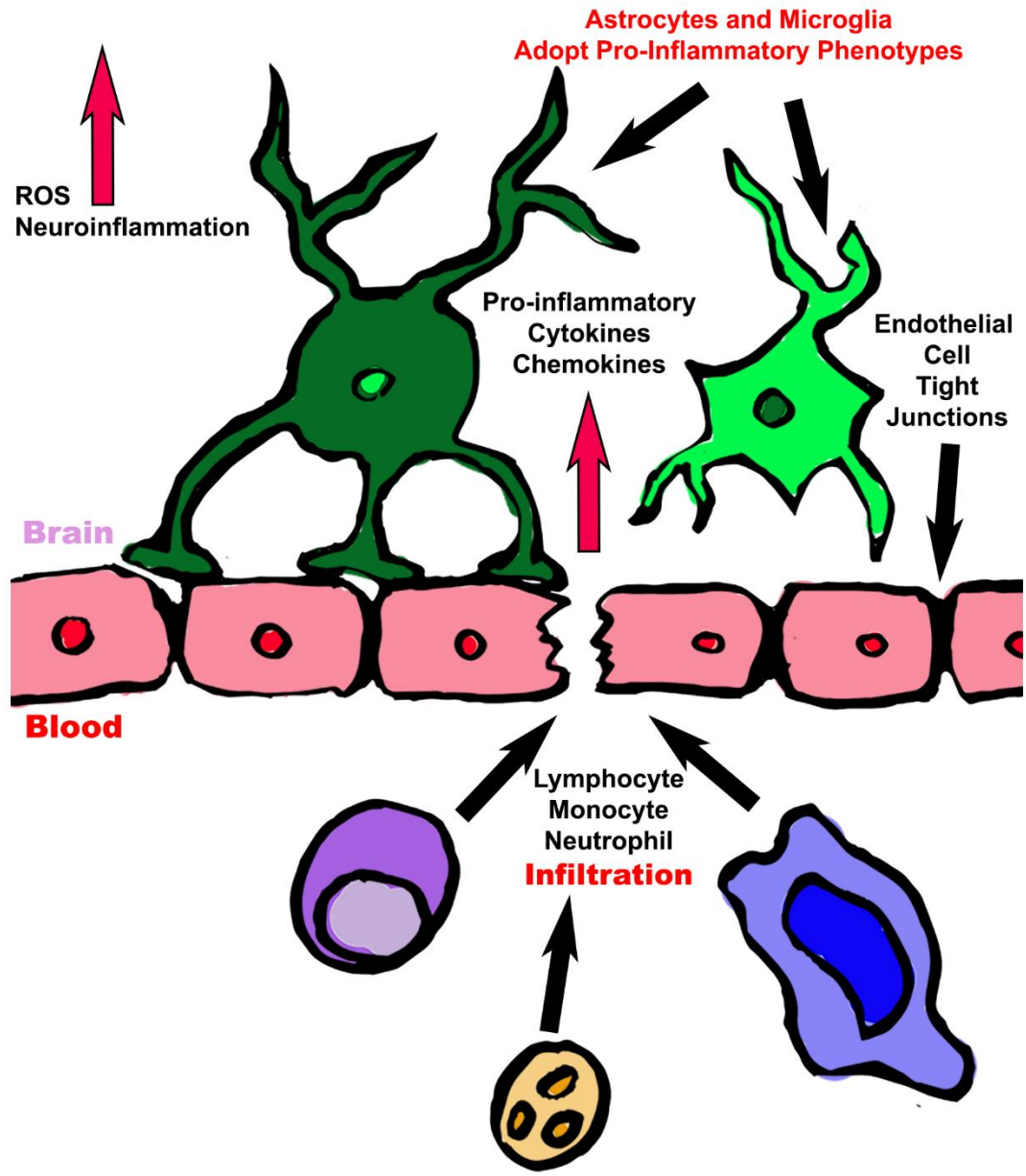


Figure 1.2 Blood Brain Barrier Disruption in Mild TBI. The blood brain barrier helps maintain homeostasis in the CNS and consists of a barrier of cells including astrocytes, pericytes, and tight junctions between endothelial cells. When this barrier loses its integrity as a result of mild TBI, toxins and peripheral lymphocytes, monocytes, and neutrophils can enter the brain. Furthermore, endothelial cells which construct the blood brain barrier can release pro-inflammatory cytokines such as interleukin- 1β and tumor necrosis factor- α . Endothelial cells of the blood brain barrier and peripheral immune cells contribute to neuroinflammation and elicit a pro-inflammatory response from astrocytes and microglia recruited to the blood brain barrier. Astrocytes and microglia adopt pro-inflammatory phenotypes characterized by changes in morphology, production of pro-inflammatory cytokines, chemokines, and reactive oxygen species (ROS), along with forgoing their homeostatic processes.

1.2.2 Excessive Glutamate Release and Excitotoxicity

Excessive extracellular glutamate has been reported immediately following TBI of all severities which seems to be a result of decreased clearance and buffering (Figure 1.3; Dorsett et al., 2017). Initially following TBI there is an increase in glutamate release and, when this persists, it can result in prolonged cognitive symptoms following injury (Guerriero et al., 2015). Furthermore, γ -aminobutyric acid (GABA), the brain's primary inhibitory neurotransmitter, is decreased following mild TBI, although this is dependent on location of measurement and time elapsed since the TBI (Yasen et al., 2018). In the weeks following a mild TBI, some researchers have found that the brain attempts to maintain homeostasis through a reversal with increased levels of GABA and decreased levels of glutamate (Friedman et al., 2017). It is unclear whether this persists or if the balance switches back to a state of increased glutamate and decreased GABA. More research needs to be done to understand the changes to glutamate and GABA in a time dependent manner, and long term, in response to mild TBI.

The NMDA ionotropic glutamate receptor has been shown to respond to primary injury from mild-moderate TBI through a loss of affinity for the magnesium ion that blocks the receptor at resting potential. This results in receptor activation and excitotoxicity acutely following TBI (Zhang, L., et al., 1996). This receptor has also been shown to be upregulated following mild TBI (Gabrieli et al., 2021). N-methyl-D-aspartic acid receptor activation allows for calcium and sodium influx into the neuron which can result in mitochondrial dysfunction, resulting caspase activation, action potential and neurotransmitter release, and protease production (Baracaldo-Santamaría et al., 2022). These receptors are also located on astrocytes which may indicate that they also contribute to excitotoxicity and oxidative stress (Lee, M. C., et al., 2010).

The EAAT glutamate transporters are expressed by both glial cells and neurons. As mentioned above, astrocytes adopt a pro-inflammatory phenotype and lose their ability to clear excessive glutamate from the synapse. Astrocytes express EAAT1 and EAAT2, with EAAT2 (known as GLT-1 in mice) being responsible for more than 90% of glutamate reuptake in the brain (Danbolt et al., 1992). Therefore, astrocytes are crucial in preventing excitotoxicity. The downregulation of EAAT2 has been well studied in various models of TBI; however, only a few studies report this downregulation in response to mild TBI and more research needs to be done to understand the expression changes in response to repetitive mild TBI (Goodrich et al., 2013; Shandra et al., 2019; Yi & Hazell, 2006).

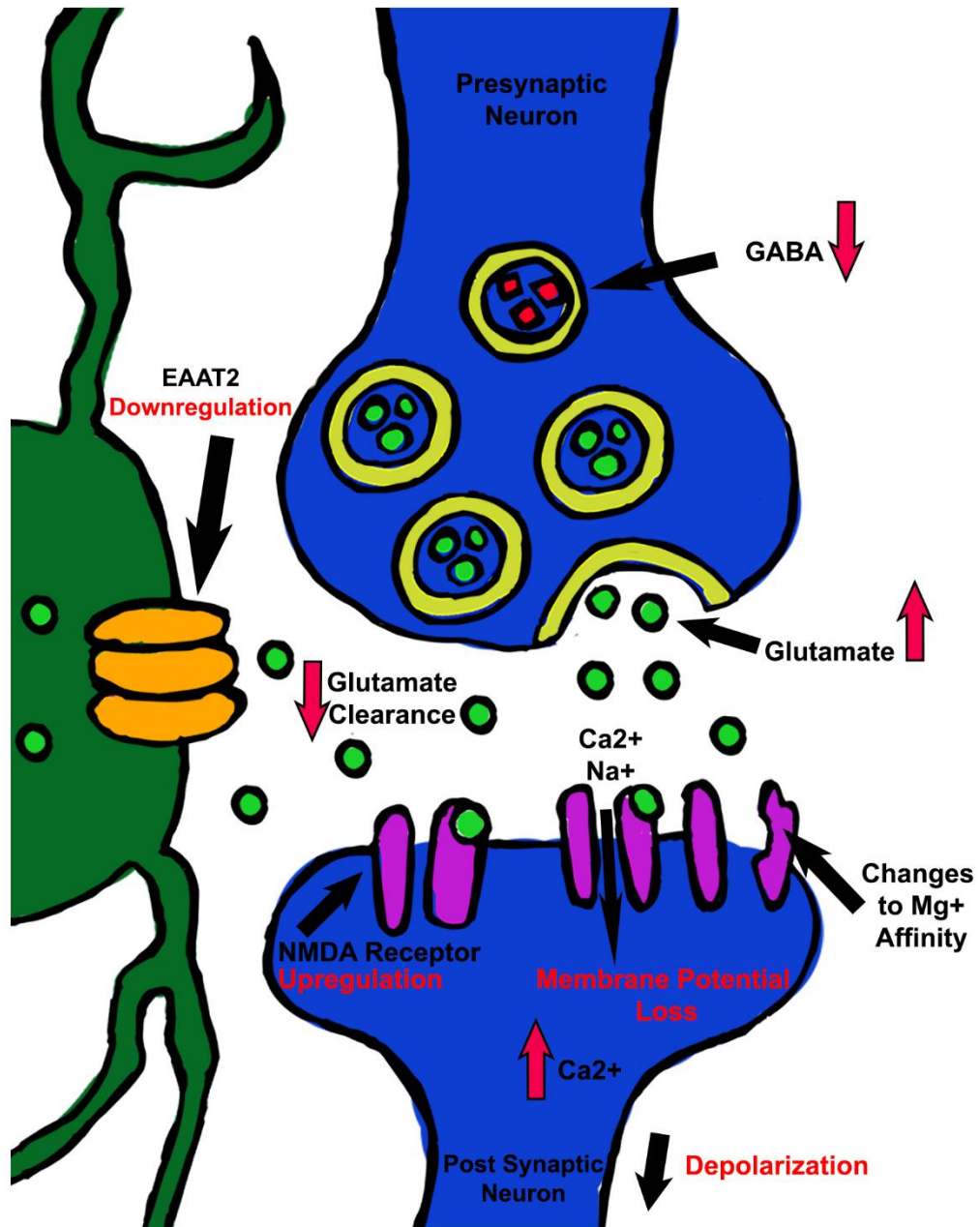


Figure 1.3 Excitotoxicity in Mild TBI. Excessive extracellular glutamate following mild TBI results from decreased clearance and buffering by astrocytes. Astrocytes adopt a pro-inflammatory phenotype and lose their ability to uptake glutamate from synapses due to downregulation of the excitatory amino acid transporter 2 (EAAT2) receptor. Furthermore, production and release of γ -aminobutyric acid (GABA), the brain's primary inhibitory neurotransmitter, by pre-synaptic neurons is decreased. In response to mild TBI, there is an upregulation of N-methyl-D-aspartic acid (NMDA) ionotropic glutamate receptors. These receptors suffer a loss of affinity for the magnesium ion (Mg^{+}) that blocks the receptor at resting potential. This allows the receptor to activate more frequently resulting in excessive influx of calcium (Ca^{2+}) and sodium (Na^{+}) ions. As a result, the post-synaptic neuron loses membrane potential which triggers depolarization and action potential. Excessive action potential generation can result in increased neurotransmitter release, protease production, excitotoxicity, oxidative stress, and ultimately, mitochondrial dysfunction, caspase activation, and neuronal cell death.

1.2.3 Oxidative Stress and Mitochondrial Damage

The previously described pathology, including BBB disruption, neuroinflammation, and excitotoxicity, can contribute to increased levels of oxidative stress and mitochondrial dysfunction. Increased levels of oxidative stress markers such as free radical species and ROS/RNS have been measured following TBI and seem to correlate with severity of TBI. Although more research into these markers following mild TBI should be explored, increased levels of NO and hydrogen peroxide have been measured in animal models and in humans with varying severities of TBI (DeWitt et al., 2009; Gahm et al., 2006). Levels of 3-nitrotyrosine (3-NT) are elevated following TBI of all severities, which indicates an increase in nitrosative stress (Abdul-Muneer et al., 2013; Sorokina et al., 2021). Evidence of oxidative and nitrosative stress, as measured by damage to lipids, DNA, and proteins are also observed following TBI. Increased levels of oxidative stress markers are measured along with a decrease in antioxidant markers, which will be discussed in further detail below. Due to the brain's high polyunsaturated

fatty acid (PUFA) content, lipid peroxidation is abundant following TBI. Increases in 4-hydroxynonenal (4-HNE) and malondialdehyde (MDA) have been observed in response to TBI of all severities, including mild and mild repetitive TBI (Emmerich et al., 2017; Vagnozzi et al., 1999; Yates et al., 2017). Damage to DNA and deficits to DNA repair mechanisms have also been observed following repetitive mild TBI (Fehily & Fitzgerald, 2017; Schwab et al., 2019a; Schwab et al., 2019b).

Along the same lines, mitochondrial DNA also suffers damage in response to the increased oxidative and nitrosative stress caused by both mild and severe TBI (Balasubramanian et al., 2020; Bulstrode et al., 2014). This, along with BBB disruption, neuroinflammation, and excitotoxicity results in mitochondrial dysfunction and neuronal cell death through apoptosis (Figure 1.4). Furthermore, dysfunctional mitochondria contribute to the generation of oxidative stress through deficits in the ETC. Altered energy metabolism is also observed in response to TBI as the brain requires more glucose. However, adenosine 5'-triphosphate (ATP) production decreases following TBI which indicates that mitochondria are unable to keep up with the increased energy demand (Lifshitz et al., 2003). Decreases in enzymatic activity from mitochondria, along with reduced oxygen usage, are further evidence of this following TBI (Lifshitz et al., 2003; Mautes et al., 2001). These effects likely contribute to excitotoxicity as mitochondria are not generating the energy needed for neuronal cells to perform active transport of ions across membranes to restore resting membrane potential.

1.2.4 Observed Changes to Autophagy and Protein Aggregation Following Mild TBI

Changes in autophagy have been observed following TBI. It seems that initially, following TBI of all severities, autophagy is accelerated as the brain attempts to clear components resulting from neuronal cell death (Au et al., 2017; Zeng, X. J., et al., 2018). Most studies on autophagy have been done in more severe models of TBI and not much research exists on changes to autophagy following mild TBI (Zeng, Z., et al., 2020). Furthermore, it seems that an increase in autophagy following TBI has a dual role, with more recent research indicating that oxidative stress contributes to the observed increase of autophagy. Consequently, studies have shown that suppression of autophagy with antioxidants or inhibitors improves TBI secondary injury pathology (Luo et al., 2011; Wang, C. Q., et al., 2017).

It is also unclear whether the overactive autophagy observed acutely following TBI persists long-term or if there is a sharp decrease in autophagy within months following TBI as the brain attempts to maintain homeostasis. Protein aggregates have also been observed following TBI of even mild severity and especially following repetitive mild TBI. This may help explain the increase in autophagy in response to TBI, and support evidence that suggests a toxic role of increased autophagy, as the brain works to clear these aggregates (Au et al., 2010). In the process, increased autophagy may also harm by degrading healthy organelles, such as mitochondria.

Toxic protein aggregates such as amyloid- β ($A\beta$), tau, neurofilament light chain protein (NfL), and α -synuclein have been observed following TBI of all severities. Proteins such as tau and NfL maintain neuronal and axonal structure which become

damaged in TBI. In the case of TBI, neurofibrillary tangles form which consist of hyperphosphorylated tau protein. Hyperphosphorylated tau has prion-like properties resulting in protein seeding as the protein moves from axon to soma where it can be released from neurons (Edwards et al., 2020). Tau hyperphosphorylation and aggregation have been observed in athletes with mild TBI and levels are positively correlated with negative patient outcome in those with mild TBI (Hossain et al., 2020). Neurofilament light chain protein is expressed along myelinated axons and its elevation, indicative of axonal injury, has been observed in mild TBI cases (McDonald et al., 2021; Shahim et al., 2017b). Amyloid- β -40 and -42 are derived from amyloid precursor protein (APP) which has roles in synapse maintenance. Amyloid precursor protein is cleaved by β - and γ -secretases to generate A β -40 and -42 which have the potential to aggregate and form senile plaques, an artifact commonly seen in AD patients (Bayer et al., 2006). These toxic aggregates can disrupt axonal transport and synaptic transmission resulting in neuronal cell death. Patients with repetitive mild TBI develop these senile A β plaques (Edwards et al., 2017). Alpha synuclein is one of the most abundant proteins present at axonal presynaptic terminals and has roles in synapse health and maintenance. The aggregation of this protein as a toxic oligomer is observed mainly in Parkinson's disease (PD) but also in AD and other dementias (Burré, 2015). Similar to those aggregating proteins described above, α -synuclein aggregates have also been observed in all severities of TBI (Impellizzeri et al., 2016). Furthermore, those individuals at high-risk for repetitive mild TBI have a >50% increased chance of developing PD (Gardner et al., 2018). The presence of toxic protein aggregates after even mild TBI, which have implications in

various neurodegenerative diseases, supports the idea that even TBI of mild severity may be a risk factor for developing these diseases.

1.2.5 Axonal Injury and Pathology Following Mild TBI

Diffuse axonal injury can be a result of primary injury due to the rapid acceleration and deceleration of the head during a TBI. Initially, diffuse axonal injury was thought to only occur following more severe forms of TBI. However, many studies have also observed diffuse axonal injury as evidenced by blood biomarkers and visualized lesions in mild TBI patients and in animal models of mild TBI (Shahim et al., 2017a; Topal et al., 2008; Xu et al., 2021). Evidence of accumulated phosphorylated tau and NfL, as reported above, are indicative of axonal injury following mild TBI. Although this may in part be due to primary injury sustained during a mild TBI, it is likely that the secondary injury mechanisms described above such as excitotoxicity, oxidative stress, and abnormal protein aggregation also contribute to axonal damage.

Axonal injury can cause abnormal axonal transport, loss of ion homeostasis, and deficits in synaptic transmission. The aberrant accumulation of proteins, synaptic vesicles, and organelles along the axon can result in axonal swelling. This gives the appearance of bulbous structures along axons in response to mild TBI (Johnson et al., 2013b). These blockages can disrupt ion homeostasis and result in increased calcium within the cell. To compensate for this, the cell increases levels of calpain, the calcium activated protease. Calpain is required for the proteolysis of voltage gated sodium channels and its increasing abundance results in more proteolysis of the channels which, in turn, results in more influx of calcium in injured neurons (Huh et al., 2006; von Reyn

et al., 2009). This contributes to excitotoxicity which, as discussed above, can result in mitochondrial dysfunction and neuronal cell death.

Along the same lines, alterations to synaptic transmission have been observed as a result of axonal injury including increases in excitatory and decreases in inhibitory neurotransmission following TBI (Witkowski et al., 2019). Furthermore, axonal injury visualized using magnetic resonance imaging (MRI) has been linked to cognitive deficits following mild TBI in patients (Wäljas et al., 2014; Zhang, K., et al., 2010). To summarize, axonal injury can result in a cascade of processes resulting in neuronal cell death and presenting as symptomology in patients with mild TBI.

1.2.6 Mild TBI Secondary Injury Pathology Symptom Presentation

The secondary injury pathology caused by mild TBI results in an array of cognitive, psychological, motor, and somatic symptoms typically referred to as post-concussive syndrome. Emotional symptoms such as anxiety, irritability, and depression have been reported in patients with mild TBI (Bergersen et al., 2017; Ponsford et al., 2012). Resulting cognitive symptoms include memory issues, attention deficits, brain fog, and focusing problems (Konrad et al., 2011; Panayiotou et al., 2010). Patients may also suffer motor symptoms such as balance and gait deficits which make them prone to a future mild TBI. Lastly, somatic symptoms can include headache, fatigue, dizziness, and sleep disturbances (Lee, J. E., et al., 2015; Prince & Bruhns, 2017).

Males and females seem to have differing outcomes following mild TBI. Women typically experience worsened overall symptomology and outcomes, but males have reportedly worsened cognitive symptoms specifically (Bazarian et al., 2010; Levin et al.,

2021). However, studies exploring symptomology in response to mild TBI in males and females are often confounded by a wide patient age range, unequal sample sizes in control and mild TBI groups, and inaccurate patient reporting. Furthermore, sex hormones, societal interactions, and perceived anxiety sensitivity also play roles in outcome differences between males and females who suffered mild TBI (Ma et al., 2019).

Symptoms resulting from mild TBI also seem to present on an individual basis, differing widely in number, type, duration, and severity. Some individuals report only a few symptoms that last a short time post-mild TBI while others report numerous symptoms that last for months to years following the injury. Approximately 15% of adults and 40% of children who sustain even a single mild TBI can have chronically persistent symptoms (McCrea et al., 2009). It is unclear why a minority of individuals have persisting symptoms, but it is possible that these individuals have persisting secondary injury pathology resulting from mild TBI. Over time, these processes deplete the body's antioxidant defenses. Deficiencies in many endogenous antioxidant compounds and associated enzymatic activities have been linked to the presentation of symptoms (Shafiee et al., 2018). It is hypothesized that patients with persistent symptoms have lasting secondary injury pathology and chronic antioxidant depletion from mild TBI.

1.3 Endogenous Antioxidant Depletion Following Mild TBI

An increased oxidative stress burden and overproduction of ROS/RNS from dysfunctional mitochondria and neuroinflammatory cells play a major role underlying mild TBI pathology. The brain is highly susceptible to damage induced by free radical

species and intracellular targets include protein sulfhydryls, lipid membranes, and DNA. To compensate for an increased oxidative burden, antioxidants are produced through transcriptional and post-transcriptional cascades (Morris, G., et al., 2019). Mild TBI disturbs the redox homeostasis resulting in a loss of essential endogenous antioxidants and a consequent further build-up of free radicals. Loss of redox homeostasis may persist following mild TBI and can result in worsened symptomology. If left untreated, and if subsequent mild TBIs are sustained, antioxidant depletion could also contribute to an increased risk of developing neurodegenerative disease.

1.3.1 Enzymatic Endogenous Antioxidant Depletion Following Mild TBI

Antioxidants are compounds that can prevent the formation of free radicals or sequester and reduce ROS/RNS through redox reactions, making them a viable therapeutic option to decrease or prevent oxidative and nitrosative stress after mild TBI (Khatri et al., 2018). The brain is particularly susceptible to oxidative damage due to its high lipid content, high oxygen consumption of about 20% of the body's basal level, and resulting energy needs to support over 80 billion neurons and greater than 200 billion glial cells (Cobley et al., 2018).

The brain has two antioxidant defense systems that can be classified as enzymatic or non-enzymatic (Lee, K. H., et al., 2020). The enzymatic endogenous antioxidant system consists of GSH/GSH peroxidases (GPx), thioredoxin, SOD, and catalase. Glutathione and GSH related enzymes will be a focus of this dissertation and will be discussed more in depth below. The thioredoxin system consists of thioredoxin and thioredoxin reductase. This system has anti-inflammatory and antioxidant abilities, and its activation

has been studied to be neuroprotective in response to various models of brain injury, including *in vivo* in models of mild TBI and ischemic damage (Baratz-Goldsten et al., 2018). There are three forms of SOD and they all function as antioxidants by having the ability to convert superoxide into hydrogen peroxide, although SOD-3 interacts with cytokines instead of oxidative species. Superoxide dismutase-1 and -2 are reduced following TBI and overexpression or administration of either seems to have a neuroprotective effect (Baranova et al., 2008; Zaghloul et al., 2014). Catalase is produced in response to oxygen and is a tetrameric protein which contains a heme group. Catalase protects cells from generated hydrogen peroxide through its conversion to water/alcohol and oxygen (Lee, K. H., et al., 2020). Although less research has been done on catalase enzymatic activity following mild TBI, a few studies have reported an acute increase in activity following TBI which may be a compensatory response to the initial oxidative stress burden (Goss et al., 1997; Kucur et al., 2005).

1.3.2 Nonenzymatic Antioxidant Depletion Following Mild TBI

The nonenzymatic endogenous antioxidant system consists of cofactors for antioxidant enzymes such as selenium, zinc, and coenzyme-q10. Coenzyme-q10 is a ubiquinone that is lipid soluble, is crucial for mitochondrial ETC function, and is embedded in some organelle membranes such as the Golgi apparatus and lysosomes (Lee, K. H., et al., 2020). It has been studied for its ability to protect against lipid peroxidation and cell membrane damage, and its ability to reduce oxidized alpha tocopherol (i.e., vitamin E; Pisoschi & Pop, 2015). Many studies have also explored coenzyme-q10 as a therapeutic for mild TBI, as discussed below (Hiebert et al., 2015).

Selenium is a crucial component of selenoproteins, selenocysteine, and selenoenzymes. These proteins have biological functions in antioxidant defense through interactions with GPx, regulating calcium, BBB maintenance, immunity, and mitochondrial biogenesis (Solovyev et al., 2021). Selenium, like coenzyme-q10, is commonly studied as a treatment for mild TBI. However, depletions in selenium and coenzyme-q10 following TBI of any severity are not very well studied. On the other hand, zinc depletion following TBI has been studied and linked to increases in neuronal cell death and excitotoxicity *in vivo* following TBI (Yeiser et al., 2002). Zinc interacts with endogenous antioxidant enzymes including playing a part in GSH metabolism and inhibiting pro-oxidant enzymes (Lee, K. H., et al., 2020). Interestingly, the location of zinc in the presynaptic bouton seems to be crucial in its neuroprotective role. Following TBI, the location of zinc changes and excessive amounts are released extracellularly which results in toxicity (Morris, D. R., & Levenson, 2013). These nonenzymatic endogenous antioxidants also interact with exogenous antioxidants which scavenge ROS/RNS such as vitamin E, vitamin A, and PUFAs.

1.3.3 Glutathione, GSH Precursor, and GSH Enzymatic Antioxidant Depletion Following Mild TBI

Glutathione is a tripeptide that functions as an essential endogenous antioxidant, protects neurons against free radical damage, and is a nonenzymatic antioxidant itself (Ross et al., 2012). Supporting enzymes such as GPx act as enzymatic antioxidants and use GSH to detoxify ROS, generating an oxidized form of GSH (GSSG) while reducing hydrogen peroxide to water. Glutathione reductase (GR) then utilizes NADPH to reduce

GSSG and replenish the GSH pool. The GSH to GSSG ratio is an important indicator of how the cell is managing oxidative stress and maintaining its redox balance (Koza et al., 2019; Ross et al., 2012).

Previous work has shown a reduction in brain GSH following TBI which may enhance the susceptibility of neurons to damage by free radicals (Koza et al., 2019). Ansari et al. (2008) measured the GSH/GSSG ratio and the activities of GPx and GR in a unilateral moderate cortical contusion model of TBI in the hippocampi of young adult rats. They found that the ratio of GSH/GSSG exhibited a significant time-dependent decrease post-TBI in the hippocampus ipsilateral to the injury, when compared to sham controls. The decrease was observed initially at 3 hours post-TBI and dropped to the lowest values at 24–48 hours post-TBI. The ratio of GSH/GSSG was still significantly lower than sham controls at 96 hours post-TBI. Furthermore, GPx and GR activities in the hippocampus also displayed time-dependent declines similar to that observed for the GSH/GSSG ratio (Ansari et al., 2008). In a clinical study, Bayir et al. (2002) measured GSH levels in cerebrospinal fluid of infants and children who had suffered severe TBI. They found that GSH levels were significantly decreased from day 1 post-TBI until day 7 post-TBI, when compared to healthy controls.

Dash et al. (2016) has shown that GSH precursors are also decreased after TBI. Methionine, when metabolized, generates S-adenosylmethionine (SAM). Homocysteine, an amino acid homologue of cysteine, is used to synthesize GSH under oxidative stress and is derived from SAM. The authors examined plasma levels of methionine and its metabolites in human patients 24 hours following mild and severe TBI. They found that

methionine and SAM levels were significantly decreased in severe TBI patients when compared to healthy controls. Furthermore, they also observed a significant decrease in GSH precursors, cysteine and glycine, in the severe TBI group when compared to controls. Mild TBI patients also showed a decrease in methionine and glycine levels; however, this decrease was less than that measured in the severe TBI patients (Dash et al., 2016).

From the above studies, it is evident that brain GSH is depleted following TBI of varying severity (Koza et al., 2019). Additional evidence suggests that endogenous GSH plays a role in protecting neurons from the devastating effects of TBI. For instance, transgenic mice deficient in GPx displayed increased oxidative stress and mitochondrial dysfunction following a TBI induced by controlled cortical impact (CCI), when compared to non-transgenic controls (Xiong et al., 2004). Al Nimer et al. (2013) also explored a genetic component of the GSH pathway in two strains of mice, dark agouti and piebald virol glaxo (PVGav1), in a weight drop model of TBI. These strains exhibit a difference in the regulation of the GSH pathway specifically at the level of the transcript for GSH S-transferase-4. The PVGav1 mice display increased GSH S-transferase-4 expression compared to dark agouti mice and demonstrated increased survival of neurons and a decrease in by-products of lipid peroxidation following TBI (Al Nimer et al., 2013). These studies further support the hypothesis that GSH plays a significant role in protecting neurons against oxidative and nitrosative stress caused by TBI.

The above studies mostly describe GSH, GPx, and GSH precursor depletion following more severe models of TBI *in vivo* (Koza et al., 2019). Less research is done

on the response of GSH, supporting enzymes, and precursors to mild TBI and repetitive mild TBI. However, supplementation of GSH and GSH precursors are commonly studied therapeutics for concussion and mild TBI which will be described below. This dissertation aims to fill a gap in the research by measuring GSH and GSH precursor depletion in patients with mild TBI and by also measuring GSH, GSSG, and GSH:GSSG in mouse models of repetitive mild and mild-moderate TBI. Furthermore, supplementation with a GSH precursor nutraceutical, Immunocal®, is explored as a treatment in these animal models.

1.3.4 Evaluation of Antioxidant Biomarker Depletion in a Patient Cohort with a History of Mild TBI

It is evident that secondary injury pathology of TBI, even of mild severity, places an increased oxidative burden on the brain. However, as discussed above, few studies to date report endogenous antioxidant depletion and even fewer studies report significantly reduced levels of nonenzymatic endogenous and exogenous antioxidants in patients with mild TBI.

De-identified patient data was obtained from a local specialized sports medicine clinic located in Englewood, Colorado. Upon presentation to the clinic, patients were evaluated by a board-certified physician who collected demographic information and a detailed medical history. A medical symptom questionnaire (MSQ) was completed by the patients and whole blood was taken for analysis of antioxidant biomarkers located in plasma, serum, red blood cells, white blood cells, or whole blood prior to the administration of any treatment or intervention. Eighty-eight (n = 88) patients, including

sixty-two (n = 62) males and twenty-six (n = 26) females, reported having at least one TBI in their lifetime and were considered to have a history of TBI. The board-certified physician confirmed that all these patients sustained TBIs of mild severity. Using physician intake notes, patients with a history of mild TBI were further categorized by number of mild TBIs sustained throughout their lifetime. Twenty-seven (n = 27) patients reported having a single mild TBI and forty (n = 40) sustained multiple mild TBIs. Patients with a history of mild TBIs were also categorized based on time elapsed since their most recent mild TBI to the clinic visit. Fourteen (n = 14) patients presented to the clinic within 1 year of their most recent mild TBI, termed as acute-subchronic mild TBI patients, and thirty-two (n = 32) patients presented to the clinic greater than 1 year since their most recent TBI, termed chronic mild TBI patients.

Antioxidant blood biomarker levels were compared between the total, male, and female populations with versus without a history of mild TBI. Emotional, energy, head, and cognitive symptoms were also analyzed between these populations to see if increased antioxidant depletion was associated with worsened symptomology. These symptoms were also qualitatively analyzed in the mild TBI subpopulations to see if number of mild TBIs sustained or time since the most recent mild TBI had different symptom severities or presentations. Lastly, we wanted to understand whether more extensive PUFA antioxidant depletion resulted in worsened symptoms in the total mild TBI population. This study is valuable in that it is one of the first to examine antioxidant depletion in human subjects with mild TBI. Furthermore, it helps to identify sex-specific differences in antioxidant depletion and symptomology and may further support the use of

antioxidant supplementation to treat mild TBI. This study is discussed in detail in Chapter Two.

1.4 Glutathione Precursor Supplementation to Treat Mild TBI

As discussed in depth in the previous sections, antioxidant depletion occurs as a result of the secondary injury pathology induced by mild TBI. Supplementation with nutraceutical compounds which act as GSH precursors designed to boost GSH, or with nutraceutical antioxidant compounds, may help alleviate the increased oxidative burden following mild TBI (Koza & Linseman, 2019; Figure 1.5). This could, in turn, treat persisting symptoms and may even reduce the risk of developing neurodegenerative disease in the future.

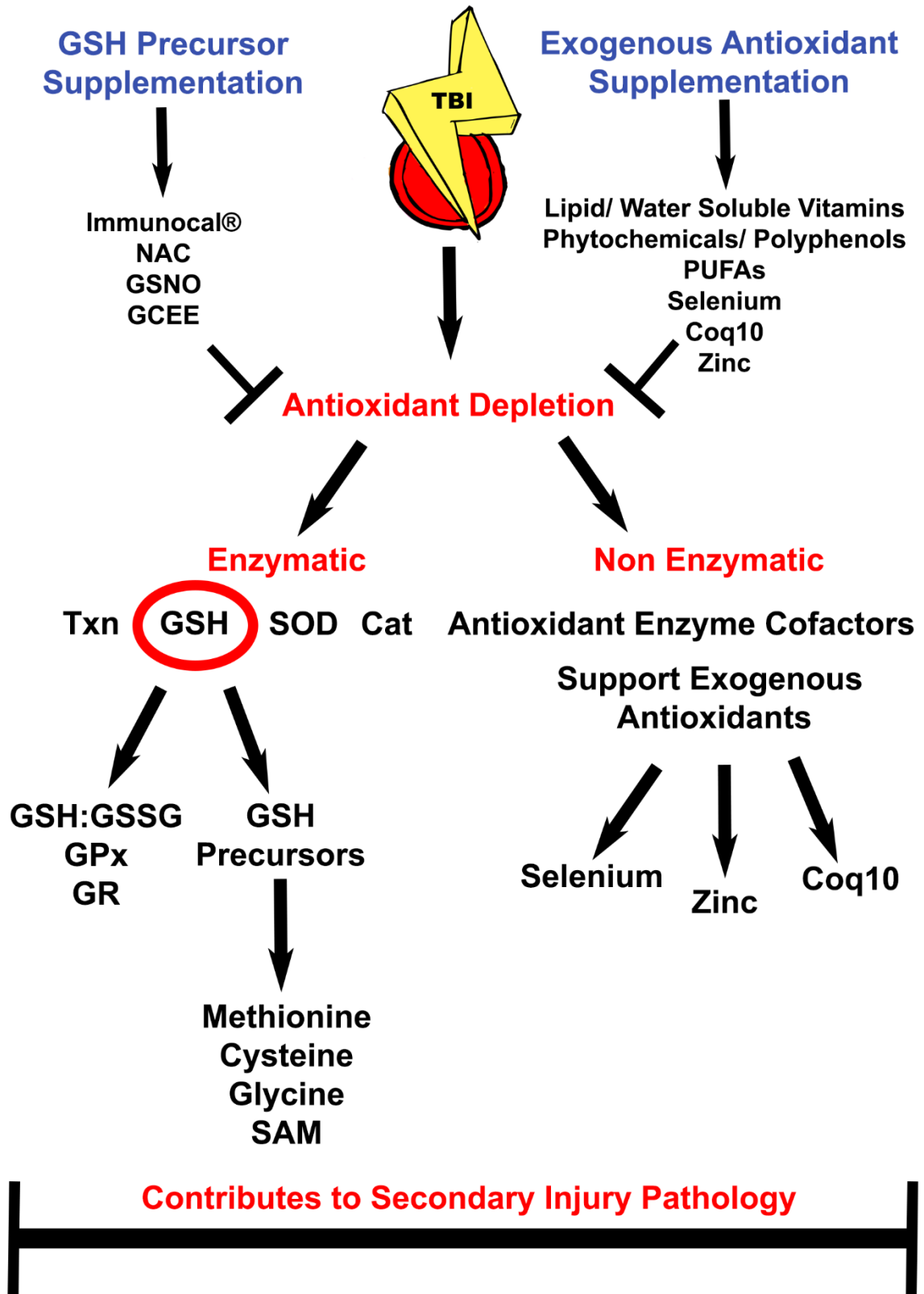


Figure 1.5 Endogenous Antioxidant Depletion from Mild TBI and Treatment with Nutraceutical Antioxidant Supplementation. To compensate for an increased oxidative burden following mild TBI, antioxidants are produced through transcriptional and post-transcriptional cascades and redox homeostasis is disrupted. The brain has two antioxidant defense systems that can be classified as enzymatic or non-enzymatic. The enzymatic endogenous antioxidant system consists of glutathione (GSH)/ GSH peroxidases (GPx), thioredoxin (Txn), superoxide dismutase (SOD), and catalase (Cat). Glutathione/GPx are a focus of this dissertation. Supporting enzymes such as GPx act as enzymatic antioxidants and use GSH to detoxify reactive oxygen species, generating an oxidized form of GSH (GSSG) while reducing hydrogen peroxide to water. Glutathione reductase (GR) then utilizes NADPH to reduce GSSG and replenish the GSH pool. The GSH to GSSG ratio is an important indicator of how the cell is maintaining its redox balance. This ratio and GSH supporting enzymes, along with precursors necessary for the production of GSH, such as methionine, cysteine, glycine, and S-adenosylmethionine (SAM) have been shown to be depleted following mild TBI. The nonenzymatic endogenous antioxidant system consists of cofactors for antioxidant enzymes such as selenium, zinc, and coenzyme-q10 (Coq10). These cofactors play roles in protecting against lipid peroxidation, oxidative stress, blood brain barrier disruption, and excitotoxicity. These nonenzymatic endogenous antioxidants also interact with exogenous antioxidants such as vitamins, phytochemicals/ polyphenols, and polyunsaturated fatty acids (PUFAs). Supplementation with compounds designed to increase the available pool of GSH, such as Immunocal®, N-acetylcysteine (NAC), S-nitrosoglutathione (GSNO), or γ -glutamylcysteine ethyl ester (GCEE), or that support exogenous antioxidants such as lipid/water soluble vitamins, phytochemicals/polyphenols, PUFAs, selenium, Coq10, or zinc could be beneficial in treating mild TBI pathology.

1.4.1 Glutathione Precursors as Treatment Options for Mild TBI

A few studies have shown the neuroprotective effects of treatment with GSH precursors post-TBI (Koza et al., 2019). N-acetylcysteine (NAC) is an antioxidant precursor to GSH and cysteine analog which can induce GSH synthesis or scavenge ROS itself. Hicdonmez et al. (2006) explored the beneficial effect of NAC in a closed head free fall cortical impact TBI model in rats. NAC was given to rats 15 minutes post-TBI and rats were sacrificed at 2 and 12 hours post-TBI. Administration of a single dose of NAC post-TBI significantly decreased MDA levels, increased SOD and GPx levels, and

protected neurons when compared to untreated rats that were subjected to TBI (Hicdonmez et al., 2006). In a clinical setting, active-duty military personnel that were exposed to blast mild TBI were given NAC for 1 week. Patients that received NAC had significantly improved symptoms when referenced to a baseline assessment as compared to patients that received a placebo. The authors also reported that patients who received NAC within 24 hours of mild TBI had an 86% chance of symptom resolution (Hoffer et al., 2013). These findings indicate that NAC can protect neurons from oxidative stress through the increased activity of antioxidants such as SOD and GPx which may also improve outcome following mild TBI (Koza & Linseman, 2019).

Another study tested the importance of the excitatory amino acid carrier type 1 (EAAC1), a membrane transporter that participates in the neuronal uptake of cysteine and maintains the levels of GSH in the brain. In this study, EAAC1 receptor knock-out mice were subjected to a CCI TBI. When mouse hippocampi were analyzed 3 and 24 hours post-TBI, superoxide production was significantly increased, and neuronal death was doubled in the EAAC1^{-/-} mice, when compared to wild-type mice subjected to TBI. Inflammation was also significantly increased in the EAAC1^{-/-} mice when compared to wild-type mice evidenced by an increase in microglial activation at 1-week post-TBI. Interestingly, pretreatment with NAC significantly reduced neuronal death and superoxide production in the EAAC1^{-/-} mice. These observations designate a crucial role for the EAAC1 transporter in GSH production and neuronal protection against the secondary injury induced by TBI (Choi, B. Y., et al., 2016).

S-nitrosoglutathione (GSNO) is a metabolite of GSH which can combat oxidative stress. GSNO has the ability to scavenge RNS and is seven-fold more capable than GSH to combat against oxidative stress caused by peroxynitrite (Khan et al., 2009). When GSNO was administered to rats 2 hours after a CCI TBI, the integrity of the BBB was preserved, apoptosis was reduced, and macrophages showed reduced inducible NO synthase (iNOS) expression when compared to vehicle-treated TBI animals. TBI animals treated with GSNO also significantly recovered neurobehavioral functions, such as motor deficits and cognitive impairment, as evaluated by the rotarod task and sensorimotor measurements when compared to untreated TBI animals (Khan et al., 2009).

Studies have also explored the neuroprotection exhibited by γ -glutamylcysteine ethyl ester (GCEE), a cell-permeable form of γ -glutamylcysteine that up-regulates GSH production in the brain. Reed et al. (2009) administered GCEE to adult rats approximately 10 min following a weight drop model of TBI, followed by euthanasia at 24 hours post-TBI. The results showed that GCEE significantly reduced levels of 3-NT and protein carbonyls to values like those of sham controls. Although many of the above-described studies explore compounds designed to increase GSH in more moderate-severe models of TBI, they provide compelling evidence for also using GSH precursors to treat mild TBI (Koza & Linseman, 2019).

1.4.2 Immunocal® as a Potential GSH Precursor Supplement for Mild TBI

Although the above studies highlight the effects of different GSH precursors against secondary injury in TBI, many of them lack an assessment of motor and cognitive function. In addition, most did not directly measure GSH or its oxidized form GSSG.

Observing the effect of GSH precursors on motor function and cognition would allow for an evaluation of recovery following TBI and would be more relevant to future clinical applications in humans. Furthermore, many of the GSH precursors discussed above have primarily been tested as *restorative* treatments for a single TBI of more moderate-severe severity. A *preventative* treatment would be highly beneficial in protecting high-risk populations from repetitive mild TBI (Koza & Linseman, 2019).

Our lab has recently studied the effects of a non-denatured whey protein supplement, Immunocal®, in a mouse model of moderate TBI induced by CCI (Ignowski et al., 2018). Unlike the above studies, Immunocal® was administered as a preventative treatment and the ability of Immunocal® to restore motor and cognitive deficits post-TBI was also measured. Immunocal® is replete with cystine and γ -glutamylcysteine and has been shown to act as a cysteine delivery system that boosts GSH levels *in vivo* (Ross et al., 2012). CD1-Elite male mice were pretreated orally with Immunocal® for a period of 28 days prior to a single moderate TBI. Following TBI, the mice were assessed for motor deficits using the beam walk and rotarod. Mice were also assessed for spatial learning and memory using Barnes maze testing. TBI mice pretreated with Immunocal® performed significantly better than untreated TBI mice in all these tests. Immunocal® pretreated mice also displayed a significantly higher preserved brain GSH/GSSG ratio measured at 72 hours post-TBI than measured in untreated TBI mice. These data indicate that Immunocal® provides ample cysteine which is converted into GSH in the brain. With supplementation of Immunocal®, cells can overcome excess ROS and RNS and maintain a balance of the GSH redox state. Furthermore, TBI mice pretreated with

Immunocal® also displayed a two-fold reduction in brain MDA and a preservation of brain-derived neurotrophic factor (BDNF), when compared to untreated TBI mice at 72 hours post-TBI. Lastly, we found that Immunocal® pretreated mice subjected to TBI displayed significantly less demyelination of the corpus callosum and decreased numbers of degenerating neurons when compared to untreated TBI mice (Ignowski et al., 2018; Koza & Linseman, 2019).

Immunocal® would be particularly beneficial for high-risk populations due to its preventative effects against secondary injury mechanisms induced by a single moderate TBI and due to its ability to significantly improve deficits in motor and cognitive function. Amelioration of secondary injury could be crucial in the long term, especially in individuals who sustain multiple mild TBIs. Furthermore, Immunocal® is easily administrable for high-risk populations. Pre-treatment with GSH precursors such as Immunocal® could lessen the severity of motor and cognitive impairments and ultimately improve an individual's quality of life after mild TBI and especially repetitive mild TBI (Koza & Linseman, 2019). Furthermore, mild and repetitive mild TBI increases the risk of developing serious neurodegenerative diseases, such as AD. Pre-treatment with Immunocal® could reduce this risk in the long term. Below, pre- and post-TBI treatment with Immunocal® is explored as a safe and effective treatment for repetitive mild and repetitive mild-moderate TBI.

1.5 Preclinical Murine Models of Repetitive Mild and Repetitive Mild-Moderate TBI Induced by CCI to Assess the Therapeutic Benefit of Immunocal®

Preclinical research has taken a systematic approach to studying TBIs of various severities and modalities to better understand the pathology associated with TBIs

sustained by human subjects. Rodent models are most used preclinically due to the small size of the animal, lower cost, and standardization of functional tests. Models of TBI can be classified as being induced by CCI, fluid percussion, weight-drop acceleration, blast injury, or non-impact head acceleration (Xiong et al., 2013). For the purposes of this dissertation, a focus will be placed on mild TBI models.

Models of mild TBI are typically closed head, although some researchers expose the skull, and most models used are either weight drop models or piston-driven/CCI (Bodnar et al., 2019). Earlier research on mild TBI (early 1990's) principally used the weight drop model while more recent research commonly uses CCI models (Bodnar et al., 2019). Publications which report using weight drop models use a falling projectile dropped through a tube. The animal's head may be fixed or allowed to rotate, the animal may or may not have surgery to expose the skull, be wearing an affixed metal disk as a "helmet", and the animal is typically on a hard or foam surface. Studies which implement weight drop models for mild TBI have significant variability concerning the weight and type of projectile, the surface used, and height from which the projectile was dropped. All of these parameters affect the injury pathology induced (Bodnar et al., 2019). Controlled cortical impact models are more standardized in that there are only two types of devices to induce the impact, two types of impact tips exist (although sizes vary), and impact depth, dwell time, angle, and velocity are highly controlled (Osier & Dixon, 2016). Therefore, a CCI model was chosen for increased replication and standardization for the study of Immunocal® treatment for repetitive mild and mild-moderate TBI.

1.5.1 Controlled Cortical Impact as a Standardized and Highly Reproducible Model of TBI

Controlled cortical impact devices allow for control, as the name suggests. This model is well regarded by many researchers and is considered to be a highly reproducible model of TBI. Although this model was used to induce mild and mild-moderate TBI as described below, it can also be used for TBI of all severities. Two main types of CCI models exist, pneumatic and electromagnetic, which are supplied by various commercial suppliers. Pneumatic devices are powered by pressurized gas and consist of a cylinder with a piston mounted to a crossbar while electromagnetic devices are smaller and able to function without a gas source. Although few studies exist on the differences between the two devices, Brody et al. (2007) reported that the electromagnetic CCI model allowed for more consistent head injury (Figure 1.6).

Typically, these devices come with a stereotaxic frame allowing for a fixed head impact. A different model, a closed-head impact model of engineered rotational acceleration (CHIMERA), exists which uses a pneumatically driven piston to induce an impact to a freely moving head allowing for rotational acceleration injury. However, this model is newer and requires more research into the pathological effects and standardization of parameters (Namjoshi et al., 2017). For CCI, different piston shapes and sizes exist which can be chosen to induce specific injuries and resulting pathology. A limitation of CCI is that it typically induces a focal contusion type of injury. This may be relevant for only a few types of mild TBIs sustained in the human population as many sports-related injuries, falls, and those sustained by military personnel are more diffuse

and include acceleration injury. A metal disc can be affixed to the skull which may help diffuse the injury, but many studies have not implemented this for milder TBI models. A CCI model is ideal for modeling repetitive mild TBI due to its high reproducibility and control over variables such as impact depth, dwell time, angle, and velocity. Below, a well-researched and replicated model of repetitive mild TBI is described along with the pathology it induces.

A



B

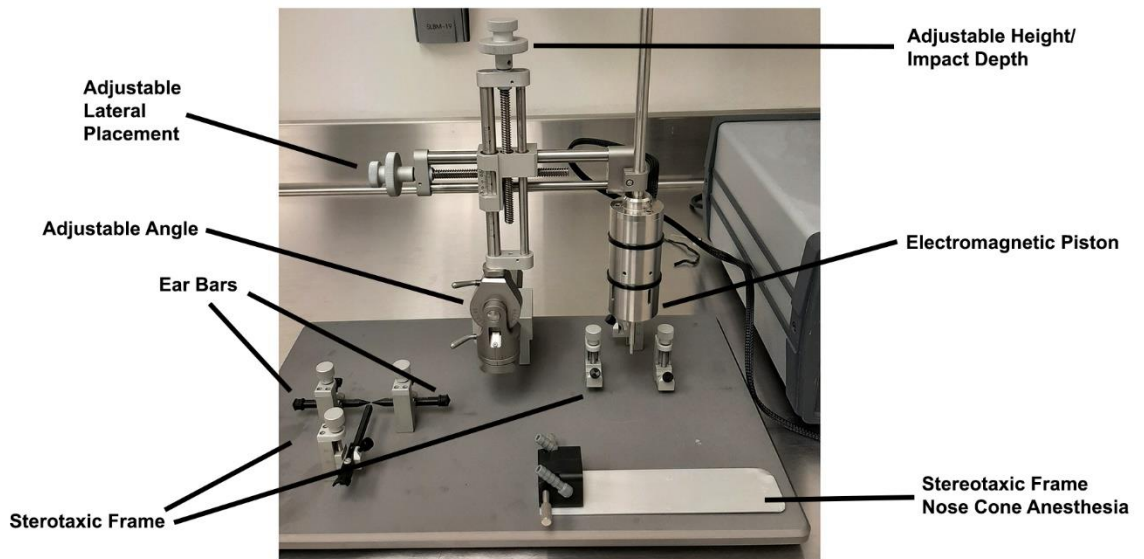


Figure 1.6 Controlled Cortical Impact Device to Induce Mild TBI. Controlled cortical impact devices allow for control and are well regarded by many researchers to be a highly reproducible model of TBI. **(A)** The model shown here is a controlled cortical impact electromagnetic device. **(B)** A stereotaxic frame is used to allow for a fixed head impact. A controlled cortical impact model is ideal for modeling repetitive mild TBI due to its high reproducibility and control over variables such as impact depth, dwell time, angle, and velocity.

1.5.2 Models of Repetitive Mild and Mild-Moderate TBI Induced by CCI Used to Assess the Therapeutic Benefit of Immunocal®

For the purposes of this dissertation, a replicated model of repetitive mild TBI induced by CCI was slightly modified and used to study Immunocal® pre- and post-TBI treatment. This technique is a well characterized model of closed head injury controlled by an electromagnetic device. In 2012, Dr. Fiona Crawford's group established a repetitive mild TBI model using CCI and characterized secondary injury pathology. This model consisted of 5 mild impacts separated by 48 hours over 10 days with each impact induced by a 5mm blunt tip. The impacts had a velocity of 5 m/s, depth of 1mm, and dwell time of 200ms. The authors reported this injury to be mild in severity because it did not cause any skull fracturing (Mouzon et al., 2012). The injury paradigm is relevant as it mimics multiple mild TBIs that may be sustained by high-risk populations such as athletes, military personnel, or the elderly who may sustain subsequent mild TBIs before recovering from an initial mild TBI. Briefly, mice were anesthetized, and the mouse's head was shaved. Mice were affixed in a stereotaxic frame so their head could not move laterally when impacted. These mice experienced anywhere from 3-30 seconds of apnea and righting reflex times anywhere from 3-6 minutes, however TBI mice righting reflex times did not differ significantly from sham mice (Mouzon et al., 2012).

The authors found deficits in motor function as evidenced by rotarod testing and a failure to return to uninjured baseline performance in repetitive mild TBI mice. Learning and spatial memory were also assessed using Barnes maze and repetitive mild TBI mice performed worse than uninjured mice. Hemorrhage ($<1\text{mm}^2$) in the cerebellum was also observed; however, skull fractures, cerebral hemorrhages, and contusions were not observed. Axonal damage and APP immunoreactivity were observed 24 hours and 10 days post-TBI. Astrogliosis and microgliosis were also observed in hippocampus and cortex with microgliosis also being present in the corpus callosum at 24 hours and 10 days post-TBI (Mouzon et al., 2012). The authors followed this original publication with two more publications looking at more long-term (6, 12, 18, and 24 months post-TBI) effects of the repetitive mild TBI model. Cognitive deficits, neuroinflammation, and white matter degeneration were still observed at these time points (Mouzon et al., 2014; Mouzon et al., 2017). Furthermore, other studies implemented this model and reported similar pathology (Maigler et al., 2021; Morin et al., 2020; Morin et al., 2021; Underwood et al., 2022). Researchers are still currently using this model, along with closely related adapted models, and have described additional pathology. Pathology including tau hyperphosphorylation, increases in nuclear factor- κ B (NF κ B) in cortex, and other behavioral changes such as reduced disinhibition by elevated plus maze have been reported (Eisenbaum et al., 2021; Morin et al., 2021).

Due to the high replicability of this CCI model, this model was adapted and used to assess the effects of Immunocal® supplementation pre- and post-repetitive *mild* TBI, as well as pre- and post-repetitive *mild-moderate* TBI of greater severity. Briefly,

Immunocal® was provided *ad libitum* in drinking water prior to, during, and following repetitive mild TBI until analysis at 2 weeks, 2 months, and 6 months following the TBIs. At each time point, astrogliosis and microgliosis were measured in cortex and MRI was used to analyze BBB disruption and macrophage activation at 2 months following the TBIs. We also analyzed astrogliosis and microgliosis in cortex, NfL in serum, and brain GSH and GSSG in mice dosed with Immunocal® and subjected to repetitive mild-moderate TBI at 72 hours post-TBIs. Results from this study are described more in depth in Chapter 3.

1.6 Pathology of ALS Results in Motor Neuron Cell Death, Skeletal Muscle Denervation, and Muscle Atrophy

The pathology of mild TBI is similar to that observed in neurodegenerative diseases, such as ALS. Furthermore, research indicates that TBI, especially sustaining multiple mild TBIs throughout an individual's lifetime, may increase the risk for developing neurodegenerative disease like ALS. Other factors, such as exposure to toxins and chemicals, along with genetic predispositions, have also been linked to the development of ALS in individuals. Although the pathology of ALS is not fully understood, key mechanisms such as protein aggregation, altered RNA metabolism, deficits in DNA damage repair mechanisms, oxidative stress, neuroinflammation, mitochondrial dysfunction, changes to axonal transport and synaptic vesicle release have been identified (Mejzini et al., 2019). These pathological changes result in motor neuron cell death, skeletal muscle denervation, loss of muscle functionality, and muscle atrophy and paralysis (Figure 1.7). These various pathological mechanisms may be targets for nutraceutical antioxidant treatments and are further described below.

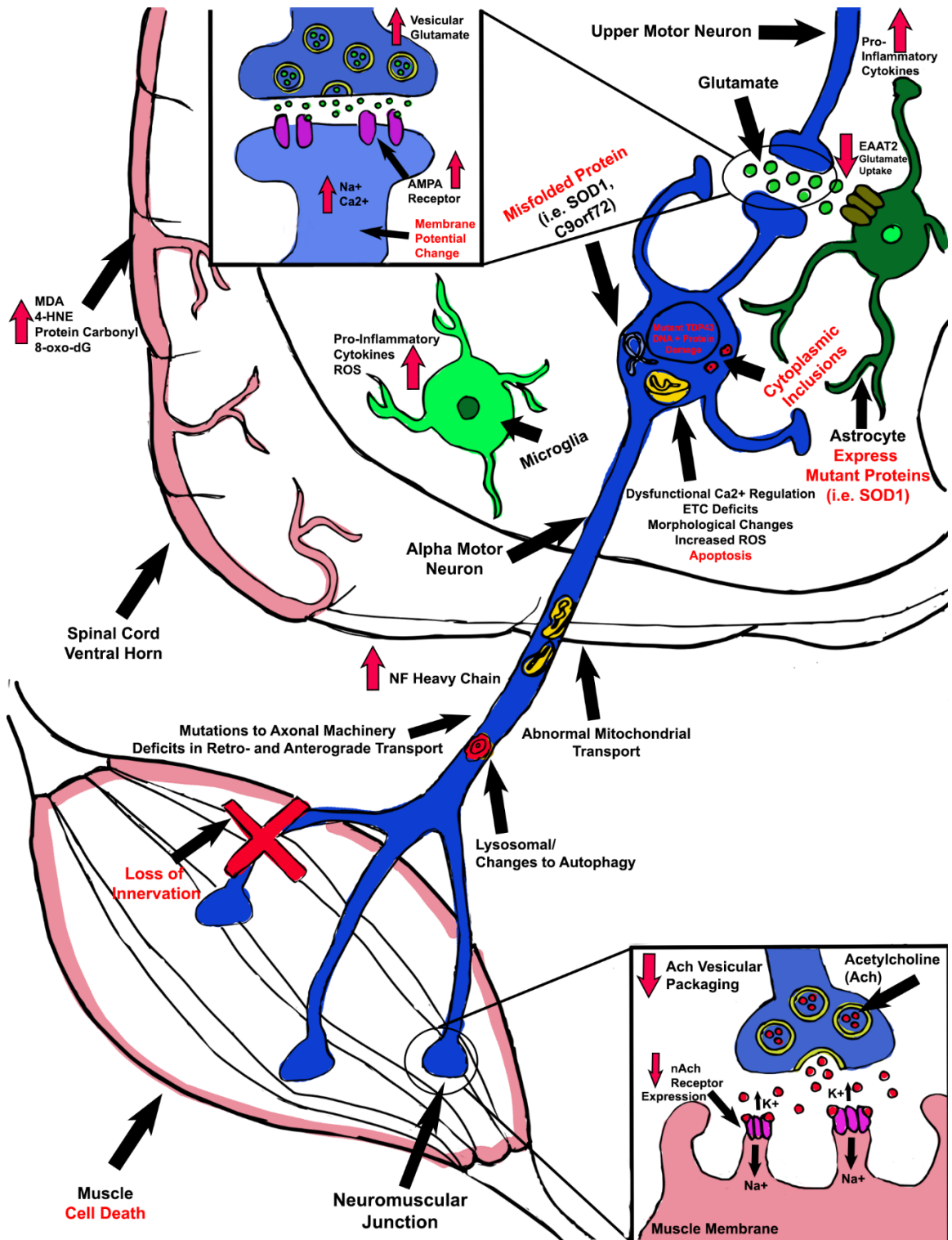


Figure 1.7 Pathology of ALS. Pathological mechanisms such as protein aggregation, altered RNA metabolism, deficits in DNA damage repair mechanisms, oxidative stress/ increased reactive oxygen species (ROS), neuroinflammation, mitochondrial dysfunction, and changes to axonal transport and synaptic vesicle release have been identified in ALS. Markers of DNA, lipid, and protein damage resulting from oxidative stress such as malondialdehyde (MDA), 4-hydroxynonenal (4-HNE), 8-oxo-2'-deoxyguanosine (8-oxo-dG), and protein carbonyls in blood, CSF, spinal cord, and/or motor cortex are elevated in ALS patients. Dysfunctional calcium ion (Ca^{2+}) regulation and mitochondrial electron transport chain (ETC), along with morphological changes to mitochondria, have also been observed in ALS. Inflammatory markers and cytokines released from astrocytes and microglia expressing mutant proteins such as superoxide dismutase-1 (SOD-1) have also been found to be upregulated in ALS. Astrocytes contribute to excitotoxicity and show decreased excitatory amino acid transporter 2 (EAAT2) transporter expression resulting in decreased uptake of glutamate from synapses. Motor neurons respond to glutamate as their primary excitatory neurotransmitter and are sensitive to excitotoxicity, particularly by α -amino-3-hydroxy-5-methyl-4-isoxazole propionic acid (AMPA) ionotropic glutamate receptors. Increased and prolonged glutamate in synapses leads to influx of sodium (Na^+) and Ca^{2+} ions, membrane potential loss, and excessive generation of action potentials. Cytoplasmic inclusions of mutant proteins such as SOD-1, TAR DNA-binding protein-43 (TDP-43), and chromosome 9 open reading frame 72 (C9orf72) have been observed in motor neurons and glial cells located in brain and spinal cord isolated from ALS patients. Evidence of defective anterograde and retrograde axonal transport such as hyperphosphorylated neurofilament (NF) heavy polypeptide chain, abnormal accumulation of mitochondria and lysosomes, and axonal spheroids containing vesicles, lysosomes, mitochondria, and microtubules, have also been observed in patients with ALS. Upper motor neurons have cell bodies in the cerebral (motor) cortex and lower/spinal motor neurons have cell bodies in the ventral horn of the spinal cord. In the case of lower/spinal motor neurons, the neurotransmitter release of acetylcholine (Ach) occurs at the neuromuscular junction to allow for movement. In ALS, Ach vesicular packaging and nicotinic Ach (nAch) receptor expression are reduced. An early event in ALS pathogenesis appears to be the retraction of motor axons away from neuromuscular junctions: this in turn, leads to loss of skeletal muscle innervation, muscle atrophy, a dying back process of motor neuron cell bodies, and resulting loss of movement.

1.6.1 Oxidative Stress and Mitochondrial Dysfunction in ALS

Oxidative stress is the excessive production of ROS/RNS in the form of free radicals. Oxidative stress markers are elevated in ALS patients (D'Amico et al., 2013). In the case of sporadic ALS, excessive oxidative stress may be due to environmental factors such as toxins, pesticides, and heavy metals, along with lifestyle habits (Bozzoni et al., 2016;

D'Amico et al., 2013). Epidemiological and case control studies have linked pesticides, agricultural chemicals, and heavy metal exposure to the development of ALS (Bonvicini et al., 2010; Sutedja et al., 2009; Weisskopf et al., 2009). Lifestyle factors such as smoking, strenuous physical activity, and stress also may increase oxidative stress and contribute to the development of ALS (de Jong et al., 2012; Scarmeas et al., 2002; Schmidt et al., 2010). Lastly, the pathology from single or repeated head trauma, even of mild severity, results in overt oxidative stress and has been researched as a potential contributor to ALS in athletes and military personnel (Beghi et al., 2010; Schmidt et al., 2010).

These factors, along with dysfunction in the mitochondrial ETC that comes with aging, likely contributes to oxidative stress in sporadic ALS cases (Barber & Shaw, 2010). In fact, mitochondrial function deficits are present prior to symptom onset (Tan, W., et al., 2014). In the aging individual, mitochondrial function is reduced, and ROS generation is increased as a byproduct of dysregulated ATP production. Furthermore, the number of damaged mitochondria with mutated DNA also increases with age and further contributes to ROS generation (Stefanatos & Sanz, 2018). Dysfunctional calcium regulation and ETC activity, along with morphological changes to mitochondria, have been observed in cell and animal models of ALS (Damiano et al., 2006; Kawamata & Manfredi, 2010; Sasaki & Iwata, 2007).

Familial ALS cases have been linked to mutations in chromosome 9 open reading frame 72 (C9orf72), TDP-43, fused in sarcoma (FUS), and SOD-1. Mutations in C9orf72 and SOD-1 account for the majority of familial ALS cases. Mutations to SOD-1 account

for 20-25% of all familial cases, making it the second most common ALS mutation behind mutations to C9orf72 (Ghasemi & Brown, 2018). Furthermore, recent data from an analysis of 22 countries has reported that, out of 2,876 prevalent mutant SOD-1 cases, 47% were familial and 53% were sporadic cases (Brown et al., 2021). Also, over 100 mutations in SOD-1 have been identified in patients with ALS (Valentine et al., 2005).

Superoxide dismutase-1 is an endogenous antioxidant enzyme with a copper binding site that can be reduced by superoxide to form dioxygen. An additional molecule of superoxide oxidizes the reduced copper ion to form hydrogen peroxide (Valentine et al., 2005). In ALS, further research is needed to understand how mutations in SOD-1 result in increased oxidative stress. Some studies have reported that SOD-1 loses its function and is unable to reduce superoxide resulting in increased levels of superoxide and peroxynitrite. Other studies have reported increased activity of SOD-1 resulting in increased production of hydrogen peroxide, hydroxyl radicals, and SOD-1 protein aggregation (Healy et al., 2020; Saccon et al., 2013). Mutated SOD-1 may also render normal SOD-1 nonfunctional (Barber & Shaw, 2010; Rosen et al., 1993). Mutations in SOD-1 also contribute to mitochondrial dysfunction as mutant SOD-1 aggregates in the mitochondrial outer membrane (Pickles et al., 2013).

Oxidative stress can result in DNA, lipid, and protein damage. Patients with ALS have increased levels of MDA, 4-HNE, 8-oxo-2'-deoxyguanosine, 3-NT, and protein carbonyls in blood, cerebrospinal fluid, spinal cord, and/or motor cortex (Barber & Shaw, 2010; D'Amico et al., 2013; Wang, Z., et al., 2019). This damage contributes to the motor neuron death that is characteristic of ALS. Furthermore, there is crosstalk between

oxidative stress and other pathological mechanisms present in ALS, such as those described below, which further contribute to motor neuron death.

1.6.2 Neuroinflammation in ALS

Inflammatory markers and cytokines released from glial and immune cells, such as IL-6, -8, and -1β , TNF- α , c-reactive protein, and interferon- γ (IFN- γ) have been found to be upregulated in ALS (Jin et al., 2020; Pronto-Laborinho et al., 2019; Tortelli et al., 2020). This dissertation will focus on the role of activated astrocytes and microglia in ALS, termed neuroinflammation, as a potential therapeutic target.

In ALS, astrocytes become toxic, release pro-inflammatory cytokines, and are typically located near dying neurons (Aebischer et al., 2011; Wang, R., et al., 2011). Astrocytes express mutated genes that have implications in ALS, including mutant SOD-1, and have been shown to cause neurotoxicity and increased levels of pro-inflammatory cytokines in culture which likely contributes to motor neuron death (Di Giorgio et al., 2007; Diaz-Amarilla et al., 2011; Yamanaka & Komine, 2018). Microglia are resident immune cells of the brain that sense the environment, exhibit macrophage activity, and respond to toxins. Like astrocytes, microglia also express ALS mutant genes, such as mutant SOD-1, and contribute to motor neuron death (Boill e et al., 2006). Both microglia and astrocytes can adopt anti- and pro-inflammatory phenotypes. Classically, an M2 phenotype is anti-inflammatory and promotes cell and tissue regeneration while an M1 phenotype is pro-inflammatory and is characterized by the generation of ROS/RNS and pro-inflammatory cytokines (Kwon & Kho, 2020). In a healthy individual, these phenotypes aren't polarized but astrocytes and microglia express these phenotypes on a

spectrum. In ALS, it seems that initially, many microglia adopt an anti-inflammatory, M2 phenotype. However, as the disease progresses, microglia take on a pro-inflammatory M1 phenotype (Beers et al., 2011; Clarke & Patani, 2020). Activated M1 microglia have been found in the motor cortex and spinal cord of ALS patients (Dols-Icardo et al., 2020; Fan et al., 2016). Lastly, there is crosstalk between astrocytes and microglia. For example, a reduction in microgliosis has been shown to decrease the activation of astrocytes (Gowing et al., 2008). Similarly, removal of astrocytes expressing mutant SOD-1 and replacement with wild-type astrocytes resulted in decreased microglial activation (Yamanaka et al., 2008). Regardless of the precise hierarchy of glial involvement in ALS pathogenesis, it is clear that these non-cell autonomous mechanisms play an important role in disease progression.

Motor neurons also express mutant genes, such as SOD-1, however, this alone does not seem to cause motor neuron death (Ilieva et al., 2009; Yamanaka et al., 2008). Furthermore, wild-type glial cells not expressing mutant ALS genes extend survival of motor neurons in animal models (Beers et al., 2006; Clement et al., 2003). These data indicate that glial cells such as astrocytes and microglia contribute to the death of motor neurons through the loss of necessary functions such as motor neuron support, homeostasis, and synapse support resulting in excitotoxicity and pro-inflammatory processes. Astrocytes and microglia also gain a toxic function through expression of mutant genes, pro-inflammatory activities, and generation of ROS/RNS, which further contribute to oxidative stress and motor neuron death.

1.6.3 Excitotoxicity in ALS

As mentioned above, healthy astrocytes have roles in synapse maintenance and neurotransmitter homeostasis. These processes include a dominant role in glutamate clearance from the synapse. In ALS, astrocytes have reduced functionality in this role which leaves excessive glutamate in the synapse and causes ionotropic glutamate receptor activation on the post-synaptic neuron (Ilieva et al., 2009; Benkler et al., 2013). Astrocytes have the EAAT2 transporter which is responsible for uptake of glutamate from the synapse, and this transporter displays decreased expression in ALS (Ferrarese et al., 2001; Foran & Trotti, 2009). Also mentioned prior, oxidative stress and mitochondrial dysfunction are both consequences and causes of excitotoxicity in ALS, as mitochondria have calcium buffering functions which become unregulated in ALS.

In general, motor neurons express a high number of AMPA receptors and exhibit an increased response to calcium influx (Kawahara & Kwak, 2005). Motor neurons respond to glutamate as their primary excitatory neurotransmitter and are sensitive to excitotoxicity, particularly by AMPA ionotropic glutamate receptors. In the case of mutant SOD-1 ALS, aggregation of mutant SOD-1 causes death of motor neurons specifically. Calcium influx through AMPA receptors can further contribute to mutant SOD-1 aggregation and the death of motor neurons (Corona & Tapia, 2007; Gregory et al., 2020; Tateno et al., 2004).

Furthermore, altered glutamate metabolism has been observed in ALS patients (Tefera et al., 2021). There is sound evidence of excitotoxicity caused by serum, plasma, and cerebral spinal fluid (CSF) isolated from ALS patients. Plasma, serum, and CSF from

ALS patients induces cytotoxicity in cultured neurons (Couratier et al., 1993; Sen et al., 2005). The neurotoxicity of CSF from ALS patients was blocked by an AMPA receptor antagonist, and an NMDA receptor antagonist showed a milder protection which suggests excitotoxicity plays a role (Couratier et al., 1993; Sen et al., 2005). Overall, it seems that glutamate excitotoxicity is an important underlying pathology observed in ALS (King et al., 2016; Milanese et al., 2011). However, it remains unclear whether this is due to increased extracellular glutamate or to changes in glutamate transporters, and what effect it has on disease phenotype. Andreadou et al. (2008) found increased plasma glutamate levels were correlated with longer disease duration in lower limb onset ALS but were not observed in bulbar onset ALS. Vesicular glutamate transporters, which package glutamate into vesicles for synaptic release, when reduced in expression in a mouse model of ALS, did protect motor neurons from death but ultimately had no effect on overall survival or disease duration (Wootz et al., 2010).

1.6.4 Observed Protein Aggregation Contributes to ALS Pathology

Protein aggregation has been observed in both sporadic and familial cases of ALS. Proteins encoded by genes such as SOD-1, TDP-43, FUS, and C9orf72 (e.g., dipeptide repeat proteins) have been observed to aggregate in ALS patients. Cytoplasmic inclusions of these proteins, classified as lewy-body like or neurofilamentous, have been observed in motor neurons and glial cells located in brain and spinal cord isolated from ALS patients (Blokhuys et al., 2013). RNA binding proteins specifically, such as TDP-43, FUS, and heterogeneous nuclear ribonucleoproteins A1/A2 (hnRNP A1/2), can become mutated and/or drawn into RNA foci and/or stress granules, and cause mislocalization of the

protein and impaired nuclear-cytoplasmic transport. Inclusions of these proteins have been observed in patients with ALS (Daoud et al., 2009; Kim, H. J., et al., 2013; Shang & Huang, 2016). Their functions and regulation of mRNA stability vary depending on the location, whether nucleus or cytoplasm, which further supports the idea that improper localization of RNA binding proteins may disrupt the regulation of mRNA and resulting in disease pathology (Wolozin & Apicco, 2015).

Aggregation of mutant SOD-1 has been observed in sporadic and familial ALS cases. Although more research is needed, SOD-1 may have similar roles to RNA binding proteins and its aggregation could have implications in the processes described above (Da Ros et al., 2021). Mutant SOD-1 does localize to RNA rich structures, support RNA metabolism, and SOD-1 inclusions do contain RNA (Butti & Patten, 2019; Da Ros et al., 2021). Aggregation of SOD-1 has been directly linked to motor neuron and glial cell death (Thomas et al., 2017; Tiwari & Hayward, 2005).

There are a few hypotheses which help explain why protein aggregation contributes to ALS disease pathology. Many observed protein aggregates in ALS have functions as RNA binding proteins or support RNA metabolism and, when these proteins are mutated and not performing their functions, there is a loss of regulation of RNA metabolism and disrupted transport of RNA from nucleus/cytoplasm. The improper formation or disintegration of stress granules also seems to play a role in ALS. Stress granules control mRNA localization, stability, and translation (Buchan, 2014). In response to stress signals, granules will sequester mRNA molecules, translation initiation factors, and RNA binding proteins such as those mentioned above. During stress, bulk translation is

inhibited but when the stress signal dissipates, translation can be reinitiated, and the stress granules disassemble due to their dynamic nature (Wolozin & Ivanov, 2019). Mutated RNA binding proteins that localize to stress granules can prevent their disassembly or can lead to aberrant formation causing a disruption in these regulatory processes (Protter & Parker, 2016). The accumulation of mutant proteins may also act in a prion-like manner, causing the aggregation of other normal and mutated proteins such as SOD-1 and TDP-43 and encouraging misfolding of these proteins (Lee, S., & Kim, 2015; Nonaka et al., 2013). Lastly, protein aggregates may also disrupt axonal transport of proteins, lipids, and mRNA which will be further described below, although the connection is not fully understood and conflicting evidence exists (Guo, W., et al., 2020).

1.6.5 Dysfunctional Axonal Transport, Synaptic Failure, Motor Neuron Death, NMJ Deterioration, and Muscle Atrophy in ALS

Increased oxidative stress, mitochondrial dysfunction, neuroinflammation, excitotoxicity, and protein aggregation can all contribute to axonal transport deficits. Mutations to axonal transport machinery such as to dynein or kinesin, or that affect microtubule stability, have been observed in ALS (Castellanos-Montiel et al., 2020; Soo et al., 2011). Excitotoxicity, oxidative stress, and mitochondrial damage are the cause and result of abnormal mitochondrial transport along axons (De Vos & Hafezparast, 2017).

Protein aggregates of TDP-43 and SOD-1 can cause aberrant activation of signaling pathways, such as activation of p38 mitogen-activated protein kinases or c-Jun kinases, which play roles in microtubule and kinesin transport (Horiuchi et al., 2013; Morfini et al., 2013; Suzuki, H., & Matsuoka, 2013). Deficits in anterograde and retrograde axonal

transport which transport mRNA, proteins, lipids, vesicles, and mitochondria have been observed in *in vivo* models of ALS. Hyperphosphorylated neurofilament heavy polypeptide chain, a marker of axonal loss, abnormal accumulation of mitochondria and lysosomes, and axonal spheroids containing vesicles, lysosomes, mitochondria, and microtubules, have all been observed in patients with familial and sporadic forms of ALS (De Vos & Hafezparast, 2017; Lu et al., 2015; Suzuki, N., et al., 2020).

Upper motor neurons have cell bodies in the cerebral (motor) cortex and lower/spinal motor neurons have cell bodies in the ventral horn of the spinal cord. Their axons allow for movement and reflex responses, with spinal motor neuron axons extending for several meters (Stifani, 2014). The synthesis of proteins and lipids occurs in the cell body; therefore, the axon is also crucial for the transport of neurotrophic factors, proteins, and mitochondria (Ikenaka et al., 2012). Furthermore, neurotransmitters in vesicles are transported along the axon for release at axon terminals. In the case of lower/spinal motor neurons, the neurotransmitter release of acetylcholine occurs at the NMJ, or the synapse between the motor neuron axon and the muscle it innervates. An early event in ALS pathogenesis appears to be the retraction of motor axons away from NMJs: this in turn, leads to loss of skeletal muscle innervation, muscle atrophy, a dying back process of motor neuron cell bodies, and resulting loss of movement. However, the precise order in which these events occur is subject to debate (Cappello & Francolini, 2017).

1.6.6 Endogenous Antioxidant Depletion Underlies ALS Pathology

All of the pathological mechanisms described above contribute to the overall antioxidant depletion observed in ALS patients (Figure 1.8). Much of the pathology

occurs prior to symptom onset and therefore goes undetected for prolonged periods. Long term oxidative stress, excitotoxicity, mitochondrial dysfunction, neuroinflammation, and accumulation of toxic protein aggregates deplete the endogenous antioxidant system. Depletions in antioxidant defense markers have been observed in ALS patients, although this is largely dependent on disease stage, progression, and duration of disease since diagnosis. As described in depth above, GSH is an endogenous antioxidant which has roles in reducing free radical oxygen. Glutathione levels, along with enzymes involved in GSH antioxidant activity such as catalase, GR, and glucose-6-phosphate dehydrogenase, have been shown to decrease with ALS disease progression and these deficiencies have been observed in both sporadic and familial forms of ALS (Babu et al., 2008; Cova et al., 2010; Golenia et al., 2014; Weiduschat et al., 2014).

SOD-1 is also a powerful cellular antioxidant. Copper and zinc binding to SOD-1 helps maintain copper homeostasis and facilitates the conversion between copper and cuperate, respectively. Many mutations to SOD-1 affect copper or zinc binding to SOD-1 rendering these processes dysfunctional in ALS (Boyd et al., 2020; Tokuda et al., 2013). As described above, mutations to SOD-1 can result in loss of function, cause increased activity and overproduction of ROS, or may inhibit functional SOD-1 and/or induce its aggregation.

On a transcriptional level, both SOD-1 and GSH play roles in, and are affected by, activation of the Nrf2 (nuclear factor erythroid 2 [NF-E2]-related factor 2 [Nrf2])–Keap1 (Kelch-like erythroid cell-derived protein with CNC homology [ECH]-associated protein 1) signaling pathway. This pathway becomes activated in response to oxidative stress.

When this occurs, cysteine residues on Keap1 are modified which results in its degradation and disassociation from Nrf2, targeting Keap1 for degradation and eliminating the interaction with Nrf2. Once freed from Keap1, Nrf2 forms a complex on antioxidant response elements in gene promoters and regulates gene expression of NAD(P)H quinone oxidoreductase 1, GSH S-transferase, and glutamate-cysteine ligase (Hemerková & Vališ, 2021). Nrf2 levels in SOD-1 mutant ALS have been found to be reduced in animal models and ALS patients (Kirby et al., 2005; Sarlette et al., 2008). Reduced response of this signaling pathway to oxidative stress helps explain why GSH and supporting enzymes are reduced in ALS patients (Harvey et al., 2009; Vargas et al., 2006). This indicates a loss of the endogenous antioxidant response to oxidative stress in ALS, although this is likely not the only pathway involved.

The Nrf2-Keap1 signaling pathway would be a viable target for treatment of ALS. Treatment using antioxidants for ALS has been well researched. Studies on Edaravone, a current FDA approved treatment for ALS which acts as an antioxidant, and other nutraceutical compounds which act as antioxidants have been explored as treatments for ALS. Natural dietary antioxidant compounds such as vitamin E (alpha tocopherol), resveratrol, epigallocatechin gallate, curcumin, and coenzyme-q10 have been well studied for ALS *in vivo* in preclinical mouse models (Carrera-Juliá et al., 2020). A large amount of research also has focused on flavonoids, or natural polyphenolic compounds. However, these compounds require more research into the feasibility of administration for patients, bioavailability, and mechanism of action. Furthermore, many published studies report conflicting data or have very small sample sizes. Below, nutraceutical

anthocyanin compounds and their phenolic acid metabolites, including cyanidin-3-*O*-glucoside and its metabolite protocatechuic acid (PCA), are discussed as possible therapeutics for ALS.

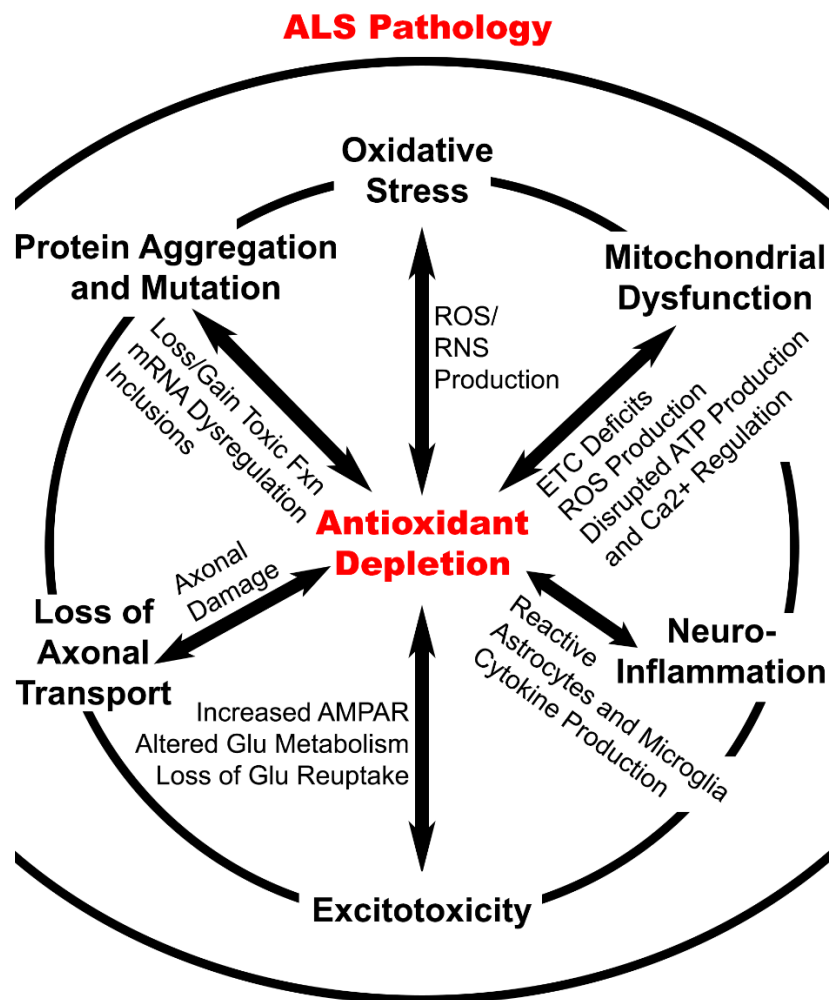


Figure 1.8 Antioxidant Depletion and ALS. Long term oxidative stress caused by increased reactive oxygen and nitrogen species (ROS/RNS) contributes to mitochondrial dysfunction characterized by electron transport chain (ETC) dysregulation, ATP production deficits, and calcium ion (Ca²⁺) dysregulation. These processes elicit neuroinflammatory responses from astrocytes and microglia. Excitotoxicity also results from increased expression of α -amino-3-hydroxy-5-methyl-4-isoxazole propionic acid (AMPA) receptors on motor neurons and altered glutamate (Glu) metabolism. These processes damage axons and, along with accumulation of toxic protein aggregates, cause loss of axonal transportation. These processes are interrelated and contribute to the overall antioxidant depletion observed in ALS patients. Much of this pathology occurs prior to symptom onset and therefore goes undetected for prolonged periods.

1.7 Berry Anthocyanin Nutraceutical Compounds and Their Phenolic Acid Metabolites as Potential Treatments for Neurodegenerative Diseases Like ALS

Berries and berry extracts have been previously studied and commonly reported to have antioxidant and anti-inflammatory properties. Due to this, they have been explored as treatments for various conditions including cardiovascular disease, cancer, and neurodegenerative disease (Winter & Bickford, 2019). Many berry extracts contain compounds known as anthocyanins, among many other compounds, which may be beneficial to treat disease. Anthocyanins are a water-soluble class of flavonoids, polyphenolic compounds that are found in both the skin and flesh of berries and fruits. Anthocyanins have roles in protecting berries from ultraviolet light and cold temperatures (Mattioli et al., 2020; Zafra-Stone et al., 2007). They are also responsible for the natural pigmentation of many berries and fruits, expressing as violet, red, and blue colors. Berries, such as blueberries, bilberries, and blackberries, are rich dietary sources of anthocyanins. However, concentration varies and is dependent on growing and storing conditions. On average, a half cup of blueberries or blackberries contains 120.8 mg and 70.4 mg of anthocyanins, respectively (Cassidy, A., 2018). The average human ingests 12.5 mg of anthocyanins daily (Eker et al., 2019). Consuming just a single cup of blueberries a day has been shown to increase anthocyanin dietary intake levels enough to prevent against cardiovascular disease (Cassidy, A., 2018).

Extractions of anthocyanins can be done organically, such as with ethanol, or using acidified water and high temperatures. The crude extraction can be separated, and the target anthocyanin can be identified through chromatographic techniques. This section will discuss the antioxidant properties of berry anthocyanins and their phenolic acid

metabolites. Specifically, cyanidin-3-*O*-glucoside, an anthocyanin compound found in blackberries and bilberries, along with its phenolic acid metabolite, PCA, will be discussed for their antioxidant, anti-inflammatory, and neuroprotective properties. These properties may be beneficial for treating neurodegenerative diseases such as ALS.

1.7.1 Nutraceutical Berry Anthocyanins and Their Antioxidant Properties

The structures of anthocyanins confer their antioxidant, anti-inflammatory, and neuroprotective properties. Anthocyanins are glycosides, containing one or more sugar molecules. They have a basic flavonoid structure but contain a positive charge at the oxygen of the C-ring and acylation of the sugar with cinnamic acids or aliphatic acids (Eker et al., 2019; Khoo et al., 2017). Free radical species can be extinguished through electron transfer and oxidation of the phenolic hydroxy groups and hydrogen atom removal from para- and ortho- phenolic groups (Mattioli et al., 2020). Common anthocyanins include pelargonidin, cyanidin, delphinidin, peonidin, petunidin, and malvidin (Winter & Bickford, 2019). The most common anthocyanin found in berries is cyanidin, whereas petunidin, peonidin, and malvidin are not as commonly found (Khoo et al., 2017).

Anthocyanins have been studied for their protection against pathology such as oxidative stress, neuroinflammation, protein aggregation, and excitotoxicity which is commonly seen in neurodegenerative disease, including ALS. Treatment with nutraceutical anthocyanin extracts, isolated compounds, and anthocyanin metabolites have been reported to be neuroprotective in *in vitro* and *in vivo* models of neurodegeneration. Anthocyanin compounds isolated from tart cherry extract had

inhibitory activity of cyclooxygenase-1 and -2 (COX-1 and -2), mediators of pro-inflammatory prostaglandins, comparative to non-steroidal anti-inflammatory pharmaceuticals *in vitro* (Seeram et al., 2001b). Shukitt-Hale et al. (2016) also studied pretreatment with tart cherry anthocyanins in rat microglial cells exposed to lipopolysaccharide (LPS) and found that levels of NO, TNF- α , and COX-2 were decreased in a time and dose dependent manner (Shukitt-Hale et al., 2016). Endothelial cells treated with an elderberry extract resulted in incorporation of anthocyanins into the cell's plasma membrane and cytosol and this uptake allowed for significant protection against hydrogen peroxide, dihydrochloride, and ascorbic acid oxidative stressors (Youdim et al., 2000). Furthermore, neuronal cultures derived from rats treated with a blueberry extract were protected from glutamate excitotoxicity (Vyas et al., 2013).

Anthocyanin rich diets and extracts have also been studied *in vivo*. A diet rich in blueberries and strawberries fed to aged rats improved cerebellar neuron beta adrenergic function which has been linked to motor learning (Bickford et al., 2000). Galli et al. (2006) also showed that hippocampal neurons isolated from rats fed a blueberry rich diet displayed increased resilience to cell death and inflammation *in vitro* (Galli et al., 2006). A strawberry extract rich in anthocyanins administered orally in an ALS mouse model prior to symptom onset resulted in delayed disease onset, increased survival, preserved grip strength, reduced astrogliosis, and protection of muscle innervation (Winter et al., 2018).

Lastly, it seems that anthocyanins also can influence the Nrf2-Keap1 signaling pathway. Although more research needs to be done to understand how anthocyanin

compounds affect this pathway in models of neurodegenerative disease, these compounds have been shown to activate this pathway in *in vitro* and *in vivo* in models of cancer, hypoxia, and oxidative stress injury (Aboonabi & Singh, 2015; Cimino et al., 2013; Kropat et al., 2013).

1.7.2 The Berry Anthocyanin, Cyanidin-3-*O*-Glucoside, and its Phenolic Acid Metabolites Including Protocatechuic Acid (PCA)

Cyanidin 3-*O*-glucoside is a cyanidin which is one of the most abundant and well-studied type of anthocyanin compounds. A systematic review by Sandoval-Ramírez et al. (2020) suggested that out of 203 possible phenolic compounds identified in human plasma and urine following anthocyanin-rich berry intake, cyanidin 3-glucoside would be best to use as a biomarker for the consumption of anthocyanins due to its frequently reported abundance (Sandoval-Ramírez et al., 2020). Cyanidin compounds, including cyanidin 3-*O*-glucoside, have been well studied for their antioxidant, anti-inflammatory, and neuroprotective properties. The neuroprotective effects of cyanidin 3-*O*-glucopyranoside were measured against hydrogen peroxide induced oxidative stress in SH-SY5Y human neuronal cells. The compound was able to inhibit ROS production, preserve mitochondrial function, and inhibit apoptosis (Tarozzi et al., 2007). Cyanidin-3-*O*-glucopyranoside treatment in PC12 cells also had a cytoprotective effect in cells exposed to hydrogen peroxide and oxygen glucose deprivation (Kang et al., 2006). Kim, S. M., et al. (2012) reported that cyanidin 3-*O*-glucoside pretreatment reduced hydrogen peroxide cytotoxicity in human brain neuroblastoma SK-N-SH cells by reducing intracellular ROS and inactivating apoptosis through Janus kinases (Kim, S. M., et al.,

2012). In an *in vitro* model of rheumatoid arthritis using synovial fibroblasts and mononuclear cells cultured with cluster of differentiation 38 (CD38) positive natural killer (NK) cells, cyanidin 3-*O*-glucoside treatment reduced pro-inflammatory cytokine production including IL-6 and IFN- γ (Wang, H., et al., 2019). Liu, F., et al. (2020) showed that cyanidin 3-*O*-glucoside was also able to prevent the formation of A β 40 beta sheet structures and reduced ROS production in response to A β 40 *in vitro* which may indicate that cyanidin 3-*O*-glucoside has anti-aggregative properties and may be beneficial to treat neurodegenerative diseases with notable protein aggregation like ALS (Liu, F., et al., 2020).

In vivo, cyanidin 3-*O*-glucoside administered immediately after spinal cord injury in rats allowed for maintenance of BBB integrity and grip strength at 14 days post-injury. Furthermore, superoxide generation, lesion volume, and neuronal cell death in spinal cord were also reduced at this time point (Kim, K. T., et al., 2011). Di Giacomo et al. (2012) also explored cyanidin 3-*O*-glucoside pretreatment in rats that suffered cerebral ischemia and found that treatment reduced lipid peroxidation, iNOS expression, and increased levels of γ -glutamyl cysteine synthase in brain at 24 hours post-ischemia.

Although further research should be done on the bioavailability of specific anthocyanin compounds, it seems that, overall, anthocyanins are absorbed relatively poorly with only 1-2% present in target organs or the blood stream following ingestion (Lila et al., 2016; Manach et al., 2005). However, their absorption and appearance in plasma is fast which may be explained by absorption via the gastric mucosa (Passamonti et al., 2003). Many factors specific to the structure of the individual anthocyanin, along

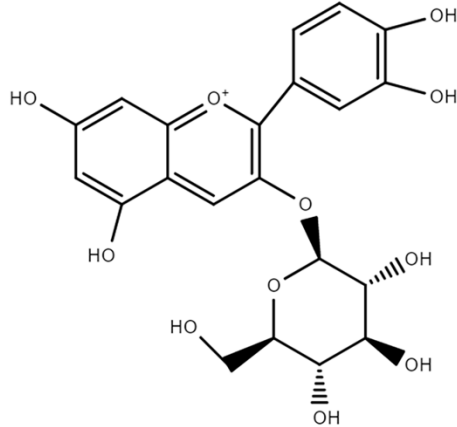
with food consumed alongside the anthocyanin, food already present in the digestive system, cooking methods, pH, temperature, and even the individual's gut microbiome contribute to the absorption of anthocyanins from the diet (Eker et al., 2019).

Anthocyanins have the ability to cross the BBB through P-glycoprotein transporters and have been measured in brain tissues after ingestion or administration (Fornasaro et al., 2016; Winter & Bickford, 2019). However, radiolabeled cyanidin 3-*O*-glucoside shows a peak at 3 hours post ingestion in rats with over 80% of intake observed in the gastrointestinal tract and only trace (<1%) in other tissues such as the brain (Felgines et al., 2010). Due to the poor availability of anthocyanins such as cyanidin 3-*O*-glucoside in the brain, metabolites of anthocyanins may have higher bioavailability and access to the brain and may therefore have greater efficacy in treating neurodegenerative diseases such as ALS.

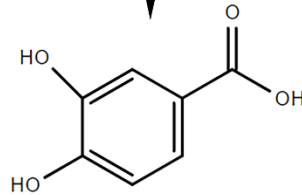
Cyanidin 3-*O*-glucoside can be metabolized into more than 20 different metabolites once in the body (de Ferrars et al., 2014). However, research indicates that the neuroprotective effects described above are most likely due to bioactive metabolites such as vanillic acid, ferulic acid, phloroglucinaldehyde, and PCA (Tan, J., et al., 2019). Protocatechuic acid is one of the major metabolites of cyanidin 3-*O*-glucoside (Figure 1.9). Animal studies report that PCA is abundant in tissues and plasma following cyanidin 3-*O*-glucoside administration (Tsuda et al., 1999). Furthermore, when 1L of blood orange juice containing 71mg of cyanidin 3-*O*-glucoside was ingested by healthy individuals, PCA accounted for 73% of the ingested cyanidin 3-*O*-glucoside in plasma (Vitaglione et al., 2007). Studies have also reported that cyanidin 3-*O*-glucoside can be

converted to its phenolic acid metabolites, including PCA, at a basic pH *in vitro* (Fleschut et al., 2006; Seeram et al., 2001a). As mentioned above, cyanidin 3-*O*-glucoside absorption occurs in the stomach and undergoes first-pass metabolism in the small intestine. In the small intestine, cyanidin 3-*O*-glucoside is hydrolyzed to aglycones and is then further degraded into phenolic compounds in the small intestine and large intestine by gut microflora. Protocatechuic acid is produced this way through cleavage of the C-ring of cyanidin 3-*O*-glucoside (Tan, J., et al., 2019). It can be further metabolized into phase II metabolites which may be responsible for some of the antioxidant and anti-inflammatory properties of PCA. Once absorbed, PCA crosses the BBB where it has been studied for its support of the endogenous antioxidant system (Krzysztoforska et al., 2019). However, for the purposes of this dissertation, PCA is focused on due to its high bioavailability in the CNS and because it is well studied in *in vitro* and *in vivo* models of neurodegenerative disease.

Cyanidin-3-O-Glucoside



First Pass Metabolism
in Small Intestine
pH 7-8



Protocatechuic Acid

Figure 1.9 Structures of Cyanidin 3-O-glucoside and its Metabolite Protocatechuic Acid. The bioavailability of the anthocyanin compound, cyanidin 3-O-glucoside, is relatively poor. Protocatechuic acid is one of the major metabolites of cyanidin 3-O-glucoside. Protocatechuic acid is abundant in tissues, including brain, and plasma following cyanidin 3-O-glucoside administration. Cyanidin 3-O-glucoside absorption occurs in the stomach and undergoes first-pass metabolism in the small intestine. In the small intestine, cyanidin 3-O-glucoside is hydrolyzed to aglycones and is then further degraded into phenolic compounds, such as protocatechuic acid in the small and large intestines by gut microflora. Protocatechuic acid is produced this way through cleavage of the C-ring of cyanidin 3-O-glucoside and once absorbed, can cross the blood brain barrier where it has been studied for its support of the endogenous antioxidant system.

1.7.2 Evidence of Antioxidant, Anti-Inflammatory, and Neuroprotective Properties of PCA in Support of Its Use as a Therapeutic Treatment for ALS

Protocatechuic acid has a lot of pharmacological potential including anticancer, antiulcer, antifibrotic, antiviral, antibacterial, and anti-atherosclerotic properties. However, for the purposes of this dissertation, a focus will be placed on the antioxidant and anti-inflammatory properties which may be beneficial in treating ALS (Figure 1.10). There is a lot of *in vitro* and *in vivo* evidence of the antioxidant, anti-inflammatory, and neuroprotective properties of PCA. More specifically, PCA has been explored in *in vivo* models of neurodegenerative disease; however, this dissertation reports the first study of PCA in a preclinical mouse model of ALS (Koza et al., 2020). Due to its well-researched neuroprotective properties, PCA was hypothesized to be a beneficial nutraceutical antioxidant compound to be used in treating ALS.

PCA has exhibited antioxidant activities *in vitro*. Oxidants such as superoxide, hydroxyl radicals, and ferric and cupric ions were dose dependently scavenged by PCA through metal chelation and radical scavenging (Li et al., 2011). Another study showed the ability of PCA to protect PC12 cells against 1-methyl-4-phenylpyridinium-induced mitochondrial dysfunction and associated loss of membrane potential, ROS generation, GSH depletion, and apoptosis (Guan et al., 2006). Winter et al. (2017b) showed that in a model of cerebellar granule neurons, PCA was able to protect against both nitrosative and oxidative stress (Winter et al., 2017c).

PCA also has been studied for its anti-inflammatory properties *in vitro*. Winter et al. (2017a) also showed that PCA prevented NO secretion in microglial cells exposed to LPS

(Winter et al., 2017a). PCA may also help to mitigate the production of pro-inflammatory cytokines and was able to decrease the expression of TNF- α and IL-1 β in RAW 264.7 cells. Protocatechuic acid also reduced iNOS and COX-2 expression in this model (Min et al., 2010). PCA can also inhibit the release of pro-inflammatory cytokines from microglia stimulated by LPS through activation of the sirtuin1/NF κ B pathway (Kaewmool et al., 2020).

In vivo, the antioxidant and anti-inflammatory effects of PCA have been tested in numerous models of neurodegenerative disease such as AD and PD. In an A β mouse model of AD, mice administered 100 and 200mg/kg PCA daily for 2 weeks while symptomatic had improved learning and memory as evidenced by T-maze test, novel object recognition, and the Morris water maze. Decreased lipid peroxidation, NO, NO synthase, and COX-2 were also observed in brain (Choi, J. R., et al., 2020). Furthermore, in an aged A β PP/PS1 mouse model of AD, daily 100mg/kg PCA treatment improved cognitive deficits assessed by Morris water maze, reduced A β inclusions in hippocampus and cortex, decreased the production of pro-inflammatory cytokines TNF- α , IL-1 β , IL-6, and also increased BDNF (Song et al., 2014). In a 1-methyl-4-phenyl-1,2,3,6-tetrahydropyridine mouse model of induced PD, 50 and 100mg/kg PCA pretreatment improved rotarod test motor function deficits and preserved dopamine and expression of tyrosine hydroxylase in the striatum (Zhang, H. N., et al., 2010). Park et al. (2019) also reported that 50mg/kg PCA administered immediately, at 6 and 12 hours, and daily for 7 days following spinal cord injury prevented blood spinal cord barrier disruption and suppressed mRNA expression of TNF- α , IL-1 β , iNOS, and COX2 at 7 days post-injury

(Park et al., 2019). Daily injection of 30mg/kg PCA for 1 week following ischemia in rats reduced astrogliosis, microgliosis, BBB disruption, oxidative stress, preserved GSH, and prevented neuronal cell hippocampal death (Kho et al., 2018). Lastly, PCA had neuroprotective effects in an animal model of TBI which shares pathology with neurodegenerative disease like ALS. Lee, S. H., et al. (2017) found that PCA injection once per day for 1-week post-TBI can preserve GSH and reduce neuronal cell death, oxidative stress, and neuroinflammation in a rat model of mild TBI induced by CCI (Lee, S. H., et al., 2017). To date, no clinical trials using human subjects have explored the effects of PCA as a treatment for neurodegenerative disease. However, based on the promising *in vitro* and *in vivo* data reporting PCA's ability to scavenge ROS/RNS, inhibit the production of pro-inflammatory cytokines, prevent pro-inflammatory pathways, and even prevent the aggregation of toxic protein aggregates, PCA should be explored as a therapeutic for ALS.

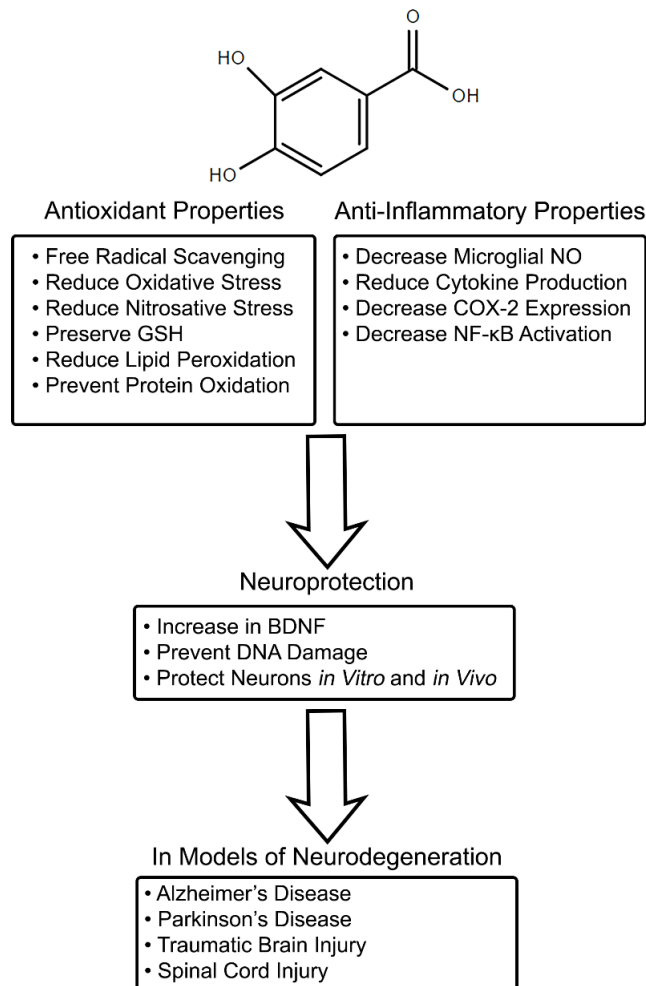


Figure 1.10 Antioxidant and Anti-Inflammatory Properties of Protocatechuic Acid in Models of Neurodegeneration. This figure summarizes *in vitro* and *in vivo* evidence of the antioxidant, anti-inflammatory, and neuroprotective properties of protocatechuic acid (PCA; structure shown). *In vitro*, PCA has been shown to scavenge superoxide, hydroxyl radicals, and ferric and cupric ions. Protocatechuic acid can also protect against loss of membrane potential, reactive oxygen species and nitric oxide (NO) generation, glutathione (GSH) depletion, and apoptosis. *In vitro*, PCA also has been studied for its anti-inflammatory properties and has been shown to reduce pro-inflammatory cytokine production, expression of cyclooxygenase-2 (COX-2), and nuclear factor-κB (NFκB) activation. *In vivo*, the antioxidant and anti-inflammatory effects of PCA have been tested in numerous models of neurotrauma and neurodegenerative disease. Protocatechuic acid has been shown to improve cognitive deficits, decrease levels of reactive oxygen and nitrogen species, pro-inflammatory cytokines, and COX-2 expression. Protocatechuic acid shows neuroprotection in these models through preservation of the blood brain barrier, GSH, and brain derived neurotrophic factor (BDNF).

1.8 The hSOD1^{G93A} Transgenic Mouse: A Preclinical Model of ALS to Explore the Potential Treatment Efficacy of PCA

Superoxide dismutase-1 was the first gene identified to be mutated in ALS in 1993. Today, greater than 170 mutations in SOD-1 have been identified, with the majority being missense mutations (Ghasemi & Brown, 2018). Mutations to SOD-1 are also observed in sporadic ALS cases that have no identified inheritance pattern and seem to contribute to pathology (Müller et al., 2022). As discussed in depth above, SOD-1 mutations may cause it to lose function or gain a toxic function, both of which contribute to ALS pathology. One of the most studied mutations in preclinical research is human mutant SOD-1 with a glycine to alanine substitution at position 93 (hSOD1^{G93A}). A mouse model of this mutation was created in 1994 and has been widely used and well-studied since (Gurney et al., 1994). Synofzik et al. (2010) analyzed the human phenotype of this mutation and reported it to be a highly homogenous phenotype that resembles that of sporadic ALS cases. In humans, this mutation leads to asymmetrical distal limb onset, upper and motor neuronal cell death, disease duration of 2-4 years following onset, and death due to respiratory failure (Synofzik et al., 2010). The hSOD1^{G93A} mouse model of ALS was chosen to study the therapeutic effect of PCA due to the expansive research done on the model for the past twenty years and due to reports of the mutation in humans matching the phenotype of the animal model.

1.8.1 Phenotype and Pathology of the hSOD1^{G93A} Mouse Model of ALS

As mentioned above, the hSOD1^{G93A} mouse model of ALS was created in 1994 by Gurney and colleagues (1994). Mice with abundant mutant hSOD1^{G93A} in the CNS displayed hind limb weakness, an inability to splay their hind legs when lifted by their

tails, impaired grooming, and thinning in their posterior around 3-4 months of age (Gurney et al., 1994). Gate abnormalities also began around this time and worsened rapidly until paralysis of one or both hind limbs around 5 months of age. Soon after, mice needed to be euthanized as the animal could no longer access food or water (Figure 1.11; Gurney et al., 1994). Pathological changes were also observed in this animal that mirrored that of ALS patients. Loss of cholinergic motor neurons, phosphorylated neurofilament proteins, and swollen axons were observed. Furthermore, researchers observed denervation of NMJs, aberrant axonal transport, and a severe loss of myelination, with the most drastic findings present in the spinal cord ventral horn (Gurney et al., 1994). The pathology observed in this initial model seems to be consistent across the model that maintains 25 copies of the mutant transgene, although other models have since been created that have fewer or more transgene copies resulting in a less or more progressive phenotype, respectively (Alexander et al., 2004; Deitch et al., 2014).

Following the initial report by Gurney et al. (1994) on the model, researchers have continued to characterize the pathology. As new findings in ALS pathology are observed, they are explored in this model. Furthermore, researchers have identified additional pathology not originally sought after in this model. For example, increased autophagy through mammalian target of rapamycin has been observed (Morimoto et al., 2007). Longitudinal MRI has been used in this model to identify motor nuclei neurodegeneration in brainstem, although this was not observed in the motor cortex even in the late stage. This finding may indicate that muscle damage occurs early in this model which may contribute to motor neuron death later in the disease (Marcuzzo et al., 2011). Sensory

neuropathies have also been identified in the dorsal spinal cord of this model (Guo, Y. S. et al., 2009). Furthermore, protein aggregates of SOD-1 and mislocalization of TDP-43 are observed in spinal cord (Shan et al., 2009; Zeineddine et al., 2017).

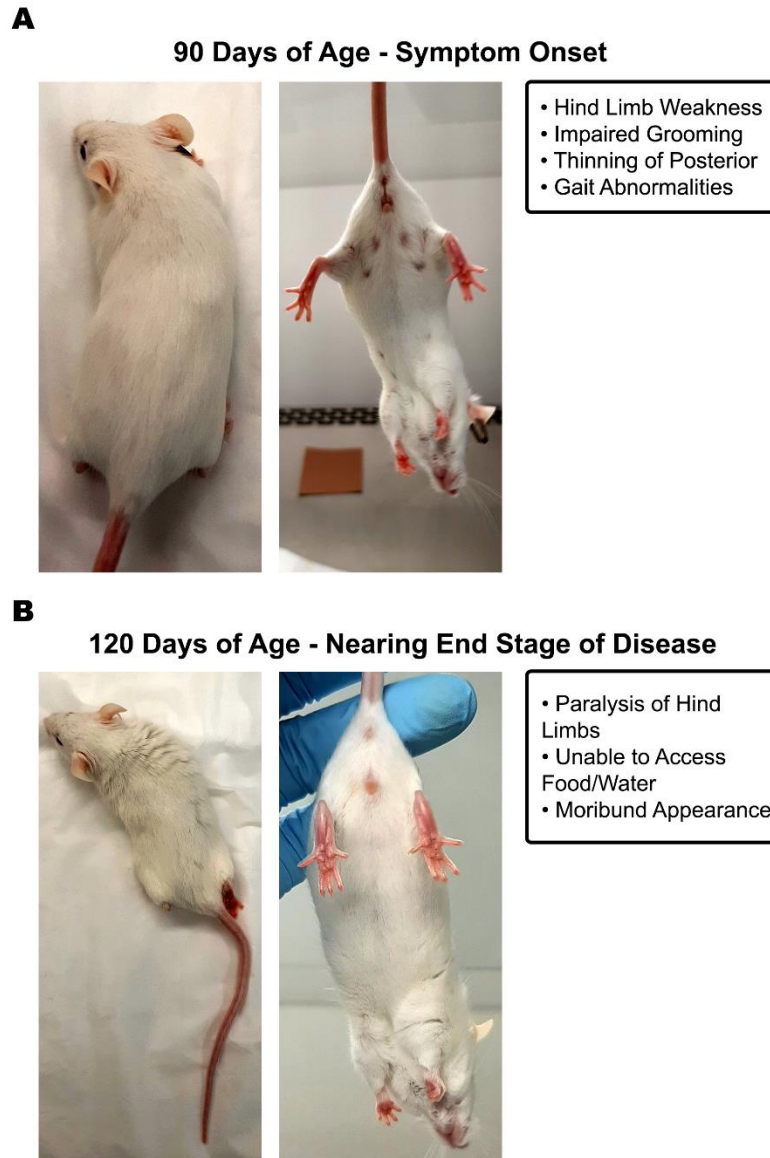


Figure 1.11 The hSOD1^{G93A} Mouse Model of ALS Disease Phenotype. One of the most studied mutations in preclinical research is human mutant superoxide dismutase-1 with a glycine to alanine substitution at position 93 (hSOD1^{G93A}). (A) Mice with abundant mutant hSOD1^{G93A} in the CNS display hind limb weakness, an inability to splay their hind legs when lifted by their tails, impaired grooming, and thinning in their posterior around 90 days of age. Gate abnormalities also begin around this time and worsen rapidly until (B) paralysis of one or both hind limbs around 125 days of age. Mice are euthanized shortly after they become unable to access food or water. Pathological changes observed in this model mirror that of ALS patients and include loss of cholinergic motor neurons, phosphorylated neurofilament proteins, and swollen axons. Furthermore, researchers have reported denervation of neuromuscular junctions, aberrant axonal transport, and a severe loss of myelination present in the spinal cord ventral horn.

1.8.2 Neuroinflammation in the hSOD1^{G93A} Mouse Model of ALS

A lot of research has focused on characterizing neuroinflammation in this model. The hSOD1^{G93A} model of ALS has a robust pro-inflammatory phenotype with pro-inflammatory cytokines TNF- α , IL-1 α , and IL-1 β increasing from 80 days to 120 days with corresponding increased expression of caspases at 120 days, close to end-stage of disease (Hensley et al., 2002). It seems that the inflammatory response occurs early prior to disease onset as Yoshihara et al. (2002) reported upregulation of TNF- α and caspase activation as early as 77 days of age which is typically a pre-symptomatic age (Yoshihara et al., 2002). Microgliosis is also observed in this model as microglia express increased levels of monocyte chemoattractant protein-1 *in vivo* and also have a heightened response to LPS when cultured (Sargsyan et al., 2009). Lastly, genetic background and sex-specific phenotypic differences have been characterized in this model (Heiman-Patterson et al., 2005).

1.8.3 Preclinical Study of PCA in the hSOD1^{G93A} Mouse Model of ALS

Due to the abundant research on the hSOD1^{G93A} mouse model of ALS, this model, bred on an FVB/NJ background, was chosen to explore the therapeutic benefit of PCA. Mice bred on this background experience disease onset around 90 days of age and survive an average of 128.9 days (Winter et al., 2018). We explore two doses of PCA, 50mg/kg/day and 100mg/kg/day, beginning at disease onset, on survival, motor function, grip strength, neuroinflammation, neuroprotection, and preservation of NMJs in this mouse model of ALS. This preclinical study is described in detail in Chapter Four (Koza et al., 2020).

**CHAPTER TWO: SIGNIFICANT AND SEX-SPECIFIC ANTIOXIDANT
BIOMARKER DEPLETION IN HISTORY OF MILD TRAUMATIC BRAIN
INJURY PATIENTS**

2.1 Abstract

Individuals with a history of mild traumatic brain injury (mTBI) are at risk for prolonged neurological effects and brain pathology, suggesting that intrinsic neuroprotective mechanisms, such as the endogenous antioxidant reservoir, may be depleted long-term. Here, we retrospectively analyzed symptoms and blood antioxidants in patients with a history of mTBI who presented to Resilience Code, a sports medicine clinic in Denver, Colorado. Significant decreases ($p<0.05$) in alpha-tocopherol, selenium, linoleic acid, taurine, docosahexaenoic acid, and total omega-3 were measured in the total mTBI population ($n=88$) versus controls ($n=82$). Male mTBI patients ($n=62$) had additional significant/trending ($p<0.10$) antioxidant depletion, whereas only a few significant/trending reductions were measured in females ($n=26$), versus sex-matched controls ($n=42$, $n=40$, respectively). Patients with mTBI reported significantly worsened emotional, energy, head, and cognitive symptoms (with sex-specific differences). Qualitative analyses suggested that multiple ($n=40$) and chronic ($n=32$) mTBI patients had worsened symptoms versus single ($n=27$) or acute-subchronic ($n=14$) mTBI patients, respectively. These results demonstrate that sex-specific antioxidant depletions persist in patients with a history of mTBI and these deficits are associated with worsened

symptomology. In conclusion, supplementation with specific antioxidants, like polyunsaturated fatty acids, may diminish symptom severity in patients suffering from the chronic neurological effects of mTBI.

2.2 Introduction

Mild traumatic brain injury (i.e., concussion; mTBI) is the most commonly occurring severity of TBI. Of the 69 million TBIs that occur each year worldwide, 80% are mTBIs (Dewan et al., 2018). Primary injury, such as disruption of cellular integrity, calcium influx, edema, and diffuse axonal injury, that occur immediately following the impact, may not be severe with mTBI (Sulhan et al., 2020). However, secondary injury pathology such as neuroinflammation, oxidative stress, blood-brain barrier (BBB) disruption, and excitotoxicity can lead to neuronal cell death following mTBI and may persist for weeks to months following injury (Bramlett & Dietrich, 2015; Ladak et al., 2019; Mckee & Daneshvar, 2015; Wang, K. K., et al., 2013).

There is an increased risk of sustaining a future mTBI in high-risk individuals, such as athletes, who already have a history of mTBI (Guskiewicz et al., 2003). Subsequent mTBIs, termed repetitive mTBI (rmTBI), can exacerbate and prolong secondary injury (Bailes et al., 2014; Bailes et al., 2013). Behavioral and cognitive symptoms have been reported in human subjects following mTBI and rmTBI, however, duration of symptoms vary depending on the individual (Abbas et al., 2015; Levin & Diaz-Arrastia, 2015; Miller et al., 2013). Furthermore, although symptoms may subside shortly following injury and the individual has returned to normal routine, underlying secondary injury pathology can persist.

Long-term secondary injury pathology from a single mTBI and especially from rmTBI has been identified as a risk factor for developing neurodegenerative disease later in life such as Alzheimer's disease (AD), Parkinson's disease, and chronic traumatic encephalopathy (CTE). Retired national football league athletes have a 3-fold increased risk of dying from AD and amyotrophic lateral sclerosis (ALS) compared to non-athletes (Lehman et al., 2012). Cerebral atrophy, tau pathology, and proteinopathies, which mirror pathology present in neurodegenerative disease, have also been observed in retired athletes with rmTBI (Gavett et al., 2011; Lolekha et al., 2010; McKee et al., 2009). More research should be done to fully understand the relationship between mTBI and the risk for developing neurodegenerative disease.

Neuroinflammation and oxidative stress are also observed following mTBI and especially in those with a history of mTBI. Prolonged and severe neuroinflammation and excitotoxicity in response to mTBI is well studied and results in the overproduction of reactive oxygen species (ROS), nitrogen species (RNS), and lipid peroxides (Cornelius et al., 2013, Abdul-Muneer et al., 2015). This leads to mitochondria dysfunction, DNA damage, and ultimately neuronal cell death. In response, the endogenous antioxidant system becomes strained resulting in antioxidant depletion (Morris, G., et al., 2019). Many studies have explored using antioxidants, such as n-acetylcysteine or alpha-tocopherol, to treat TBI in animal models and a few in clinical trials (Wu, A., et al., 2010; Niu et al., 2018; Maynard et al., 2019; Ismail et al., 2020; Kyyriäinen et al., 2021). Resulting antioxidant depletion likely contributes to lasting symptoms observed in

patients with a history of mTBI, however, the few clinical studies focusing on antioxidant treatments for mTBI do not measure symptom resolution.

Few studies to date have measured antioxidant depletion in patients with a history of mTBI. Furthermore, no studies to date explore sex-specific differences in antioxidant depletion in patients with a history of mTBI. We hypothesized that patients with a history of mTBI show significant antioxidant depletion and worsened symptoms, with sex-specific differences, when compared to patients with no history of mTBI. We aimed to test this hypothesis and fill a gap in the literature by retrospectively studying antioxidant levels in blood from male and female patients with a history of mTBI that presented to Resilience Code, a sports medicine clinic in Denver, CO. Antioxidant biomarkers were measured in serum, plasma, red blood cells (RBCs), white blood cells (WBCs), and whole blood from total, male, and female patients with a history mTBI and compared to patients with no history of mTBI. We also analyzed self-reported emotional, energy, head, and cognitive symptoms in these patients. Furthermore, we performed a qualitative analysis to see if number of mTBIs sustained or time since most recent mTBI influenced symptom severity and frequency. Lastly, we compared symptomology in history of mTBI patients with less versus more severe polyunsaturated fatty acid (PUFA) biomarker depletion. These data, although preliminary, provide insight into sex-specific differences in antioxidant biomarker depletion and symptomology associated with a history of mTBI. These data also tell us how symptom severity and frequency differ based on number of mTBIs sustained and time since a patient's last mTBI. Finally, these data support further

exploration of antioxidant treatments, such as PUFA supplementation, to ameliorate chronic neurological effects of mTBI.

2.3 Methods

2.3.1 Participant Population

Data from 170 patients, admitted to a sports medicine clinic between 11/2017-9/2020, (Resilience Code; Englewood, Colorado) were retrospectively analyzed for this study. Patients were evaluated by a board-certified physician who collected demographic information and medical history. Patients also completed a medical symptom questionnaire (MSQ) and provided blood for analysis of biomarkers (detailed below) prior to the administration of any treatment. Patients with active cancer at the time of visit were excluded. A total of 88 patients, including 62 males and 26 females, having at least one TBI in their lifetime, were considered to have a history of TBI based on patient reporting and medical history. The board-certified physician confirmed all history of TBI patients as having TBIs of mild severity. The 88 patients with a history of mTBI were further categorized by number of mTBIs sustained throughout their lifetime and time elapsed since their most recent mTBI to the clinic visit. A total of 27 patients reported sustaining a single mTBI, 40 sustained multiple mTBIs, and 21 patients did not report this information and were not included in analyses of these populations. A patient was included in the multiple mTBI group if they sustained more than one mTBI throughout their lifetime, regardless of time elapsed between mTBIs. Of the 88 history of mTBI patients, 14 patients presented to the clinic within 1 year of their most recent mTBI, termed as acute-subchronic mTBI patients, and 32 patients presented to the clinic greater

than 1 year since their most recent TBI, termed chronic mTBI patients. A total of 42 patients did not report this information and were not included in analyses of these populations. Of the 170 total patients, 82 patients, consisting of 42 males and 40 females, never reported having a mTBI in their lifetime and were considered to have no history of mTBI. Demographic information for these populations is displayed in Tables 2.1 and 2.2. A flow diagram of patients and analyses performed are displayed in Supplementary Figure 1.

2.3.3 Blood collection, Processing, and Analysis

Blood samples were obtained from all 170 patients. However, n values for each biomarker analyzed in blood vary and are reported for each individual biomarker as blood from each patient was not analyzed for every biomarker. Blood samples were obtained by a certified phlebotomist at Resilience Code and were processed according to manufacturer's protocols to isolate serum, plasma, RBCs, or WBCs. Blood was stored at Resilience Code at 4°C for no longer than 8 hours prior to being shipped to Vibrant America Clinical Labs (San Carlos, CA) or Genova Diagnostics (Asheville, North Carolina) for analysis of biomarkers in serum, plasma, RBC, WBCs, or whole blood.

2.3.4 Medical Symptom Questionnaire

The presence, frequency, and severity of symptoms at the time of the clinic visit were gathered using a 71-item electronic MSQ that took an average of 15 minutes to complete. A modified MSQ was used as previously described (Lukaszuk et al., 2018). Of the total 170 patients, 139 patients completed the MSQ. A total of 69 of the 88 patients with a history of TBI, consisting of 45 males and 24 females, completed the MSQ. A total of 64

out of 82 patients without a history of TBI, including 32 males and 32 females, completed the MSQ. Some patients did not complete every question in the MSQ so n values for individual symptoms vary and are reported. The presence of specific symptoms and symptom severity were reported on a 4-point Likert scale with 0 indicating never or almost never having the specific symptom, 1 being occasionally having the symptom but the effect is not severe, and 4 being frequently having the symptom and the effect is severe. Symptom categories pertain to weight, skin, nose, mouth, cognition, chest, joints, heart, head, eyes, energy, emotions, ears, digestion, and other. Each individual symptom falls under one of these 15 categories and a total score for each symptom category is calculated for each patient by adding up the scores for the individual symptoms under the category. A total symptom score is also calculated for each patient by adding up all scores for each symptom category. A higher symptom category or total symptom score indicates increased symptom severity and frequency of symptoms. A total symptom score of 0 is the lowest score possible and a score of 284 is the highest score possible.

2.3.5 Statistics

All data was analyzed using SPSS Statistical Software (IBM Corp., Version 25, Armonk, NY) and graphs and heatmap visualizations were created in using R Studio (R Studio Team [2021]. RStudio: Integrated Development for R. RStudio, Inc., Boston, MA) for Windows. Continuous data in tables and text are reported as mean \pm standard error of the mean (SEM), unless stated otherwise. Antioxidant blood biomarker and MSQ data for total, male, and female patients without versus with a history of mTBI and for total

history of mTBI patients with levels of high versus low PUFA biomarkers are displayed graphically as boxplots using R Studio ggplot2 package and geom_boxplot function (Wickham, 2016). Boxplot components are displayed as follows: lower whisker = smallest observation greater than or equal to lower hinge-1.5 * interquartile range (IQR), lower hinge = 25% quantile, middle line = median at 50% quantile, diamond = mean, upper hinge = 75% quantile, upper whisker = largest observation less than or equal to upper hinge+1.5 * IQR, outlying points = data beyond end of upper or lower whiskers (McGill et al., 1978). Due to the clinical nature of the data, which was mostly non-normally distributed with unequal variances, as analyzed by Shapiro-Wilk and Levene's tests, respectively, nonparametric statistical tests were used to analyze all data (detailed below). Only one value for taurine in plasma was excluded from analysis from a female patient with a history of mTBI as this value was an extreme outlier. No other values were excluded. Statistical differences were considered significant if $p < 0.05$ and trending significant if $p < 0.10$. All de-identified data was compiled and checked by at least two separate researchers. Data was also analyzed and checked by two separate researchers.

2.3.5.1 Demographic Analysis of Total, Male, and Female Patients Without Versus with a History of mTBI and in Patients with a History of mTBI

The Mann Whitney U-Test was used to analyze differences in age between total, male, and female patients without versus with a history of mTBI and in patients. The association of history of mTBI or reported cause of most recent mTBI and sex was analyzed using the Pearson Chi Square Test.

2.3.5.2 Analysis of Antioxidant Blood Biomarker Levels and MSQ Data from Total, Male, and Female Patients Without Versus with a History of mTBI

Blood biomarker levels and MSQ symptoms pertaining to emotional state, energy, head, and cognition in total patients without a history of mTBI versus with a history of mTBI, male patients without a history of mTBI versus with a history of mTBI, female patients without a history of mTBI versus with a history of mTBI were analyzed using the nonparametric Mann Whitney U-Test.

2.3.5.3 Heatmap Analysis of MSQ Data from Single, Multiple, Acute, Chronic, and No History of mTBI Patients.

N values were too low for quantitative analysis of blood biomarkers levels and MSQ data in patients with a single mTBI versus a history of multiple mTBI or between patients with acute- subchronic mTBI versus chronic mTBI. Therefore, differences in MSQ scores between these groups pertaining to emotional state, energy, head, and cognition were visualized using a heatmap using R Studio ggplot2 package and geom_tile function (Wickham, 2016). Briefly, MSQ scores were converted to z scores to allow for normalization of individual symptom scores and symptom category scores, which exhibit different scoring ranges, for patients with single mTBI, multiple mTBI, and no history of mTBI. This was also done for patients with acute-subchronic mTBI, chronic mTBI, and no history of mTBI to allow for symptom severity comparison between these groupings. The z score average was calculated for each individual symptom/symptom total category score. An increased z score corresponds to an increased symptom score indicating a severe and frequent symptom. Each row represents an individual symptom/symptom

category total, and each column represents the average score for the different populations. Rows and columns were not clustered. The lightest grey shade corresponds to a z score of -0.30 and the darkest shade corresponds to 0.40 for single, multiple, no mTBI patients and to -0.30 and 0.80, respectively, for no, acute, and chronic, mTBI patients.

2.3.5.4 Analysis of MSQ Data from Patients with a History of mTBI with High Versus Low Levels of PUFA Biomarkers

Blood biomarker levels for alpha-linolenic acid and linoleic acid in plasma and total omega-6, total omega-3, and docosahexaenoic acid in RBCs, termed a PUFA biomarker grouping, were divided into quartiles for all history of mTBI patients. A score of 1-4, corresponding to the quartile the patient's blood biomarker level was in (1 being the lowest quartile and 4 being the highest quartile), was given for each biomarker for each history of mTBI patient who had measurements for all PUFA biomarkers listed above. Quartile scores for the PUFA biomarkers were added for each patient and the patient was given a total PUFA score which had a possible range of 5-19. Patients with high versus low PUFA scores were divided into two groups based on a median split (median=12). Patients with a score of 11 or less (n=20; range = 5-11) were considered to have a low PUFA score (I.e., PUFA depletion) and patients with a score of 12 or more (n=23; range=12-19) were considered to have a high PUFA score. The PUFA biomarker score for patients with low versus high PUFA scores were significantly different as analyzed the Mann Whitney U-Test. Medical symptom questionnaire scores in total history of mTBI patients with high versus PUFAs were analyzed by the Mann Whitney U-Test.

2.3.6 Study Approval

All patients granted Resilience Code specific, written authorization to disclose their medical records for research purposes. This study was retrospective and all protected health information was de-identified prior to compilation of data and analysis. Each patient was assigned a random global unified identifier which was used on all reports and forms associated with the study to maintain anonymity. Therefore, this study was determined to be exempt from The University of Denver's Institutional Review Board.

2.4 Results

2.4.1 Patient population

Antioxidant biomarker levels measured by either Vibrant America Clinical Labs or Genova Diagnostics in whole blood, or components such as serum, plasma, RBCs, or WBCs, along with demographic information and medical history, were compiled from a total of 170 (n=104 males, n=66 females) patients who presented to Resilience Code, a specialized sports medicine clinic in Denver, CO. Blood and MSQ responses, which inquired about a variety of symptoms and their severities and frequencies, were taken at initial clinic visit prior to treatment. A total of 88 patients reported sustaining at least one mTBI in their lifetime and were considered to have a history of mTBI whereas 82 patients never reported having a mTBI and had no history of mTBI.

The average age of patients with mTBI was significantly lower ((38.95 ± 1.81) y, $p=0.003$) than those without a history of mTBI ((46.16 ± 1.85) y). Male patients with a history of mTBI were driving this difference as they had a significantly lower average age ((37.55 ± 2.09) y, $n=62$, $p=0.001$) than males without mTBI ((48.62 ± 2.66) y, $n=42$;

Table 2.1). Average age was not significantly different between female patients with ((42.31±3.50) y, n=26, $p=0.694$) versus without a history of mTBI ((43.58±2.55) y, n=40; Table 2.1). Research has shown that antioxidant deficiency occurs in individuals aged 65 years and older (Kozakiewicz et al., 2019; Muralidharan et al., 2017). Populations with and without a history of mTBI have an average age that is well below 65 years. Furthermore, increased oxidative stress and inflammation, which could result in antioxidant depletion, occur following TBI (Abdul-Muneer et al., 2015; Cornelius et al., 2013). Our history of mTBI population is significantly younger than the population without mTBI and we would expect these younger patients to have more robust antioxidant systems. Findings of antioxidant depletion in these younger patients in response to mTBI would be even more convincing. Therefore, age was not considered to be a confounding factor in the results to follow.

Patients with a history of mTBI were further divided into populations based on reported number of mTBIs sustained in their lifetime and time elapsed since their most recent mTBI (Table 2.2). Forty-six (n=46) history of mTBI patients, including 29 males and 17 females, reported the cause of their most recent mTBI as sport, fall, car accident, or blunt injury and a significant association was found between sex and the cause of most recent mTBI ($p<0.000$; Table 2.2). A flow diagram of patients and analyses performed are displayed in Supplementary Figure 1.

Table 2.1 Age and Sex of Patients Without and with a History of mTBI. Age is displayed for total (n=170), male, and female patients without versus with a history of mTBI. Age is reported in years as mean \pm SEM (range). The Mann Whitney U-Test was used to analyze continuous data and Pearson Chi Square Test was used to analyze categorical data differences between groups. Significant *p* values (*p*<0.05) are displayed as bolded text.

	Patients without history of mTBI (n = 82)	Patients with history of mTBI (n = 88)	<i>p</i>-value
Age	46.16 \pm 1.85 (17 - 83)	38.95 \pm 1.81 (16 - 80)	0.003
Males	n = 42	n = 62	0.010
Females	n = 40	n = 26	
Male age	48.62 \pm 2.66 (24 - 83)	37.55 \pm 2.09 (16 - 80)	0.001
Female age	43.58 \pm 2.55 (17 - 77)	42.31 \pm 3.50 (19 - 78)	0.694

Table 2.2 Age, Sex, and Cause of Most Recent mTBI for Patients with a History of mTBI. Age is displayed for mTBI patient populations. Acute-subchronic mTBI patients presented to the clinic ≤ 1 year and chronic mTBI patients presented to the clinic > 1 year since their most recent mTBI. Age is reported in years as mean \pm SEM (range). The Mann Whitney U-Test was used to analyze continuous data and Pearson Chi Square Test was used to analyze categorical data differences between groups. Significant p values ($p < 0.05$) are displayed as bolded text.

	Patients with history of mTBI (n = 88)	<i>p</i>-value
Male age (n = 62)	37.55 \pm 2.09 (16 - 80)	0.247
Female age (n = 26)	42.31 \pm 3.50 (19 - 78)	
Cause of most recent mTBI (Both sexes; n = 88) (Not reported; n = 42)	Sport: n = 31 Fall: n = 9 Car accident: n = 3 Blunt injury: n = 3	
Males (n = 62) (Not reported; n = 33)	Sport: n = 27 Fall: n = 1 Car accident: n = 0 Blunt injury: n = 1	< 0.000
Females (n = 26) (Not reported; n = 9)	Sport: n = 4 Fall: n = 8 Car accident: n = 3 Blunt injury: n = 2	
Patients single mTBI	n = 27	
Age (Both sexes)	41.26 \pm 3.20 (21 - 72)	
Male age (n = 18)	38.94 \pm 3.98 (21 - 72)	0.275
Female age (n = 9)	45.89 \pm 5.32 (22 - 70)	
Patients with multiple mTBI	n = 40	
Age (Both sexes)	39.78 \pm 2.84 (16 - 79)	
Male age (n = 25)	38.60 \pm 3.43 (16 - 79)	0.699
Female age (n = 15)	41.73 \pm 5.06 (19 - 78)	
Patients with acute-subchronic mTBI	n = 14	
Age (Both sexes)	30.21 \pm 3.97 (19 - 78)	
Male age (n = 7)	26.00 \pm 1.54 (20 - 31)	0.805
Female age (n = 7)	34.43 \pm 7.75 (19 - 78)	
Patients with chronic mTBI	n = 32	
Age (Both sexes)	42.16 \pm 2.75 (21 - 70)	
Male age (n = 18)	36.11 \pm 3.30 (21 - 67)	0.009
Female age (n = 14)	49.93 \pm 3.81 (24 - 70)	

2.4.2 Sex-Specific Antioxidant Depletion in Patients with Versus Without a History of mTBI.

Animal studies indicate that secondary injury resulting from mTBI may persist for months or longer following injury (Chaban et al., 2020; Sun et al., 2019). Therefore, we hypothesized that prolonged oxidative stress and inflammation may result in depletion of the endogenous antioxidant system. We aimed to fill a gap in the literature and analyzed differences in antioxidant biomarker levels between total patients with and without a history of mTBI. Biomarker levels that were not significant or trending significantly different between these patients are displayed in Supplementary Table 1. All biomarkers were not measured in every patient, therefore, sample sizes for individual biomarkers vary and are reported.

Patients with a history of mTBI had significantly lower levels of alpha-tocopherol ((13.30±0.47) mg/L, n=87, $p=0.004$) and selenium ((137.32±2.80) ng/mL, $p=0.033$, n=48) in serum compared to patients without mTBI (alpha-tocopherol; (15.99±0.76) mg/L, n=80; selenium; (155.98±7.66) ng/mL, n=37; Figure 2.1A, 2.1D). Patients with a history of mTBI also had significantly lower linoleic acid ((1125.74±26.08) µmol/L, n=88, $p=0.003$) and taurine ((43.69±1.72) µmol/L, n=86, $p<0.000$) in plasma when compared to patients without mTBI (linoleic acid; (1268.83±34.37) µmol/L, n=81; taurine; (52.68±2.47) µmol/L, n=77; Figure 2.2B, 2.2C). Lastly, patients with a history of mTBI had significant decreases in docosahexaenoic acid ((6.47±0.30) %, n=48, $p=0.042$) and total omega-3 ((8.13±0.36) %, n=48, $p=0.038$) in RBCs compared to patients without

mTBI (docosahexaenoic acid; (7.51 ± 0.33) %, $n=37$; total omega-3; (9.46 ± 0.44) %, $n=37$; Figure 2.3A, 2.3B).

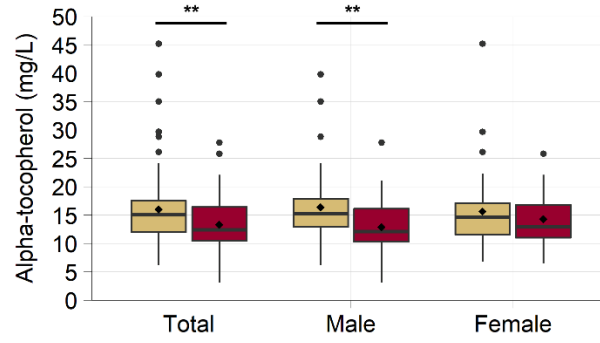
Increased oxidative stress markers are reported in healthy adult males compared to females (Ide et al., 2002; Kander et al., 2017). Furthermore, females exhibit higher antioxidant capacity than males which may be due to sex hormones (Borrás et al., 2003; Demirbag et al., 2005; Vina et al., 2011). Males and females may have dissimilar antioxidant capacities in responses to mTBI secondary pathology. To explore this, antioxidant biomarkers were compared between males and females with versus without a history of mTBI.

Males with a history of mTBI displayed significantly or trending significantly decreased alpha-tocopherol ((12.88 ± 0.54) mg/L, $n=61$, $p=0.002$) and selenium ((134.00 ± 2.92) ng/mL, $n=30$, $p=0.072$) in serum compared to males without mTBI (alpha-tocopherol; (16.36 ± 1.05) mg/L, $n=41$; selenium; (145.42 ± 4.87) ng/mL, $n=16$; Figure 2.1A, 2.1D). Males with a history of mTBI also had significant or trending significant decreases in plasma biomarkers such as linoleic acid ((1114.27 ± 30.91) $\mu\text{mol/L}$, $n=62$, $p=0.072$) and taurine ((43.47 ± 2.24) $\mu\text{mol/L}$, $n=62$, $p=0.005$) when compared to males without a history of mTBI (linoleic acid; (1244.27 ± 53.49) $\mu\text{mol/L}$, $n=41$; taurine; (52.73 ± 4.22) $\mu\text{mol/L}$, $n=40$; Figure 2.2B, 2.2C). Lastly, males with a history of mTBI had significantly or trending significantly depleted levels of docosahexaenoic acid ((6.27 ± 0.39) %, $n=30$, $p=0.068$) and total omega-3 ((7.83 ± 0.43) %, $n=30$, $p=0.046$) when compared to males without mTBI (docosahexaenoic acid; (7.58 ± 0.46) %, $n=16$; total omega-3; (9.66 ± 0.61) %, $n=16$; Figure 2.3A and 2.3B). All

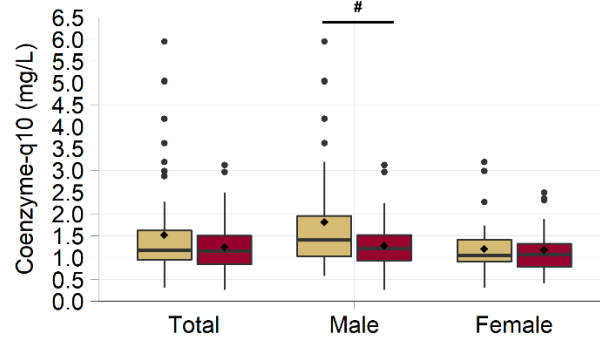
these biomarkers were significantly decreased in total patients with versus without a history of mTBI. Interestingly, male patients with a history of mTBI also had additional significant or trending significant decreases in coenzyme-q10 ((1.27 ± 0.07) mg/L, $n=61$, $p=0.051$) and cysteine ((23.25 ± 2.31) nmol/mL, $n=30$, $p=0.094$) in serum, alpha-linolenic acid ((27.56 ± 1.38) μ mol/L, $n=62$, $p=0.088$) in plasma, and total omega-6 ((23.35 ± 1.12) %, $n=30$, $p=0.035$) in RBCs when compared to males without mTBI (coenzyme-q10; (1.81 ± 0.20) mg/L, $n=41$; cysteine; (27.56 ± 2.81) nmol/mL, $n=16$; alpha-linolenic acid; (33.07 ± 2.46) μ mol/L, $n=41$; total omega-6; (27.28 ± 1.26) %, $n=16$; Figures 2.1B, 2.1C, 2.2A, and 2.3C).

Female patients with a history of mTBI only had significant or trending significant decreases in linoleic acid ((1153.08 ± 49.09) μ mol/L, $n=26$, $p=0.053$) and taurine ((44.25 ± 2.24) μ mol/L, $n=24$, $p=0.017$) in plasma compared to females without mTBI (linoleic acid; (1294.00 ± 43.21) μ mol/L, $n=40$; taurine; (52.62 ± 2.43) μ mol/L, $n=37$; Figure 2.2B, 2.2C).

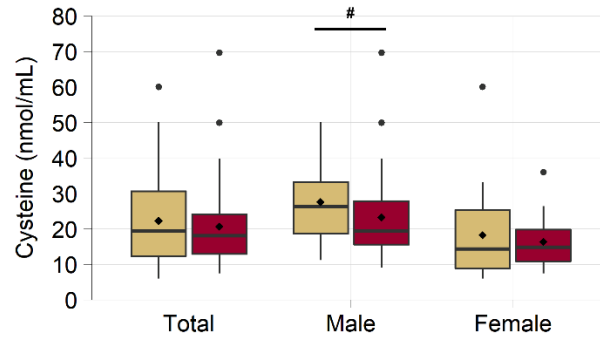
A



B



C



D

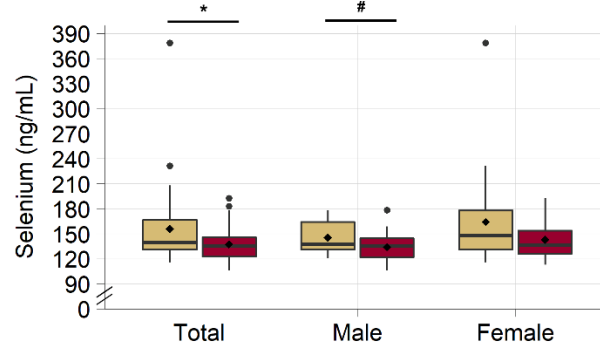
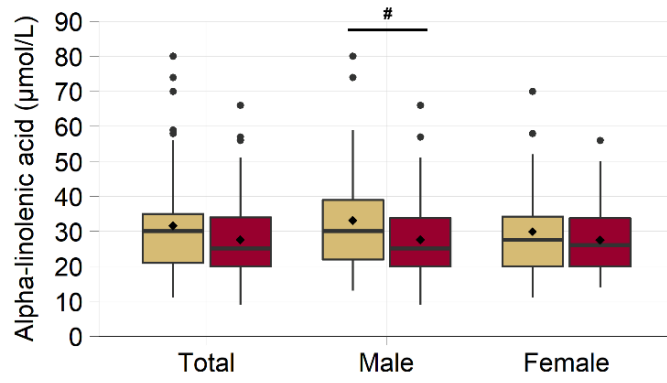
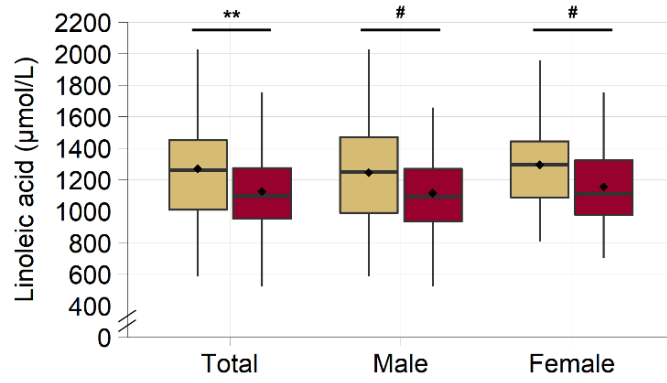


Figure 2.1 Significantly or Trending Significantly Reduced Levels of Serum Antioxidant Biomarkers in Total, Male, and Female Patients Without Versus with a History of mTBI. In each graph, the gold plot represents populations without a history of mTBI and the crimson plot represents populations with a history of mTBI. **(A)** Alpha-tocopherol levels in serum for total patients without (n=80) versus with a history of mTBI (n=87), male patients without (n=41) versus with history of mTBI (n = 61), and female patients without (n = 39) versus with a history of mTBI (n = 26). **(B)** Coenzyme-q10 levels in serum for total patients without (n=80) versus with history of mTBI (n=87), male patients without (n=41) versus with history of mTBI (n=61), and female patients without (n=39) versus with history of mTBI (n=26). **(C)** Cysteine levels in serum for total patients without (n=37) versus with history of mTBI (n=48), male patients without (n=16) versus with history of mTBI (n=30), and female patients without (n=21) versus with history of mTBI (n=18). **(D)** Selenium levels in serum for total patients without (n=37) versus with history of mTBI (n=48), male patients without (n=16) versus with history of mTBI (n=30), and female patients without (n=21) versus with history of mTBI (n=18). Boxplots represent the minimum, maximum, median, mean (diamond symbol), first/third quantile, and outlying values (\leq/\geq lower/upper hinge +1.5* interquartile range). Statistical differences are analyzed by the Mann Whitney U-Test. # indicates $p<0.10$, * indicates $p<0.05$, and ** indicates $p<0.01$.

A



B



C

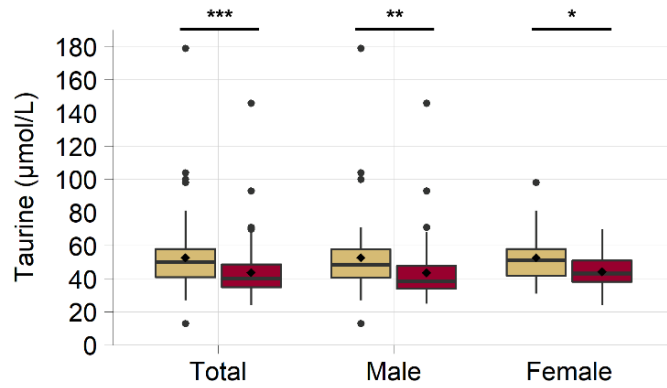


Figure 2.2 Significantly or Trending Significantly Reduced Levels of Plasma Antioxidant Biomarkers in Total, Male, and Female Patients Without Versus with a History of mTBI. In each graph, the gold plot represents populations without a history of mTBI and the crimson plot represents populations with a history of mTBI. **(A)** Alpha-linolenic levels in plasma for total patients without (n=81) versus with history of mTBI (n=88), male patients without (n=41) versus with history of mTBI (n=62), and female patients without (n=40) versus with history of mTBI (n=26). **(B)** Linoleic acid levels in plasma for total patients without (n=81) versus with history of mTBI (n=88), male patients without (n=41) versus with history of mTBI (n=62), and female patients without (n=40) versus with history of mTBI (n=26). **(C)** Taurine levels in plasma for total patients without (n=77) versus with history of mTBI (n=86), male patients without (n=40) versus with history of mTBI (n=62), and female patients without (n=37) versus with history of mTBI (n=24). Boxplots represent the minimum, maximum, median, mean (diamond symbol), first/third quantile, and outlying values (\leq/\geq lower/upper hinge +1.5* interquartile range). Statistical differences are analyzed by the Mann Whitney U-Test. # indicates $p<0.10$, * indicates $p<0.05$, ** indicates $p<0.01$, and *** indicates $p<0.001$.

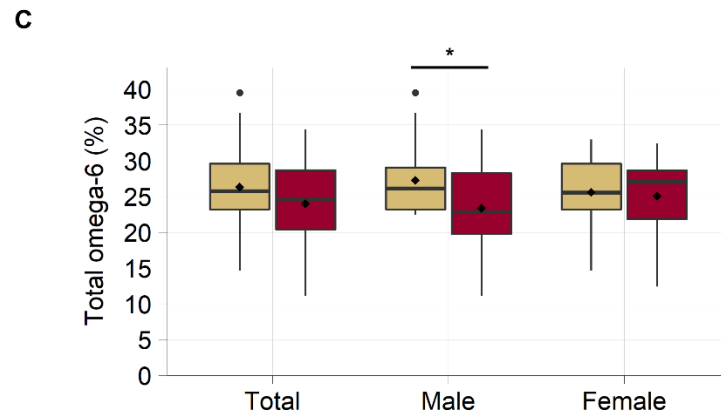
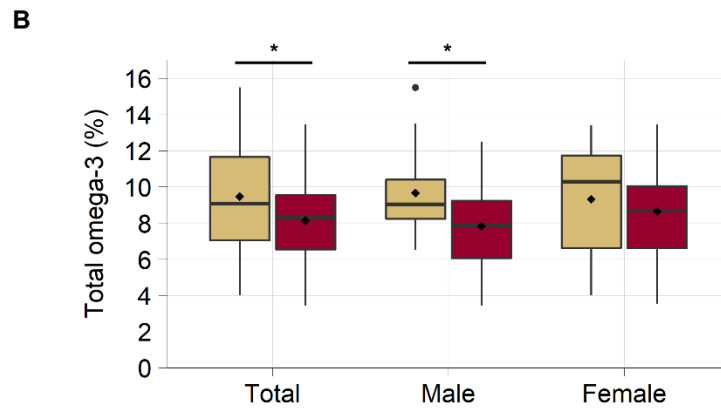
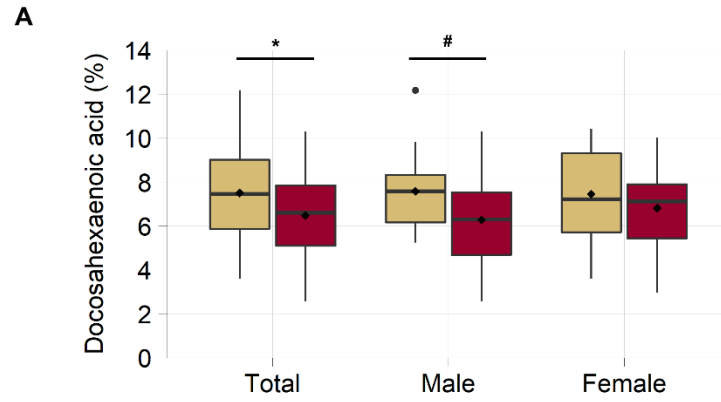


Figure 2.3 Significantly or Trending Significantly Reduced Levels of RBC Antioxidant Biomarkers in Total, Male, and Female Patients Without Versus with a History of mTBI. In each graph, the gold plot represents populations without a history of mTBI and the crimson plot represents populations with a history of mTBI. **(A)** Docosahexaenoic acid levels in RBCs for total patients without (n=37) versus with history of mTBI (n=48), male patients without (n=16) versus with history of mTBI (n=30), and female patients without (n=21) versus with history of mTBI (n=18). **(B)** Total omega-3 levels in RBCs for total patients without (n=37) versus with history of mTBI (n=48), male patients without (n=16) versus with history of mTBI (n=30), and female patients without (n=21) versus with history of mTBI (n=18). **(C)** Total omega-6 levels in RBCs for total patients without (n=37) versus with history of mTBI (n=48), male patients without (n=16) versus with history of mTBI (n=30), and female patients without (n=21) versus with history of mTBI (n=18). Boxplots represent the minimum, maximum, median, mean (diamond symbol), first/third quantile, and outlying values (\leq/\geq lower/upper hinge +1.5* interquartile range). Statistical differences are analyzed by the Mann Whitney U-Test. # indicates $p<0.10$ and * indicates $p<0.05$.

2.4.3 Sex-Specific Differences in Emotional, Energy, Head, and Cognitive Symptom Symptomology in Patients with Versus Without a History of mTBI.

Neuropsychological, emotional, and cognitive symptoms have been shown to persist for months to years following mTBI for some individuals (Cooksley et al., 2018, Theadom et al., 2018). The majority of our mTBI patient population presented to the clinic with persisting symptoms which were self-reported using the MSQ. We analyzed emotional, energy, head, and cognitive symptoms in patients with versus without a history of mTBI. Some patients did not complete the MSQ or did not answer every question so n values for individual questions and scores vary and are reported.

Patients with a history of mTBI had a trending significantly greater total symptom score (54.81 ± 3.87 , $n=69$, $p=0.069$) when compared to patients without mTBI (45.48 ± 3.78 , $n=64$; data not shown). Total patients with a history of mTBI had a significantly increased emotions total score (5.29 ± 0.49 , $n=69$, $p=0.016$) when compared to patients without mTBI (3.58 ± 0.38 , $n=64$; Figure 2.4A). Significantly increased emotional symptoms included anxiety/fear (1.65 ± 0.17 , $n=69$, $p=0.049$), depression (1.30 ± 0.16 , $n=69$, $p=0.024$), and mood swings (1.20 ± 0.13 , $n=69$, $p=0.019$) when compared to patients without mTBI (anxiety/fear; 1.14 ± 0.14 , $n=64$; depression; 0.78 ± 0.12 , $n=64$; mood swings; 0.80 ± 0.10 , $n=64$; Figure 2.4B-D). A significantly greater energy total symptom score was also observed in patients with a history of mTBI (5.14 ± 0.51 , $n=69$, $p=0.046$) versus patients without mTBI (3.44 ± 0.34 , $n=64$, Figure 2.5A). Significantly or trending significantly increased energy symptoms in patients with a history of mTBI included apathy/lethargy (1.38 ± 0.18 , $n=69$, $p=0.026$), hyperactivity

(0.62 ± 0.13 , $n=68$, $p=0.060$), and restlessness (1.20 ± 0.15 , $n=69$, $p=0.006$) when compared to patients with no mTBI (apathy/ lethargy; 0.80 ± 0.15 , $n=64$; hyperactivity; 0.30 ± 0.09 , $n=64$; restlessness; 0.63 ± 0.10 , $n=64$, Figure 2.5B, D, and E). For head and cognitive symptoms, history of mTBI patients only had trending significantly increased scores for faintness (0.59 ± 0.12 , $n=69$, $p=0.072$) and confusion (0.80 ± 0.14 , $n=69$, $p=0.055$), respectively, when compared to patients without mTBI (faintness; 0.31 ± 0.09 , $n=64$; confusion; 0.52 ± 0.13 , $n=64$; Figure 2.6B, 7B).

Previous literature has reported differences in male and female patient outcomes, which includes symptomology, following mTBI (Styrke et al., 2013; Mikolić et al., 2021). Therefore, symptom severity and frequency for emotion, energy, head, and cognitive symptoms were also analyzed for male and female patients with and without a history of mTBI to see if sex-specific differences existed. For all symptom data, an increased score indicates more severe and frequent affective symptomology.

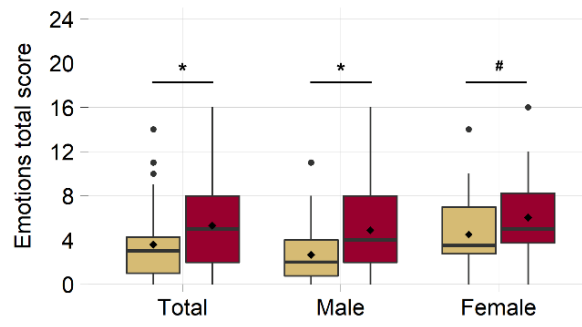
Parallel to the total mTBI patients, males with a history of mTBI had a significantly increased emotions total score (4.89 ± 0.63 , $n=45$, $p=0.024$) when compared to males without mTBI (2.66 ± 0.47 , $n=32$; Figure 2.4A). Significantly or trending significantly increased emotional symptoms in males with a history of mTBI included anxiety/fear (1.47 ± 0.20 , $n=45$, $p=0.016$), depression (1.18 ± 0.20 , $n=45$, $p=0.089$), and mood swings (1.20 ± 0.16 , $n=45$, $p=0.007$) when compared to males without mTBI (anxiety/fear; 0.78 ± 0.19 , $n=32$; depression; 0.66 ± 0.19 , $n=32$; mood swings; 0.56 ± 0.12 , $n=32$; Figure 2.4B - D). For emotional symptoms, in contrast to the total history of mTBI patients, males with a history of mTBI only had significantly or trending significantly increased

scores for hyperactivity (0.5 ± 0.16 , $n=44$, $p=0.073$) and restlessness (1.04 ± 0.16 , $n=45$, $p=0.014$) when compared to males without mTBI (hyperactivity; 0.16 ± 0.07 , $n=32$; restlessness; 0.47 ± 0.10 , $n=32$; Figure 2.5D and 5E). Male patients with a history of mTBI had a significantly increased head symptom total score (3.07 ± 0.46 , $n=45$, $p=0.029$) including significantly or trending significantly increased faintness (0.42 ± 0.11 , $n=45$, $p=0.012$), headaches (0.91 ± 0.20 , $n=45$, $p=0.060$), and insomnia (1.38 ± 0.23 , $n=45$, $p=0.035$) when compared to males without mTBI, of which faintness was only significant in the total mTBI population (total head score; 1.44 ± 0.27 , $n=32$; faintness; 0.06 ± 0.04 , $n=32$; headaches; 0.38 ± 0.13 , $n=32$; insomnia; 0.65 ± 0.18 , $n=31$; Figure 2.6A - 6D). Similar to the total history of mTBI population, males with history of mTBI did not have a significantly increased or trending increased total cognitive score (4.16 ± 0.73 , $n=45$, $p=0.199$) but did have a trending significantly increased symptom score for confusion (0.64 ± 0.16 , $n=45$, $p=0.077$) compared to males without mTBI (total cognitive score; 2.84 ± 0.71 , $n=32$; confusion; 0.38 ± 0.18 , $n=32$; Figure 2.7A and 7B). History of mTBI males had additional significant or trending significant increases in cognitive symptom scores for difficulty deciding (0.73 ± 0.16 , $n=45$, $p=0.065$), slurred speech (0.13 ± 0.08 , $n=45$, $p=0.085$), and stuttering (0.20 ± 0.06 , $n=45$, $p=0.091$) versus males without mTBI (difficulty deciding; 0.41 ± 0.18 , $n=32$; slurred speech; 0.00 ± 0.00 , $n=32$; stuttering; 0.06 ± 0.04 , $n=32$; Figure 2.7C, 7E, and 7F).

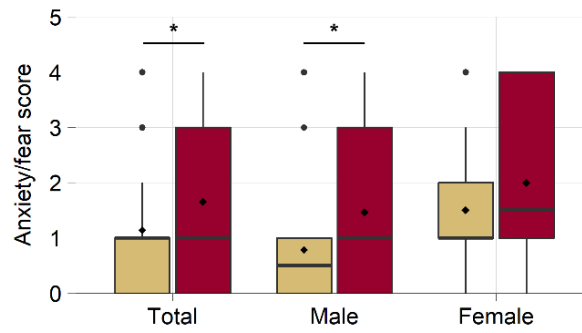
Females with history of mTBI only had significantly increased scores for depression (1.54 ± 0.26 , $n=24$, $p=0.039$) when compared to females without mTBI (0.91 ± 0.16 , $n=32$; Figure 2.4C). While mTBI males only had significantly or trending significantly

increased scores for hyperactivity and restlessness, female mTBI patients showed a significant increase in total energy score (7.13 ± 0.89 , $n=24$, $p=0.016$) which included significant or trending significant increases for apathy/lethargy (2.17 ± 0.33 , $n=24$, $p=0.005$), fatigue (2.79 ± 0.29 , $n=24$, $p=0.085$), and restlessness (1.50 ± 0.30 , $n=24$, $p=0.081$) versus females without mTBI (total energy score; 4.34 ± 0.55 , $n=32$; apathy/lethargy; 1.00 ± 0.23 , $n=32$; fatigue; 2.13 ± 0.26 , $n=32$; restlessness; 0.78 ± 0.17 , $n=32$; Figure 2.5A - 5E). In contrast to males with mTBI, females with a history of mTBI had no head symptoms that were significantly or trending significantly increased compared to females without mTBI (Figure 2.6). Furthermore, females with a history of mTBI only had a trending significantly increased score for poor concentration (1.96 ± 0.32 , $n=24$, $p=0.061$) for cognitive symptoms when compared to females without mTBI (1.22 ± 0.23 , $n=32$; Figure 2.7D). These data indicate that males exhibit increased symptom severity and frequency for more symptoms but that female patients show increased symptom severity and frequency for energy symptoms in response to mTBI.

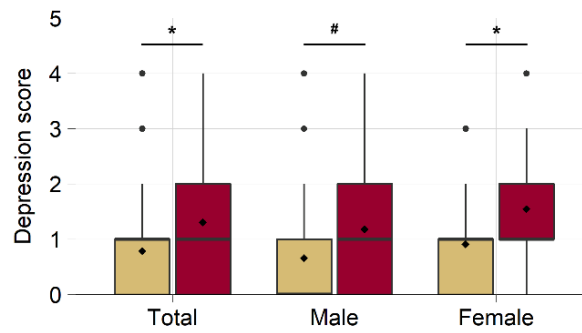
A



B



C



D

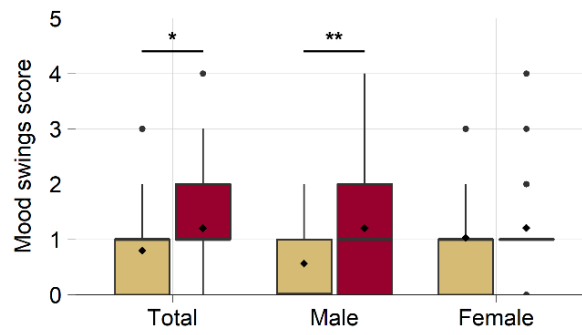


Figure 2.4 Significantly or Trending Significantly Worsened Symptoms Pertaining to Emotional State in Total, Male, and Female Patients with Versus Without a History of mTBI. In each graph, the gold plot represents populations without a history of mTBI and the crimson plot represents populations with a history of mTBI. **(A)** Emotion symptom category total score for total patients without (n=64) versus with history of mTBI (n=69), male patients without (n=32) versus with history of mTBI (n=45), and female patients without (n=32) versus with history of mTBI (n=24). **(B)** Anxiety/fear symptom score for total patients without (n=64) versus with history of mTBI (n=69), male patients without (n=32) versus with history of mTBI (n=45), and female patients without (n=32) versus with history of mTBI (n=24). **(C)** Depression symptom score for total patients without (n=64) versus with history of mTBI (n=69), male patients without (n=32) versus with history of mTBI (n=45), and female patients without (n=32) versus with history of mTBI (n=24). **(D)** Mood swing symptom score for total patients without (n=64) versus with history of mTBI (n=69), male patients without (n=32) versus with history of mTBI (n=45), and female patients without (n=32) versus with history of mTBI (n=24). Boxplots represent the minimum, maximum, median, mean (diamond symbol), first/third quartile, and outlying values (\leq/\geq lower/upper hinge +1.5* interquartile range). Statistical differences are analyzed by the Mann Whitney U-Test. # indicates $p<0.10$, * indicates $p<0.05$, and ** indicates $p<0.01$.

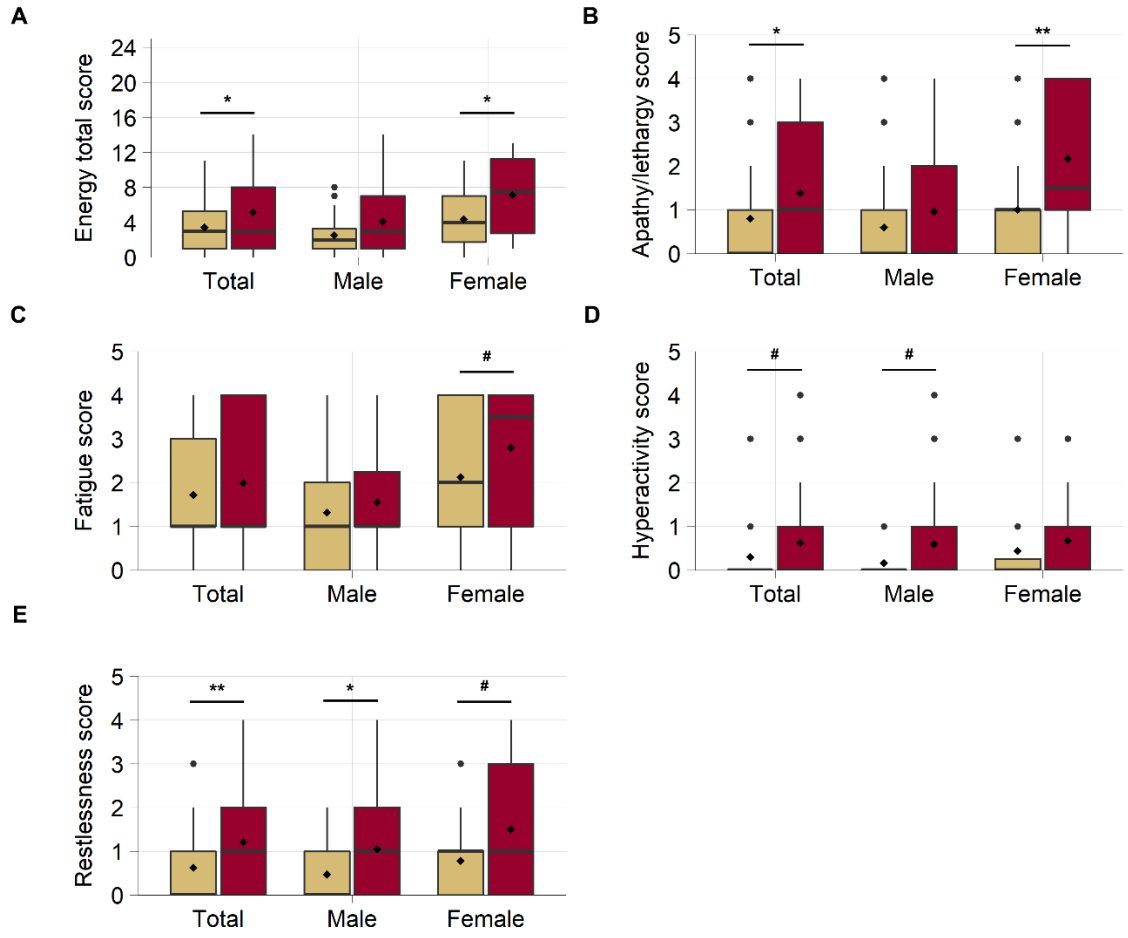
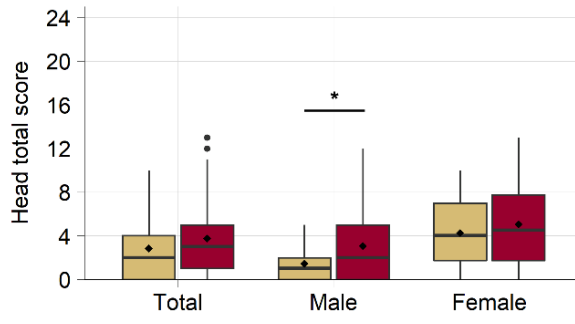
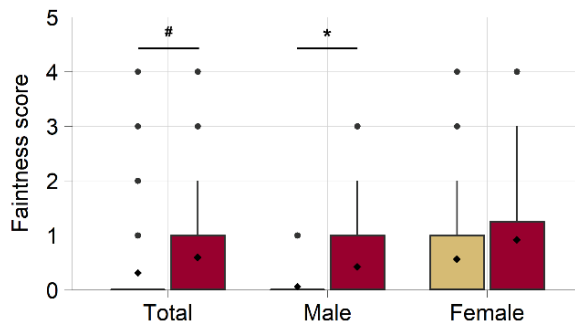


Figure 2.5 Significantly or Trending Significantly Worsened Symptoms Pertaining to Energy in Total, Male, and Female Patients with Versus Without a History of mTBI. In each graph, the gold plot represents populations without a history of mTBI and the crimson plot represents populations with a history of mTBI. **(A)** Energy symptom category total score for total patients without (n=64) versus with history of mTBI (n=69), male patients without (n=32) versus with history of mTBI (n=45), and female patients without (n=32) versus with history of mTBI (n=24). **(B)** Apathy/lethargy symptom score for total patients without (n=64) versus with history of mTBI (n=69), male patients without (n=32) versus with history of mTBI (n=45), and female patients without (n=32) versus with history of mTBI (n=24). **(C)** Fatigue symptom score for total patients without (n=64) versus with history of mTBI (n=68), male patients without (n=32) versus with history of mTBI (n=44), and female patients without (n=32) versus with history of mTBI (n=24). **(D)** Hyperactivity symptom score for total patients without (n=64) versus with history of mTBI (n=68), male patients without (n=32) versus with history of mTBI (n=44), and female patients without (n=32) versus with history of mTBI (n=24). **(E)** Restlessness symptom score for total patients without (n=64) versus with history of mTBI (n=69), male patients without (n=32) versus with history of mTBI (n=45), and female patients without (n=32) versus with history of mTBI (n=24). Boxplots represent the minimum, maximum, median, mean (diamond symbol), first/third quantile, and outlying values (\leq/\geq lower/upper hinge +1.5* interquartile range). Statistical differences are analyzed by the Mann Whitney U-Test. # indicates $p<0.10$, * indicates $p<0.05$, and ** indicates $p<0.01$.

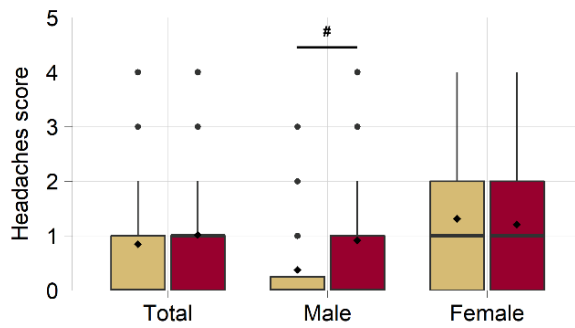
A



B



C



D

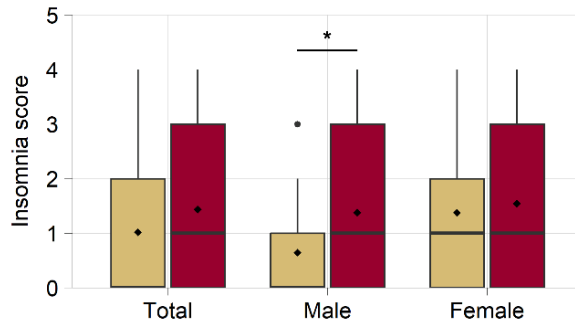


Figure 2.6 Significantly or Trending Significantly Worsened Head Symptoms in Total, Male, and Female Patients with Versus Without a History of mTBI. In each graph, the gold plot represents populations without a history of mTBI and the crimson plot represents populations with a history of mTBI. **(A)** Head symptom total score for total patients without (n=64) versus with history of mTBI (n=69), male patients without (n=32) versus with history of mTBI (n=45), and female patients without (n=32) versus with history of mTBI (n=24). **(B)** Faintness symptom score for total patients without (n=64) versus with history of mTBI (n=69), male patients without (n=32) versus with history of mTBI (n=45), and female patients without (n=32) versus female patients with history of mTBI (n=24). **(C)** Headache symptom score for total patients without (n=64) versus with history of mTBI (n=69), male patients without (n=32) versus with history of mTBI (n=45), and female patients without (n=32) versus with a history of mTBI (n=24). **(D)** Insomnia symptom score for total patients without (n=63) versus with history of mTBI (n=69), male patients without (n=31) versus with a history of mTBI (n=45), and female patients without (n=32) versus with a history of mTBI (n=24). Boxplots represent the minimum, maximum, median, mean (diamond symbol), first/third quartile, and outlying values (\leq/\geq lower/upper hinge +1.5* interquartile range). Statistical differences are analyzed by the Mann Whitney U-Test. # indicates $p<0.10$ and * indicates $p<0.05$.

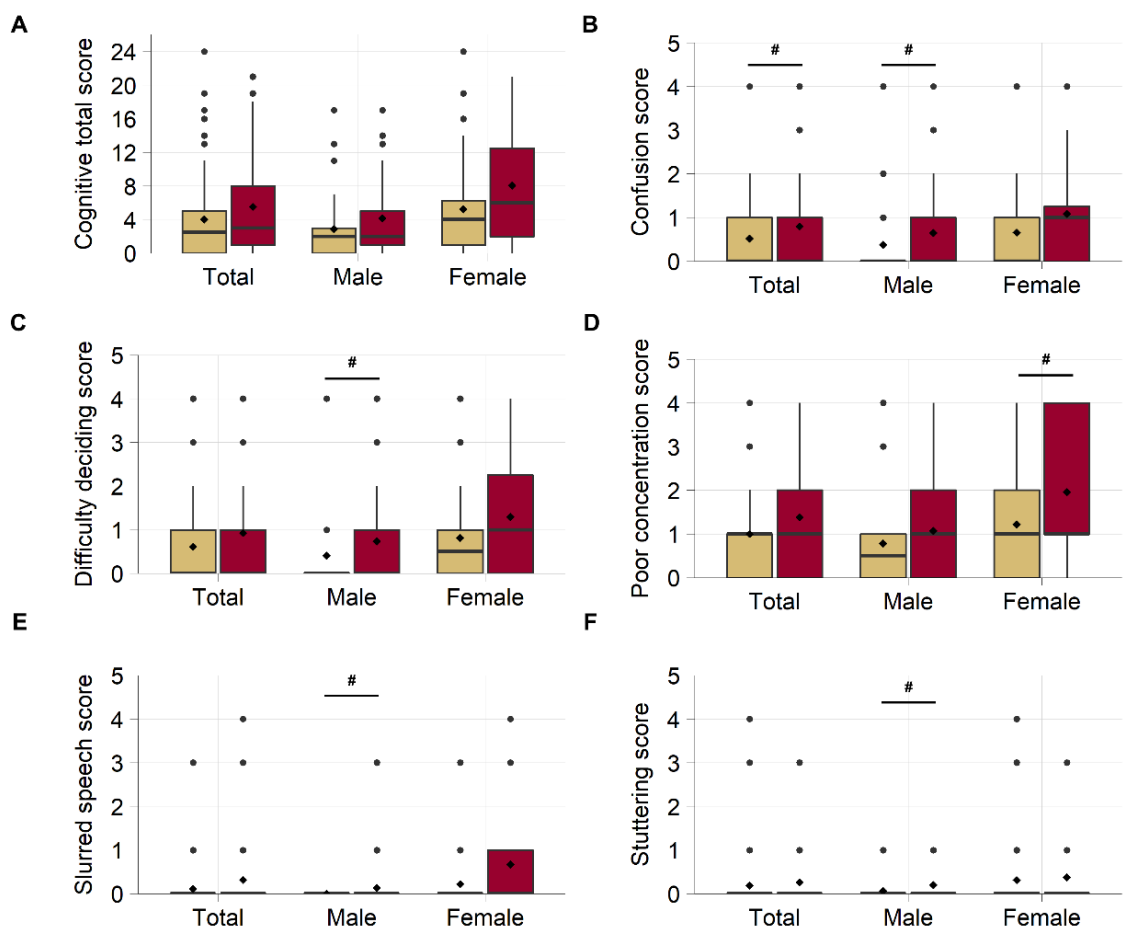


Figure 2.7 Trending Significantly Worsened Symptoms Pertaining to Cognition in Total, Male, and Female Patients with Versus Without a History of mTBI. In each graph, the gold plot represents populations without a history of mTBI and the crimson plot represents populations with a history of mTBI. **(A)** Cognitive symptom total score for total patients without (n=64) versus with history of mTBI (n=69), male patients without (n=32) versus with history of mTBI (n=45), and female patients without (n=32) versus female patients with history of mTBI (n=24). **(B)** Confusion symptom score for total patients without (n=64) versus with history of mTBI (n=69), male patients without (n=32) versus with history of mTBI (n=45), and female patients without (n=32) versus with history of mTBI (n=24). **(C)** Difficulty deciding symptom score for total patients without (n=64) versus with history of mTBI (n=69), male patients without (n=32) versus with history of mTBI (n=45), and female patients without (n=32) versus with history of mTBI (n=24). **(D)** Poor concentration symptom score for total patients without (n=64) versus with history of mTBI (n=69), male patients without (n=32) versus with history of mTBI (n=45), and female patients without (n=32) versus with history of mTBI (n=24). **(E)** Slurred speech symptom score for total patients without (n=64) versus with history of mTBI (n=69), male patients without (n=32) versus with history of mTBI (n=45), and female patients without (n=32) versus with history of mTBI (n=24). **(F)** Stuttering symptom score for total patients without (n=64) versus with history of mTBI (n=69), male patients without (n=32) versus with history of mTBI (n=45), and female patients without (n=32) versus with history of mTBI (n=24). Boxplots represent the minimum, maximum, median, mean (diamond symbol), first/third quantile, and outlying values (\leq/\geq lower/upper hinge +1.5* interquartile range). Statistical differences are analyzed by the Mann Whitney U-Test. # indicates $p < 0.10$.

2.4.4 Multiple mTBI Patients Seemed to Have Worsened and More Frequent Symptomology Compared to Patients Who Sustained a Single mTBI.

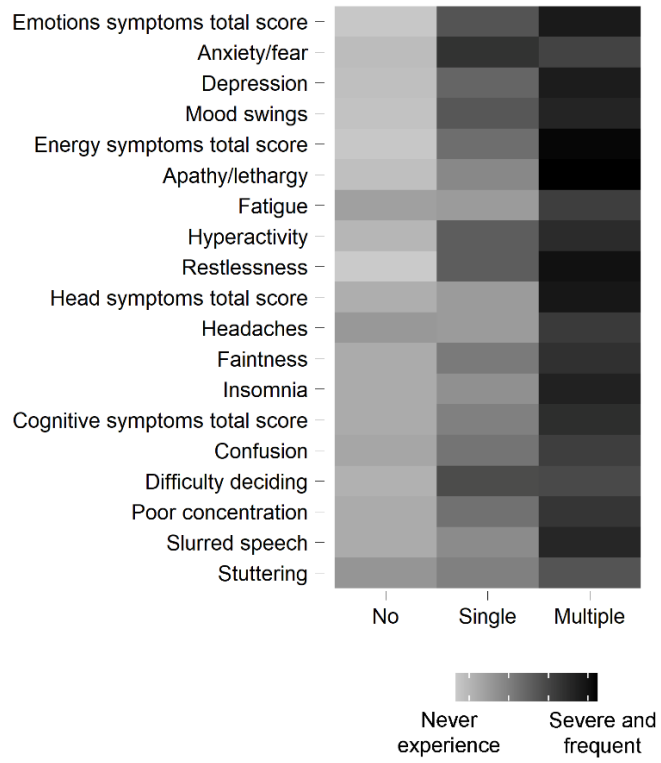
Sixty-seven (n=67) of the 88 history of mTBI patients reported either sustaining a past single mTBI (n=27) or multiple mTBIs (n=40). A patient was included in the multiple mTBI group if they sustained more than one mTBI throughout their lifetime, regardless of time elapsed between mTBIs. Previous data indicates that patients who suffer multiple mTBIs may have exacerbated secondary pathology which could lead to worsened symptoms (Bailes et al., 2014, Miller et al., 2013). Therefore, a qualitative heatmap visualization was created to allow for a comparison of increased symptom

severity and frequency for the previously mentioned emotional, energy, head, and cognitive symptoms in patients with multiple mTBI when compared to patients with a past single mTBI and no mTBI (Figure 2.8A). Patients with multiple mTBI seem to have worsened symptom severity and frequency, as indicated by the darker shade of grey for symptom scores, when compared to patients with a past single or no history of mTBI.

2.4.5 Chronic mTBI Patients Seemed to Have Worsened and More Frequent Emotional, Energy, and Cognitive, but Not Head Symptoms, When Compared to Acute-Subchronic mTBI Patients.

We also wanted to know whether symptom severity and frequency improved with increased time elapsed since the mTBI. History of mTBI patients were divided into groups based on the amount of time that has passed since their most recent mTBI to the clinic visit. Of the 88 history of mTBI patients, 46 reported the date of their most recent mTBI. Fourteen (n=14) patients suffered acute-chronic mTBI and presented to the clinic within 1 year of their most recent mTBI. Thirty-two (n=32) patients suffered chronic mTBI with their most recent mTBI > 1 year since presenting to the clinic. Emotional, energy, head, and cognitive symptom scores between no, acute-subchronic, and chronic mTBI patients were also qualitatively analyzed using a heatmap visualization (Figure 2.8B). As indicated by a darker grey shade, it appears that patients with chronic mTBI have worsened and more frequent symptoms in all categories aside for hyperactivity and most head symptoms when compared to acute-subchronic and no mTBI patients.

A



B

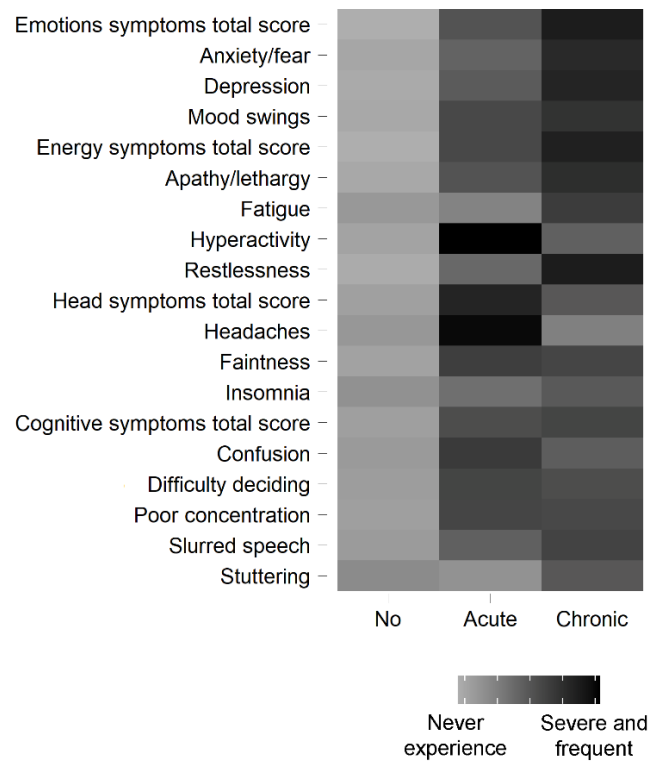


Figure 2.8 Qualitative Differences in Emotional, Energy, Head, and Cognitive Symptom Severity and Frequency Between Patients with No History of mTBI Versus Patients with a Past Single mTBI or with a History of Multiple mTBI and Between Patients with No History of mTBI Versus Patients with Acute-Subchronic mTBI or Chronic mTBI. Total/individual symptom scores between (**A**) patients with no history of mTBI (No; n=82), single mTBI (Single; n=27), and multiple mTBI (Multiple; n=40) or between (**B**) patients with no history of mTBI (No; n=82), acute-subchronic mTBI (Acute; n=14), and chronic mTBI (Chronic; n=32) are displayed in a heatmap for qualitative comparison of symptom severity between these groups. Acute-subchronic mTBI patients presented to the clinic ≤ 1 year and chronic mTBI patients presented > 1 year since their most recent mTBI. A lighter shade indicates a lower symptom score/lessened severity/less frequent, and a darker shade indicates a higher score/worsened severity/increased frequency.

2.4.6 History of mTBI Patients with Lower Levels of PUFA Biomarkers Have Significantly Worsened and Increased Frequency of Symptoms When Compared to mTBI Patients with Higher Levels of PUFA Biomarkers.

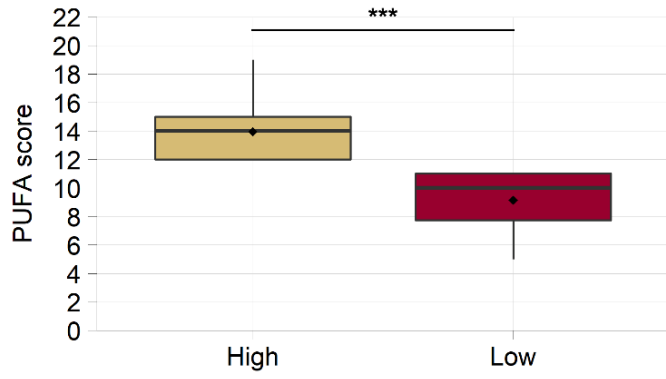
Supplementation with PUFAs prior to and following TBI have been shown to reduce neuronal cell death, inflammation, and oxidative stress and improve cognitive function following TBI (Bailes & Mills, 2010; Mills et al., 2011; Pu et al., 2013; Pu et al., 2017). It can be hypothesized that higher PUFA levels could result in improved outcome and less severe symptomology in humans following TBI. Our data indicate that PUFAs such as total omega-3, total omega-6, linoleic acid, alpha-linolenic acid, and docosahexaenoic acid are depleted with mTBI. Therefore, we suspected that greater depletion in these antioxidants may be responsible for worsened symptomology in patients with a history of mTBI.

Patients with a history of mTBI that had biomarker data for all PUFAs analyzed (linoleic acid and alpha-linolenic acid in plasma and total omega-3, total omega-6, and docosahexaenoic acid in RBCs) and MSQ responses (n=43) were divided into patients

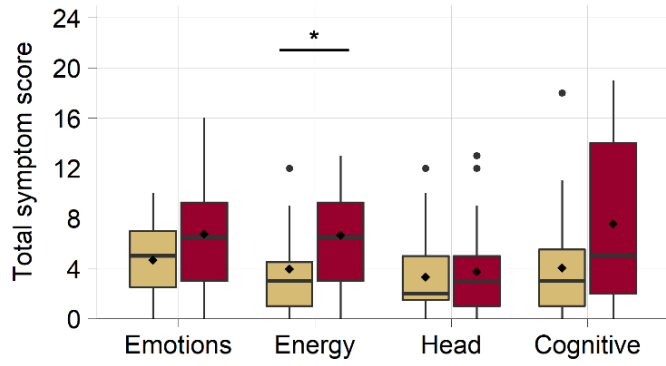
with a low (n=20) and high level of PUFAs (n=23). History of mTBI patients with a low level of PUFAs had a significantly lower level of PUFAs (9.15 ± 0.47 , $p<0.000$) when compared to mTBI patients with a high level (13.96 ± 0.42 , Figure 2.9A). Overall, history of mTBI patients with a low PUFA score had a significantly higher total symptom score (65.15 ± 6.46), indicating worsened symptom severity and increased frequency, when compared to patients with a higher PUFA score (47.39 ± 6.34 , $p=0.028$, data not shown). Emotional, energy, head, and cognitive total symptom scores were analyzed between these patients. Of these, the energy total symptom score was significantly increased in history of mTBI patients with low levels of PUFAs (6.65 ± 0.86) versus those with higher levels (3.96 ± 0.81 , $p=0.022$, Figure 2.9B).

History of mTBI patients with low PUFA levels had significantly increased scores for energy symptoms for fatigue (2.60 ± 0.31 , $p=0.038$), apathy/lethargy (1.80 ± 0.31 , $p=0.035$), and restlessness (1.60 ± 0.27 , $p=0.023$) when compared to patients with high levels (fatigue; 1.70 ± 0.29 ; apathy/lethargy; 1.09 ± 0.33 ; restlessness; 0.91 ± 0.26 ; Figure 2.9C). Patients with a history of mTBI with low levels of PUFAs also had significantly increased symptom scores for anger/irritability (1.75 ± 0.28 , $p=0.018$) for emotional symptoms and confusion (1.50 ± 0.34 , $p=0.023$) for cognitive symptoms when compared to patients with high levels (anger/irritability; 0.87 ± 0.16 ; confusion; 0.48 ± 0.17 ; Figure 2.9C). These data indicate that mTBI patients with lower levels of PUFA biomarkers have worsened symptomology when compared to patients with higher levels.

A



B



C

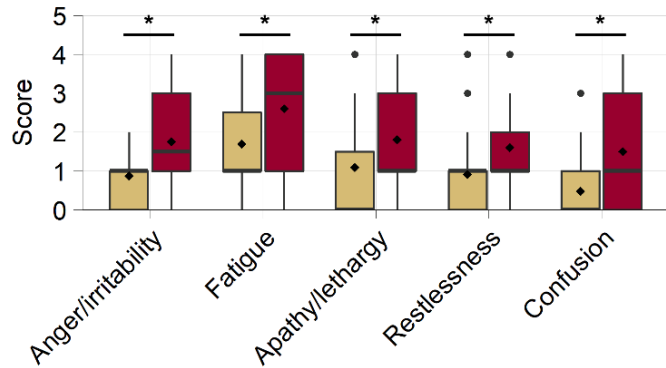


Figure 2.9 Significantly Worsened Symptoms Pertaining to Emotional State, Energy, Head Symptoms, or Cognition in Total History of mTBI Patients with PUFA Biomarker Depletion When Compared to History of mTBI Patients with Higher Levels of PUFA Biomarkers. In each graph, the gold plot represents history of mTBI populations with a high PUFA biomarker score (n=23) and the crimson bar represents populations with a low PUFA biomarker score (n=20). **(A)** Polyunsaturated fatty acid biomarker scores were significantly different for total history of mTBI patients with a high versus low PUFA biomarker score. **(B)** MSQ symptom total scores analyzed in history of mTBI patients with a high versus low PUFA score. **(C)** Significantly worsened symptoms analyzed in history of mTBI patients with a high versus low PUFA biomarker score. Boxplots represent the minimum, maximum, median, mean (diamond symbol), first/third quartile, and outlying values (\leq/\geq lower/upper hinge +1.5* interquartile range). The Mann Whitney U-Test was used to analyze statistical differences in PUFA scores and symptom scores. * indicates $p<0.05$ and *** indicates $p<0.001$.

2.5 Discussion

We retrospectively analyzed antioxidant biomarkers and symptomology in patient cohorts with and without a history of mTBI from a local sports medicine clinic in Denver, CO. We found that the total population with a history of mTBI had significantly depleted levels of biomarker antioxidants including alpha-tocopherol and selenium in serum, linoleic acid and taurine in plasma, and docosahexaenoic acid and total omega-3 in RBCs when compared to patients without mTBI. Male patients with a history of mTBI, compared to males without mTBI, showed significant or trending significant depletions in all antioxidant biomarkers that were depleted in the total mTBI population. Furthermore, male patients with a history of mTBI had additional significant or trending significant decreases in coenzyme-q10 and cysteine in serum, alpha-linolenic acid in plasma, and total omega-6 in RBCs when compared to males without mTBI. On the other hand, female mTBI patients only showed significantly or trending significantly decreased linoleic acid and taurine in plasma, which were depleted in the total population with a

history of mTBI, when compared to female without mTBI. Overall, patients with a history of mTBI have significant antioxidant biomarker depletion and male patients seem to show more extensive antioxidant depletion than female patients in response to mTBI.

The secondary injury pathology response to TBI, even of mild severity, can include neuroinflammation, oxidative stress, BBB disruption, mitochondrial dysfunction, and excitotoxicity. Previous research has shown that this pathology can persist for weeks to months following a mTBI (Bramlett & Dietrich, 2015; Ladak et al., 2019; Mckee & Daneshvar, 2015; Wang, K. K., et al., 2013). Neuroinflammation consists of infiltrating macrophages as a result of BBB disruption and activated resident microglia and astrocytes which generate ROS/RNS and contribute to the oxidative burden (Abdul-Muneer et al., 2015). Excessive glutamate release and subsequent calcium overload results in excitotoxicity. Excitotoxicity, along with increased oxidative stress, can initiate apoptotic signaling pathways within mitochondria leading to neuronal cell death (Cornelius et al., 2013). When these processes persist, the endogenous antioxidant system becomes depleted as brain endogenous antioxidants like superoxide dismutase (SOD) or glutathione (GSH) work to remove and neutralize ROS/RNS. Only a few *in vivo* studies report antioxidant depletion following more severe TBI (Bayir et al., 2002; Tyurin et al., 2000). However, no studies, to date, report extensive antioxidant depletion in human subjects in response to mTBI. The data presented here are novel in that they confirm significant antioxidant depletion in patients with a history of mTBI.

Our data also suggests that there are sex-specific differences in antioxidant depletion in response to a history of mTBI. Previous studies have shown that male subjects have

increased ROS/RNS species, increased markers of oxidative damage such as thiobarbituric reactive substances, and reduced antioxidants such as SOD, GSH peroxidase, and catalase, when compared to females (Ide et al., 2002; Kander et al., 2017; Ruszkiewicz et al., 2019). Total antioxidant capacity is also higher in females (Borrás et al., 2003; Demirbag et al., 2005; Vina et al., 2011). Female sex hormones such as 17 β -estradiol and progesterone, are neuroprotective and play a role in increasing activity of the endogenous antioxidant system (Ruszkiewicz et al., 2019). Furthermore, studies have shown that female sex hormones are neuroprotective against TBI (Pooley et al., 2018; Shahrokhi et al., 2012). In response to TBI of greater severity and in animal studies of TBI, oxidative stress as evidenced by lipid peroxidation and protein carbonylation was increased in males with TBI (Bayir et al., 2004; Lazarus et al., 2015; Wagner et al., 2004). Since healthy males already have increased oxidative burden and reduced antioxidant potential, our findings support that, in response to the overt and prolonged oxidative stress caused by a history of mTBI, males have more extensive antioxidant depletion.

Severity and frequency of emotional, energy, head, and cognitive symptoms were also analyzed in total, male, and female populations with a history of mTBI. Total patients with mTBI had significant or trending significant increases in the total emotion symptom score which included anxiety/fear, depression, and mood swings, the total energy symptom score which included apathy/lethargy, hyperactivity, and restlessness, only faintness for head symptoms, and no significant increase in cognitive symptom scores. Males and females exhibited sex-specific differences in trending or significantly

increased symptom scores. It seems that male patients with a history of mTBI had worsened symptom severity and frequency for most symptoms, particularly for head and cognitive symptoms, whereas females exhibited less overall symptomology but more severe symptom severity and frequency for energy symptoms. Sustained increased oxidative burden leading to extensive antioxidant depletion can present in physical symptoms. Many of the antioxidants observed to be depleted in our history of mTBI patients have implications in reducing oxidative stress, act as neuroprotective agents, and have anti-inflammatory properties. When depleted long-term, physical symptoms may manifest and antioxidant depletion may contribute to the development of neurodegenerative disease.

Patients with a history of mTBI were further divided based on number of TBIs sustained and time since their last mTBI. Qualitative analysis indicated that multiple mTBI patients had worsened symptom scores for all categories when compared to single mTBI and patients without mTBI. Multiple mTBIs can exacerbate secondary injury and healthy adults who have mTBIs report worse cognitive and emotional symptoms (Bailes et al., 2014; Bailes et al., 2013). Chronic mTBI patients also showed worsened symptom scores for emotional, energy, and cognitive symptoms when compared to acute-subchronic mTBI and no mTBI patients. Interestingly, acute-subchronic mTBI patients had worsened symptoms for hyperactivity and most head symptoms. Persisting symptoms from mTBI occur in 10-15% of patients which typically include headache, sleep disturbances, and fatigue (Marshall et al., 2012). This minority of patients with

persisting symptoms likely represent our chronic mTBI patients as they presented to the clinic with continuing symptoms greater than 1 year since their mTBI.

Alpha-tocopherol has implications in nerve protection and cognitive function, resulting in neurological symptoms when depleted (Traber, 2014). Selenium is a trace mineral that plays roles in the formation of selenoproteins, including GSH peroxidase, which performs antioxidant activities, and its depletion has been linked to immune dysfunction, decreased neurotransmitter production, and depressed mood states (Shreenath et al., 2021). Both alpha-tocopherol and selenium were significantly or trending significantly depleted in total and male patients with a history of mTBI which may explain the worsened head and cognitive symptoms reported particularly by male patients with mTBI.

Taurine, which was depleted in all history of mTBI populations, is a sulfur-containing amino acid that has anti-inflammatory roles, can reduce superoxide generation, prevents apoptosis, supports energy metabolism, and protects against excitotoxicity (Jong et al., 2012; Schaffer & Kim, 2018). Depletion of taurine can result in depression and anxiety, symptoms that were significantly or trending significantly worsened in all history of mTBI populations.

Taurine is synthesized from cysteine. Although taurine was found to be depleted in all mTBI populations, cysteine was only found to be trending significantly depleted in males with a history of mTBI. Cysteine is an amino acid necessary for protein synthesis, a precursor to many sulfur containing molecules, and is necessary for GSH synthesis. Cysteine plays roles in redox homeostasis and has implications for numerous

neurodegenerative diseases (Paul et al., 2018). Cysteine depletion in males with mTBI may explain the worsened head and cognitive symptoms. GSH was measured in WBCs but was not significantly depleted. Findings of cysteine depletion, but not GSH, could be due to the difference in location of measurement.

Coenzyme-q10 was trending significantly depleted in males with mTBI and is a component of the mitochondrial electron transport chain. It has roles in energy metabolism and mitochondrial function, with implications in neurodegenerative disease (Paul et al., 2018). Males had deficiencies in many of the antioxidant biomarkers with implications in neurodegenerative disease and also had increased symptomology for head and cognitive symptoms. The connection between antioxidant depletion in response to mTBI and neurodegenerative disease should be further explored.

Polyunsaturated fatty acids found to be depleted in mTBI populations in this study include linoleic acid, alpha-linolenic acid, total omega-3, total omega-6, and docosahexaenoic acid. Polyunsaturated fatty acids provide structure and support to both neurons and glia (Bazinet & Layé, 2014). The brain is particularly enriched in arachidonic acid and docosahexaenoic acid, which were measured in this study. Depletions in PUFAs, particularly docosahexaenoic acid, have been associated with mood changes including depression and bipolar disorder (McNamara et al., 2013). Male mTBI patients had significantly or trending significantly decreased levels of linoleic acid, alpha-linolenic acid, total omega-3, total omega-6, and docosahexaenoic acid when compared to male patients without mTBI. which may explain their reported worsened emotional, head, and cognitive symptoms.

Polyunsaturated fatty acid biomarkers have been well studied in *in vivo* models as treatments for TBI. Supplementation with PUFA biomarkers, such as docosahexaenoic acid and omega-3, result in neuroprotection and decreased inflammation and oxidative stress following TBI (Bailes & Mills, 2010; Mills et al., 2011; Pu et al., 2013; Pu et al., 2017). Furthermore, PUFA supplementation can preserve BBB integrity, reduce neurological impairment, and preserve brain derived neurotrophic factor levels (Bailes et al., 2020; Kumar, P. R., et al., 2014; Zhang, E., et al., 2020). We found that mTBI patients with lower levels of PUFAs had significantly worsened anger/irritability for emotional symptoms, confusion for cognitive symptoms, and energy total score which included significantly worsened fatigue, apathy/lethargy, and restlessness. These data support the use of antioxidant treatments, such as supplementation with PUFAs, to treat mTBI.

There are several limitations to the present study. Due to the retrospective nature of this study, we could not collect additional information for participants who were missing information resulting in varying n values for biomarker levels and symptom scores. Furthermore, patients presented to the clinic within a wide range of time elapsed since their most recent mTBI or didn't report the date of their last mTBI. We also recognize that there may not be a direct correlation between antioxidant depletion and the presentation of certain symptoms and that environmental and social factors may contribute to the reported symptoms and antioxidant depletion observed. Future studies should include larger sample sizes, complete medical history and lifestyle information, and thorough information pertaining to the nature of the mTBI. Biomarker measurements

and symptom responses should be obtained ideally at regular intervals from the first mTBI. However, this study is valuable in that it is the first of its kind to analyze numerous antioxidant biomarkers and a comprehensive list of symptoms in male and female patients with a history of mTBI.

The data presented here show that overall, patients with a history of mTBI have significant antioxidant biomarker depletion and worsened symptomology than patients without a history of mTBI. Furthermore, sex-specific differences exist in antioxidant biomarker depletion and symptom response to history of mTBI. The data support the use of sex-specific antioxidant supplementation following mTBI particularly in patients with chronic symptoms and those who have suffered from multiple mTBIs as they may be beneficial for improved symptomology caused by mTBI.

CHAPTER THREE: IMMUNOCAL® LIMITS GLIOSIS IN MOUSE MODELS OF REPETITIVE MILD-MODERATE TRAUMATIC BRAIN INJURY

3.1 Abstract

3.1.1 Objective

Successive traumatic brain injuries (TBIs) exacerbate neuroinflammation and oxidative stress. No therapeutics exist for populations at high risk of repetitive mild TBIs (rmTBIs). We explored the preventative therapeutic effects of Immunocal®, a cysteine-rich whey protein supplement and glutathione (GSH) precursor, for rmTBI and repetitive mild-moderate TBI (rmmTBI).

3.1.2 Methods

Mice were treated with Immunocal® prior to, during, and following rmTBI induced by controlled cortical impact until analysis at 2 weeks, 2 months, and 6 months following the last rmTBI. Astrogliosis and microgliosis were measured in cortex at each time point and edema and macrophage infiltration by MRI was analyzed at 2 months post-rmTBI. The dosing regimen was repeated in mice subjected to rmmTBI. Astrogliosis, microgliosis, neurofilament light (NfL) in serum, and GSH and glutathione disulfide (GSSG) were measured 72 hours post-rmmTBI.

3.1.3 Results

Immunocal® significantly reduced astrogliosis at 2 weeks and 2 months post-rmTBI. Macrophage activation was observed at 2 months post-rmTBI but Immunocal®

had no significant effect on this endpoint. We did not observe significant microgliosis or edema after rmTBI. Increases in astrogliosis, microgliosis, serum NFL, and reductions in the GSH:GSSG ratio, were observed 72 hours post-rmmTBI. Immunocal® only significantly reduced microgliosis after rmmTBI.

3.1.4 Interpretation

Astrogliosis persists for 2 months post-rmTBI. Inflammation, neuronal damage, and altered redox homeostasis present acutely following rmmTBI. Immunocal® significantly limited gliosis in these models; however, its neuroprotection was, to some extent, overwhelmed by repetitive injury. Treatments that modulate distinct aspects of TBI pathophysiology, used with Immunocal®, may show more protection in rmTBI models.

3.2 Introduction

Each year, approximately 69 million individuals worldwide sustain a traumatic brain injury (TBI), defined as an injury resulting from an impact to the head (Dewan et al., 2018). In the United States, 1.5 million individuals suffer a TBI of which 80,000 experience long-term disability (Flanagan, 2015). In 2010, the lifetime economic burden of TBI for the United States was estimated to be \$76.5 billion (Seifert, 2007). Clearly, TBI has severe emotional, physical, and economic consequences.

Primary injury from TBI occurs immediately and results from mechanical forces from the impact (Harish et al., 2015). Secondary injury is progressive and includes neuroinflammation, blood brain barrier (BBB) disruption, oxidative stress, excitotoxicity, and cell death (Hiebert et al., 2015; Jassam et al., 2017; Pearn et al., 2017). These processes contribute to symptoms and cognitive and motor deficits following TBI

(Decker et al., 2018; Honan et al., 2015; Voormolen et al., 2019; Wang, G., et al., 2018; Yin et al., 2016). Approximately 80% of TBIs sustained worldwide are mild in severity (McCrory et al., 2013). Repetitive TBIs (rTBIs), even of mild severity, can prolong and worsen TBI secondary injury (Bailes et al., 2013; Dhillon et al., 2020; Fehily & Fitzgerald, 2017; Fujita et al., 2012; Mouzon et al., 2017). Cognitive and motor deficits may or may not result from rmTBI, however, pathology can persist. Continual treatment of secondary injury is necessary for patients that suffer rmTBI as they may have an increased risk for neurodegeneration (Edwards et al., 2017; Faden & Loane, 2015; Gao et al., 2017).

Currently, there are no FDA approved preventative treatments for individuals, such as athletes and military personnel, who sustain rmTBI. The current study investigated Immunocal® as a preventative and restorative treatment for rmTBI and repetitive mild-moderate TBI (rmmTBI). Immunocal® is a non-denatured whey protein supplement that contains a large amount of cystine and glutamylcysteine, which can be converted to cysteine after crossing the BBB (Baruchel & Viau, 1996; Ross et al., 2012; Shih et al., 2006). Cysteine is the limiting substrate in the production of glutathione (GSH), a key endogenous antioxidant which has been shown to play significant roles in mitigating oxidative stress from neurodegeneration and neurotrauma (Bannai & Tateishi, 1986; Koza & Linseman, 2019; Mazzetti et al., 2015). We have previously shown that Immunocal® enhances the synthesis of GSH in neurons and provides neuroprotection *in vitro* and *in vivo* (Ross et al., 2012; Ross et al., 2014; Winter et al., 2017b).

Here, we analyzed the effect of Immunocal® treatment in mouse models of rmTBI or rmmTBI induced by controlled cortical impact (CCI), adapted from a well-established model (Mouzon et al., 2014; Mouzon et al., 2017; Mouzon et al., 2012). We have previously studied Immunocal® in a mouse model of single moderate TBI induced by CCI and found that supplementation with Immunocal® for 28 days prior to TBI preserved the ratio of GSH:glutathione disulfide (GSSG). Immunocal® also significantly reduced inflammation, axonal demyelination, and lipid peroxidation, ultimately offering neuroprotection (Ignowski et al., 2018). In this study, we explored the potential therapeutic effects of Immunocal® treatment in models of repetitive TBI. Mice were treated with Immunocal® 28 days prior to, during, and following 5 rmTBIs or 3 rmmTBIs induced by CCI and the effects of Immunocal® treatment were assessed on recovery, edema, macrophage infiltration, astrogliosis, microgliosis, serum neurofilament light (NfL), and brain GSH:GSSG, using ex vivo and in vivo (magnetic resonance imaging, MRI) techniques

3.3 Methods

3.3.1 Animal Care and Treatment

Animal work was performed under approved protocols to study rmTBI (#1011533; approved: 2/7/2017; expired: 2/6/2020) or rmmTBI (#1638687; approved: 8/27/2020; expires: 8/26/2023) by the Institutional Animal Care and Use Committee (IACUC) at the University of Denver. Male CD1-Elite mice (aged 35 days) were purchased from Charles River Laboratories (Hollister, CA) and maintained at the University of Denver animal

facility on a 12h light/dark cycle with food and water provided *ad libitum*. Mice acclimated for two weeks prior to the study.

3.3.2 Mice Subjected to rmTBI for Analysis at 2 Weeks, 2 Months, and 6 Months Post-TBI

Mice were divided into three groups with 23 mice in each group: Sham, untreated rmTBI, or Immunocal®-treated rmTBI. Immunocal®-treated rmTBI mice were dosed with a 3% w/v solution in sterile drinking water provided *ad libitum* for 5 days/week over 28 days prior to, during the rmTBIs, and until euthanasia. A similar dosing regimen yielded therapeutic effects in mice subjected to single moderate TBI (Ignowski et al., 2018). Body weights were obtained weekly. A magnetic resonance imaging (MRI) session was performed on 11 (n=3-4 per group) of the mice analyzed at 2 months post-rmTBI. Immunohistochemical staining of cortex with glial fibrillary acidic protein (GFAP) and ionized calcium-binding adaptor molecule 1 (Iba-1) to measure astrogliosis and microgliosis, respectively, from mice analyzed at 2 weeks, (n=9 per group), 2 months (n=9 per group), and 6 months (n=5 per group) post-rmTBI. N values vary due to unviable tissue or high/low outliers resulting in exclusion.

3.3.3 Repetitive mTBI Procedure

Five rmTBIs were performed with an inter-concussion interval of 48 hours over 10 consecutive days. Following the 28-day Immunocal® dosing, the first mTBI was induced by CCI using the Leica Impact One system (Leica Biosystems, Buffalo Grove, IL). Briefly, mice were anesthetized using an isoflurane vaporizer (VetEquip, Inc., Livermore, CA), their head was shaved, and they were placed into a stereotaxic frame (Braintree

Scientific Inc., Braintree, MA) to prevent movement during impact. The impactor probe (5mm diameter) was directly centered along the midline at bregma. A mTBI was administered with an impact depth of 1mm at a velocity of 5m/s (dwell time 200msec) as previously described (Mouzon et al., 2017; Mouzon et al., 2014; Mouzon et al., 2012). Untreated and Immunocal®-treated rmTBI mice were subjected to rmTBI (Supplementary Table 2). Apnea times greater than 5s were not observed or recorded. Sham were not subjected to impact but were otherwise treated identically to rmTBI mice. Mice recovered from anesthesia on a thermal pad and their righting reflex times were measured. Righting reflex was the point at which the animal was able to maintain a sternal position. Mice returned to their home cage once ambulatory.

3.3.4 Mice Subjected to rmmTBI and Analysis at 72 Hours Post-TBI

Mice were divided into three groups with 7 mice in each group: Sham, untreated rmmTBI, or Immunocal®-treated rmmTBI. Two Immunocal®-treated rmmTBI and 1 untreated rmmTBI mouse were euthanized prior to study conclusion due to adverse effects from the rmmTBI (e.g., difficulties with ambulation, seizure activity). The dosing regimen and body weight assessment was performed as described above. During and following the rmmTBIs until euthanasia, mice were monitored for distress. Mice were euthanized at 72 hours post-rmmTBI. Immunohistochemical staining of cortex for GFAP to measure astrogliosis and Iba-1 to measure microgliosis, brain GSH and GSSG, and serum NfL were performed for all mice subjected to rmmTBI. However, n values vary slightly due to unviable tissue or high/low outliers resulting in exclusion.

3.3.5 Repetitive mmTBI Procedure

Three mmTBIs were performed with an inter-concussion interval of 48 hours over 5 consecutive days. Repetitive mmTBIs were performed as described above with the following modifications. A concave 3mm metallic disk was affixed to the shaved head along the midline at bregma using tissue adhesive. Mice were in a stereotaxic frame and the impactor probe administered an impact depth of 2mm at a velocity of 5.5m/s (dwell time 200msec) to induce mmTBI (Supplementary Table 2). Untreated and Immunocal®-treated rmmTBI mice underwent mmTBI and were monitored for TBI-induced apnea (discontinuation of normal respiration). Sham animals were not subjected to impact but were otherwise treated identically to rmmTBI mice. Mice recovered from anesthesia on a thermal pad, their righting reflex times were measured, and returned to their home cage once ambulatory.

3.3.6 MRI Analysis of BBB Disruption/Edema and Activated Macrophages

3.3.6.1 Magnetic Resonance Imaging

All mouse brain MRI acquisitions were performed in the Colorado Animal Imaging Shared Resource (University of Colorado Anschutz Medical Campus) under an approved animal IACUC protocol #00596 (expires 11/7/2022). Briefly, the animals were anesthetized with 1.5-2% Isoflurane, positioned inside a warmed animal holder and inserted into the Bruker 9.4 Tesla/ 20 cm BioSpec MRI scanner with a mouse head phase-array RF coil. A multi-parametric high-resolution MR protocol was applied (Dahl et al., 2020; Frey et al., 2014; Pierce A. M., et al., 2019; Serkova et al., 2010): “T2w-turboRARE MRI” (structural MRI, 48 microns in-plane resolution)→ “T2wMRI-MSME

mapping with 16 echoes” (with/ without iron oxide nanoparticles Ferumoxytol for macrophage imaging)→ “T1wMRI-MSME” (with/ without gadolinium contrast MultiHance for BBB breakdown)→ EPS DWI with 6-gradients (for restricted diffusion/ brain edema).

3.3.6.2 Quantitative Image Analysis

All injured areas were assessed by placing region of interest (ROIs) on T2wMRI axial and sagittal slices. The changes in T2-relaxation times were assessed in the injured and control cortex from the T2w-maps in pre- and post-ferumxytol scans (24 hrs apart) to assess iron accumulation if macrophages. Increased T1-signal intensities in T1W post-gadolinium MRI scans were used to assess the areas of BBB leakage. Increased pparent diffusion coefficient (ADC) values from DWI for the left and right hemisphere were taken in two brain slices, anterior and posterior to bregma, were used to characterize brain edema. Change in T2-weighted values for the left and right hemisphere were also averaged for each mouse. All analysis was performed using Bruker ParaVision NEO360 v2.0 software

3.3.7 Euthanasia and Sample Collection

Mice were euthanized with an overdose of isoflurane and decapitated at respective study endpoints. For rmmTBI mice, trunk blood was collected. Whole brain was removed, washed in 1X phosphate buffered saline (PBS, pH= 7.4) and placed into a 1mm cut stainless steel brain matrix (Plastics One, Roanoke, VA) submerged in ice cold Gey’s balanced salt solution (Sigma Aldrich, St. Louis, MO). Using a razor blade, each brain was sectioned and used as shown in Supplementary Figure 2.

3.3.8 Immunohistochemical Staining of GFAP and Iba-1 in Cortex

3.3.8.1 Tissue Processing

The brain section was washed with ice cold Grey's solution and placed in 4% paraformaldehyde at 4°C overnight. Each section was washed with cold 1X PBS and placed in 30% sucrose in 1X PBS for cryopreservation. Sections were frozen in optimal cutting temperature (OCT) compound with liquid nitrogen and stored at -80°C. Prior to sectioning, tissue was allowed to acclimate in the microtome cryostat for 30 minutes. Brain was cut in 20µm sections, collecting every viable tissue section onto the surface of Fisherbrand Superfrost Colorfrost Plus coated slides (Fisher Scientific, Pittsburgh, PA) and stored at -20°C.

3.3.8.2 Immunohistochemical Staining

Slides equilibrated at room temperature for 30 minutes. Sections were outlined with Liquid Blocker Super PAP Pen (Daido Sangyo Co., Tokyo, Japan) and washed twice with 1X PBS to remove residual OCT. Tissue underwent a standard staining protocol using primary antibodies against GFAP and Iba-1, Cy3- or Alexa Fluor 488-conjugated secondary antibodies, and Hoechst nuclear stain, as previously described (Ignowski et al., 2018). Two slides with 6 sections of cortex per mouse were stained for Iba-1 and GFAP.

3.3.9 Immunofluorescence Microscopy of GFAP and Iba-1-Stained Cortex

Three 20X images per section were captured by a blinded researcher using a Zeiss Axio Observer epi fluorescence microscope (locations shown in Supplementary Figure 3). Iba-1 and GFAP images were captured on the Alexa Fluor 488 and Cy3 channel, respectively.

3.3.10 Quantification of Astrocyte and Microglia Number in Cortex

Iba-1 and GFAP images were quantified by two blinded researchers. Using Adobe Photoshop CC 19.1.7 (Adobe Inc., San Jose, CA), background staining was removed by setting a black point for the image in an area of high background staining. The count tool was then used to label positively stained GFAP and Hoechst cells, counted as astrocytes, or positively stained Iba-1 and Hoechst cells, counted as microglia. An average of the total number of astrocytes or microglia counted for each mouse was obtained from 18-36 images per mouse.

3.3.11 Measurement of Serum NfL by Enzyme-Linked Immunosorbent Assay (ELISA)

3.3.11.1 Blood Processing

Trunk blood was collected into 200 μ L serum capillary top sample tubes (SAI Infusion Technologies, Lake Villa, IL) and clotted for 1 hour at room temperature prior to centrifugation at 4000rpm for 10 minutes at 4°C. Supernatant was collected and serum was isolated and stored at -80°C.

3.3.11.2 ELISA

Manufacturer's protocols were followed for mouse Neurofilament Light ELISA assay kit (Aviva Systems Biology, San Diego, CA). Samples were diluted 1:2 with provided standard diluent and run in duplicate. Optical density (O.D.) absorbance was read at 450nm using a spectrophotometer and relative O.D. with corrected absorbance was calculated for standard and sample. Values for NfL concentration were interpolated from the standard curve and an average NfL concentration was calculated for each mouse.

3.3.12 Colorimetric Detection of Brain GSH and GSSG

3.3.12.1 Tissue Processing

Brain sections (Supplementary Figure 2) were frozen in liquid nitrogen and stored at -80°C. Brain sections were homogenized in 250µL of ice cold 100mM phosphate buffer (pH=7) using a dounce homogenizer. The homogenate was centrifuged at 14,000rpm for 10 minutes at 4°C and supernatant was removed. An aliquot was taken for protein assay determination. One volume of cold 5% 5-sulfo-salicylic acid (Sigma-Aldrich, St/ Louis, MO) was added to remaining samples which were incubated for 10 minutes at 4°C. Samples were centrifuged at 14,000rpm for 10 minutes at 4°C and supernatant was analyzed.

3.3.12.2 Colorimetric Detection Assay

Manufacturer's protocols were followed for the Glutathione Colorimetric Detection Kit (Invitrogen, Waltham, MA). Samples were diluted by adding 1.5 volumes of provided 1X assay buffer and run in duplicate. O.D. absorbance was read at 405nm using a spectrophotometer and the relative O.D. with corrected absorbance was calculated for standards and samples. Values for GSH and GSSG were interpolated from standard curves and normalized based on protein concentration. Average values for GSH and GSSG were calculated for each mouse and the GSH:GSSG ratio was calculated.

3.3.13 Statistical analysis

Data were statistically analyzed and graphs (showing mean \pm standard error of the mean (SEM)) were created using GraphPad Prism 5.01 for Windows (GraphPad Software, San Diego, CA). Statistical differences between groups were evaluated using a

one-way ANOVA with *post-hoc* Tukey's test at each time point for body weight, righting reflex, ADC and T-2 weighted values, quantification of astrocytes and microglia, NFL levels, and GSH, GSSG, and GSH:GSSG measurements. A *post-hoc* Dunnett's Multiple Comparison test was also used for GSH. Statistical differences in righting reflex between and within groups were analyzed by a paired t-test. Statistical differences between groups were analyzed by an unpaired t-test for apnea values. Differences were statistically significant when $p < 0.05$ for all analyses.

3.4 Results

3.4.1 Immunocal®-Treatment Effects on Body Weight and Righting Reflex Times After rmTBI

Sham, untreated rmTBI, and Immunocal®-treated rmTBI mice were analyzed at 2 weeks (n=9 per group), 2 months (n=9 per group), and 6 months (n=5 per group) post-rmTBI. Body weights were monitored weekly (Figure 3.1A-C). There were no significantly sustained changes in percentage of peak body weight between groups. Righting reflex times, indicative of TBI and impairment, were measured immediately following each rmTBI or sham surgery and combined for mice analyzed at all time points post-rmTBI (Grin'kina et al., 2016). Righting reflex times for untreated and Immunocal®-treated rmTBI mice did not significantly differ but were significantly increased versus sham mice (Figure 3.1D).

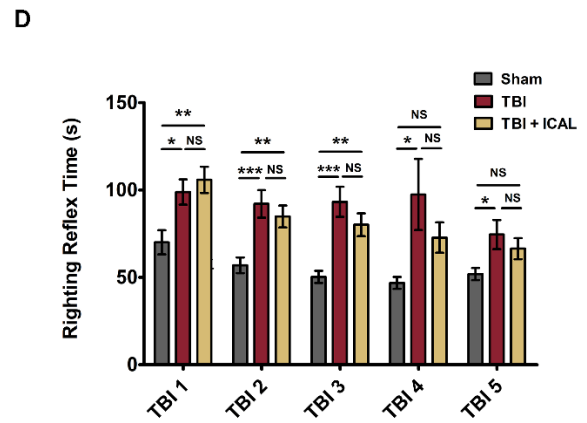
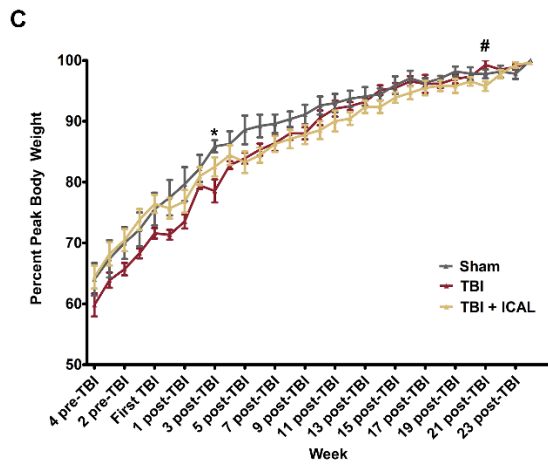
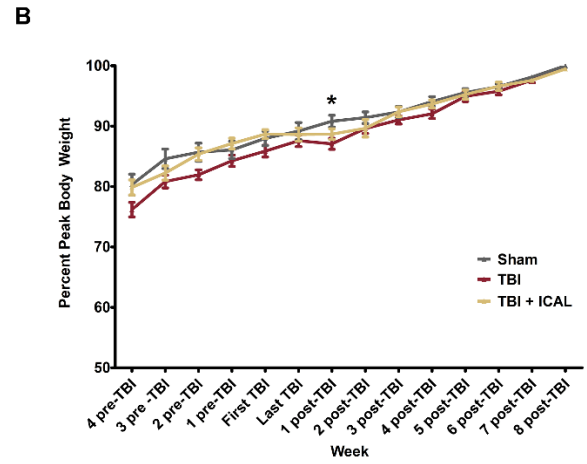
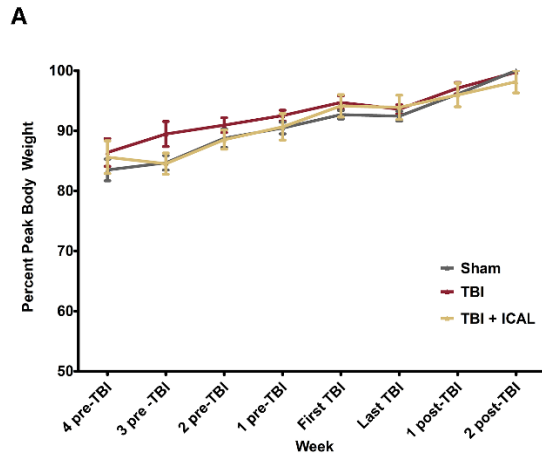


Figure 3.1 Percent of Peak Body Weight and Righting Reflex Times of Mice Subjected to Sham Surgery (Sham) or Untreated (TBI) and Immunocal®-Treated (TBI + ICAL) Mice Subjected to Repetitive Mild TBI (rmTBI). Body weight of untreated TBI, TBI + ICAL, and sham mice was assessed once per week beginning with Immunocal® treatment at 4 weeks (28 days) prior to the first mTBI, during the mTBI's, and continuing until euthanasia for analysis at (A) 2 weeks (n=9 mice per group), (B) 2 months (n=9 mice per group), and (C) 6 months (n=5 mice per group) post-last rmTBI or sham surgery. Body weight is expressed as the percentage of peak body weight at each time point. No significant differences in percent of peak body weight were observed at any time points for mice analyzed at (A) 2 weeks post-rmTBI. For mice analyzed at (B) 2 months post-rmTBI, untreated TBI mice had significantly lower percent of peak body weight only at 1-week post-last mTBI when compared to sham mice (p=0.031). No significant differences in percent of peak body weight were observed between TBI + ICAL mice and sham or untreated TBI mice at any time points for mice analyzed at 2 months post-last TBI. For mice analyzed at (C) 6 months post-rmTBI, untreated TBI mice had a significantly lower percent of peak body weight compared to sham mice only at 3 weeks post-rmTBI (p=0.017). TBI + ICAL mice had a significantly lower percent of peak body weight compared to TBI mice only at 21 weeks post-rmTBI (p=0.019). No significant differences in percent of peak body weight were observed between TBI + ICAL and sham mice at any time points. All data in (A) - (C) are displayed as the mean \pm SEM and a one-way ANOVA with post-hoc Tukey's test was used to analyze data at each time point (* indicates p<0.05 for untreated TBI versus sham mice and # indicates p<0.05 for TBI + ICAL versus TBI mice). Righting reflex times for sham, TBI, and TBI + ICAL mice analyzed at (D) all time points (2 weeks, 2 months, and 6 months post- last rmTBI; n=23 per group) were measured immediately following each mTBI or sham surgery after anesthesia was discontinued. Untreated TBI mice had significantly increased righting reflex times compared to sham mice following all mTBIs, however, TBI + ICAL mice only exhibited significantly increased righting reflex times compared to sham mice following the first three TBI's. All data in (D) are displayed as the mean \pm SEM and righting reflex times between groups are analyzed by a one-way ANOVA with post-hoc Tukey's test for each TBI day number (* indicates p<0.05, ** indicates p<0.01, *** indicates p<0.001, and NS indicates p>0.05 or nonsignificant).

3.4.2 MRI Analysis of Immunocal®-Treatment Effects on Macrophage

Activation After rmTBI

Groups were analyzed by MRI at 2 months post-rmTBI. Gadolinium contrast was used to determine edema. Since the mTBIs were performed at midline at bregma, the ADC values for the left and right hemispheres at bregma were averaged. No significant

differences were observed between sham, untreated rmTBI, and Immunocal®-treated rmTBI mice ($p=0.742$; Figure 3.2A). It seems that rmTBI did not induce significant edema 2 months post-rmTBI.

Iron-oxide T2-weighted contrast was used to measure macrophage activation in mice. This contrast consists of nanoparticles which accumulate in activated macrophages after circulation and is indicative of increased brain inflammation. Change in T2 values were averaged for the left and right hemisphere. Untreated rmTBI mice had significantly increased average T2 values versus sham mice, indicating accumulation of iron-oxide nanoparticles in macrophages ($p=0.025$). Immunocal® treatment did not protect against this as Immunocal®-treated rmTBI mice did not have significantly values versus untreated rmTBI mice (Figure 3.2B).

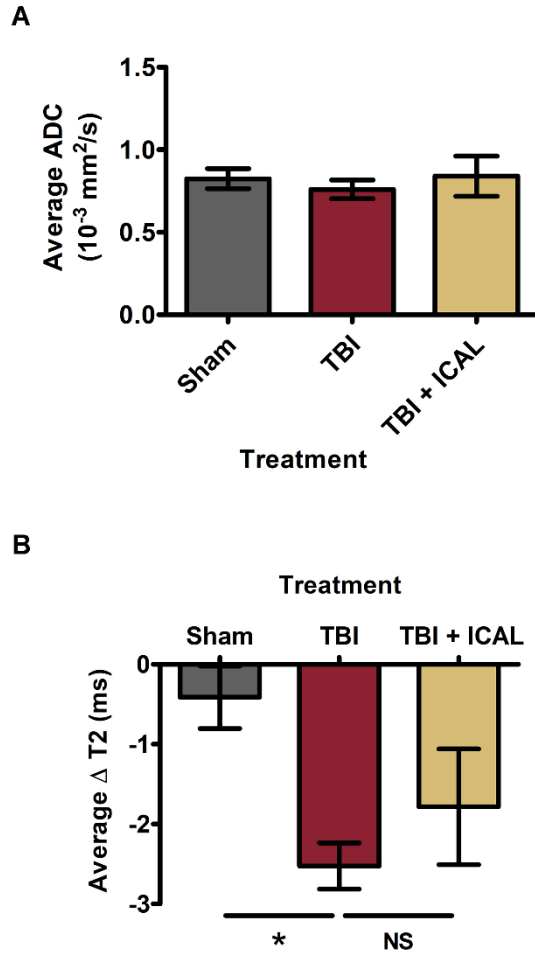


Figure 3.2 Repetitive Mild Traumatic Brain Injury (rmTBI) Did Not Result in Edema but Did Cause an Increase in Inflammation as Analyzed by Magnetic Resonance Imaging (MRI). Iron oxide T2-weighted brain MRI analysis was performed on untreated (TBI) and Immunocal® pre- and post-treated (TBI + ICAL) mice subjected to rmTBI, or mice subjected to sham surgery (Sham) at 2 months post-last mTBI or sham surgery (n=3-4 per group). Averaged apparent diffusion coefficient (ADC) values for the left and right hemisphere (**A**), which indicate edema when increased, were not significantly different between groups (p=0.742). The average combined left and right hemisphere change (Δ) in T2-weighted values (**B**) are significantly decreased in untreated TBI mice when compared to sham mice which is indicative of the accumulation of the iron nanoparticle contrast in activated macrophages (p=0.025). No significant differences in the average change in T2-weighted values were observed between TBI + ICAL and sham mice or untreated TBI mice. All MRI data are displayed as the mean \pm SEM and are analyzed by a one-way ANOVA with post-hoc Tukey's test (* indicates p<0.05 and NS indicates p>0.05 or non-significant).

3.4.3 Immunocal®-Treatment Significantly Reduces Astrogliosis at 2 Weeks and 2 Months After rmTBI

Neuroinflammation has been reported *in vivo* in response to closed skull rmTBI (Hoogenboom et al., 2019). The rmTBI model used to model our rmTBI model showed significant GFAP and Iba-1 immunoreactivity in brain at 24 hours and 6 months post-rmTBI versus sham mice (Mouzon et al., 2014; Mouzon et al., 2012). We anticipated astrogliosis and microgliosis around the injury site out to 6 months post-rmTBI. Cortices of mice were stained for GFAP, Iba-1, and Hoechst to analyze astrogliosis, microgliosis, and nuclei, respectively. Astrocytes or microglia, counted as GFAP or Iba-1 (and Hoechst) positive cells, respectively, were quantified and averaged for groups analyzed at 2 weeks, 2 months, and 6 months post-TBI (Figure 3.3 and 3.4).

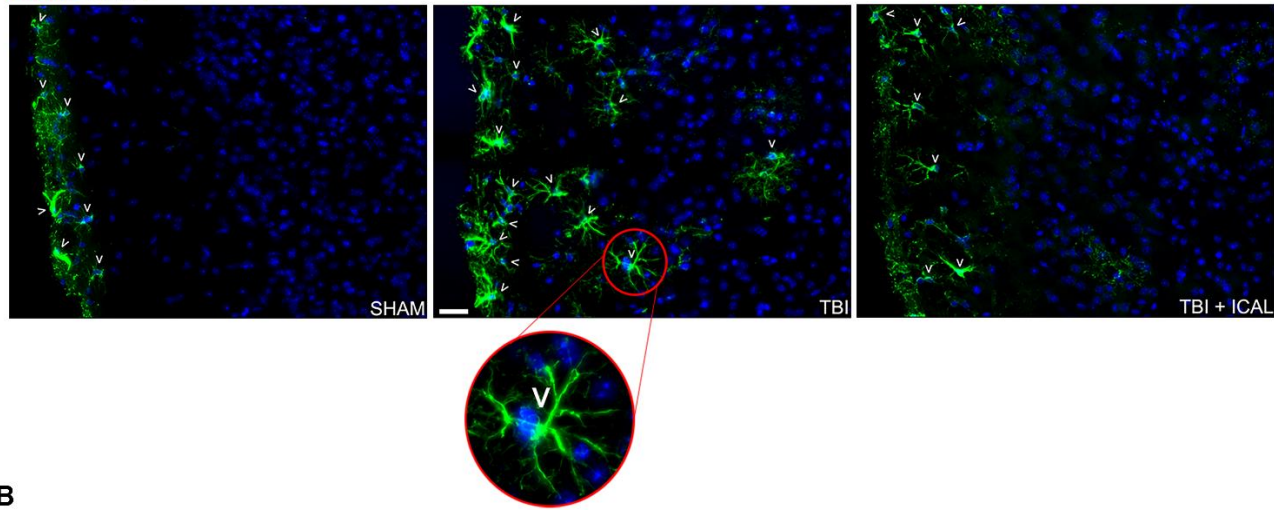
Untreated rmTBI mice had significantly increased average number of astrocytes in cortex versus sham mice when analyzed at 2 weeks ($p=0.011$) and 2 months ($p=0.002$) post-rmTBI (Figure 3.3B). Immunocal®-treatment essentially prevented astrogliosis evidenced by significantly decreased average number of astrocytes in cortex versus untreated rmTBI mice and no significant differences versus sham mice at 2 weeks ($p=0.011$) and 2 months post-rmTBI ($p=0.002$). No significant differences were observed between groups 6 months post-rmTBI ($p=0.216$; Figure 3.3B).

No significant differences in the number of microglia were observed between groups at 2 weeks ($p=0.229$), 2 months ($p=0.450$), or 6 months ($p=0.291$) post-rmTBI (Figure 3.4B). It seems that rmTBI induced sustained astrogliosis at 2 weeks and 2 months, but

not 6 months, post-rmTBI. Immunocal® prevented the increase in astrogliosis, however, microgliosis was not observed in this mouse model of rmTBI.

A

GFAP DAPI



B

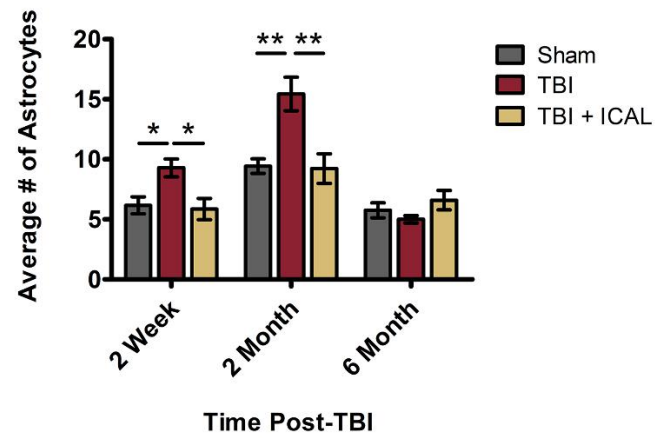
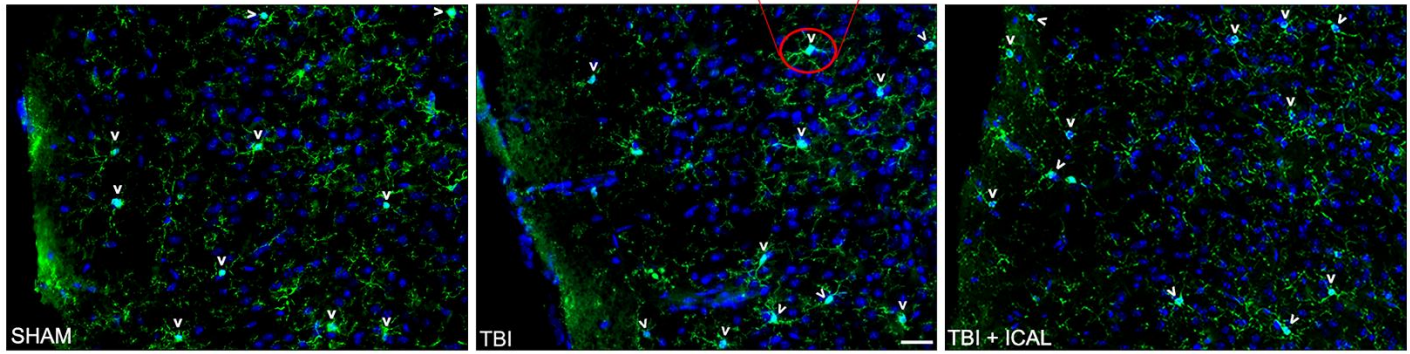


Figure 3.3 Immunocal®-Treatment Pre- and Post-Repetitive Mild Traumatic Brain Injury (rmTBI) Significantly Reduced Astrogliosis in the Cortex of Mice Subjected to rmTBI When Analyzed at 2 Weeks and 2 Months, but Not at 6 Months Post-Last rmTBI. Representative images of cortex stained for GFAP (green) and DAPI (blue), to label astrocytes and nuclei, respectively, from mice subjected to sham surgery (SHAM) and Immunocal® pre- and post-treated mice (TBI + ICAL) and untreated mice (TBI) subjected to rmTBI analyzed at **(A)** 2 months post-rmTBI. White arrows indicate GFAP and DAPI positive cells, counted as astrocytes. Scale bar =20µm. Quantification of the average number (#) of astrocytes in cortex stained with GFAP and DAPI, as described in **(A)** is shown for sham, untreated TBI, and TBI + ICAL mice analyzed at **(B)** 2 weeks (n=6-7 mice per group), 2 months (n=7-9 mice per group), and 6 months (4-5 mice per group) post-rmTBI. The average number of astrocytes in the cortex of untreated TBI mice was significantly increased at 2 weeks (p=0.011) and 2 months (p=0.002) post-rmTBI compared to sham mice. Immunocal®-treatment pre- and post-rmTBI significantly reduced the average number of astrocytes in the cortex in mice subjected to rmTBI at 2 weeks (p=0.011) and 2 months (p=0.002) post-rmTBI when compared to untreated TBI mice and showed no significant difference compared to sham mice. No significant differences in the average number of astrocytes in the cortex were observed between groups analyzed at 6 months post-rmTBI (p=0.216). All astrocyte quantification data are displayed as the mean ± SEM and are analyzed by a one-way ANOVA with post-hoc Tukey's test at each time point (* indicates p<0.05 and ** indicates p<0.01).

A

Iba-1 DAPI



146

B

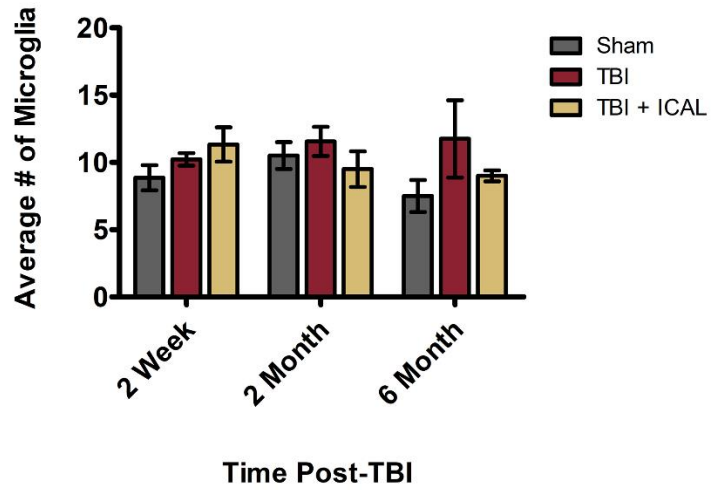


Figure 3.4 Microgliosis Was Not Observed in the Cortex of Mice Subjected to Repetitive Mild Traumatic Brain Injury (rmTBI) When Analyzed at 2 Weeks, 2 Months, or 6 Months Post-Last mTBI. Representative images of cortex stained for Iba-1 (green) and DAPI (blue), to label microglia and nuclei, respectively, from mice subjected to sham surgery (SHAM) and untreated mice (TBI) and Immunocal®-treated pre- and post-rmTBI mice (TBI + ICAL) subjected to rmTBI analyzed at (A) 2 weeks post-rmTBI. White arrows indicate Iba-1 and DAPI positive cells, counted as microglia. Scale bar=20µm. Quantification of the average number (#) of microglia in cortex stained with Iba-1 and DAPI, as described in (A) is shown for sham, untreated TBI, and TBI + ICAL mice analyzed at (B) 2 weeks (n=7-9 mice per group), 2 months (n=8-9 mice per group), and 6 months (n=4 mice per group) post-rmTBI. No significant differences of the average number of microglia in the cortex were observed between sham, TBI, and TBI + ICAL mice at 2 weeks ($p=0.229$), 2 months ($p=0.450$), or 6 months ($p=0.291$) post-rmTBI. All microglia quantification data are displayed as the mean \pm SEM and are analyzed by a one-way ANOVA with post-hoc Tukey's test at each time point.

3.4.4 Immunocal®-Treatment Effects on Body Weight, Apnea, and Righting

Reflex Times After rmmTBI

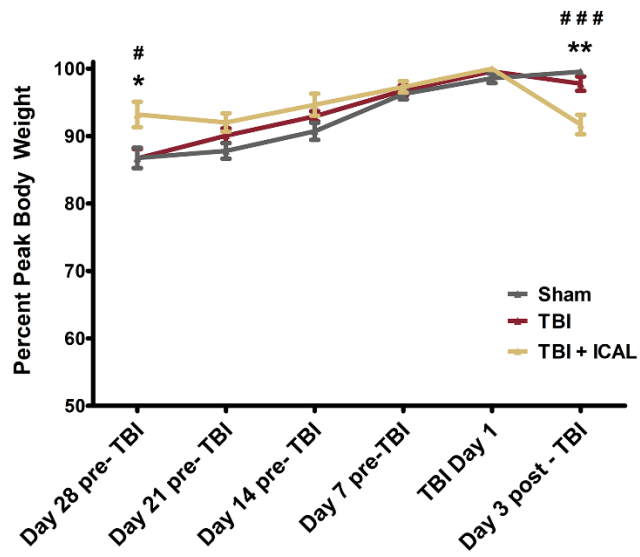
We next performed an analysis in a mouse model of rmmTBI of increased severity which we hypothesized would elicit a more robust injury response. Mice were divided into sham, untreated rmmTBI, and Immunocal®-treated rmmTBI mice. Mice were analyzed 72 hours post-rmmTBI (n=5-7 per group).

Body weight was assessed weekly. Percentage of peak body weight for Immunocal®-treated rmmTBI mice was significantly increased day 28 prior to the first TBI versus sham and untreated rmmTBI mice ($p=0.023$). There were no significant differences between untreated rmmTBI and sham mice at any time point. Immunocal®-treated rmmTBI mice displayed a small but significantly decreased percentage of peak body weight versus sham and untreated rmmTBI mice 3 days post-rmmTBI ($p=0.000$; Figure 3.5A).

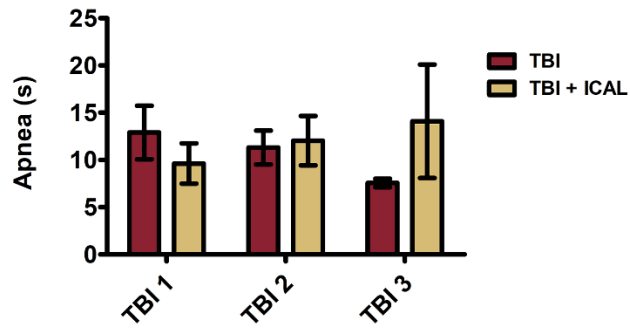
Untreated and Immunocal®-treated rmmTBI mice experienced apnea which suggests this model is increased in severity. Sham mice did not experience apnea and are not shown. No significant differences in average apnea times between groups were found following the mmTBI procedures (Figure 3.5B).

Righting reflex times for all groups were measured immediately following each mmTBI or sham surgery (Fig 3.5C). Righting reflex times for untreated and Immunocal®-treated rmmTBI mice did not significantly differ but were significantly increased versus sham mice (Fig 3.5C).

A



B



C

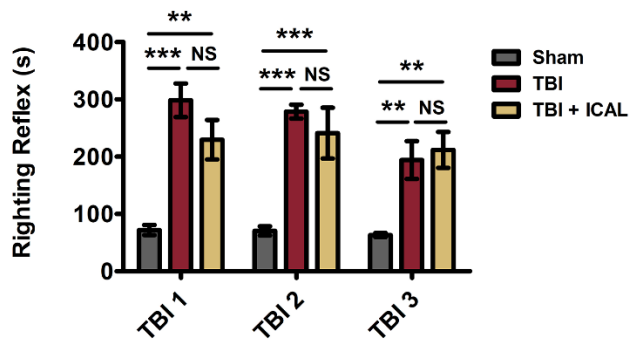


Figure 3.5 Percent of Peak Bodyweight, Apnea, and Righting Reflex Times of Mice Subjected to Sham Surgery (Sham) or Untreated (TBI) and Immunocal®-Treated (TBI + ICAL) Mice Subjected to Repetitive Mild-Moderate Traumatic Brain Injury (rmmTBI) Analyzed at 72 Hours Post-Last TBI. Bodyweight of sham, untreated TBI, and TBI + ICAL mice was assessed once per week beginning with Immunocal® treatment at 4 weeks (28 days) prior to the first mmTBI, during the mmTBI's, and continuing until euthanasia for analysis at **(A)** 72 hours (3 days) post-rmmTBI or sham surgery (n=5-7 mice per group). Bodyweight is expressed as the percentage of peak body weight at each time point. Data are displayed as the mean ± SEM. Bodyweight for TBI + ICAL mice was significantly increased at day 28 pre-TBI (p=0.023) and significantly decreased at 72 hours post-TBI (p=0.000) when compared to both sham and untreated TBI mice. Bodyweight data are displayed as the mean ± SEM and are analyzed by a one-way ANOVA with post-hoc Tukey's test at each time point (* indicates p<0.05 and ** indicates p<0.01 for TBI + ICAL versus untreated TBI mice. # indicates p<0.05 and ### indicates p<0.001 for TBI + ICAL versus sham mice). Apnea times were recorded immediately after each TBI impact or sham surgery for mice analyzed at **(B)** 72 hours post-rmmTBI or sham surgery (n=5-7 mice per group). Mice subjected to sham surgery did not display apnea and are not shown. Both untreated TBI and TBI + ICAL mice experienced apnea but no significant differences were observed between these groups following TBI 1 (p=0.383), TBI 2 (p=0.822), or TBI 3 (p=0.261). Data are displayed as the mean ± SEM and are analyzed by an unpaired t-test for each TBI number. Righting reflex times for mice analyzed at **(C)** 72 hours post-rmmTBI were measured immediately following each mmTBI or sham surgery after anesthesia was discontinued (n=5-7 mice per group). Untreated TBI and TBI + ICAL mice had significantly increased righting reflex times compared to sham mice following TBI 1 (p<0.000), TBI 2 (p<0.000), and TBI 3 (p=0.001). No significant differences in righting reflex times were observed between untreated TBI and TBI + ICAL following any TBI. All righting reflex data are displayed as the mean ± SEM and are analyzed one-way ANOVA with post-hoc Tukey's test for each TBI number (** indicates p<0.01, *** indicates p<0.001, and NS indicates p>0.05 or nonsignificant).

3.4.5 Analysis of Immunocal®-Treatment Effects on Increases in Serum NfL

Induced by rmmTBI

Neurofilament light chain is a subunit of neurofilament proteins, scaffolding proteins that are highly expressed in myelinated axons. Increased NfL in serum are indicators of neuroaxonal injury resulting from neurodegeneration and rmTBI (Khalil et al., 2018; Ojo et al., 2015; Pham et al., 2021).

We evaluated if rmmTBI induced increased levels of serum NfL and if Immunocal®-treatment would prevent this. Serum was analyzed for NfL by ELISA all groups 72 hours post-rmmTBI. Untreated rmmTBI mice exhibited a significant increase of NfL versus sham mice ($p=0.035$). Immunocal®-treated rmmTBI mice did not significantly differ from untreated rmmTBI or sham mice (Figure 3.6). These data indicate that rmmTBI induced neuronal damage, however, Immunocal®-treatment did not significantly decrease this.

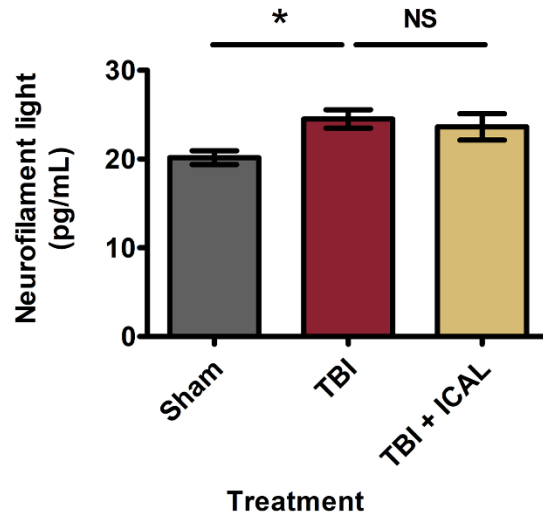


Figure 3.6 Repetitive Mild-Moderate Traumatic Brain Injury (rmmTBI) Results in Acute Neuronal Damage in Mice Analyzed at 72 Hours Post-Last mmTBI.

Quantification of neurofilament light (NfL) levels, an indication of acute neuronal damage, in serum detected by enzyme-linked immunosorbent assay from mice subjected to sham surgery (SHAM) and untreated mice (TBI) and Immunocal®-treated pre- and post-rmmTBI mice (TBI + ICAL) subjected to rmmTBI analyzed at 72 hours post-rmmTBI or sham surgery (n=4-5 mice per group). NfL levels were significantly elevated in untreated TBI mice when compared to sham mice (p=0.035), however, no differences were observed between untreated TBI and TBI + ICAL mice or TBI + ICAL and sham mice. Neurofilament light data are displayed as the mean ± SEM and are analyzed by a one-way ANOVA with post-hoc Tukey's test (* indicates p<0.05 and NS indicates p>0.05 or nonsignificant).

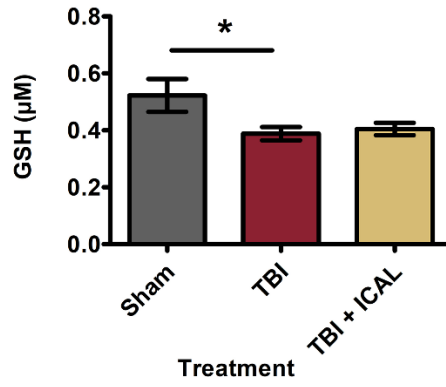
3.4.6 Analysis of Immunocal®-Treatment Effects on Changes in Brain GSH and GSSG Induced by rmmTBI

Glutathione, an endogenous antioxidant, can protect against reactive oxygen (ROS) and nitrogen species (RNS) and maintain redox homeostasis. Upon reacting with ROS/RNS, GSH oxidizes to GSSG. The ratio of GSH:GSSG is indicative of redox status (Dwivedi et al., 2020). Immunocal® contains cystine which can be converted to cysteine, the limiting substrate in GSH synthesis (Bannai & Tateishi, 1986; Ross et al., 2012) We have previously shown that Immunocal® enhances GSH synthesis in neurons and that a

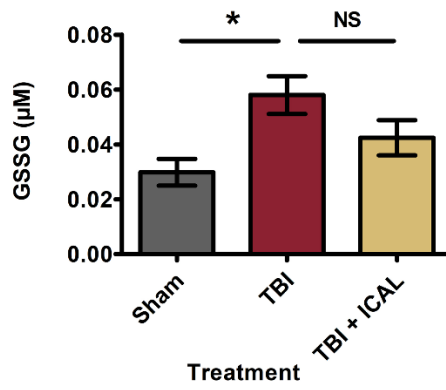
similar dosing regimen preserves GSH:GSSG in a mouse model of single moderate TBI (Ignowski et al., 2018; Ross et al., 2012; Ross et al., 2014; Winter et al., 2017b).

Therefore, GSH and GSSG were measured in brain from all groups analyzed 72 hours post-rmmTBI. A significant difference was found in GSH levels between all groups and, although a Tukey's *post-hoc* analysis did not identify differences, a Dunnett's Multiple Comparison test identified a significant GSH decrease in untreated rmmTBI versus sham mice ($p=0.046$; Figure 3.7A). Brain GSSG was significantly increased in untreated rmmTBI mice versus sham mice ($p=0.022$; Figure 3.7B). Immunocal®-treated rmmTBI mice showed no significant differences in GSH or GSSG versus untreated rmmTBI or sham mice. No significant differences in GSH:GSSG were observed between untreated and Immunocal®-treated rmmTBI mice although both groups showed a significant decrease versus sham mice ($p=0.003$; Figure 3.7C). It seems that rmmTBI decreases GSH and significantly increases GSSG, resulting in a decreased brain GSH:GSSG ratio, that Immunocal®-treatment did not alter.

A



B



C

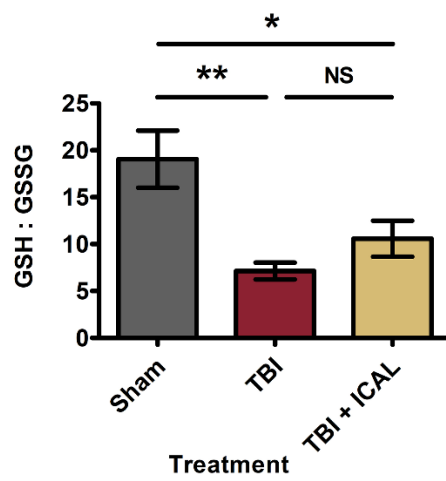


Figure 3.7 Repetitive Mild-Moderate Traumatic Brain Injury (rmmTBI) Reduced Glutathione (GSH) and Significantly Increased Glutathione Disulfide (GSSG) in Brain of Mice Analyzed at 72 hours Post-Last mmTBI. Quantification of GSH measured in brain homogenate isolated from mice subjected to sham surgery (SHAM) and untreated mice (TBI) and Immunocal®-treated pre- and post-rmmTBI mice (TBI + ICAL) exposed to rmmTBI analyzed at **(A)** 72 hours post-rmmTBI or sham surgery (n=5-6 mice per group). Glutathione (GSH) levels were significantly different between groups (p=0.046). A post-hoc Tukey's test was unable to identify which groups were significantly different but a post-hoc Dunnett's Multiple Comparison test identified a significant difference between untreated TBI and sham mice. All GSH data are displayed as mean ± SEM. Quantification of glutathione disulfide (GSSG) as measured in brain homogenate of sham, untreated TBI, and TBI + ICAL analyzed at **(B)** 72 hours post-rmmTBI or sham surgery (n=5-6 mice per group). Untreated TBI mice had significantly elevated levels of GSSG when compared to sham mice (p=0.022). No significant differences in GSSG levels were observed in TBI + ICAL mice when compared to untreated TBI mice or sham mice. All GSSG data are displayed as mean ± SEM and analyzed by a one-way ANOVA with post-hoc Tukey's test (* indicates p<0.05 and NS indicates p >0.05 or nonsignificant). The ratio of GSH:GSSG as measured in brain homogenate of sham, untreated TBI, and TBI + ICAL analyzed at **(C)** 72 hours post-TBI or sham surgery (n=5-6 mice per group). Both untreated TBI and TBI + ICAL mice had a significantly reduced ratio of GSH: GSSG when compared to sham mice (p=0.003). No significant differences were observed between untreated TBI mice and TBI + ICAL mice. GSH: GSSG data are displayed as the mean ± SEM and are analyzed by a one-way ANOVA with post-hoc Tukey's test (* indicates p<0.05, ** indicates p<0.01, and NS indicates p>0.05 or nonsignificant).

3.4.7 Immunocal®-Treatment Significantly Reduces Microgliosis at 72 Hours

After rmmTBI

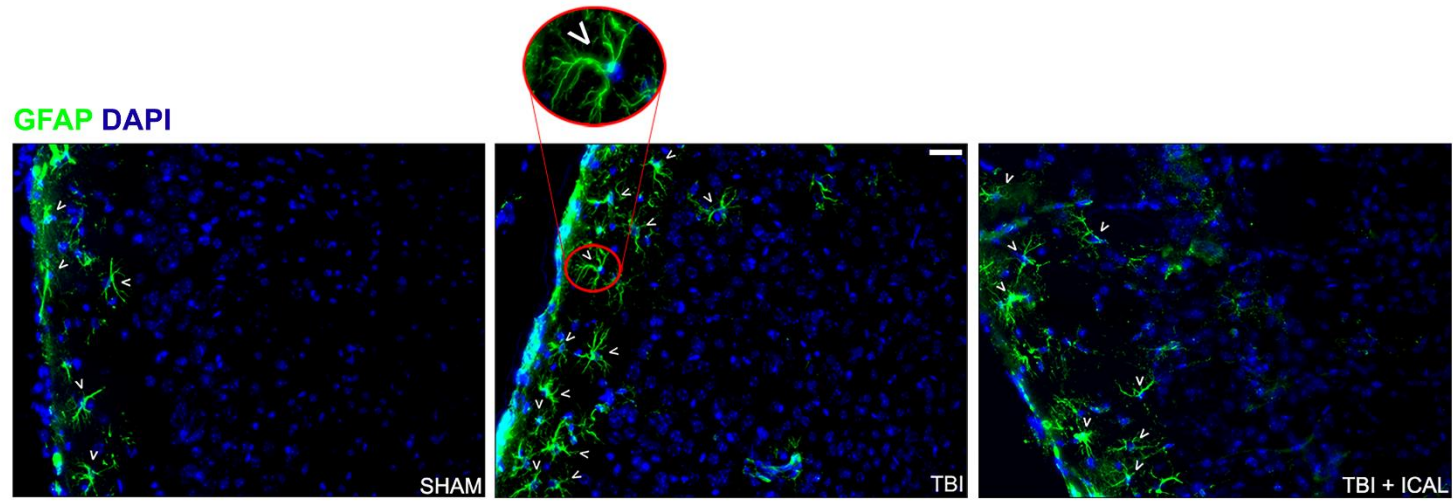
Astrogliosis, and prevention of astrogliosis with Immunocal® treatment were observed at 2 weeks and 2 months following rmTBI. We hypothesized that we would observe astrogliosis at a much earlier time point, 72 hours post-rmmTBI and evaluated if Immunocal®-treatment would attenuate this effect. Although microgliosis was not observed in the rmTBI model, we analyzed microgliosis to see if it was induced by a more severe rmmTBI model and if Immunocal®-treatment would mitigate this effect. Cortices from all groups were stained for GFAP, Iba-1, and Hoechst to analyze

astrogliosis, microgliosis, and nuclei, respectively 72 hours post-rmmTBI (Figure 3.8A and 3.9A). Astrocytes or microglia, counted as GFAP or Iba-1 (and Hoechst) positive cells, respectively, were quantified and averaged for all groups (Figure 3.8B and 3.9B).

A significant increase in the average number of astrocytes in cortex of untreated rmmTBI mice was observed versus sham mice at 72 hours post-rmmTBI ($p=0.033$, Figure 3.8B). However, Immunocal®-treatment did not significantly reduce the average number of astrocytes versus untreated rmmTBI mice at this time point.

Interestingly, a significant increase in the average number of microglia in the cortex of untreated rmmTBI mice was observed versus sham mice at 72 hours post-rmmTBI ($p=0.021$; Figure 3.9B). Immunocal®-treated rmmTBI mice showed a significantly decreased average number of microglia versus untreated rmmTBI mice and no difference from sham mice ($p=0.021$). Both astrogliosis and microgliosis are present in the cortex of mice 72 hours post-rmmTBI, however, Immunocal® only prevents microgliosis at this early time point.

A



B

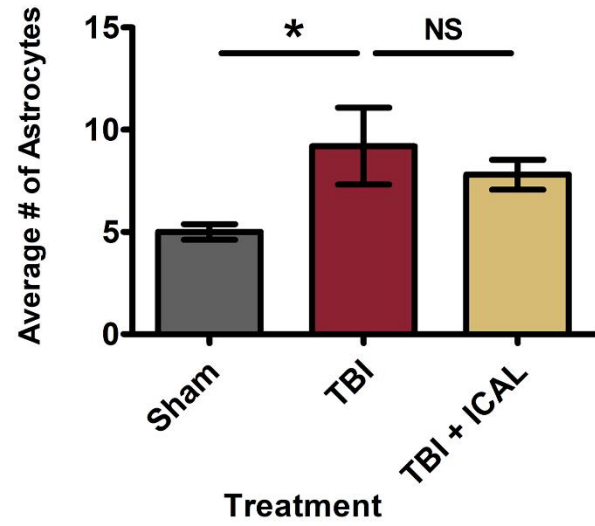
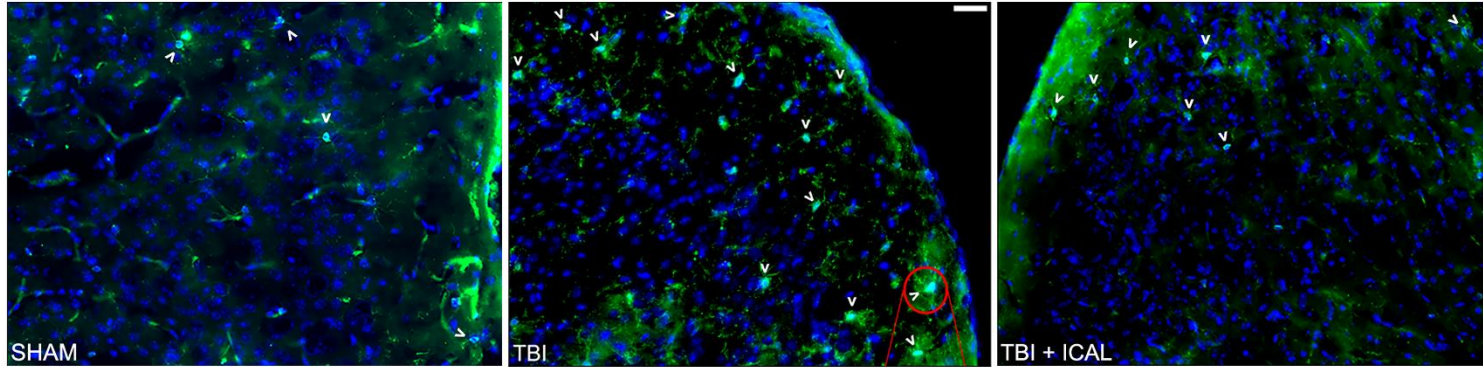


Figure 3.8 Significant Astrogliosis Present in the Cortex of Mice Subjected to Repetitive Mild-Moderate-Traumatic Brain Injury (rmmTBI) When Analyzed at 72 Hours Post-ast mmTBI. Representative images of cortex stained for glial fibrillary acidic protein (GFAP; green) and DAPI (blue), to label astrocytes and nuclei, respectively, from mice subjected to sham surgery (SHAM) and untreated mice (TBI) and Immunocal®-treated pre- and post-rmmTBI mice (TBI + ICAL) exposed to rmmTBI analyzed at **(A)** 72 hours post-rmmTBI. White arrows indicate GFAP and DAPI positive cells, counted as astrocytes. Scale bar=20µm. Quantification of the average number of astrocytes in cortex stained with GFAP and DAPI, as described in **(A)** is shown for sham, TBI + ICAL, and untreated TBI mice analyzed at **(B)** 72 hours post-rmmTBI (5-7 mice per group). The average number of astrocytes in the cortex of untreated TBI mice was significantly increased compared to sham mice ($p=0.033$). No significant differences were observed between TBI + ICAL mice versus sham or untreated TBI mice. Astrocyte quantification data are displayed as the mean \pm SEM and are analyzed by a one-way ANOVA with post-hoc Tukey's test (* indicates $p<0.05$ and NS indicates $p>0.05$ or nonsignificant).

A

Iba-1 DAPI



B

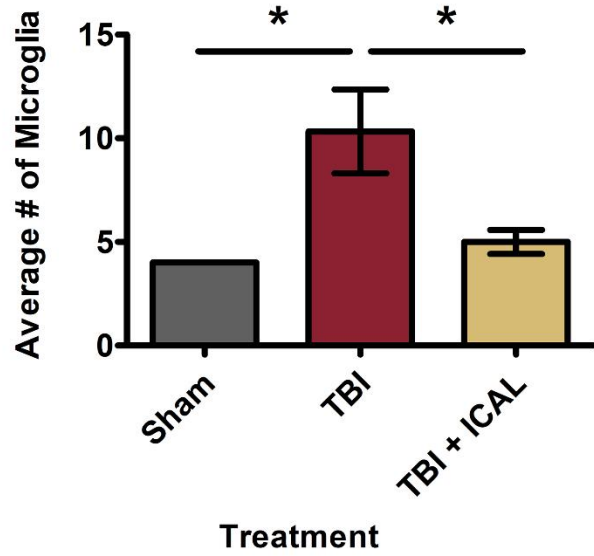


Figure 3.9 Immunocal®-Treatment Pre- and Post-Repetitive Mild-Moderate TBI (rmmTBI) Significantly Reduced Microgliosis in the Cortex of Mice When Analyzed at 72 Hours Post-Last mmTBI. Representative images of cortex stained for ionized calcium-binding adapter molecule 1 (Iba-1; green) and DAPI (blue), to label microglia and nuclei, respectively, from mice subjected to sham surgery (SHAM) and untreated mice (TBI) and Immunocal®-treated pre- and post-rmmTBI mice (TBI + ICAL) exposed to rmmTBI analyzed at (A) 72 hours post-rmmTBI. White arrows indicate Iba-1 and DAPI positive cells, counted as microglia. Scale bar=20µm. Quantification of the average number of microglia in cortex stained with Iba-1 and DAPI, as described in (A) is shown for sham, TBI, and TBI + ICAL mice analyzed at (B) 72 hours post-rmmTBI (n=3 mice per group). The average number of microglia in cortex of untreated TBI mice was significantly increased compared to sham mice (p=0.021). Immunocal®-treatment pre- and post-rmmTBI significantly reduced the average number of microglia in the cortex at this time point when compared to untreated TBI mice (p=0.021). No significant differences in the average number of microglia were observed between TBI + ICAL mice versus sham mice. Microglia quantification data are displayed as the mean ± SEM and are analyzed as a one-way ANOVA with post-hoc Tukey's test (* indicates p<0.05).

3.5 Discussion

There is a need for preventative and restorative treatments for individuals at high-risk for rTBI. Although symptoms may not arise or subside following rTBI, pathology may persist (Dhillon et al., 2020; Bramlett & Dietrich, 2015; Mouzon et al., 2017). Repetitive mTBI can cause cumulative injury to the brain, resulting in an enhanced susceptibility to neurodegeneration (Edwards et al., 2017; Faden & Loane, 2015; Gao et al., 2017). We investigated Immunocal®, a whey protein supplement shown to preserve brain GSH and provide neuroprotection in a mouse model of single moderate TBI, as a preventative and restorative treatment in models of rTBI (Ignowski et al., 2018; Ross et al., 2012; Winter et al., 2017b). First, mice were administered Immunocal® for 28 days prior to, during, and following CCI rTBI. Brain was analyzed for BBB disruption/edema and macrophage activation by MRI at 2 months post-rmTBI and cortex for astrogliosis and microgliosis by immunohistochemistry at 2 weeks, 2 months, and 6 months post-rmTBI.

We repeated the study design using a more severe rmmTBI model and analyzed cortex again for microgliosis and astrogliosis, serum for NfL, and brain GSH and GSGG to measure more extensive damage and potential neuroprotection with Immunocal® treatment earlier at 72 hours post-rmmTBI.

We observed significant astrogliosis, but not microgliosis, in cortex around the injury site at 2 weeks and 2 months post-rmTBI which Immunocal® significantly reduced. Mouzon et al. (2014) also did not report microgliosis in the cortex at 6 and 12 months post-rmTBI, however, microgliosis in corpus callosum was observed at these timepoints (Mouzon et al., 2014). Microgliosis in cortex in rmTBI mouse models is not observed chronically (Fidan et al., 2016; Hoogenboom et al., 2019). The rmTBI model may not be severe enough to elicit prolonged microgliosis in cortex. Microglia display heterogeneity in brain and increased numbers are observed in the substantia nigra, dentate gyrus, basal ganglia, and olfactory bulb in mice (Lawson et al., 1992; Tan, Y. L., et al., 2020). Microgliosis could have been present in sensitive areas or may subside before 2 weeks following rmTBI.

Macrophage infiltration was observed 2 months post-rmTBI by MRI. However, no significant edema was observed. Furthermore, we quantified Iba-1 positive cells as microglia, so the observed macrophage activation could be due to supraependymal, epileptus, or pericyte cells, which reside near the injury (Jordan & Thomas, 1988).

We observed a more robust injury response to rmmTBI. Clinically, NfL in serum is elevated following rTBI (Al Nimer et al., 2015; Hossain et al., 2019; Shahim et al., 2017b; Shahim et al., 2020). We've shown that rmmTBI increases NfL in serum from

mice 72 hours post-rmmTBI, although Immunocal®-treatment had no effect. We also observed increased astrogliosis and microgliosis in cortex in response to rmmTBI. Similarly, astrogliosis and microgliosis in cortex 1-7 days post-TBI is reported following more severe rTBI (Chen, H., et al., 2017; Petraglia et al., 2014). Interestingly, Immunocal®-treatment only prevented microgliosis in this model.

Lastly, we measured a decreased GSH:GSSG ratio at 72 hours post-rmmTBI. Increased oxidative stress in brain results from TBI and leads to antioxidant depletion and cell death (Cornelius et al., 2013; Morris, G., et al., 2019). Glutathione is an endogenous antioxidant that maintains redox homeostasis in brain. We did not observe GSH preservation or an increased GSH:GSSG ratio in Immunocal®-treated rmmTBI mice. We have previously shown that Immunocal® pre-treatment prevented an approximately 25% reduction in brain GSH:GSSG in a single moderate TBI mouse model (Ignowski et al., 2018). The repetitive nature of the model used here may cause sustained oxidative stress. Therefore, Immunocal® was unable to keep up with the increased oxidative burden and sustain brain GSH.

We observed that Immunocal®-treatment significantly limited astrogliosis in the rmTBI model and microgliosis in the rmmTBI model. Immunocal® offers its therapeutic effects through enhancing GSH synthesis, however, astrocytes and microglia synthesize GSH differently. Lindenau et al. (1998) reported increased GSH peroxidase (GPx) localization and activity was only measured in activated astrocytes following excitotoxicity but not in resting astrocytes (Lindenau et al., 1998). However, GPx localizes to resting microglia and more activity was observed in activated microglia

versus astrocytes. Higher GPx activity is beneficial in protecting microglia from ROS produced intrinsically or by nearby microglia (Lindenau et al., 1998). Astrocytes produce GSH to support neurons and increase GSH in neurons when cultured together (Dringen et al., 1999). Microglia synthesis of GSH is coupled to glutamate uptake which may be abundant following injury. Persson et al. (2006) reported that, in response to toxins, GSH synthesis and release was protective to microglia (Persson et al., 2006). Microglia may become resilient through GSH synthesis whereas astrocytes synthesize GSH to protect neurons. Furthermore, microglia have a higher cytosolic concentration of GSH in culture than either astrocytes or neurons (Chatterjee et al., 1999; Hirrlinger et al., 2000). In the more severe model of rmmTBI, a decrease in microgliosis and not astrogliosis may result from Immunocal® supplementation because microglia synthesize GSH for their own protection.

Although this study is beneficial in that it further characterizes pathology induced by rmTBI and rmmTBI and highlights the ability of Immunocal® supplementation to reduce gliosis in these models, there are limitations. The present study only used male mice, however, further preclinical study should use both sexes. Furthermore, this study should be followed up with a more thorough analysis of oxidative stress and inflammatory biomarkers in brain taken at regular intervals from both the rmTBIs and rmmTBIs to see what effect Immunocal® supplementation has on reducing lipid peroxidation, DNA damage, and pro-inflammatory cytokine production.

In summary, rmTBI can induce lasting gliosis out to 2 months post-rmTBI. Furthermore, inflammation, neuronal damage, and altered redox homeostasis present

acutely following rmmTBI. These findings support the use of easily administered preventative and restorative treatments, such as Immunocal®, for patients at high-risk for rTBI. Preventative and restorative Immunocal® supplementation for rmTBI and rmmTBI significantly limited gliosis. However, we believe that the repetitive nature of these models induces pathology that cannot be ameliorated by a single agent. Additional treatments (e.g., anti-glutamatergic compounds, lipid-based free radical scavengers like vitamin E or omega-3 fatty acids, and mitochondrial protective agents), used with a GSH precursor such as Immunocal®, may produce a synergistic therapeutic effect in more severe models of rTBI. The data presented here are important in that they show the limits of GSH-based neuroprotection in repetitive models of TBI. As shown previously, Immunocal® supplementation offers significant neuroprotection and brain GSH preservation in single moderate TBI and for rmTBI³². However, pathology induced by repetitive TBI of increased severity exceeds the treatment capacity of a single-agent like Immunocal®

**CHAPTER FOUR: PROTOCATECHUIC ACID EXTENDS SURVIVAL,
IMPROVES MOTOR FUNCTION, DIMINISHES GLIOSIS, AND SUSTAINS
NEUROMUSCULAR JUNCTIONS IN THE hSOD1^{G93A} MOUSE MODEL OF
AMYOTROPHIC LATERAL SCLEROSIS**

4.1 Abstract

Amyotrophic lateral sclerosis (ALS) is a devastating disorder characterized by motor neuron apoptosis and subsequent skeletal muscle atrophy caused by oxidative and nitrosative stress, mitochondrial dysfunction, and neuroinflammation. Anthocyanins are polyphenolic compounds found in berries that possess neuroprotective and anti-inflammatory properties. Protocatechuic acid (PCA) is a phenolic acid metabolite of the parent anthocyanin, kuromanin, found in blackberries and bilberries. We explored the therapeutic effects of PCA in a transgenic mouse model of ALS that expresses mutant human Cu, Zn-superoxide dismutase-1 with a glycine to alanine substitution at position 93. These mice display skeletal muscle atrophy, hindlimb weakness, and weight loss. Disease onset occurs at approximately 90 days old and end stage is reached at approximately 120 days old. Daily treatment with PCA (100mg/kg) by oral gavage beginning at disease onset significantly extended survival (121 days old in untreated vs. 133 days old in PCA-treated) and preserved skeletal muscle strength and endurance as assessed by grip strength testing and rotarod performance. Furthermore, PCA reduced astrogliosis and microgliosis in spinal cord, protected spinal motor neurons from

apoptosis, and maintained neuromuscular junction integrity in transgenic mice. PCA lengthens survival, lessens the severity of pathological symptoms, and slows disease progression in this mouse model of ALS. Given its significant preclinical therapeutic effects, PCA should be further investigated as a treatment option for patients with ALS.

4.2 Introduction

Amyotrophic lateral sclerosis (ALS), also known as Lou Gehrig's disease, is a devastating, progressive, and fatal neurodegenerative disease that affects motor neurons of the central nervous system. ALS patients exhibit a median survival of only 2–3 years following diagnosis, with death typically caused by respiratory failure (Oskarsson et al., 2018). ALS presents as either a sporadic or familial disease. Sporadic ALS cases account for approximately 90% of all patients and do not have an obvious genetic cause. Familial ALS accounts for the remaining 10% of patients and has been linked to mutations in genes such as Cu, Zn-superoxide dismutase-1 (SOD-1), chromosome 9 open reading frame 72 (C9orf72), fused in sarcoma, and TAR DNA-binding protein-43 (TDP-43) (Kumar, V., et al., 2019). Although ALS is classified as a rare disease, with a prevalence of 5 in 100,000 people living in the United States, the effects of the disease are calamitous for those who are afflicted (Oskarsson et al., 2018).

ALS is characterized pathologically by the death of motor neurons, axonal retraction away from the neuromuscular junctions (NMJs), skeletal muscle atrophy, and ultimately, death. The pathogenesis underlying both familial and sporadic forms of ALS has been extensively studied but is still not completely understood. Protein aggregation, disrupted axonal transport, perturbed RNA metabolism, excitotoxicity, neuroinflammation,

mitochondrial dysfunction, and oxidative stress have all been identified as underlying mechanisms and contributing factors in ALS. In the context of motor neuron degeneration, neuroinflammation and oxidative stress appear to be major pathogenic mechanisms. Both astrocytes and microglia can adopt distinct anti- or pro-inflammatory phenotypes, depending on signals from the surrounding environment. These anti- or pro-inflammatory phenotypes are neuroprotective or neurotoxic to motor neurons, respectively. Astrocytes, although beneficial to neurons in their resting state, become reactive and contribute to motor neuron death in various models of ALS (Diaz-Amarilla et al., 2011; Haidet-Phillips et al., 2011; Ramírez-Jarquín et al., 2017; Tyzack et al., 2017). Reactive astrocytes have also been shown to impair the process of autophagy in motor neurons, resulting in increased protein aggregation and reduced motor neuron health in *in vivo* and *in vitro* models of ALS (Madill et al., 2017; Rudnick et al., 2017; Tripathi et al., 2017). Microglia also contribute significantly to the neuroinflammation in ALS. Microglia have been shown to induce astrocyte reactivity by releasing pro-inflammatory cytokines, resulting in an inability of astrocytes to protect motor neurons (Liddel et al., 2017; Meissner et al., 2010). Microglia also become pro-inflammatory and have been found to display an ALS-specific phenotype that contributes to rapid disease progression and increased motor neuron loss (Brettschneider et al., 2012; Chiu et al., 2013; Graber et al., 2010; Xiao et al., 2007).

Oxidative stress is another mechanism that has been identified as a causative factor in ALS. Increased oxidative stress burden correlates positively with disease severity (D'Amico et al., 2013; Ikawa et al., 2015). Superoxide and nitric oxide have been found

to be elevated in ALS (Almer et al., 1999; Lee, J., et al., 2009). Oxidative stress markers such as glutathione peroxidase, malondialdehyde, glutathione status, and 8-oxodeoxyguanosine demonstrate significant alterations in ALS patients (Mitsumoto et al., 2008; Blasco et al., 2017). Furthermore, mitochondrial dysfunction and mutations in genes that affect mitochondrial processes have been linked to ALS (Carrì et al., 2017; Lopez-Gonzalez et al., 2016; Palomo & Manfredi, 2015; Pickles et al., 2016; Walczak et al., 2019). Specifically, in the case of ALS caused by mutations in SOD-1, the mutant SOD-1 protein has been shown to aggregate within mitochondria, resulting in mitochondrial dysfunction and mitochondrial oxidative stress (Abu-Hamad et al., 2017; Pickles et al., 2016). Given the above findings, a beneficial therapeutic approach for ALS may be to reduce both neuroinflammation and oxidative stress.

Currently, only two drugs, Riluzole and Edaravone, have been approved by the U.S. Food and Drug Administration (FDA) to treat ALS. Riluzole is administered orally, only has a modest effect on slowing disease progression, and shows an extension of life of only a few months (Kumar, V., et al., 2019). Edaravone has been shown to delay disease progression by only 33% when compared to a placebo, is costly, and must be administered intravenously (Bhandari et al., 2018). Unfortunately, both Riluzole and Edaravone have only modest effects on disease progression and survival. Furthermore, both drugs are expensive and display substantial side effects. Many other therapeutics have failed in the clinic or are still undergoing clinical trials. However, no new pharmacological therapies are immediately on the horizon for ALS patients.

Nutraceuticals, natural bioactive compounds found in foods, may be safe, easy to administer, and cost-effective therapeutic treatments for ALS. More specifically, anthocyanins, a type of flavonoid, may be beneficial to ALS patients due to their substantial antioxidant and anti-inflammatory properties (Kelsey et al., 2011). Anthocyanins vary in color from red to blue and are responsible for the vibrant coloring of many fruits and vegetables (Murukan & Murugan, 2018). We have previously demonstrated a therapeutic effect of an anthocyanin-enriched strawberry extract in a transgenic mouse model of ALS that expresses mutant human SOD-1 with a glycine to alanine substitution at position 93 (hSOD1^{G93A}; Winter et al., 2018). This strawberry extract is enriched in callistephin, an anthocyanin derived from pomegranates and strawberries (Kelsey et al., 2011; Winter et al., 2017c). We have also shown that callistephin suppresses apoptosis induced by mitochondrial oxidative stress and protects neurons from glutamate excitotoxicity in vitro (Kelsey et al., 2011; Winter et al., 2017c). *In vivo*, we found that hSOD1^{G93A} mice treated with strawberry anthocyanin extract beginning at 60 days old showed delayed disease onset, improved grip strength throughout the disease, and significantly extended survival when compared to untreated hSOD1^{G93A} littermate mice. Furthermore, treated mice displayed significantly decreased astrogliosis in the spinal cord and preserved NMJs in gastrocnemius muscle when compared to untreated littermate mice (Winter et al., 2018). These findings indicate that anthocyanin compounds may have therapeutic potential in ALS. However, despite their potential benefits, parent anthocyanins suffer from poor bioavailability. In contrast, their

phenolic acid metabolites typically display much higher bioavailability and most can readily cross the blood brain barrier (Losada-Barreiro et al., 2017).

Here, we examined the therapeutic potential of protocatechuic acid (PCA) in the hSOD1^{G93A} preclinical mouse model of ALS. PCA is a phenolic acid metabolite of kuromanin, the parent anthocyanin found in blackberries, bilberries, and black rice. We have previously shown that kuromanin protects neurons from oxidative stress induced by glutamate excitotoxicity, nitrosative stress induced by nitric oxide, and it also suppresses mitochondrial oxidative stress and the consequent apoptosis by preserving mitochondrial glutathione (Kelsey et al., 2011; Winter et al., 2017c). In a similar manner, PCA protects neurons against nitrosative and oxidative stress and reduces nitric oxide production in microglial cells treated with lipopolysaccharide, demonstrating both antioxidant and anti-inflammatory activities (Winter et al., 2017a). Based on our previous findings, we tested the therapeutic effects of PCA in the hSOD1^{G93A} mouse model of ALS.

4.3 Materials and Methods

4.3.1 The hSOD1^{G93A} Mouse Model of ALS

FVB/NJ mice harboring a human transgene coding for a mutated form of SOD-1 with a glycine to alanine substitution at position 93 were obtained from The Jackson Laboratory (Bar Harbor, ME, USA). Mice were bred and maintained at the University of Denver animal facility under a standard 12h light/dark cycle with food and water provided *ad libitum*. Genotyping to identify transgenic mice was carried out by a third-party company, Transnetyx Inc. (Cordova, TN, USA). All procedures were performed in accordance with two protocols approved by the institutional animal care and use

committee at the University of Denver. The initial protocol (927091) was approved on 21 July 2016 and the second protocol (1454889) was approved on 12 July 2019.

4.3.2 Survival Data

For the survival study, mice were divided into four groups consisting of 15 mice each. The first group consisted of non-transgenic wild-type (WT) age- and sex-matched littermate controls. The other three groups consisted of age- and sex-matched transgenic hSOD1^{G93A} littermate mice, either untreated or treated with either 50 or 100mg/kg PCA. PCA was dissolved in sterile deionized water and was administered once per day as a 0.25mL dose by oral gavage 5 days/week. Oral gavage treatment of PCA began at disease onset (90 days of age) and continued until mice reached end stage, defined as the point at which a mouse no longer had the ability to right itself within 15s after being placed on its side. PCA-treated and untreated hSOD1^{G93A} littermate mice were euthanized at end stage by an overdose of inhaled isoflurane (Vet One, Boise, ID, USA). The WT littermate control mouse was euthanized at end stage of whichever hSOD1^{G93A} littermate mouse lived the longest, regardless of treatment.

4.3.3 Paw Grip Endurance and Rotarod Testing

Hind limb strength was assessed by paw grip endurance (PaGE) testing twice per week beginning at disease onset. Briefly, mice were placed on top of a standard wire cage lid which was suspended a few inches above the bench top. Mice were briefly allowed to acclimate before the cage lid was smoothly inverted to prompt the mouse to grip the wire with both its fore and hind limbs. A stopwatch was started as soon as the cage lid was inverted and the time was measured to determine how long the mouse could hold on

before its hind legs released their grip from the cage lid, expressed as latency to fall. Care was taken not to jostle the lid during this time. The stopwatch was stopped at a maximum of 30s. Mice were given five scored attempts and the highest and lowest scores were excluded from the final score. Final scores are reported as an average of the three remaining scored attempts \pm standard error of the mean (SEM) for each time point. Time points correspond to the age of the animal at the time that testing was performed and are reported as a range of several days since multiple sets of animals having slightly different ages were tested concomitantly.

Motor function and endurance were assessed by accelerating rotarod testing once per week beginning at disease onset. Mice were placed on a rod, 30mm in diameter, rotating at 4rpm. Each animal was placed in one lane and subjected to three trials. The lane was cleaned before the next mouse was tested to prevent interference. Once the mice were acclimated to the initial speed of 4rpm, the rod was accelerated from 4 to 40rpm over the course of 5min. The time was stopped when the mouse fell off the rotating rod, expressed as latency to fall. Mice were given three scored attempts reported as an average \pm SEM for each time point. Time points correspond to the age of the animal at the time that testing was performed and are reported as a range of several days since multiple sets of animals having slightly different ages were tested concomitantly.

4.3.4 Analysis of Mice at End Stage of the Untreated hSOD1^{G93A} Littermate Mouse

For assessment of Nissl-stained motor neuron counts, glial fibrillary acidic protein (GFAP) and ionized calcium-binding adapter molecule 1 (Iba-1) staining, NMJ area,

perimeter, and Sholl analysis, mice were divided into three groups consisting of approximately 10 mice per group. The first group consisted of non-transgenic WT age- and sex-matched littermate controls. The other two groups consisted of age- and sex-matched transgenic hSOD1^{G93A} littermate mice, either untreated or treated with 100mg/kg PCA orally as described above. PCA treatment continued until the untreated hSOD1^{G93A} littermate mouse reached end stage. At that point, mice from all 3 groups were euthanized and spinal cord and gastrocnemius muscles were collected.

4.3.5 Analysis of Mice at 105 Days of Age

We observed the greatest improvements in motor function as assessed by rotarod and PaGE testing between 97 and 114 days of age in PCA-treated hSOD1^{G93A} mice. Therefore, we analyzed the gastrocnemius muscle wet weight, vesicular acetylcholine transporter (VAChT) and alpha-bungarotoxin (BTx) co-stained gastrocnemius muscle, and 4-hydroxynonenal (4-HNE)-stained spinal cord ventral horn from a separate cohort of mice at 105 days of age. This cohort consisted of both WT and hSOD1^{G93A} mice with or without PCA treatment, with each treatment group containing approximately 10 mice. Mice receiving PCA were given a daily dose of 100mg/kg beginning at 90 days of age and continuing until the mice reached 105 days of age. At 105 days of age, mice from all 3 groups were euthanized and gastrocnemius muscles and lumbar spinal cord were collected.

4.3.6 Tissue Preparation and Cryosectioning

Following euthanasia, the thoracolumbar portion of the spinal column, containing the lumbar spinal cord, and gastrocnemius muscle were removed. Each specimen was

washed with 1X phosphate-buffered saline (PBS, pH 7.4), and placed in 4% paraformaldehyde at 4°C overnight. Each specimen was then washed again and allowed to sit in 1X PBS for 20min. Gastrocnemius muscle was placed in 30% sucrose in 1X PBS and allowed to sink for cryoprotection. The lumbar spinal cord was placed in 6% trichloroacetic acid (Sigma-Aldrich, St. Louis, MO, USA) in deionized water for 6 days for decalcification. Following decalcification, the lumbar spinal cord was placed in 30% sucrose until saturated. Both gastrocnemius muscle and spinal cord were frozen rapidly in optimal cutting temperature (OCT) compound with liquid nitrogen and stored at -80°C until sectioning took place. Prior to sectioning, tissue was allowed to acclimate in the microtome cryostat for at least 20min. For gastrocnemius muscle and spinal cords, sections of 30µm in length were cut and every viable tissue section was collected onto the surface of Fisherbrand Superfrost Colorfrost Plus coated slides (Fisher Scientific, Pittsburgh, PA, USA). Slides were stored at -20°C until subjected to immunohistochemistry.

4.3.7 Immunohistochemistry of Spinal Cord Sections

Prior to staining, slides were allowed to equilibrate at room temperature for at least 30min. Tissue sections on the slides were then outlined with a hydrophobic pen (Liquid Blocker Super PAP Pen; Daido Sangyo Co., Tokyo, Japan) and washed twice with 1X PBS to remove any residual OCT. Tissue was then incubated at room temperature in blocking buffer, containing 5% (w/v) bovine serum albumin (BSA) and 1X PBS containing 0.2% triton-X 100 for 90min. For astrocyte staining, primary antibody to GFAP (Abcam, Cambridge, MA, USA) was then prepared as a 1:500 dilution in 1X PBS

containing 0.2% triton-X 100 and 2% BSA (w/v). For microglial staining, primary antibody to Iba-1 (Abcam, Cambridge, MA, USA) was prepared as a 1:167 dilution in PBS containing 0.2% triton-X 100 and 2% BSA (w/v). For 4-HNE staining, primary antibody to 4-HNE (Alpha Diagnostic Intl. Inc., San Antonio, TX, USA) was prepared as a 1:500 dilution in PBS containing 0.2% triton-X 100 and 2% BSA (w/v). Tissue was incubated in primary antibody overnight at 4°C. Tissue was washed 3–4 times with 1X PBS to remove any unbound primary antibody. FITC-conjugated donkey anti-rabbit antibody (Jackson ImmunoResearch Laboratories, West Grove, PA, USA) or Alexa Fluor 488-conjugated donkey anti-goat antibody (Jackson ImmunoResearch Laboratories, West Grove, PA, USA) were then prepared at 1:500 dilutions (v/v) in 1X PBS containing 0.2% triton-X100 and 2% BSA (w/v) and Hoechst nuclear stain (Sigma-Aldrich, St. Louis, MO, USA) at a 1:500 dilution to detect GFAP and Iba-1, and to label nuclei, respectively. For 4-HNE staining, FITC-conjugated donkey anti-rabbit antibody (Jackson ImmunoResearch Laboratories, West Grove, PA, USA) was prepared at 1:500 dilution (v/v) in 1X PBS containing 0.2% triton-X100 and 2% BSA (w/v) and Hoechst nuclear stain (Sigma-Aldrich, St. Louis, MO, USA) at a 1:500 dilution to detect 4-HNE and to label nuclei, respectively. Sections were incubated with secondary antibodies at room temperature for 90min, then washed 3–4 times with 1X PBS. ProLong Gold anti-fade reagent (Thermo Fisher Scientific, Eugene, OR, USA) was used as mounting medium and slides were sealed with coverslips. Stained slides were stored in the dark at –20°C until imaging took place. Twelve sections of spinal cord were stained for Iba-1, GFAP, and 4-HNE per mouse.

4.3.8 Imaging and Quantification of Spinal Cord Sections Stained for Iba-1 and GFAP at End Stage of the Untreated hSOD1^{G93A} Littermate Mouse

Tissue was imaged using a Zeiss Axio Observer epifluorescence microscope to capture a single image of each ventral horn on the 20X objective. Imaging was performed by blinded researchers. For Iba-1 and GFAP, images were captured on the Alexa Fluor 488 channel and the exposure time was set appropriately for the untreated hSOD1^{G93A} littermate and kept constant when imaging the PCA-treated hSOD1^{G93A} and WT littermate mice. At least 6 ventral horns per animal were imaged and analyzed for fluorescence intensity using Adobe Photoshop CC software for both Iba-1 and GFAP staining. For both Iba-1 and GFAP quantification, the ventral horn image of the untreated hSOD1^{G93A} littermate control mouse with the most background was chosen, and the green channel input level was adjusted so that background staining was best eliminated. This value was recorded and used for each subsequent image, including those taken from the WT control littermate and the PCA-treated hSOD1^{G93A} littermate mice such that all images were adjusted by an equivalent amount. After the channel levels were adjusted, the ventral horn was outlined using the lasso tool and green channel values for mean pixel intensity and pixel area were recorded for each ventral horn image. Total pixel intensity of the green channel was obtained by multiplying the pixel intensity and pixel area. An average of the total pixel intensity was taken for each mouse. Quantification was performed twice by two different and blinded researchers. An average of the pixel intensities for each mouse was obtained. For analysis, the average total pixel intensity for the WT littermate control mouse for each group was set at 100% and the average total

pixel intensities for the untreated hSOD1^{G93A} littermate control and PCA-treated hSOD1^{G93A} littermate mice were calculated as percentages relative to the WT littermate control mouse. Mean raw GFAP and Iba-1 fluorescence intensity in the lumbar spinal cord ventral horn in the untreated hSOD1^{G93A} littermate mice and WT littermate mice were also counted and statistically compared to verify a significant disease effect.

4.3.9 Nissl Staining of Spinal Cord Sections

Prior to staining, slides were allowed to equilibrate at room temperature for at least 30min. Slides were then washed twice with 1X PBS to remove any residual OCT. Tissue was then incubated in 70% ethanol and then 95% ethanol for 3 min each. Slides were then incubated in 100% ethanol for 3min and then 5 min, changing the ethanol between each incubation. Slides were then washed in deionized water 3–4 times. A Cresyl Violet Counterstain Solution (Bioenno Tech, Santa Anna, CA, USA) was applied to each slide for 3min. De-staining was then performed by washing briefly in 70mM acetic acid solution. Slides were rinsed in deionized water 3 times. Lastly, slides were incubated sequentially in solutions of 70%, 95%, and 100% ethanol as described above. Slides were mounted with ProLong Gold anti-fade reagent and were sealed with coverslips. Stained slides were stored in the dark at –20°C until imaging took place. Two slides from each mouse spinal cord were stained for Nissl with 6 sections per slide.

4.3.10 Imaging and Quantification of Nissl-Stained Spinal Cord Sections at End Stage of the Untreated hSOD1^{G93A} Littermate

A single image of each ventral horn was captured on the 20X objective using bright field by blinded researchers. At least six ventral horns for each mouse were imaged. Any

neuron greater than 20 μ m in length along its longest axis was considered to be a viable alpha motor neuron. Using Adobe Photoshop CC, the contrast was set to the WT littermate and kept the same within the group to ensure consistency in staining. Next, the ruler tool was used to measure all motor neurons greater than 20 μ m. For each mouse, the average number of alpha motor neurons was taken. Quantification was performed twice by two different and blinded researchers. Each average of the untreated hSOD1^{G93A} littermate and 100mg/kg PCA-treated hSOD1^{G93A} littermate mouse were calculated as a percent of the average of the WT littermate control mouse (set at 100%). The mean numbers of alpha motor neurons in the lumbar spinal cord ventral horn in the untreated hSOD1^{G93A} littermate mice and WT littermate mice were also statistically compared to verify a significant disease effect.

4.3.11 Alpha-Bungarotoxin and VAcHT Staining of Gastrocnemius Sections

Prior to staining, slides were allowed to equilibrate at room temperature for at least 30min. Tissue sections on the slides were then outlined with a hydrophobic pen and washed twice with 1X PBS to remove any OCT. Tissue was then incubated at room temperature in blocking buffer, containing 5% (w/v) BSA and 0.2% triton-X 100 in 1X PBS for 90min. For analysis of NMJ area, perimeter, and complexity, the slides were then incubated for 90min with alpha-BTx conjugated to Alexa Fluor® 594 (ThermoFisher Scientific Inc., Rockford, IL, USA) at a 1:200 dilution in blocking buffer containing Hoechst nuclear stain at a dilution of 1:500. For analysis of NMJ innervation, slides were stained with primary antibody to VAcHT (C-terminal) (Sigma-Aldrich, St. Louis, MO, USA) which was prepared as a 1:500 dilution in PBS containing 0.2% triton-

X 100 and 2% BSA (w/v). Tissue was incubated in primary antibody overnight at 4°C. FITC-conjugated donkey anti-rabbit antibody (Jackson ImmunoResearch Laboratories, West Grove, PA, USA) was then prepared at a 1:500 dilution (v/v) and alpha-BTx conjugated to Alexa Fluor® 594 (ThermoFisher Scientific Inc., Rockford, IL, USA) was prepared at a 1:200 dilution in 1X PBS containing 0.2% triton-X100 and 2% BSA (w/v) and Hoechst nuclear stain (Sigma-Aldrich, St. Louis, MO, USA) at a 1:500 dilution to detect VAcHT on the presynaptic axon terminal, NMJs, and to label nuclei, respectively. Slides were washed with 1X PBS 3–4 times and then mounted using ProLong Gold anti-fade reagent and sealed with coverslips. Stained slides were stored in the dark at –20°C until imaging took place.

4.3.12 Imaging and Area, Perimeter, and Sholl Analysis Quantification of Gastrocnemius Sections Stained with Alpha-Bungarotoxin at End Stage of the Untreated hSOD1^{G93A} Littermate Mouse

Neuromuscular junctions (20–25) were imaged for each mouse by blinded researchers on the 40X objective for all mice that were euthanized at end stage of the untreated hSOD1^{G93A} littermate control mice. Using the magic wand tool in Adobe Photoshop CC, the area was measured, in pixels, for each NMJ. This was achieved by outlining the outside of each NMJ, pressing “Record Measurements”, and taking the provided “Area” value. The perimeter, in pixels, of each NMJ was also measured by tracing the NMJ inside and outside, pressing “Record Measurements”, and taking the provided “Perimeter” value. An average perimeter and area were calculated for each mouse from all the values recorded for the mouse. Quantification was performed twice by two

different and blinded researchers. The untreated hSOD1^{G93A} and 100mg/kg PCA-treated hSOD1^{G93A} littermate mice averages were calculated as a percent of the WT littermate mouse, which was set at 100%. Mean NMJ pixel area and perimeter in the untreated hSOD1^{G93A} littermate mice and WT littermate mice were also statistically compared to verify a significant disease effect. The Sholl analysis was also performed on the same NMJ images that were used to analyze area and perimeter. Briefly, using ImageJ, the red (BTx) channel was separated from all channels and the NMJ was isolated using the plugins “Despeckle” and “Find Edges”. The edges of the NMJ were traced with “Simple Neurite Tracer” and “Analyze Skeleton” plugins. Each NMJ was circled by hand and pasted into a new image. The plugin “Skeletonize” was run to draw a line around the border of the NMJ. The “Sholl Analysis” plugin was run to decide a point in the center of the NMJ and to draw concentric circles around that point at a radius increasing by 10 pixels. Mean Sholl analysis values of NMJ complexity, or the number of intersections formed between the concentric circles and the skeleton of the NMJ, were reported for each untreated hSOD1^{G93A} and 100mg/kg PCA-treated hSOD1^{G93A} littermate mouse to be taken as a percent of the WT littermate control mouse (set at 100%). Mean Sholl analysis values from untreated hSOD1^{G93A} littermate mice and WT littermate mice were also statistically compared to verify a significant disease effect.

4.3.13 Analysis of Gastrocnemius Muscle Wet Weight at 105 Days of Age

Gastrocnemius muscle from all 105-day-old mice were placed into a tared weigh boat on a standard analytical balance to obtain muscle wet weight. Weights of gastrocnemius muscle were taken from WT, 100mg/kg PCA-treated hSOD1^{G93A}, and untreated

hSOD1^{G93A} littermate mice. Each gastrocnemius muscle wet weight from the untreated hSOD1^{G93A} littermate mouse and 100mg/kg PCA-treated hSOD1^{G93A} littermate mouse was calculated as a percent of the average of the WT littermate control mouse (set at 100%).

4.3.14 Imaging of Gastrocnemius Sections Stained with Alpha-BTx and VACht at 105 Days of Age

Neuromuscular junctions (20–25) were captured on the Rhodamine channel for each mouse by blinded researchers on the 20X objective for all mice that were euthanized at 105 days of age. VACht was captured on the Alexa Fluor 488 channel for each NMJ. Representative images are shown from a WT, untreated hSOD1^{G93A} mouse, and a 100mg/kg PCA-treated hSOD1^{G93A} mouse.

4.3.15 Imaging of Quantification of 4-HNE-Stained Spinal Cord Sections at 105 Days of Age

A single image of each ventral horn on the 20X objective was captured for each mouse. Imaging was performed by blinded researchers. Images were captured on the Alexa Fluor 488 channel (pseudo-colored red) and the exposure time was set appropriately for the untreated hSOD1^{G93A} littermate and kept constant when imaging the PCA-treated hSOD1^{G93A} and WT littermate mice. Two littermate groups were analyzed and 6 ventral horns per animal were imaged and analyzed for fluorescence intensity using Adobe Photoshop CC software. The ventral horn image of the untreated hSOD1^{G93A} littermate control mouse with the most background was chosen, and the red channel input level was adjusted so that background staining was best eliminated. This value was

recorded and used for each subsequent image, including those taken from the WT control littermate and the PCA-treated hSOD1^{G93A} littermate mice such that all images were adjusted by an equivalent amount. After the channel levels were adjusted, the ventral horn was outlined using the lasso tool and red channel values for mean pixel intensity and pixel area were recorded for each ventral horn image. Total pixel intensity of the red channel was obtained by multiplying the pixel intensity and pixel area. An average of the total pixel intensity was taken for each mouse. Quantification was performed once by a blinded researcher. An average of the pixel intensities for each mouse was obtained. For analysis, the average total pixel intensity for the WT littermate control mouse for each group was set at 100% and each individual total pixel intensity for each ventral horn for the untreated hSOD1^{G93A} littermate control and PCA-treated hSOD1^{G93A} littermate mice were calculated as percentages relative to the average total pixel intensity of the WT littermate control mouse. Mean raw 4-HNE fluorescence intensity in the lumbar spinal cord ventral horn in the untreated hSOD1^{G93A} littermate mice and WT littermate mice were also counted and statistically compared to verify a significant disease effect.

4.3.16 Statistical Analysis

Histological analyses were performed on at least 6 mice per treatment group. Differences between untreated and PCA-treated hSOD1^{G93A} littermate mice for Iba-1, GFAP, and 4-HNE intensity, NMJ area and perimeter, Nissl-stained counts, and gastrocnemius muscle wet weight were analyzed using a paired t-test. PaGE and rotarod were analyzed using an unpaired t-test at each time point. Correlation analysis of PaGE data and survival were analyzed using a Pearson correlation. Mean NMJ Sholl analysis

values were analyzed using a one-way analysis of variance (ANOVA) with *post-hoc* Tukey's test. Survival Kaplan–Meier curves and body weight data were analyzed using a log-rank test. For all analyses, differences were statistically significant when $p < 0.05$.

4.4 Results

4.4.1 PCA Orally Administered Beginning at Disease Onset Results in a Significant Extension of Survival but Does Not Preserve Body Weight in the hSOD1^{G93A} Mouse Model of ALS

In order to determine the therapeutic benefit of PCA in an ALS mouse model, we first evaluated the ability of PCA to extend the lifespan of hSOD1^{G93A} mice. Mice were dosed by oral gavage with either 50 or 100mg/kg PCA beginning at 90 days of age. This time point corresponds with average disease onset. At this age, mice typically display gait disturbances, decreased weight, and lower limb tremors (Mancuso et al., 2011). Mice were dosed by oral gavage with PCA until end stage, assessed by the ability of the mouse to right itself to sternum when placed on its side. Administration of both 50 and 100mg/kg PCA significantly extended median survival in hSOD1^{G93A} mice to 129 and 133 days, respectively, when compared to untreated hSOD1^{G93A} mice, which exhibited a median survival of 121 days ($p=0.0025$; Figure 4.1A). This impressive extension of survival indicates that PCA is slowing the disease progression in hSOD1^{G93A} ALS mice. Body weight of the hSOD1^{G93A} mice was assessed twice per week and is expressed as a percentage of peak body weight at each time point. Despite significantly extended survival, administration of PCA had no significant effect on the decline in body weight in the hSOD1^{G93A} mouse model of ALS (Figure 4.1B).

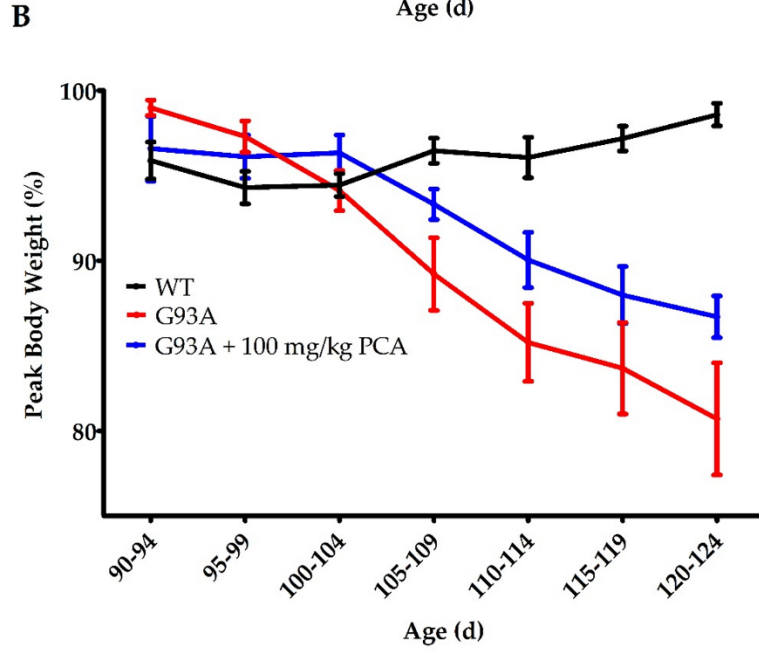
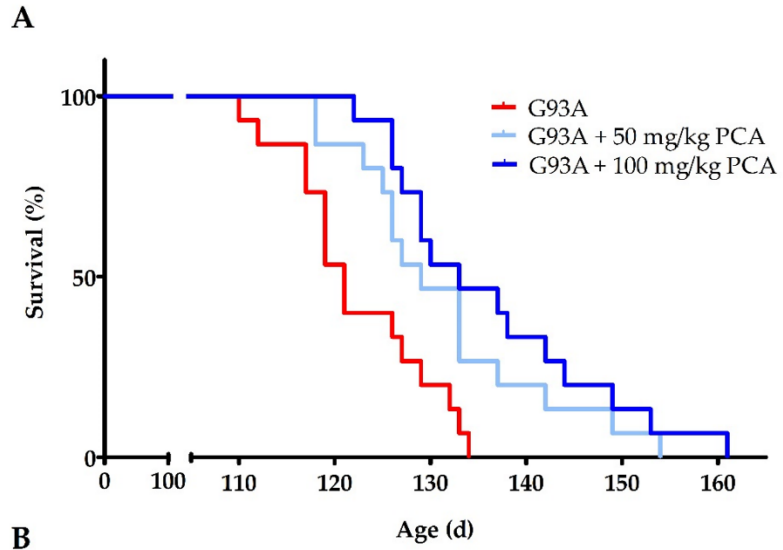


Figure 4.1 PCA Treatment Extends Survival in the hSOD1^{G93A} Mouse Model of ALS. (A) Survival of hSOD1^{G93A} mice (untreated or treated with 50 or 100mg/kg PCA) and wild-type mice (WT). Oral administration of either 50 or 100mg/kg PCA beginning at disease onset (90 days of age) significantly extended median survival in hSOD1^{G93A} mice to 129 and 133 days, respectively, when compared to untreated hSOD1^{G93A} mice, which exhibited a median survival of 121 days. Curves are significantly different as determined by log-rank (Mantel–Cox) test ($p=0.0025$; $n=15$ mice per group). (B) Body weight of hSOD1^{G93A} mice (untreated or treated with 100mg/kg PCA) and WT mice. Body weight was assessed twice per week and is expressed as the percent of peak body weight at each time point. Data are displayed as the mean \pm SEM with $n=15$ mice for each group.

4.4.2 PCA Treatment Improves Grip Strength and Motor Performance in the hSOD1^{G93A} Mouse Model of ALS

Since the dose of 100mg/kg PCA had a more pronounced effect on survival than the 50mg/kg PCA dose, grip strength and motor function were assessed in mice dosed with 100mg/kg PCA. hSOD1^{G93A} mice treated with 100mg/kg PCA were further evaluated using PaGE testing and rotarod testing in order to assess motor function (Weydt et al., 2003). PaGE testing was performed twice a week beginning at disease onset until end stage of disease to assess grip strength. Administration of 100mg/kg PCA beginning at disease onset significantly increased the latency to fall as assessed by PaGE testing at 100 to 114 days of age when compared to the untreated hSOD1^{G93A} littermate controls ($p<0.05$, Figure 4.2A). PaGE data were also analyzed for differences between male and female mice. PCA-treated male hSOD1^{G93A} mice did not show a significantly increased latency to fall at any time points when compared to the untreated male hSOD1^{G93A} littermate controls (Figure 4.2B). However, PCA-treated male hSOD1^{G93A} mice did trend towards a significant increase in latency to fall at 95–99 ($p=0.118$, Figure 4.2B) and 100–104 days of age ($p=0.115$). PCA-treated female hSOD1^{G93A} mice displayed a

significantly increased latency to fall as assessed by PaGE testing at 105–109 ($p<0.001$, Figure 4.2C) and 110–119 ($p<0.05$, Figure 2C) days of age when compared to untreated female hSOD1^{G93A} littermate controls. Lastly, we sought to understand the relationship between PaGE testing and survival in PCA-treated hSOD1^{G93A} mice. We averaged latency to fall as assessed by PaGE testing at 100–114 days of age from male and female hSOD1^{G93A} mice treated with 100mg/kg PCA beginning at disease onset. The latency to fall at these time points was chosen to be averaged because PCA-treated hSOD1^{G93A} displayed an increased latency to fall as assessed by PaGE testing at these time points when compared to untreated hSOD1^{G93A} littermate mice. The average latency to fall over these time points was correlated with the days lived for each mouse. Average latency to fall at 100–114 days and days lived was positively and significantly correlated in PCA-treated hSOD1^{G93A} mice ($r=0.558$, $p<0.05$, Figure 4.2D).

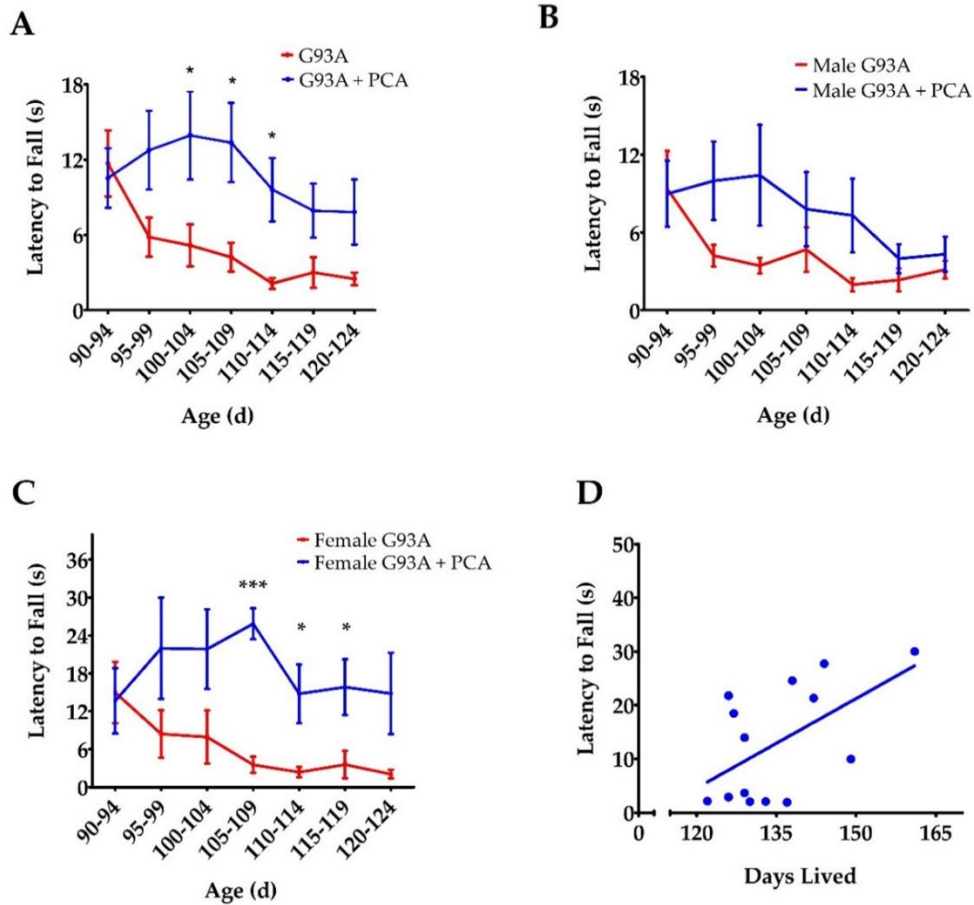


Figure 4.2 PCA Treatment Improves Grip Strength as Assessed by PaGE in the hSOD1^{G93A} Mouse Model of ALS. (A) PaGE testing of hSOD1^{G93A} mice (untreated or treated with 100mg/kg PCA) beginning at disease onset. PaGE testing was performed twice a week beginning at 90 days of age and is expressed as latency to fall. PaGE data are expressed as the mean \pm SEM for each time point; n=15 mice per group. * indicates p<0.05 in comparison to untreated hSOD1^{G93A} littermate controls. All data were analyzed using an unpaired t-test at each time point. (B) PaGE testing of male hSOD1^{G93A} mice (untreated or treated with 100mg/kg PCA) beginning at disease onset. PaGE data are expressed as the mean \pm SEM for each time point; n=9 mice per group. All data were analyzed using an unpaired t-test at each time point. (C) PaGE testing of female hSOD1^{G93A} mice (untreated or treated with 100mg/kg PCA) beginning at disease onset. PaGE data are expressed as the mean \pm SEM for each time point; n=6 mice per group. All data were analyzed using an unpaired t-test at each time point. * indicates p<0.05 in comparison to untreated hSOD1^{G93A} littermate controls. *** indicates p<0.001 in comparison to untreated hSOD1^{G93A} littermate controls. (D) Increased average PaGE latency to fall between 100 and 114 days of age is significantly correlated with longer survival of 100mg/kg PCA-treated hSOD1^{G93A} mice. PaGE data from 100–114 days of age are expressed as the mean for each mouse; n=14 mice. All data were analyzed using a Pearson correlation (r=0.558, p<0.05).

For further motor function analysis, rotarod testing was performed once a week beginning at disease onset until end stage of disease. This behavioral assay also showed an impressive enhancement in the motor function of PCA-treated hSOD1^{G93A} mice when compared to untreated hSOD1^{G93A} littermates. Administration of 100mg/kg PCA beginning at disease onset significantly but transiently increased the latency to fall as measured by rotarod testing at 97 and 104 days of age when compared to the untreated hSOD1^{G93A} littermate control mice ($p < 0.001$, Figure 4.3A). The results of these behavioral tests indicate that oral administration of PCA beginning at disease onset significantly improves balance, grip strength, and motor coordination in the hSOD1^{G93A} mouse model of ALS.

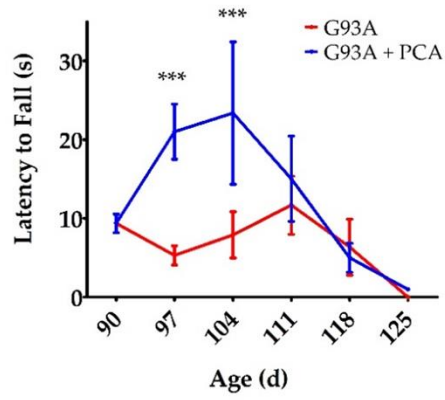
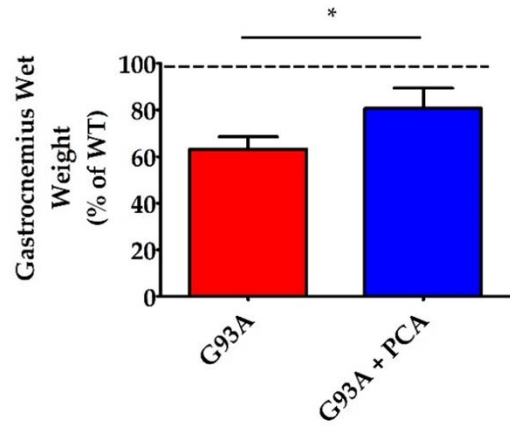
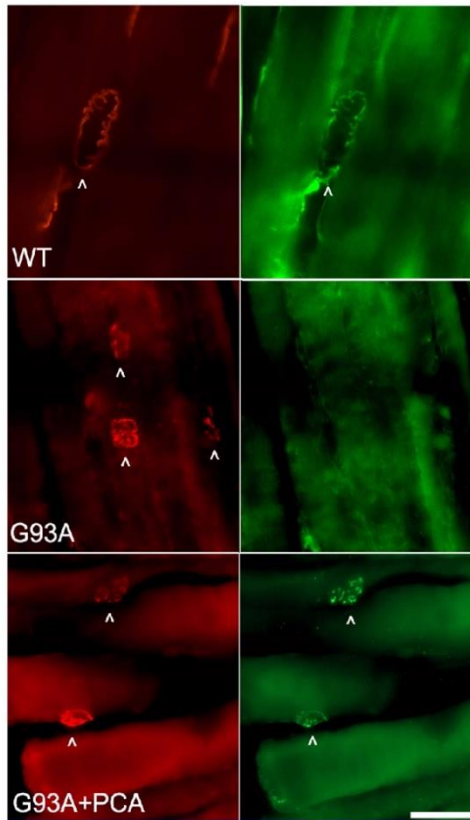
A**B****C**

Figure 4.3 PCA Treatment Improves Motor Function as Assessed by Rotarod and Also Preserves Gastrocnemius Muscle Weight and Neuromuscular Junction (NMJ) Innervation at 105 Days of Age in the hSOD1^{G93A} Mouse Model of ALS. (A) Rotarod testing of hSOD1^{G93A} mice (untreated or treated with 100mg/kg PCA beginning at disease onset). Rotarod testing was performed beginning at 90 days of age and extending through end stage and is expressed as latency to fall. Rotarod data are represented as the mean \pm SEM for each time point; n=10 mice per group. *** indicates $p < 0.001$ in comparison to untreated hSOD1^{G93A} littermate controls. All data were analyzed using an unpaired t-test at each time point. (B) Quantification of gastrocnemius muscle weights. Data are expressed as a percent of the wild-type (WT) littermate mouse muscle weight and are shown as the mean \pm SEM; n=7 mice per group. * indicates $p < 0.05$ compared to untreated hSOD1^{G93A} control mice (paired t-test). Mean gastrocnemius wet weight for the untreated hSOD1^{G93A} mouse (0.0912 ± 0.0070) is significantly decreased when compared to the WT littermate control mouse (0.1433 ± 0.0055) ($p = 0.0002$; n=7 mice per group). (C) Representative images of gastrocnemius muscle from wild-type control mice (WT), untreated hSOD1^{G93A} mice (G93A), and hSOD1^{G93A} mice treated orally with 100mg/kg PCA beginning at disease onset (G93A+PCA). Mice were euthanized at 105 days of age and gastrocnemius muscles were stained with alpha-BTx (red) and VACHT (green) to label NMJs and innervation of NMJs, respectively. Scale bar=20 μ m. Arrowheads point to NMJs stained positively with alpha-BTx and VACHT.

4.4.3 PCA Treatment Preserves Gastrocnemius Muscle Wet Weight, Protects NMJ Innervation, and Reduces Oxidative Stress in the hSOD1^{G93A} Mouse Model of ALS at 105 Days of Age

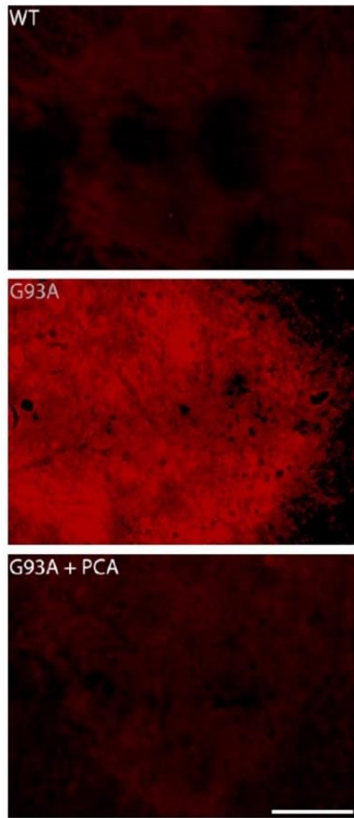
We observed the greatest improvements in motor function as assessed by rotarod and PaGE testing between 97 and 114 days of age in PCA-treated hSOD1^{G93A} mice. Therefore, we next analyzed gastrocnemius muscle weight at 105 days of age, the time point at which we saw the greatest behavioral therapeutic effect of PCA. Wet muscle weight isolated from untreated hSOD1^{G93A} mice ($0.091\text{g} \pm 0.007$) was significantly decreased when compared to WT littermate mice ($0.143\text{g} \pm 0.006$) ($p < 0.01$, Figure 4.3B). PCA-treated mice exhibited a significant preservation of gastrocnemius muscle wet weight when compared to untreated hSOD1^{G93A} littermate mice. PCA-treated hSOD1^{G93A}

mice had a mean muscle wet weight of 80% of the WT littermate mice, while untreated hSOD1^{G93A} mice had a mean muscle weight of only 63% of WT littermate mice ($p < 0.05$, Figure 4.3B). These results show that PCA treatment significantly delayed atrophy of the gastrocnemius muscle in the hSOD1^{G93A} mouse model of ALS. To support these findings, we stained gastrocnemius muscle isolated at 105 days of age with alpha-BTx and VACht in order to visualize innervated NMJs. Although these findings are preliminary, they indicate that PCA-treated mice exhibit a protection of NMJ innervation when compared to untreated hSOD1^{G93A} littermate mice, as evidenced by retention of the overlapping staining of alpha-BTx and VACht in the treated mouse NMJs (Figure 4.3C).

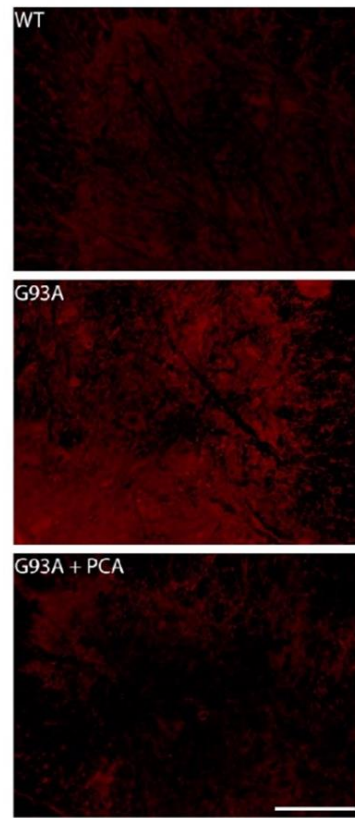
Oxidative stress is an underlying pathology of ALS and contributes to motor neuron death and subsequent skeletal muscle atrophy and deficits in motor function (D'Amico et al., 2013; Ikawa et al., 2015). Therefore, we also analyzed the effect of PCA on the production of 4-HNE in the lumbar spinal cord ventral horn of the hSOD1^{G93A} mouse model of ALS. Lumbar spinal cord isolated at 105 days of age from two littermate groups was stained with antibodies against 4-HNE to measure lipid peroxidation. Untreated hSOD1^{G93A} mice in both groups exhibit significantly higher raw 4-HNE fluorescence units ($((11.70 \pm 0.78) \times 10^6)$ and $((6.56 \pm 0.88) \times 10^6)$) when compared to their WT littermate control mice ($((7.83 \pm 0.16) \times 10^6)$ and $((4.17 \pm 0.24) \times 10^6)$), respectively. These data indicate profound lipid peroxidation in the ventral horn ($p < 0.01$ and $p < 0.05$, Figure 4.4A and 4.4C, respectively). Administration of 100mg/kg PCA beginning at disease onset significantly reduced lipid peroxidation in the ventral horn of the lumbar spinal cord in

the hSOD1^{G93A} mouse model of ALS relative to the untreated littermate control ($p < 0.01$ and $p < 0.05$, Figure 4.4B and 4.4D, respectively).

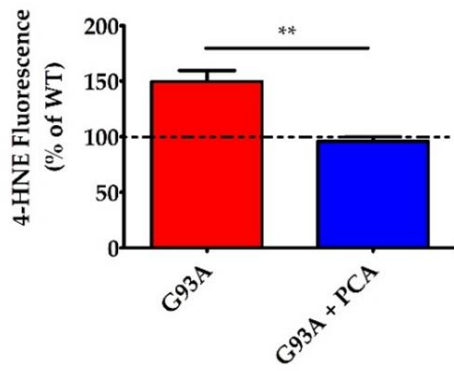
A



C



B



D

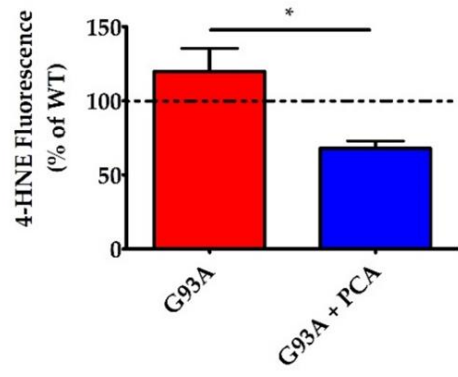


Figure 4.4 PCA Treatment Significantly Reduces Lipid Peroxidation in the Ventral Horn of the Spinal Cord in the hSOD1^{G93A} Mouse Model of ALS. (A,C)

Representative images of lumbar spinal cord ventral horns stained for 4-HNE from two littermate groups of wild-type control mice (WT), untreated hSOD1^{G93A} mice (G93A), and hSOD1^{G93A} mice treated orally with 100mg/kg PCA beginning at disease onset (G93A+PCA). Mice were euthanized at 105 days of age and ventral horns were stained with an antibody to 4-HNE to measure lipid peroxidation. Scale bar=70µm. **(B)**

Quantification of spinal cord ventral horns stained with 4-HNE as described and shown in A. The 4-HNE fluorescence intensity of untreated and PCA-treated hSOD1^{G93A} littermate mice were normalized and expressed as a percentage of mean 4-HNE fluorescence measured in the WT littermate control mouse. Data are expressed as the mean ± SEM; 6 ventral horns were imaged per mouse. ** indicates p<0.01 compared to the untreated hSOD1^{G93A} control littermate (paired t-test). Raw mean 4-HNE fluorescence units for the untreated hSOD1^{G93A} mouse (11.70±0.78)×10⁶ are significantly higher than the WT littermate mouse (7.83±0.16)×10⁶ (p<0.01) **(D)**

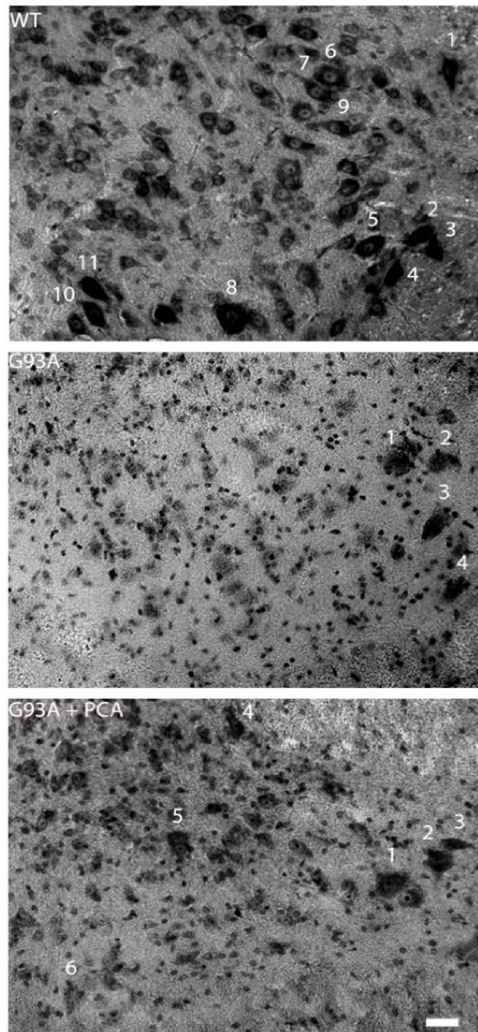
Quantification of spinal cord ventral horns stained with 4-HNE as described and shown in C. The 4-HNE fluorescence intensity of untreated and PCA-treated hSOD1^{G93A} littermate mice were normalized and expressed as a percentage of mean 4-HNE fluorescence measured in the WT littermate control mouse. Data are expressed as the mean ± SEM; 6 ventral horns were imaged per mouse. * indicates p<0.05 compared to the untreated hSOD1^{G93A} control littermate (paired t-test). Raw mean 4-HNE fluorescence units for the untreated hSOD1^{G93A} mouse (6.56±0.88)×10⁶ are significantly higher than the WT (4.17±0.24)×10⁶ (p<0.05).

4.4.4 PCA Treatment Significantly Preserves Motor Neurons in the Ventral Horn of the Spinal Cord in the hSOD1^{G93A} Mouse Model of ALS

It was evident that PCA had a beneficial therapeutic effect, as evidenced by the extension of survival and motor function improvements in the hSOD1^{G93A} mouse model of ALS. However, the effects of PCA on inflammation, motor neuron preservation, and neuromuscular junction integrity needed to be studied in order to support the survival and behavioral assay results. Lumbar spinal cord was isolated at end stage of the untreated hSOD1^{G93A} littermate control mouse and Nissl staining was performed so that neuronal cell bodies could be identified. The number of alpha motor neurons, with somas typically greater than 20µm along the longest axis, were counted in the ventral horn of the lumbar

spinal cord of untreated and PCA-treated hSOD1^{G93A} littermate mice. These values were normalized and expressed as a percentage of the number of alpha motor neurons counted in the WT littermate control mouse. The cell bodies of alpha motor neurons are located in the ventral horn of the lumbar spinal cord and their axons project to innervate skeletal muscle fibers of the leg muscles including the gastrocnemius muscle. The hSOD1^{G93A} mouse model of ALS exhibits a rapidly progressive lower limb muscular atrophy and subsequent paralysis as a result of alpha motor neuron death in the ventral horn of the spinal cord and retraction of motor axons away from the NMJs (Mancuso et al., 2011). As anticipated, untreated hSOD1^{G93A} mice exhibited nearly 60% fewer alpha motor neurons in the lumbar spinal cord ventral horn than their healthy WT littermates (Figure 4.5A). However, when 100mg/kg PCA was administered beginning at disease onset, the average alpha motor neuron count in the ventral horn of the lumbar spinal cord was significantly increased in comparison to the untreated hSOD1^{G93A} littermate mouse ($p < 0.05$, Figure 4.5B). These findings may contribute to the observed improvements in motor function as assessed by rotarod and PaGE testing.

A



B

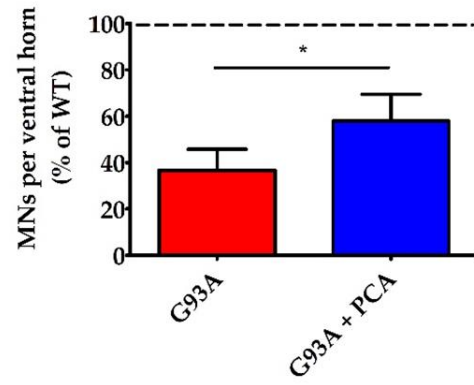


Figure 4.5 PCA Treatment Significantly Preserves Motor Neurons in the Ventral Horn of the Spinal Cord in the hSOD1^{G93A} Mouse Model of ALS. (A) Representative images of lumbar spinal cord ventral horns from wild-type control mice (WT), untreated hSOD1^{G93A} control mice (G93A) and hSOD1^{G93A} mice treated orally with 100mg/kg PCA beginning at disease onset (G93A+PCA). Mice were euthanized at end stage of the untreated hSOD1^{G93A} littermate control mouse and ventral horns were Nissl stained to label neuronal cell bodies. Stained soma were measured along the longest axis and cells were considered alpha motor neurons if the length was greater than 20µm. Scale bar=20µm. (B) Quantification of Nissl-stained alpha motor neurons as described in A. The number of alpha motor neurons in the ventral horns of lumbar spinal cord of untreated and PCA-treated hSOD1^{G93A} littermate mice were normalized and expressed as a percentage of the number of alpha motor neurons measured in the WT littermate control mouse. Data are expressed as the mean ± SEM; n=7 mice per group; 4–6 ventral horns were imaged per mouse. * indicates p<0.05 compared to untreated hSOD1^{G93A} littermate controls (paired t-test). Mean number of alpha motor neurons present in the ventral horn lumbar spinal cord for the untreated hSOD1^{G93A} littermate mouse (1.92±0.47) is significantly less than that of the WT (5.55±0.57) (p=0.004; n=7 mice per group). Abbreviations used: MNs = motor neurons.

4.4.5 PCA Treatment Significantly Reduces Astrogliosis and Microgliosis in the Ventral Horn of the Spinal Cord in the hSOD1^{G93A} Mouse Model of ALS

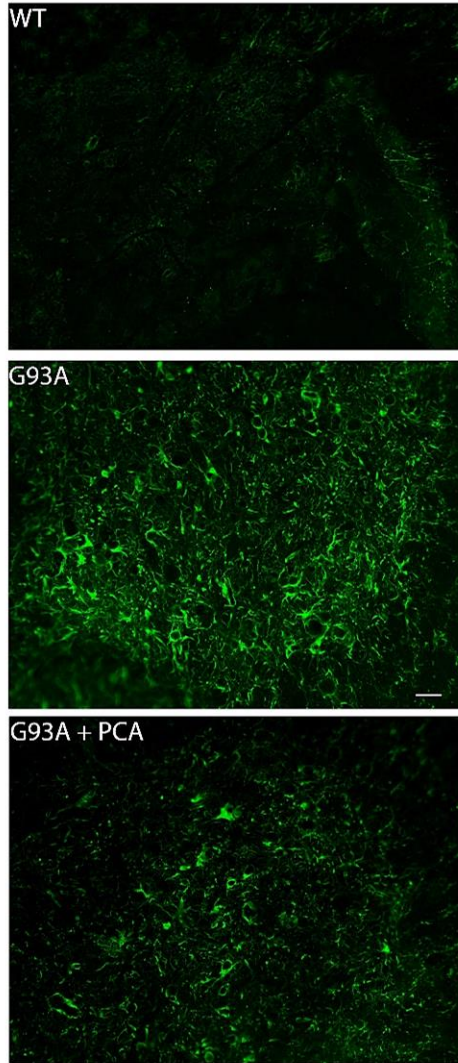
A robust neuroinflammatory response in the central nervous system of the hSOD1^{G93A} mouse model contributes to the motor neuron death and muscle atrophy producing the ALS-like phenotype (Mancuso et al., 2011). Therefore, we next analyzed the effect of PCA on astrogliosis and microgliosis in the lumbar spinal cord ventral horn of the hSOD1^{G93A} mouse model of ALS. Lumbar spinal cord isolated at end stage of the untreated hSOD1^{G93A} littermate mouse was stained with antibodies against GFAP and Iba-1 to identify astrocytes and microglia, respectively. Untreated hSOD1^{G93A} mice exhibit significantly higher raw mean GFAP fluorescence units ((3.21±0.46)×10⁶) when compared to WT littermate control mice ((0.97±0.16)×10⁶) indicating profound astrogliosis in the ventral horn (p=0.001, Figure 4.6A).

Microgliosis is also present in the lumbar spinal cord ventral horn of untreated hSOD1^{G93A} mice, as these mice exhibited significantly higher raw mean Iba-1 fluorescence units ($(3.41 \pm 0.52) \times 10^6$) when compared to healthy WT littermate control mice ($(1.56 \pm 0.29) \times 10^6$) ($p < 0.05$, Figure 4.7A).

Administration of 100mg/kg PCA beginning at disease onset significantly reduced astrogliosis in the ventral horn of the lumbar spinal cord in the hSOD1^{G93A} mouse model of ALS from a mean 394% increase to a mean 258% increase in GFAP fluorescence units relative to the WT littermate control ($p < 0.05$, Figure 4.6B).

Administration of PCA also significantly reduced microgliosis in the ventral horn lumbar spinal cord in the hSOD1^{G93A} mouse model of ALS from a mean 248% increase to a mean 156% increase in Iba-1 fluorescence units relative to the WT littermate control ($p < 0.05$, Figure 4.7B). From these data, we conclude that PCA significantly reduces gliosis which may ultimately protect alpha motor neurons in the ventral horn of the lumbar spinal cord in the hSOD1^{G93A} mouse model of ALS.

A



B

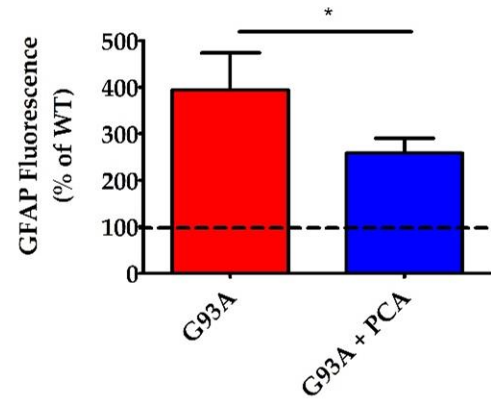
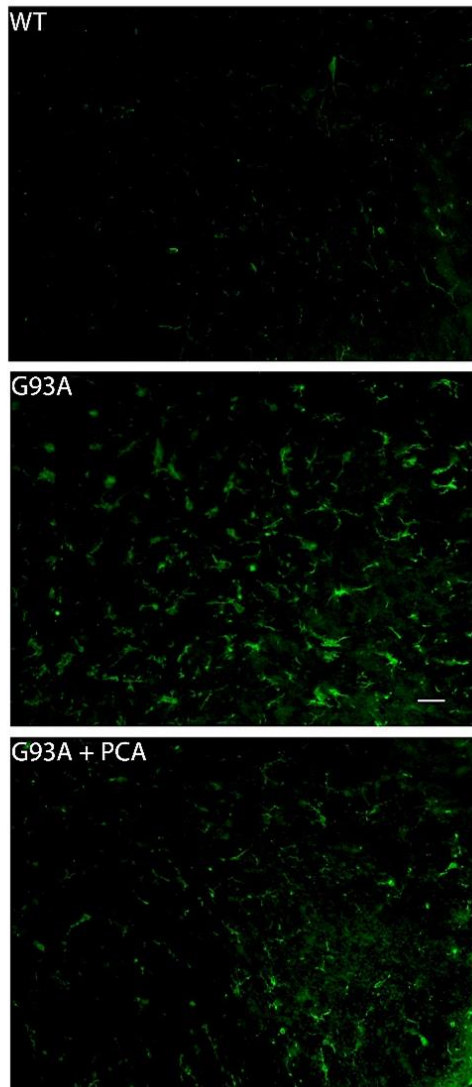


Figure 4.6 PCA Treatment Significantly Reduces Astrogliosis in the Ventral Horn of the Spinal Cord in the hSOD1^{G93A} Mouse Model of ALS. (A) Representative images of lumbar spinal cord ventral horns stained for GFAP from wild-type control mice (WT), untreated hSOD1^{G93A} mice (G93A), and hSOD1^{G93A} mice treated orally with 100mg/kg PCA beginning at disease onset (G93A+PCA). Mice were euthanized at end stage of the untreated hSOD1^{G93A} littermate control mouse and ventral horns were stained with an antibody to GFAP to label astrocytes. Scale bar=20 μ m. (B) Quantification of spinal cord ventral horns stained with GFAP as described in A. GFAP fluorescence intensity of untreated and PCA-treated hSOD1^{G93A} littermate mice were normalized and expressed as a percentage of GFAP fluorescence measured in the WT littermate control mouse. Data are expressed as the mean \pm SEM; n=10 mice per group; 4–6 ventral horns were imaged per mouse. * indicates $p < 0.05$ compared to untreated hSOD1^{G93A} controls (paired t-test). Raw mean GFAP fluorescence units for the untreated hSOD1^{G93A} mice ($(3.21 \pm 0.46) \times 10^6$) are significantly higher than the WT ($(0.97 \pm 0.16) \times 10^6$) ($p = 0.001$; n=10 mice per group).

A



B

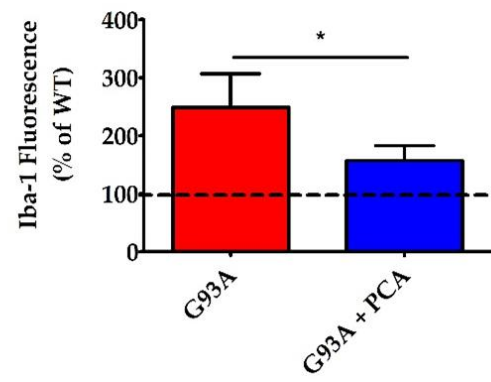


Figure 4.7 PCA Treatment Significantly Reduces Microgliosis in the Ventral Horn of the Spinal Cord in the hSOD1^{G93A} Mouse Model of ALS. (A) Representative images of lumbar spinal cord ventral horns stained for Iba-1 from wild-type control mice (WT), untreated hSOD1^{G93A} mice (G93A), and hSOD1^{G93A} mice treated orally with 100mg/kg PCA beginning at disease onset (G93A+PCA). Mice were euthanized at end stage of the untreated hSOD1^{G93A} littermate mouse and ventral horns were stained with an antibody to Iba-1 to label microglia. Scale bar=20µm. (B) Quantification of spinal cord ventral horns stained with Iba-1 as described in A. Iba-1 fluorescence intensity of untreated and PCA-treated hSOD1^{G93A} littermate mice were normalized and expressed as a percentage of Iba-1 fluorescence measured in the WT littermate control mouse. Data are expressed as the mean ± SEM; n=6 mice per group; 4–6 ventral horns were imaged per mouse. * indicates p=0.05 compared to untreated hSOD1^{G93A} controls (paired t-test). Raw mean Iba-1 fluorescence units for the untreated hSOD1^{G93A} mouse ((3.41±0.52)×10⁶) are significantly higher than the WT ((1.56±0.29)×10⁶) (p<0.05; n=6 mice per group).

4.4.6 PCA Treatment Significantly Preserves Neuromuscular Junctions of the Gastrocnemius Muscle in the hSOD1^{G93A} Mouse Model of ALS

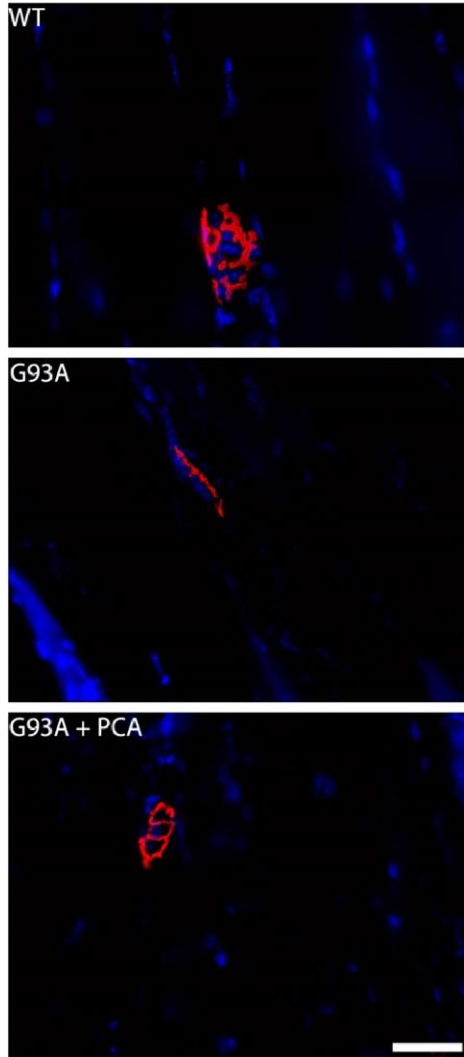
After determining that PCA has neuroprotective and anti-inflammatory effects in the ventral horn of the lumbar spinal cord isolated from hSOD1^{G93A} mice, we sought to analyze NMJs in gastrocnemius muscle in order to further elucidate how administration of PCA improved motor deficits. Neuromuscular junctions represent the synapse between the alpha motor neuron axon terminal and the gastrocnemius muscle fiber. In the hSOD1^{G93A} mouse model of ALS, NMJs become weakened and break down as the alpha motor neuron cell body dies and the axon retracts away from the muscle. This results in skeletal muscle atrophy and paralysis characteristically seen in this mouse model (Mancuso et al., 2011).

To analyze the NMJs, gastrocnemius muscle was isolated at end stage of the untreated hSOD1^{G93A} littermate mouse and stained with alpha-bungarotoxin. Alpha-bungarotoxin binds to nicotinic acetylcholine receptors found on the gastrocnemius

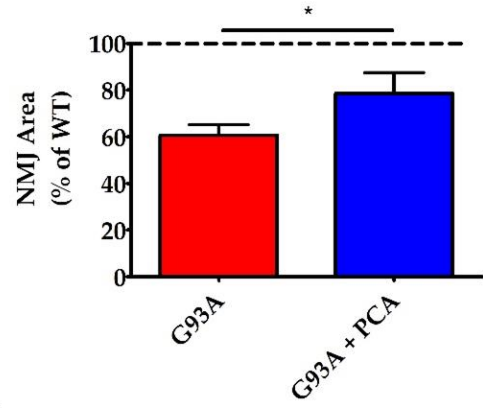
muscle. Mean NMJ area, perimeter, and Sholl analysis values of untreated and PCA-treated hSOD1^{G93A} littermate mice were normalized and expressed as a percentage of the corresponding NMJ values measured in the WT littermate control mouse. Untreated hSOD1^{G93A} mice exhibited an overall decreased NMJ pixel area (11,842±1204) when compared to WT littermate control mice (17,966±818) ($p=0.01$, Figure 4.8A).

Furthermore, untreated hSOD1^{G93A} mice also exhibited an overall decreased NMJ pixel perimeter (731±40) when compared to the healthy WT littermate control mice (1141±95) ($p=0.0007$, Figure 4.8A). Administration of 100 mg/kg PCA beginning at disease onset significantly preserved NMJ area yielding an average NMJ pixel area of 79% of the WT littermate mice compared to the untreated hSOD1^{G93A} littermate mice, which had an average area of 61% of the WT littermate mice ($p<0.05$, Figure 4.8B). Furthermore, PCA significantly preserved NMJ perimeter in the hSOD1^{G93A} mouse model of ALS. PCA-treated hSOD1^{G93A} mice exhibited a mean NMJ pixel perimeter of 81% of WT littermate mice versus untreated hSOD1^{G93A} littermate mice, which exhibited a mean of 64% of WT littermate mice ($p<0.05$, Figure 4.8C). Untreated hSOD1^{G93A} mice also exhibited an overall decreased NMJ mean Sholl analysis value (62±1.6) when compared to WT littermate mice (97±4.3) ($p<0.001$, Figure 4.8D). More importantly, PCA-treated hSOD1^{G93A} littermates exhibited a significantly greater mean Sholl analysis value (79±6.8) when compared to untreated hSOD1^{G93A} littermate mice ($p<0.05$, Figure 4.8D). These findings indicate that PCA protects the synapse between the alpha motor neuron axon and the gastrocnemius muscle, ultimately allowing for improved motor function and mobility.

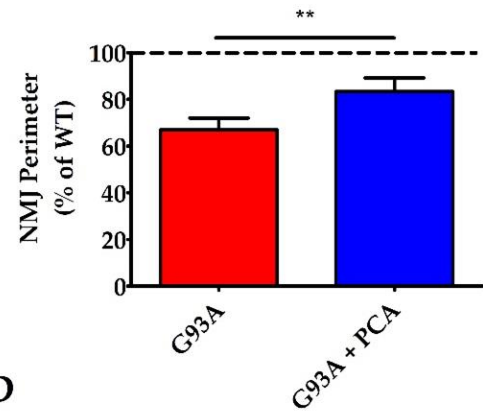
A



B



C



D

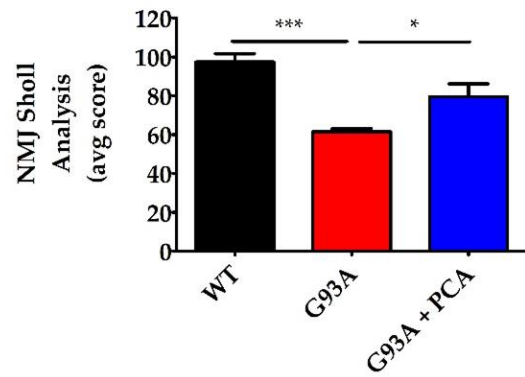


Figure 4.8 PCA Treatment Significantly Preserves Neuromuscular Junctions (NMJ) in the Gastrocnemius Muscle in the hSOD1^{G93A} Mouse Model of ALS. (A)

Representative images of gastrocnemius muscle from wild-type control mice (WT), untreated hSOD1^{G93A} mice (G93A), and hSOD1^{G93A} mice treated orally with 100mg/kg PCA beginning at disease onset (G93A+PCA). Mice were euthanized at end stage of the untreated hSOD1^{G93A} littermate mouse and gastrocnemius muscles were stained with alpha-BTx (red) and Hoechst (blue) to label NMJs and nuclei, respectively. Scale bar=40 μ m. **(B)** Quantification of gastrocnemius NMJ area stained with alpha bungarotoxin as described in A. The NMJ area, measured in pixels by tracing the outside of the neuromuscular junction, of untreated and PCA-treated hSOD1^{G93A} littermate mice were normalized and expressed as a percentage of NMJ area measured in the WT littermate control mouse. Data are expressed as the mean \pm SEM; n=8 mice per group; 20–25 NMJs were imaged per mouse. * indicates $p < 0.05$ compared to untreated hSOD1^{G93A} control mice (paired t-test). Mean NMJ pixel area for the untreated hSOD1^{G93A} littermate mouse (11,842 \pm 1204) is significantly less than the WT littermate control mouse (17,966 \pm 818) ($p = 0.01$; n=8 mice per group). **(C)** Quantification of gastrocnemius NMJ perimeter stained with alpha bungarotoxin as described in A. The NMJ perimeter, measured in pixels by tracing the inside and outside of the NMJ, of untreated and PCA-treated hSOD1^{G93A} littermate mice were normalized and expressed as a percentage of NMJ perimeter measured in the WT littermate control mouse. Data are expressed as the mean \pm SEM; n=9 mice per group; 20–25 neuromuscular junctions were imaged per mouse. ** indicates $p < 0.01$ compared to untreated hSOD1^{G93A} controls (paired t-test). Mean NMJ pixel perimeter for the untreated hSOD1^{G93A} littermate mouse (730.9 \pm 39.37) is significantly less than the WT littermate control mouse (1141 \pm 94.52) ($p = 0.0007$; n=9 mice per group). **(D)** Quantification of gastrocnemius NMJ Sholl analysis stained with alpha bungarotoxin as described in A. WT, untreated, and PCA-treated hSOD1^{G93A} littermate mice were given a mean Sholl analysis value, which represents the number of intersections that the NMJ makes with concentric circles every 10 pixels from a center point. Data are expressed as the mean \pm SEM; n=8 mice per group; 20–25 neuromuscular junctions were imaged per mouse. * indicates $p < 0.05$ and *** indicates $p < 0.001$ compared to WT littermate control mice (one-way ANOVA with post-hoc Tukey's test).

4.5 Discussion

Plant-derived polyphenolic compounds exhibit anti-inflammatory, antioxidant, and neuroprotective capabilities; therefore, they have the potential to be safe, cost-effective, and successful agents in treating neurodegenerative diseases such as ALS. The catechol, protocatechuic acid (PCA), is a phenolic acid metabolite of kuromanin, an

anthocyanin found in foods such as blackberries, bilberries, and black rice. Here, we demonstrate that PCA extends survival, improves motor function, reduces gliosis, protects motor neurons, and preserves NMJs in the hSOD1^{G93A} mouse model of ALS. To ensure that PCA was non-toxic and had therapeutic potential, we first studied the effects of PCA on survival. We found that daily administration of 100 mg/kg PCA by oral gavage beginning at disease onset significantly extended survival of hSOD1^{G93A} mice when compared to untreated hSOD1^{G93A} littermate control mice. PCA-treated hSOD1^{G93A} mice also exhibited significantly improved motor function as assessed by rotarod and PaGE testing when compared to untreated hSOD1^{G93A} littermate control mice. To supplement these findings, we also analyzed gastrocnemius muscle weight at 105 days of age, a time point at which we observed significant peak motor performance in PCA-treated hSOD1^{G93A} mice. We found a preservation of muscle wet weight in PCA-treated hSOD1^{G93A} littermate mice when compared to untreated littermate controls at 105 days of age. At this time point, we also observed that PCA-treated hSOD1^{G93A} mice seemed to display a preservation of NMJ innervation in gastrocnemius muscle when compared to untreated hSOD1^{G93A} mice. Indeed, PCA administration preserved motor function and muscle weight well into the disease course, indicating that this compound was able to slow the progression of motor symptoms, which could indicate improved quality of life.

We next sought to determine how PCA was able to elicit a significant improvement in survival and motor function. We analyzed the ventral horn of the lumbar spinal cord at end stage of untreated hSOD1^{G93A} littermate mice and found that PCA-

treated hSOD1^{G93A} mice had significantly reduced astrogliosis, microgliosis, and increased motor neuron count when compared to untreated hSOD1^{G93A} littermate control mice. Furthermore, we analyzed NMJs within the gastrocnemius muscle isolated from PCA-treated hSOD1^{G93A} mice at end stage of the untreated hSOD1^{G93A} littermate control mice and measured them in terms of overall area, perimeter, and complexity (via Sholl analysis). We found that oral treatment with PCA significantly preserved NMJ area, perimeter, and complexity when compared to untreated hSOD1^{G93A} littermate control mice. Furthermore, at 105 days of age, we analyzed gastrocnemius muscle stained with alpha-BTx along with antibodies against VACHT. We wanted to visualize the NMJs and their innervation by presynaptic cholinergic neurons. Representative images indicate that administration of PCA was able to protect the innervation of the NMJ at this time point. Although we did not quantitatively assess NMJ innervation, the combined results of preserved NMJ size and complexity at end stage of the untreated hSOD1^{G93A} littermate control mice, along with a preservation of gastrocnemius muscle wet weight and improved motor performance at 105 days of age, indicate that PCA has a beneficial effect on preserving skeletal muscle performance. Taken together, these findings indicate that PCA exhibits neuroprotective properties while also reducing gliosis *in vivo* and therefore, should be further explored as a therapeutic for ALS.

In future studies, we plan to further examine the mechanism of action of PCA in mitigating the deleterious effects of ALS. We have previously shown that PCA exhibits antioxidant activity due to its catechol structure. PCA has the ability to chelate metal ions, act as a reducing agent, and scavenge free radical species including nitric oxide

(Kelsey et al., 2011; Winter et al., 2017a). In the current study, we performed a preliminary analysis and explored the effect of PCA on lipid peroxidation in the ventral horn of lumbar spinal cord isolated at 105 days of age from two groups of WT, untreated hSOD1^{G93A}, and PCA-treated hSOD1^{G93A} littermate mice. Ventral horn was stained with 4-HNE, a byproduct of lipid peroxidation, and fluorescence intensity was measured. These data show that untreated hSOD1^{G93A} mice had significantly higher levels of 4-HNE fluorescence intensity in the ventral horn when compared to their WT littermates, a result that has previously been shown by others (Seo et al., 2011). Furthermore, PCA-treated hSOD1^{G93A} mice exhibited significantly lower levels of 4-HNE fluorescence intensity when compared to their untreated hSOD1^{G93A} littermate controls. These data are further supported by previous research indicating that PCA has the ability to protect cells from mitochondrial dysfunction and apoptosis *in vitro* and *in vivo* (Liu, Y.M., et al., 2008; Semaming et al., 2015). Furthermore, PCA is able to increase glutathione and superoxide dismutase activity and decrease lipid peroxidation *in vitro* (Lende et al., 2011; Nakamura et al., 2001). An increase in free radical species, release of pro-inflammatory cytokines by microglia and astrocytes, and mitochondrial dysfunction all contribute to the oxidative stress burden seen in ALS patients (Almer et al., 1999; Lopez-Gonzalez et al., 2016; McGeer et al., 2002; Pickles et al., 2016). Consequently, markers such as glutathione peroxidase and malondialdehyde have been found to be elevated in the serum, plasma, and urine of ALS patients (Mitsumoto et al., 2008; Blasco et al., 2017). Research has demonstrated that oxidative stress heavily contributes to motor neuron death in ALS and PCA has been studied for its antioxidant properties. Therefore, it is

possible that PCA is aiding in the preservation of motor neuron viability by reducing the oxidative stress burden through free radical scavenging or by an upregulation of endogenous antioxidant activity. Each of these potential mechanisms should be evaluated in future studies.

Acting in parallel with oxidative stress in the pathogenesis of ALS is neuroinflammation. For example, mutant SOD-1 contributes to the death of motor neurons and promotes microgliosis and astrogliosis in the spinal cord. In the hSOD1^{G93A} mouse model of ALS, glial cells, such as astrocytes and microglia, overexpress mutant SOD-1. This is toxic to motor neurons and causes an accelerated disease progression. It is theorized that ALS disease onset induced by expression of mutant SOD-1 is non-cell autonomous and that glial cells play a central role in motor neuron death (Di Giorgio et al., 2007; Yamanaka et al., 2008). Microglial cells expressing mutant SOD-1 become activated and release pro-inflammatory cytokines and free radical species (Meissner et al., 2010; Zhao et al., 2010). Furthermore, mutant SOD1-expressing microglia release increased nitric oxide, superoxide, and decreased insulin-like growth factor-1 when compared to WT microglia in the presence of lipopolysaccharide (Xiao et al., 2007). Neuroinflammatory microglia also contribute to the activation of astrocytes. Activated astrocytes lose the ability to promote motor neuron survival, phagocytosis, and synaptogenesis (Liddel et al., 2017). Furthermore, activated astrocytes expressing mutant SOD-1 contribute to the death of primary spinal motor neurons (Nagai et al., 2007). *In vitro*, PCA has the ability to reduce pro-inflammatory cytokines and nitric oxide production in lipopolysaccharide treated microglial cultures (Min et al., 2010;

Winter et al., 2017c). *In vivo*, PCA treatment reduces cyclooxygenase-2, interleukin-1 β , interleukin-6, tumor necrosis factor- α , and prostaglandin E2 expression in inflammatory models in rats and mice (Min et al., 2010; Nakamura et al., 2001; Tsai et al., 2012). In the hSOD1^{G93A} mouse model of ALS, we have found that PCA significantly reduces both astrogliosis and microgliosis in the ventral horn of the lumbar spinal cord. While further study is required to determine whether reducing the presence of these cells also reduces the release of pro-inflammatory factors, our data suggest that the reduction in the presence of reactive astrocytes and microglia could be a principal mechanism by which PCA preserves motor neuron survival and overall motor function in hSOD1^{G93A} mice.

In the hSOD1^{G93A} mouse model of ALS, NMJs become weakened and break down as the alpha motor neuron cell body dies and the axon retracts away from the muscle. This results in skeletal muscle atrophy and paralysis characteristically seen in this mouse model. Since PCA-treated hSOD1^{G93A} mice exhibited neuroprotection in the ventral horn of the lumbar spinal cord, we aimed to explore the preservation of the NMJ which represents the synapse between the alpha motor neuron axon terminal and the gastrocnemius muscle fiber. In the hSOD1^{G93A} mouse model of ALS, detachment of nerve terminals from the neuromuscular junction can be seen as early as 10 weeks of age (Narai et al., 2009). Although no previous research has explored the effect of PCA treatment on NMJs in mice, we found that PCA was able to preserve the size and complexity of NMJs in hSOD1^{G93A} mice. These findings help further explain the improved motor function measured by rotarod and PaGE testing in PCA-treated

hSOD1^{G93A} mice. However, the precise mechanism by which PCA protects the NMJs is currently unknown.

This study is valuable in that it highlights the ability of PCA to significantly reduce neuronal death and gliosis in a mouse model of ALS. However, the therapeutic benefits of PCA are not limited to ALS. Oxidative stress and neuroinflammation contribute to the pathology and subsequent neuronal death observed in many neurodegenerative diseases such as Alzheimer's disease (AD) and Parkinson's disease (PD). PCA has been previously studied in mouse models of AD and was able to improve spatial learning, decrease inflammatory cytokine expression, and increase expression of brain-derived neurotrophic factor in the APP/PS1 mouse model of familial AD (Song et al., 2014). Furthermore, a diet high in date palm fruits, which contain high amounts of phenolic compounds, including PCA, improved spatial learning deficits, and resulted in a reduction in lipid peroxidation and restoration of antioxidant enzymes in the [APPsw]/Tg2576 mouse model of AD (Subash et al., 2015a; Subash et al., 2015b). In cell models of PD, PCA treatment resulted in a significant upregulation of antioxidant enzymes and inhibited the activation of nuclear factor- κ B and expression of inducible nitric oxide synthase (Zhang, Z., et al., 2015). PCA was also able to prevent apoptosis, reduce reactive oxygen species (ROS) production, decrease activation of caspase-3, and enhance SOD activity in *in vitro* models of PD (An et al., 2006; Guan et al., 2006). *In vivo*, PCA was able to improve motor function and ameliorate PD pathology in the substantia nigra in both MPTP and 6-hydroxydopamine mouse models of PD (Zhang, H.N, et al., 2010; Zhang, Z., et al., 2015). Interestingly, PCA has been shown *in vitro* to

inhibit aggregation of pathogenic proteins including amyloid beta peptide and alpha-synuclein (Hornedo-Ortega et al., 2016). Therefore, it will be of interest in future studies to determine whether PCA attenuates aggregation of mutant SOD-1 or TDP-43 in models of ALS.

4.6 Conclusion

This preclinical study is the first to explore the therapeutic benefits of PCA in a mouse model of ALS. Our findings of the neuroprotective and anti-inflammatory effects of PCA in the hSOD1^{G93A} mouse model of ALS are supported by previous studies showing similar effects of PCA in other models of neurodegeneration. Although PCA has been well studied in other disease models (e.g., AD and PD), it should be further studied in additional models of ALS, such as C9orf72 and TDP-43 ALS, to further elucidate its benefit for treating ALS in a diverse patient population. A thorough analysis of the effect of PCA treatment on levels of biomarkers relating to oxidative stress and neuroinflammation should also be performed. It would be important to measure the effect of PCA treatment on levels of pro-inflammatory cytokines and intracellular levels of ROS (superoxide anion, nitric oxide) in lumbar spinal cord and gastrocnemius muscle in the hSOD1^{G93A} model and other mouse models of ALS, and to analyze these levels over the time course of the disease. Such an analysis would allow for identification of predictive biomarkers for the efficacy of PCA treatment and ALS disease progression. Furthermore, other phenolic acid metabolites of anthocyanin compounds (e.g., 4-hydroxybenzoic acid, gallic acid, and syringic acid) should be studied for similar benefits in ALS and other neurodegenerative diseases. Our findings indicate that nutraceutical

phenolic compounds, such as PCA, have the potential to help treat patients with ALS and should be investigated as possible therapeutics for this devastating disorder.

CHAPTER FIVE: CONCLUSIONS AND FUTURE DIRECTIONS

5.1 Summary of Major Findings

As described in Chapter Two, patients with a history of mild TBI, when compared to patients who have never sustained a TBI in their lifetime, have significantly depleted antioxidant biomarkers. Despite many studies exploring antioxidant treatments for TBI of all severities, this is the first study, to date, which reports extensive antioxidant depletion in humans with a history of mild TBI (Mozaffari et al., 2021). In our mild TBI patient cohort, we also found that patients had significantly worsened emotional, energy, head, and cognitive symptoms when compared to patients without TBI. The number of mild TBIs sustained, and time since the patient's most recent mild TBI, also seemed to influence symptom presence, frequency, and severity. We also identified sex-specific differences in antioxidant depletion and symptomology. Finally, we found that mild TBI patients with more severe PUFA depletion had worsened energy and cognitive symptoms when compared to patients with less severe PUFA depletion. Antioxidant depletion results from mild TBI pathogenesis, especially neuroinflammation and oxidative stress. Prolonged neuroinflammation and oxidative stress deplete the endogenous antioxidant reserves which may, in turn, result in the expression of symptoms and prolongation of secondary injury pathology.

Nutraceutical supplementation with exogenous antioxidants, or with supplements that increase levels of endogenous antioxidants, may help treat mild TBI secondary injury

pathology and, in turn, ameliorate symptomology. Secondary injury pathology from a single mild TBI can be exacerbated and further prolonged if subsequent mild TBIs are sustained. In Chapter Three, the therapeutic benefit of Immunocal®, a whey protein supplement previously studied to increase levels of GSH *in vivo*, was tested in mouse models of repetitive mild and mild-moderate TBI (Ross et al., 2012). We found that Immunocal® treatment significantly reduced astrogliosis present in the cortex of mice at 2 weeks and 2 months following repetitive mild TBI. In the model of repetitive mild-moderate TBI, we found that Immunocal® treatment significantly reduced microgliosis in cortex.

Persistent TBI secondary injury, when left untreated, could contribute to neurodegenerative disease like ALS. ALS pathology shares similarities with that of TBI and repetitive mild TBI. Furthermore, nutraceutical treatments that have antioxidant and/or anti-inflammatory properties can also be used to treat ALS pathology. Chapter Four reports the anti-neuroinflammatory and neuroprotective effects of PCA in the hSOD1^{G93A} mouse model of ALS (Koza et al., 2020). PCA is a phenolic anthocyanin metabolite which has been well studied for its ROS/RNS scavenging abilities resulting in reduction of oxidative stress and neuroprotection. In the hSOD1^{G93A} mouse model of ALS, we found that PCA administration beginning at disease onset significantly extended survival and improved motor function. On a cellular level, PCA reduced astrogliosis and microgliosis, protected motor neurons in spinal cord and preserved neuromuscular junctions in gastrocnemius muscle (Koza et al., 2020). These findings support the use of

PCA to treat ALS and align with previous research which shows PCA confers neuroprotection in other models of neurodegeneration.

There are several important considerations when using nutraceutical treatments to treat mild TBI and ALS which are further discussed below. Furthermore, the relationship between prolonged secondary injury pathology and antioxidant depletion resulting from repetitive mild TBI and the development of ALS is discussed below.

5.2 Evidence for, Potential Benefits, and Limitations of Supplementing the Endogenous Antioxidant System with Exogenous Nutraceutical Antioxidants to Treat Mild Single and Repetitive TBI

In the mild TBI patient cohort described in Chapter Two, we found that patients had significantly decreased levels of antioxidants including alpha-tocopherol and selenium in serum, linoleic acid and taurine in plasma, and docosahexaenoic acid and total omega-3 in RBCs. Males with a history of mild TBI showed additional significant or trending significant decreases in coenzyme-q10 and cysteine in serum, alpha-linolenic acid in plasma, and total omega-6 in RBCs. On the other hand, female patients with a history of mild TBI only showed significantly or trending significantly decreased linoleic acid and taurine in plasma. Sex-specific treatment with these antioxidant compounds may be beneficial in treating mild TBI. Moreover, Immunocal®, a supplement which increases levels of the endogenous antioxidant, GSH, could be used in conjunction with these treatments.

5.2.1. Evidence for Antioxidant Nutraceutical Compound Supplementation to Treat Antioxidant Depletion Resulting from Mild Single and Repetitive TBI

The antioxidant biomarkers found to be depleted in our mild TBI cohort fall into categories of amino acids, vitamins, nonenzymatic endogenous antioxidants, and PUFAs. Previous research supporting supplementation of these compounds for mild TBI is discussed in this section.

Taurine, an essential amino sulfonic acid, is well-studied for its importance in brain health and as a treatment for TBI. Supporting our findings of taurine depletion in response to TBI, Seki et al. (2005) found that taurine in CSF showed a significant decrease at 67 hours post-TBI in patients and remained lower until the last measurement at 5 days post-TBI (Seki et al., 2005). Taurine plays roles in regeneration of the CNS, neurotransmission, calcium homeostasis/excitotoxicity, and redox reactions (Niu et al., 2018). Su et al. (2014) supplemented rats subjected to moderate fluid percussion injury with 200 mg/kg intravenous taurine once daily for 1 or 7 days post-TBI. They found that taurine supplementation improved functional recovery, and reduced GFAP, edema and cytokine expression at 7 days post-TBI (Su et al., 2014). The same dosing regimen also allowed for improved reaction time, neuroprotection, improved cerebral blood flow, and greater mitochondrial ETC activity in another study in rats subjected to fluid percussion injury (Wang, Q., et al., 2016). Clinically, supplementation of 30 mg/kg/day of taurine for 14 days following TBI in patients reduced levels of IL-6 in serum at 14 days post-TBI and improved clinical outcome at 30 days post-TBI (Vahdat et al., 2021).

Vitamin E is a fat-soluble vitamin which is administered in the form of alpha tocopherol, the form of vitamin E used by the body. Alpha tocopherol interacts with free radical oxygen and lipid peroxy radicals to prevent lipid peroxidation (Morris, D. R., & Levenson, 2013). Alpha-tocopherol has been studied for its ability to reduce oxidative stress through reduction of superoxide, preserve BDNF, support synaptic plasticity, and improve spatial learning memory in animal models of mild TBI (Aiguo et al., 2010; Dobrovolny et al., 2018). Conte et al. (2004) subjected Tg2576 AD mice to repetitive mild TBI and supplemented mice with vitamin E. Vitamin E supplementation reduced lipid peroxidation and prevented A β aggregation when compared to TBI AD mice fed a normal diet (Conte et al., 2004). These findings support the idea that a decrease in vitamin E and subsequent increase in lipid peroxidation may contribute to the development of neurodegenerative disease, such as AD, in patients who sustain multiple mild TBIs. Although supplementation with a high dose regimen of intravenous vitamin E for one-week post-TBI has been explored in a human clinical trial and shown to reduce mortality following severe TBI, no human studies to date have looked at vitamin E as a treatment for mild TBI (Institute of Medicine, 2011; Razmkon et al., 2011).

Nonenzymatic endogenous antioxidants such as coenzyme-q10 and selenium, both depleted in the mild TBI patients in our study, have been explored as potential treatments for TBI. Coenzyme-q10 is produced by mitochondria and is present in an oxidized form known as ubiquinone, and a reduced form, ubiquinol. Increased ubiquinone as a result of mitochondrial damage induced by TBI can contribute to oxidative stress and reduced energy production (Allan et al., 2019). A few studies have tested coenzyme-q10

supplementation as a treatment for TBI *in vivo*, however, no human studies exist. In a weight drop moderate TBI model in rats, supplementation with coenzyme-q10 immediately and at 24 hours post-TBI resulted in reduced lipid peroxidation, neuronal loss, and edema in brain when compared to untreated controls at 48 hours post-TBI (Kalayci et al., 2011). Another study explored coenzyme-q10 supplementation 30 minutes prior to TBI in a CCI rat model of TBI and found that expression of molecular pathways pertaining to free radical production and metabolism differed between treated and untreated rats (Pierce, J. D., et al., 2017).

Selenium is essential to the activity of GPx with its deficiency directly related to a decrease in GPx activity (Wilke et al., 1992). Selenium treatment has been studied in humans with TBI. In one study, treatment with intravenous selenium for 10 days following TBI improved functional and neurological outcome in patients even out to 6 months following severe blunt injury TBI (Khalili et al., 2017). On the other hand, in another clinical trial, intravenous selenium administration within 8 hours of a moderate-severe TBI did not show any improved outcome in patients 2 months post-TBI as measured by unresponsiveness, organ failure, and length of hospital stay (Moghaddam et al., 2017).

Polyunsaturated fatty acid compounds are responsible for maintaining membrane fluidity and neurotransmission in the brain where they are enriched (Kumar, P. R., et al., 2014). We found PUFA depletion in our mild TBI cohort. Deficiencies in PUFAs, particularly omega-3 fatty acids, have been linked to cognitive deficits in humans (Cook et al., 2019; Danthiir et al., 2011). Supplementation with fish oil supplements enriched in

omega-3 fatty acids or intraperitoneal injection of omega-3 fatty acids beginning at 2 hours post-TBI and continuing for 2 weeks resulted in the initiation of angiogenesis, reduced necrosis of striatal and cortical neurons, and improvement in spatial and learning deficits at 35 days following CCI TBI in mice (Pu et al., 2017). In contrast to many antioxidants described above, signaling pathways altered by PUFA administration have been explored in response to TBI. Signaling pathways such as those responsible for glial waste clearance and increased autophagy have been shown to be regulated by PUFA supplementation following TBI *in vivo*. These findings may explain the beneficial effects these compounds have on restoring cognition in models of TBI (Chen X., et al., 2018; Zhang, E., et al., 2020).

Although many studies have explored the use of nutraceutical antioxidant compounds to treat TBI preclinically, more rigorous testing should be conducted. There is a need for replicating study results, increasing the number of animals tested, and enriching our understanding of the mechanism of action and signaling pathways affected by these antioxidants. Deepening our understanding of how these compounds treat TBI would help encourage clinical testing of these nutraceutical antioxidants. Furthermore, many of the above studies focus on more severe models of TBI. More research into these compounds as treatments for single and repetitive mild or mild-to-moderate TBI should be performed.

5.2.2 Benefits and Limitations to Immunocal® Supplementation for Mild TBI

Immunocal® is a whey protein supplement that is replete with cystine which can cross the blood brain barrier where it is converted to cysteine, the limiting precursor for

GSH synthesis (Dringen et al., 1999). Immunocal® has been shown to increase GSH levels in vivo (Ross et al., 2012). Our lab has previously studied Immunocal® in an animal model of single moderate TBI induced by CCI (Ignowski et al., 2018). In this model, Immunocal® offered neuroprotection, protected against demyelination in the corpus callosum, prevented lipid peroxidation, and preserved BDNF and the ratio of GSH:GSSG. As shown in Chapter Three, Immunocal® can reduce astrogliosis observed at 2 weeks and 2 months following repetitive mild TBI and microgliosis at 72 hours following repetitive mild-moderate TBI. It is clear that Immunocal® has a therapeutic benefit in both single moderate and repetitive mild models of TBI induced by CCI.

Although we did observe increased astrogliosis, microgliosis, reduced GSH, and an increase in serum NfL in the repetitive mild-moderate TBI model, we only found that Immunocal® reduced microgliosis. This model was considered mild-moderate and consisted of 3 repetitive TBIs. Mice were analyzed at 72 hours post-TBI. This is soon after the TBIs and GSH turnover time in brain is slow. Chang et al. (1997) supplemented 2-month-old mice with cysteine and analyzed GSH and GSSG activity from 20 minutes to 108 hours after administration. They found that brain GSH had a half-life of 59.5 hours and turnover time of 85.7 hours (rate = 0.012 h^{-1} ; Chang et al., 1997). For comparison, the liver and kidneys of rats have rapid GSH turnover rates with half-lives of 1-5 hours, for comparison (Potter & Tran, 1993). Since we did observe a reduction of microgliosis in cortex with Immunocal® treatment, we hypothesized that microglia were able to synthesize GSH resulting in a reduction in localized ROS/RNS and consequent reduction of additional microglia activation/recruitment, but that whole cortex GSH levels were not

replenished within 72 hours. If we had analyzed GSH:GSSG levels at a later time point following the repetitive mild-moderate TBIs, we may have observed a preservation of GSH. Microglia also more efficiently synthesize GSH than astrocytes which may explain why we saw a reduction in microgliosis but not astrogliosis. Glutathione peroxidase and GR activity have been shown to be higher in cultured microglia under oxidative stress when compared to astrocytes which indicates microglia can more efficiently reduce oxidative stress through GSH synthesis resulting in less activation of nearby microglia (Hirrlinger et al., 2000). Overall, the repetitive mild-moderate injury paradigm may be too severe for a single agent like Immunocal®. Immunocal® could be used in conjunction with the above discussed exogenous antioxidant nutraceuticals to allow for greater neuroprotection.

5.3 Prolonged Antioxidant Depletion in Mild TBI May Contribute to the Development of Neurodegenerative Diseases such as ALS

Following even mild TBI, but especially in response to repetitive mild TBI, secondary injury processes have been shown to continue long term, for months to years. Neuroinflammation has been found to continue for greater than a year in animal models of mild repetitive TBI and for up to 18 years in humans in response to more severe TBI (Johnson et al., 2013a; Mouzon et al., 2014; Ramlackhansingh et al., 2011). Axonal degeneration, particularly in corpus callosum, has also been observed years following TBI and especially following repetitive TBI (Johnson et al., 2013a; Mouzon et al., 2014). Although not as well researched long-term following mild TBI, a few studies have reported that protein aggregates of tau and A β persist out to a year in human and animal models of TBI (Iwata et al., 2002; Marklund et al., 2021).

There is less research on oxidative stress long-term in response to mild TBI; however, oxidative stress markers have been shown to persist for years following more severe TBI (Mackay et al., 2006). On the same note, no research to date, besides that described in Chapter Two, has measured antioxidant biomarker levels following mild TBI long-term in humans. However, many preclinical studies have shown that treatments which reduce oxidative stress, such as those described previously, also decrease secondary injury pathology (Ignowski et al., 2018; Khalili et al., 2017; Lee, S. H., et al., 2017; Pu et al., 2017; Sharma et al., 2020). Further research needs to be done to fully understand the time course of oxidative stress and antioxidant imbalance following mild TBI and repetitive mild TBI.

Pathology resulting from mild single and repetitive TBI is similar to that observed in neurodegenerative disease. Furthermore, long-term deficits in cognition, symptoms which mirror that of neurodegenerative disease, have been reported following TBI (Xiong et al., 2018). Recent research suggests that mild TBI is a risk factor for developing neurodegenerative disease and suggests that prolonged neuroinflammation and oxidative stress are driving factors. It is hypothesized that depletion of the body's antioxidant defenses is consequent of, and a contributor to, pathology following mild TBI and that antioxidant nutraceutical supplements administered for mild TBI, especially of repetitive nature, which aim to reduce oxidative stress and neuroinflammation, could decrease the risk for developing neurodegenerative diseases such as ALS.

5.4 Future Directions to Explore the Connection Between Repetitive Mild TBI and ALS

Recent research has suggested that mild TBI, especially repetitive mild TBI, increases an individual's risk for developing neurodegenerative disease. Pathology such as neuroinflammation, oxidative stress, and excitotoxicity are observed in both TBI and neurodegenerative disease. Researchers believe that this pathology, namely oxidative stress and neuroinflammation, are key mechanisms responsible for the increased risk of developing neurodegenerative disease (Cruz-Haces et al., 2017). As previously described, these pathological conditions are hallmarks of ALS. In fact, TBI pathology mirrors that of motor neuron disease such as motor cortex atrophy, progressive neuronal cell death in brain and spinal cord, increased levels and aggregation of TDP-43, and muscle atrophy (Wright et al., 2017).

A few meta-analysis and epidemiological studies have found a correlation between individuals at high-risk for repetitive mild TBI and ALS. An analysis of 7,325 male professional soccer players between the years of 1970-2001 showed a very significant dose-dependent relationship between duration of involvement in professional soccer and the risk for ALS (Chiò et al., 2005). A second study by Chiò et al. (2009b) compared professional soccer players to professional athletes with low risk for repetitive mild TBI such as cyclists and basketball players. Again, a highly significant risk of ALS was identified for soccer players, but none was identified for the other athletes (Chiò et al., 2009b). Chen, H., et al. (2007) found that, although sustaining a single head injury throughout an individual's lifetime did not significantly increase the risk for ALS compared to individuals without head injury, individuals with more than one head injury

or a head injury within 10 years, had a significantly increased risk of developing ALS when compared to individuals with no injuries. Furthermore, sustaining multiple head injuries within the past 10 years resulted in a 10-fold greater risk of developing ALS (Chen, H., et al., 2007).

Although these studies indicate that high-risk populations for repetitive mild TBI may be at a greater risk for developing ALS, there may be other genetic, environmental, and lifestyle factors not considered which could be contributing to this increased risk. For example, an initial study found that Gulf War veterans had an increased incidence of developing ALS with a peak of 3.19 times the expected incidence rate (Haley, 2003). A follow up study by Horner et al. (2008) indicated that the increased ALS incidence in this population was time-limited and therefore could be due to environmental factors (Horner et al., 2008). Subsets of patients that sustain repetitive mild TBI may be more susceptible to developing ALS due to a variety of factors. A review of the literature by Franz et al. (2019) reports that factors like genetic predisposition, such as carrying the apolipoprotein E type 4 allele, sustaining TBIs during the ages of 35-54 years, or maintaining high levels of physical activity, although alone do not increase the risk of developing ALS, could contribute to an increased risk in patients that sustain repetitive mild TBI (Franz et al., 2019; Scarmeas et al., 2002; Schmidt et al., 2010). Preclinical studies which allow for greater control of these factors are necessary to increase our understanding of the potential contributions of repetitive TBI to the development of ALS.

A study by Evans et al. (2015) was one of two studies to explore the potential connection between mild TBI and ALS in preclinical animal models. The authors

examined the effect of a single mild TBI on lifespan, disease progression, motor function, muscle electrical activity, inflammation, and isoprostane levels in brain and spinal cord of hSOD1^{G93A} mice. Interestingly, they found that a single mild TBI at 84 days of age (prior to disease onset at 125 days of age in this low transgene copy model) did not have any effect on disease onset or survival (Evans et al., 2015). However, they did measure greater impairment in motor function, muscle activity abnormalities, and increased inflammation, isoprostanes, and edema in brain and spinal cord in hSOD1^{G93A} mice subjected to mild TBI (Evans et al., 2015). Although a single mild TBI worsened pathology in the hSOD1^{G93A} mouse model of ALS, it did not have any effect on disease onset, progression or survival.

Previous research suggests that specifically repetitive mild TBI may increase the risk of developing ALS. The second preclinical study to explore the connection between mild TBI and ALS was performed by Alkaslasi et al. (2021). Researchers subjected wild-type and hSOD1^{G93A} Sprague-Dawley rats to bilateral mild TBI induced by CCI beginning at 60 days of age and continuing once per week for 5 weeks. They found that hSOD1^{G93A} rats subjected to repetitive mild TBI showed earlier disease onset and shortened survival time when compared to sham surgery hSOD1^{G93A} rats. Interestingly, repetitive mild TBI hSOD1^{G93A} rats that experienced worsened acute symptoms, such as significantly worsened motor performance on rotarod and locomotor testing, exhibited significantly increased corticospinal motor neuron death and worsened outcomes later in life when compared to repetitive mild TBI hSOD1^{G93A} rats that didn't experience as severe symptoms acutely following the TBIs (Alkaslasi et al., 2021).

A future direction would be to induce repetitive mild TBI at 50 days of age, which is prior to disease onset at 90 days of age, in the hSOD1^{G93A} mouse model of ALS described in Chapter Four (Koza et al., 2020). It would be interesting to see if repetitive, instead of a single mild TBI, has any effect on disease onset and survival in this mouse model. Motor function could be measured prior to disease onset (50 days of age) and bi-weekly until end-stage of disease. Pathology including neuroinflammation, motor neuron survival, oxidative stress markers, antioxidants/ antioxidant enzyme expression in brain, spinal cord, and gastrocnemius muscle, along with neuromuscular junction innervation and complexity in gastrocnemius muscle, should be examined at disease onset (90 days of age), 105 days of age, and end-stage (approximately 125 days of age) of disease. Furthermore, this study design could be implemented in other mouse models of ALS such as the TDP-43 and C9orf72 genetic mouse models to see if repetitive mild TBI has the same effect regardless of the underlying genetic cause of ALS.

If survival is reduced, disease onset is earlier, and pathology is worsened in these models with repetitive mild TBI, it would be interesting to implement interventions using antioxidant nutraceuticals such as those found to be depleted in our mild TBI cohort from Chapter Two, Immunocal®, or PCA. Informed decisions would need to be made as to when to deliver these agents (preventative or restorative), ideal concentrations, combinations, and continuation of administration. However, if administration of these antioxidant nutraceuticals delayed disease onset, prolonged survival, and reduced pathology in hSOD1^{G93A}, TDP-43, or C9orf72 mutant mice subjected to repetitive mild TBI, this could support the hypothesis that secondary injury pathology is playing a major

role in the development of ALS. Furthermore, inducing repetitive mild TBI early in low transgene copy number versions of these genetic models, which may develop ALS phenotypes after an extended period of time, could allow one to study more prolonged secondary injury and resulting antioxidant depletion with an opportunity to implement antioxidant nutraceutical treatments beginning at various time points following the TBIs.

Unfortunately, there are no sporadic ALS animal models or sporadic models of neurodegeneration currently available. The above models are familial models with known disease courses. Clinical longitudinal studies would ultimately need to be performed in high-risk populations, such as professional athletes or military personnel. Antioxidant nutraceutical interventions could also be implemented. However, these studies would be lengthy, costly, and require high patient compliance which present as challenges.

5.5 Timing, Bioavailability, and Impact of External Factors with PCA Treatment

In Chapter Four, data from PCA administration beginning at disease onset in the hSOD1^{G93A} mouse model of ALS was reported. Oral administration of PCA extended survival and improved motor function in the hSOD1^{G93A} mouse. PCA was also able to reduce astrogliosis and microgliosis, protect motor neurons in spinal cord, and preserve NMJs in gastrocnemius muscle (Koza et al., 2020).

As described previously, PCA is a phenolic anthocyanin metabolite of cyanidin 3-*O*-glucoside and is well studied for its antioxidant, anti-inflammatory, and neuroprotective properties. Although the mechanism of action of PCA was not explored in Chapter Four, based on previous *in vitro* and *in vivo* data, it is hypothesized that PCA acts as an antioxidant and reduces the oxidative stress burden present in ALS. This results in a

reduction of other pathology, including neuroinflammation, and ultimately, neuroprotection. *In vitro*, PCA has been shown to significantly reduce ROS generation and pro-inflammatory cytokine production and preserve endogenous antioxidant levels such as GSH (Guan et al., 2006; Kaewmool et al., 2020; Li et al., 2011; Min et al., 2010; Winter et al., 2017a). *In vivo*, PCA has been studied in other models of neurodegeneration, such as AD and PD, and has been shown to improve cognitive function, decrease levels of oxidative stress markers, offer neuroprotection, and preserve GSH (Choi, J. R., et al., 2020; Kho et al., 2018; Lee, S. H., et al., 2017; Park et al., 2019; Song et al., 2014; Zhang, H. N., et al., 2010). Our study was the first to explore the therapeutic benefit of PCA for ALS; however, more research needs to be done in other models of ALS such as in TDP-43 or C9orf72 mutant models (Koza et al., 2020). Furthermore, a thorough analysis of the mechanism of action of PCA in ALS should be studied. Future studies should measure levels of ROS/RNS markers (hydrogen peroxide, superoxide, NOS, iNOS), production of pro-inflammatory cytokines, Nrf2 and JNK expression, and p53-dependent apoptotic factors. The mechanism of action of PCA which allows for the therapeutic benefit described in Chapter Four should ideally be identified prior to clinical studies with PCA.

Clinical studies should also take into consideration timing and bioavailability of PCA. As stated in Chapter Four, we began PCA treatment at disease onset (Koza et al., 2020). This administration timepoint was chosen because, unfortunately, many ALS patients are not diagnosed until after symptoms have begun and pathology is long underway. In fact, a review of the literature by Richards et al. (2020) found that patients are typically

diagnosed 10-16 months following disease onset (Richards et al., 2020). Therefore, there is a need for therapeutics that reduce pathology, slow disease progression, and extend survival at or following disease onset. Further study should be done to understand how late in disease progression PCA loses its beneficial effects against ALS pathology.

As previously described, PCA is readily bioavailable when cyanidin 3-*O*-glucoside is ingested through diet and metabolized into PCA. As of now, PCA as a commercial supplement in pure form is not available. Therefore, patients must obtain PCA through diet. Being one of the major metabolites of cyanidin 3-*O* glucoside, PCA accounts for 73% of ingested cyanidin 3-*O*-glucoside and has been measured in brain, plasma, and serum, peaking 1 hour after ingestion, at nmol concentrations (Vitaglione et al., 2007; Zhang, Y. J., et al., 2011; Zheng et al., 2019). However, PCA has a short half-life of 2.9 minutes in plasma when 50 mg/kg PCA was administered to mice (Chen, W., et al., 2012). These pharmacokinetics should be considered when determining optimal dosage and administration for humans.

Finally, PCA could have improved antioxidant and anti-inflammatory effects when combined with other phenolic compounds or flavonoids. A few studies have shown increased beneficial neuroprotective effects of PCA when combined with other nutraceutical antioxidant compounds. For example, PCA, when combined with ginkgolide B, a ginkgolide terpenoid lactone well studied for its antioxidant effects, showed improved neuroprotection and reduction of ROS in an *in vitro* model of PD. Furthermore, in an *in vivo* model of PD, the combination improved motor function, protected neurons, and increased antioxidant enzymatic activity in brain when compared

to PCA administration alone (Wu, T., et al., 2020). Another study by Zhang, Z., et al. (2015) explored the synergistic effect of chrysin, a polyphenolic compound, and PCA. Chrysin was able to enhance the effects of PCA allowing for greater protection against 6-hydroxydopamine in PC12 cells and neuroprotection in zebrafish and mouse models of PD marked by a reduction in ROS/RNS, increase in antioxidant enzymes, reduction of lipid peroxidation, and inhibition of NF κ B (Zhang, Z., et al., 2015). Although more research needs to be done to fully understand the synergism between PCA and other antioxidant nutraceuticals, especially in models of ALS, a future direction could be formulating a supplement with a variety of nutraceutical antioxidant compounds, including PCA, which synergize to yield enhanced antioxidant and anti-inflammatory activities.

5.6 Conclusion

In conclusion, secondary injury pathology from mild single and repetitive TBI, namely oxidative stress and neuroinflammation, can persist long-term. As a result, the endogenous antioxidant system becomes depleted and further contributes to pathological changes following single and repetitive mild TBI. Data in Chapter Two supports this and describes sex-specific antioxidant depletion in a cohort of patients with a history of mild TBI. These findings present a potential for treatment using nutraceutical compounds which have antioxidant and anti-neuroinflammatory properties and that help to increase endogenous antioxidant activity. An example of this would be Immunocal®, a whey protein supplement designed to increase levels of GSH in brain, which was shown in

Chapter Three to reduce gliosis in mouse models of repetitive mild and mild-moderate TBI.

Furthermore, pathology present following mild TBI mirrors that of neurodegenerative disease. Oxidative stress and neuroinflammation resulting from TBI have been shown previously to be driving factors in increasing the risk for developing neurodegenerative disease. More specifically, research has shown that repetitive TBI, even of mild severity, may increase the risk for developing ALS. A future direction would be to explore this connection and test the repetitive TBI models described in Chapter Three in the hSOD1^{G93A} ALS mouse model used in Chapter Four to see if repetitive TBI prior to disease onset has any effect on disease onset, progression, survival, and pathology. Future research should also explore the potential benefits of antioxidant nutraceutical supplementation in hSOD1^{G93A} ALS mice, and other preclinical mouse models of ALS, subjected to repetitive mild TBI.

Finally, Chapter Four described the therapeutic, neuroprotective, and anti-inflammatory effects of PCA in the hSOD1^{G93A} ALS mouse model (Koza et al., 2020). Phenolic acid metabolites, such as PCA, have antioxidant and anti-inflammatory properties that would be beneficial in treating neurodegenerative diseases like ALS. Although the mechanism of action of PCA alone should be further investigated, a combination of PCA with other nutraceutical antioxidant compounds may act synergistically to treat oxidative stress, neuroinflammation, and other pathology observed in neurodegenerative disease.

REFERENCES

- Abbas, K., Shenk, T. E., Poole, V. N., Breedlove, E. L., Leverenz, L. J., Nauman, E. A., ... Robinson, M. E. (2015). Alteration of default mode network in high school football athletes due to repetitive subconcussive mild traumatic brain injury: a resting-state functional magnetic resonance imaging study. *Brain connect*, *5*(2), 91–101. doi:10.1089/brain.2014.0279.
- Abdul-Muneer, P. M., Chandra, N., & Haorah, J. (2015). Interactions of oxidative stress and neurovascular inflammation in the pathogenesis of traumatic brain injury. *Mol Neurobiol*, *51*(3), 966–979. doi:10.1007/s12035-014-8752-3.
- Abdul-Muneer, P. M., Schuetz, H., Wang, F., Skotak, M., Jones, J., Gorantla, S., ... Haorah, J. (2013). Induction of oxidative and nitrosative damage leads to cerebrovascular inflammation in an animal model of mild traumatic brain injury induced by primary blast. *Free Radic Biol Med*, *60*, 282–291. doi:10.1016/j.freeradbiomed.2013.02.029.
- Aboonabi, A., & Singh, I. (2015). Chemopreventive role of anthocyanins in atherosclerosis via activation of Nrf2-ARE as an indicator and modulator of redox. *Biomed Pharmacother*, *72*, 30–36. doi:10.1016/j.biopha.2015.03.008.
- Abu-Hamad, S., Kahn, J., Leyton-Jaimes, M. F., Rosenblatt, J., & Israelson, A. (2017). Misfolded SOD1 accumulation and mitochondrial association contribute to the selective vulnerability of motor neurons in familial ALS: Correlation to human

disease. *ACS Chem Neurosci*, 8(10), 2225–2234.

doi:10.1021/acschemneuro.7b00140.

Aebischer, J., Cassina, P., Otsmane, B., Moumen, A., Seilhean, D., Meininger, V., ...
Raoul, C. (2011). IFN γ triggers a LIGHT-dependent selective death of
motoneurons contributing to the non-cell-autonomous effects of mutant SOD1.
Cell Death Differ, 18(5), 754–768. doi:10.1038/cdd.2010.143.

Aiguo Wu, Zhe Ying, & Gomez-Pinilla, F. (2010). Vitamin E protects against oxidative
damage and learning disability after mild traumatic brain injury in rats.
Neurorehabil Neural Repair, 24(3), 290–298. doi:10.1177/1545968309348318.

Al Nimer, F., Ström, M., Lindblom, R., Aeinehband, S., Bellander, B. M., Nyengaard, J.
... & Piehl, F. (2013). Naturally occurring variation in the Glutathione-S-
Transferase 4 gene determines neurodegeneration after traumatic brain injury.
Antioxid Redox Signal, 18(7), 784–794. doi:10.1089/ars.2011.4440.

Al Nimer, F., Thelin, E., Nyström, H., Dring, A. M., Svenningsson, A., Piehl, F., Nelson,
D. W., & Bellander, B. M. (2015). Comparative assessment of the prognostic
value of biomarkers in traumatic brain injury reveals an independent role for
serum levels of neurofilament light. *PLoS One*, 10(7), e0132177.
doi:10.1371/journal.pone.0132177.

Alexander, G. M., Erwin, K. L., Byers, N., Deitch, J. S., Augelli, B. J., Blankenhorn, E.
P., & Heiman-Patterson, T. D. (2004). Effect of transgene copy number on

survival in the G93A SOD1 transgenic mouse model of ALS. *Brain Res Mol Brain Res*, 130(1-2), 7–15. doi:10.1016/j.molbrainres.2004.07.002.

Alkaslasi, M. R., Cho, N. E., Dhillon, N. K., Shelest, O., Haro-Lopez, P. S., Linaval, N. T., ... Thomsen, G. M. (2021). Poor corticospinal motor neuron health is associated with increased symptom severity in the acute phase following repetitive mild TBI and predicts early ALS onset in genetically predisposed rodents. *Brain Sci*, 11(2), 160. doi:10.3390/brainsci11020160.

Allan, K., Hayes, K., Thomas, M., & Barnard, K. (2019). Coenzyme Q10 supplementation in traumatic brain injury: a scoping review protocol. *JBI Database System Rev Implement Rep*, 17(9), 1901–1908. doi:10.11124/JBISRIR-2017-003984.

Almer, G., Vukosavic, S., Romero, N., & Przedborski, S. (1999). Inducible nitric oxide synthase up-regulation in a transgenic mouse model of familial amyotrophic lateral sclerosis. *J Neurochem*, 72(6), 2415–2425. doi:10.1046/j.1471-4159.1999.0722415.x.

An, L. J., Guan, S., Shi, G. F., Bao, Y. M., Duan, Y. L., & Jiang B. (2006). Protocatechuic acid from *Alpinia oxyphylla* against MPP⁺-induced neurotoxicity in PC12 cells. *Food Chem Toxicol*, 44(3), 436–443. doi:10.1016/j.fct.2005.08.017.

- Andreadou, E., Kapaki, E., Kokotis, P., Paraskevas, G. P., Katsaros, N., Libitaki, G., ... Vassilopoulos, D. (2008). Plasma glutamate and glycine levels in patients with amyotrophic lateral sclerosis. *In vivo*, *22*(1), 137–141.
- Andriessen, T. M., Jacobs, B., & Vos, P. E. (2010). Clinical characteristics and pathophysiological mechanisms of focal and diffuse traumatic brain injury. *J Cell Mol Med*, *14*(10), 2381–2392. doi:10.1111/j.1582-4934.2010.01164.x.
- Ansari, M. A., Roberts, K. N., & Scheff, S. W. (2008). Oxidative stress and modification of synaptic proteins in hippocampus after traumatic brain injury. *Free Radic Biol Med*, *45*(4), 443–452. doi:10.1016/j.freeradbiomed.2008.04.038.
- Armada-Moreira, A., Gomes, J. I., Pina, C. C., Savchak, O. K., Gonçalves-Ribeiro, J., Rei, N., ... Vaz, S. H. (2020). Going the extra (synaptic) mile: Excitotoxicity as the road toward neurodegenerative diseases. *Front Cell Neurosci*, *14*, 90. doi:10.3389/fncel.2020.00090.
- Au, A. K., Aneja, R. K., Bayır, H., Bell, M. J., Janesko-Feldman, K., Kochanek, P. M., & Clark, R. (2017). Autophagy biomarkers beclin 1 and p62 are increased in cerebrospinal fluid after traumatic brain injury. *Neurocrit Care*, *26*(3), 348–355. doi:10.1007/s12028-016-0351-x.
- Au, A. K., Bayır, H., Kochanek, P. M., & Clark, R. S. (2010). Evaluation of autophagy using mouse models of brain injury. *Biochim Biophys Acta*, *1802*(10), 918–923. doi:10.1016/j.bbadis.2009.10.010.

- Babu, G. N., Kumar, A., Chandra, R., Puri, S. K., Singh, R. L., Kalita, J., & Misra, U. K. (2008). Oxidant-antioxidant imbalance in the erythrocytes of sporadic amyotrophic lateral sclerosis patients correlates with the progression of disease. *Neurochem Int*, 52(6), 1284–1289. doi:10.1016/j.neuint.2008.01.009.
- Bailes, J. E., Abusuwwa, R., Arshad, M., Chowdhry, S. A., Schleicher, D., Hempeck, N., ... Sears, B. (2020). Omega-3 fatty acid supplementation in severe brain trauma: case for a large multicenter trial. *J Neurosurgery*, 1–5. doi:10.3171/2020.3.JNS20183.
- Bailes, J. E., Dashnaw, M. L., Petraglia, A. L., & Turner, R. C. (2014). Cumulative effects of repetitive mild traumatic brain injury. *Prog Neurol Surg*, 28, 50–62. doi:10.1159/000358765.
- Bailes, J. E., & Mills, J. D. (2010). Docosahexaenoic acid reduces traumatic axonal injury in a rodent head injury model. *J neurotrauma*, 27(9), 1617–1624. doi:10.1089/neu.2009.1239.
- Bailes, J. E., Petraglia, A. L., Omalu, B. I., Nauman, E., & Talavage, T. (2013). Role of subconcussion in repetitive mild traumatic brain injury. *J Neurosurg*, 119(5), 1235–1245. doi:10.3171/2013.7.JNS121822.
- Balasubramanian, N., Srivastava, A., Pawar, N., Sagarkar, S., & Sakharkar, A. J. (2020). Repeated mild traumatic brain injury induces persistent variations in mitochondrial DNA copy number in mesocorticolimbic neurocircuitry of the rat. *Neurosci Res*, 155, 34–42. doi:10.1016/j.neures.2019.06.003.

- Bannai, S., & Tateishi, N. (1986). Role of membrane transport in metabolism and function of glutathione in mammals. *J Membr Biol*, *89*(1), 1–8.
doi:10.1007/BF01870891.
- Baracaldo-Santamaría, D., Ariza-Salamanca, D. F., Corrales-Hernández, M. G., Pachón-Londoño, M. J., Hernandez-Duarte, I., & Calderon-Ospina, C. A. (2022). Revisiting excitotoxicity in traumatic brain injury: From bench to bedside. *Pharmaceutics*, *14*(1), 152. doi:10.3390/pharmaceutics14010152.
- Baranova, A. I., Wei, E. P., Ueda, Y., Sholley, M. M., Kontos, H. A., & Povlishock, J. T. (2008). Cerebral vascular responsiveness after experimental traumatic brain injury: the beneficial effects of delayed hypothermia combined with superoxide dismutase administration. *J Neurosurg*, *109*(3), 502–509.
doi:10.3171/JNS/2008/109/9/0502.
- Baratz-Goldstein, R., Deselms, H., Heim, L. R., Khomski, L., Hoffer, B. J., Atlas, D., & Pick, C. G. (2016). Thioredoxin-mimetic-peptides protect cognitive function after mild traumatic brain injury (mTBI). *PloS one*, *11*(6), e0157064.
doi:10.1371/journal.pone.0157064.
- Barber, S. C., & Shaw, P. J. (2010). Oxidative stress in ALS: Key role in motor neuron injury and therapeutic target. *Free Radic Biol Med*, *48*(5), 629–641.
doi:10.1016/j.freeradbiomed.2009.11.018.

- Baruchel, S., & Viau, G. (1996). In vitro selective modulation of cellular glutathione by a humanized native milk protein isolate in normal cells and rat mammary carcinoma model. *Anticancer res*, *16*(3A), 1095-1099.
- Bayer, T. A., Wirths, O., Majtényi, K., Hartmann, T., Multhaup, G., Beyreuther, K., & Czech, C. (2001). Key factors in Alzheimer's disease: beta-amyloid precursor protein processing, metabolism and intraneuronal transport. *Brain Pathol*, *11*(1), 1–11. doi:10.1111/j.1750-3639.2001.tb00376.x.
- Bayir, H., Kagan, V. E., Tyurina, Y. Y., Tyurin, V., Ruppel, R. A., Adelson, P. D., ... Kochanek, P. M. (2002). Assessment of antioxidant reserves and oxidative stress in cerebrospinal fluid after severe traumatic brain injury in infants and children. *Pediatr Res*, *51*(5), 571–578. doi:10.1203/00006450-200205000-00005.
- Bayir, H., Marion, D. W., Puccio, A. M., Wisniewski, S. R., Janesko, K. L., Clark, R. S., & Kochanek, P. M. (2004). Marked gender effect on lipid peroxidation after severe traumatic brain injury in adult patients. *J neurotrauma*, *21*(1), 1–8. doi:10.1089/089771504772695896.
- Bazarian, J. J., Blyth, B., Mookerjee, S., He, H., & McDermott, M. P. (2010). Sex differences in outcome after mild traumatic brain injury. *J Neurotrauma*, *27*(3), 527–539. doi:10.1089/neu.2009.1068.
- Bazinet, R. P., & Layé, S. (2014). Polyunsaturated fatty acids and their metabolites in brain function and disease. *Nat Rev Neurosci*, *5*(12), 771–785. doi:10.1038/nrn3820.

- Beers, D. R., Henkel, J. S., Xiao, Q., Zhao, W., Wang, J., Yen, A. A., ... Appel, S. H. (2006). Wild-type microglia extend survival in PU.1 knockout mice with familial amyotrophic lateral sclerosis. *Proc Natl Acad Sci U S A*, *103*(43), 16021–16026. doi:10.1073/pnas.0607423103.
- Beers, D. R., Zhao, W., Liao, B., Kano, O., Wang, J., Huang, A., ... Henkel, J. S. (2011). Neuroinflammation modulates distinct regional and temporal clinical responses in ALS mice. *Brain Behav Immun*, *25*(5), 1025–1035. doi:10.1016/j.bbi.2010.12.008.
- Beghi, E., Logroscino, G., Chiò, A., Hardiman, O., Millul, A., Mitchell, D., ... Traynor, B. J. (2010). Amyotrophic lateral sclerosis, physical exercise, trauma and sports: results of a population-based pilot case-control study. *Amyotroph Lateral Scler*, *11*(3), 289–292. doi:10.3109/17482960903384283.
- Benkler, C., Ben-Zur, T., Barhum, Y., & Offen, D. (2013). Altered astrocytic response to activation in SOD1(G93A) mice and its implications on amyotrophic lateral sclerosis pathogenesis. *Glia*, *61*(3), 312–326. doi:10.1002/glia.22428.
- Bergersen, K., Halvorsen, J. Ø., Tryti, E. A., Taylor, S. I., & Olsen, A. (2017). A systematic literature review of psychotherapeutic treatment of prolonged symptoms after mild traumatic brain injury. *Brain Inj*, *31*(3), 279–289. doi:10.1080/02699052.2016.1255779.

- Bhandari, R., Kuhad, A., & Kuhad, A. (2018). Edaravone: A new hope for deadly amyotrophic lateral sclerosis. *Drugs Today*, 54(6), 349–360.
doi:10.1358/dot.2018.54.6.2828189.
- Bickford, P. C., Gould, T., Briederick, L., Chadman, K., Pollock, A., Young, D., ... Joseph, J. (2000). Antioxidant-rich diets improve cerebellar physiology and motor learning in aged rats. *Brain Res*, 866(1-2), 211–217. doi:10.1016/s0006-8993(00)02280-0.
- Blasco, H., Garcon, G., Patin, F., Veyrat-Durebex, C., Boyer, J., Devos, D., ... Corcia, P. (2017) Panel of oxidative stress and inflammatory biomarkers in ALS: A pilot study. *Can J Neurol Sci*, 44(1), 90–95. doi:10.1017/cjn.2016.284.
- Blokhuis, A. M., Groen, E. J., Koppers, M., van den Berg, L. H., & Pasterkamp, R. J. (2013). Protein aggregation in amyotrophic lateral sclerosis. *Acta Neuropathol*, 125(6), 777–794. doi:10.1007/s00401-013-1125-6.
- Bodnar, C. N., Roberts, K. N., Higgins, E. K., & Bachstetter, A. D. (2019). A systematic review of closed head injury models of mild traumatic brain injury in mice and rats. *J Neurotrauma*, 36(11), 1683–1706. doi:10.1089/neu.2018.6127.
- Boillée, S., Yamanaka, K., Lobsiger, C. S., Copeland, N. G., Jenkins, N. A., Kassiotis, ... Cleveland, D. W. (2006). Onset and progression in inherited ALS determined by motor neurons and microglia. *Science*, 312(5778), 1389–1392.
doi:10.1126/science.1123511.

- Bonvicini, F., Marcello, N., Mandrioli, J., Pietrini, V., & Vinceti, M. (2010). Exposure to pesticides and risk of amyotrophic lateral sclerosis: a population-based case-control study. *Ann Ist Super Sanita*, *46*(3), 284–287. doi:10.4415/ANN_10_03_10.
- Borrás, C., Sastre, J., García-Sala, D., Lloret, A., Pallardó, F. V., & Viña, J. (2003). Mitochondria from females exhibit higher antioxidant gene expression and lower oxidative damage than males. *Free Radic Biol Med*, *34*(5), 546–552. doi:10.1016/s0891-5849(02)01356-4.
- Boyd, S. D., Ullrich, M. S., Calvo, J. S., Behnia, F., Meloni, G., & Winkler, D. D. (2020). Mutations in superoxide dismutase 1 (Sod1) linked to familial amyotrophic lateral sclerosis can disrupt high-affinity zinc-binding promoted by the copper chaperone for Sod1 (Ccs). *Molecules*, *25*(5), 1086. doi:10.3390/molecules25051086.
- Bozzoni, V., Pansarasa, O., Diamanti, L., Nosari, G., Cereda, C., & Ceroni, M. (2016). Amyotrophic lateral sclerosis and environmental factors. *Funct Neurol*, *31*(1), 7–19. doi:10.11138/fneur/2016.31.1.007.
- Bramlett, H. M., & Dietrich, W. D. (2015). Long-term consequences of traumatic brain injury: Current status of potential mechanisms of injury and neurological outcomes. *J Neurotrauma*, *32*(23), 1834–1848. doi:10.1089/neu.2014.3352.
- Brettschneider, J., Toledo, J. B., Van Deerlin, V. M., Elman, L., McCluskey, L., Lee, V. M., & Trojanowski, J. Q. (2012). Microglial activation correlates with disease

progression and upper motor neuron clinical symptoms in amyotrophic lateral sclerosis. *PLoS ONE*, 7(6), e39216. doi:10.1371/journal.pone.0039216.

Brody, D. L., Mac Donald, C., Kessens, C. C., Yuede, C., Parsadonian, M., Spinner, M., ... Bayly, P. V. (2007). Electromagnetic controlled cortical impact device for precise, graded experimental traumatic brain injury. *J Neurotrauma*, 24(4), 657–673. doi:10.1089/neu.2006.0011.

Brown, C. A., Lally, C., Kupelian, V., & Flanders, W. D. (2021). Estimated prevalence and incidence of amyotrophic lateral sclerosis and SOD1 and C9orf72 genetic variants. *Neuroepidemiology*, 55(5), 342–353. doi:10.1159/000516752.

Buchan JR. (2014). mRNP granules. Assembly, function, and connections with disease. *RNA Biol*, 11(8):1019–1030. doi:10.4161/15476286.2014.972208.

Bulstrode, H., Nicoll, J. A., Hudson, G., Chinnery, P. F., Di Pietro, V., & Belli, A. (2014). Mitochondrial DNA and traumatic brain injury. *Ann Neurol*, 75(2), 186–195. doi:10.1002/ana.24116.

Burré J. (2015). The synaptic function of α -synuclein. *J Parkinson's Dis*, 5(4), 699–713. doi:10.3233/JPD-150642.

Butti, Z., & Patten, S. A. (2019). RNA Dysregulation in amyotrophic lateral sclerosis. *Front Genet*, 9, 712. doi:10.3389/fgene.2018.00712.

- Cappello, V., & Francolini, M. (2017). Neuromuscular junction dismantling in amyotrophic lateral sclerosis. *Int J Mol Sci*, *18*(10), 2092. doi:10.3390/ijms18102092.
- Carrera-Juliá, S., Moreno, M. L., Barrios, C., de la Rubia Ortí, J. E., & Drehmer, E. (2020). Antioxidant alternatives in the treatment of amyotrophic lateral sclerosis: A comprehensive review. *Front Physiol*, *11*, 63. doi:10.3389/fphys.2020.00063.
- Carrì, M. T., D'Ambrosi, N., & Cozzolino, M. (2017). Pathways to mitochondrial dysfunction in ALS pathogenesis. *Biochem Biophys Res Commun*, *483*(4), 1187–1193. doi:10.1016/j.bbrc.2016.07.055.
- Carroll, L. J., Cassidy, J. D., Holm, L., Kraus, J., Coronado, V. G., & WHO Collaborating Centre Task Force on Mild Traumatic Brain Injury (2004). Methodological issues and research recommendations for mild traumatic brain injury: the WHO Collaborating Centre Task Force on Mild Traumatic Brain Injury. *J Rehabil Med*, (43 Suppl), 113–125. doi:10.1080/16501960410023877.
- Cassidy A. (2018). Berry anthocyanin intake and cardiovascular health. *Mol Aspects Med*, *61*, 76–82. doi:10.1016/j.mam.2017.05.002.
- Cassidy, J. D., Carroll, L. J., Peloso, P. M., Borg, J., von Holst, H., Holm, L., ... WHO Collaborating Centre Task Force on Mild Traumatic Brain Injury (2004). Incidence, risk factors and prevention of mild traumatic brain injury: Results of the WHO Collaborating Centre Task Force on Mild Traumatic Brain Injury. *J Rehabil Med*, (43 Suppl), 28–60. doi:10.1080/16501960410023732.

- Castellanos-Montiel, M. J., Chaineau, M., & Durcan, T. M. (2020). The neglected genes of ALS: Cytoskeletal dynamics impact synaptic degeneration in ALS. *Front Cell Neurosci*, *14*, 594975. doi:10.3389/fncel.2020.594975.
- Chaban, V., Clarke, G., Skandsen, T., Islam, R., Einarsen, C. E., Vik, A., ... Pischke, S. E. (2020). Systemic inflammation persists the first year after mild traumatic Brain injury: Results from the prospective Trondheim mild traumatic brain injury Study. *J Neurotrauma*, *37*(19), 2120–2130. doi:10.1089/neu.2019.6963.
- Chang, M. L., Klaidman, L. K., & Adams, J. D., Jr (1997). The effects of oxidative stress on in vivo brain GSH turnover in young and mature mice. *Mol Chem Neuropathol*, *30*(3), 187–197. doi:10.1007/BF02815097.
- Chatterjee, S., Noack, H., Possel, H., Keilhoff, G., & Wolf, G. (1999). Glutathione levels in primary glial cultures: Monochlorobimane provides evidence of cell type-specific distribution. *Glia*, *27*(2), 152–161.
- Chen, H., Desai, A., & Kim, H. Y. (2017). Repetitive closed-head impact model of engineered rotational acceleration induces long-term cognitive impairments with persistent astrogliosis and microgliosis in mice. *Journal of Neurotrauma*, *34*(14), 2291–2302. doi: 10.1089/neu.2016.4870.
- Chen, H., Richard, M., Sandler, D. P., Umbach, D. M., & Kamel, F. (2007). Head injury and amyotrophic lateral sclerosis. *Am J Epidemiol*, *166*(7), 810–816. doi:10.1093/aje/kwm153.

- Chen, W., Wang, D., Wang, L. S., Bei, D., Wang, J., See, W. A., ... Liu, Z. (2012). Pharmacokinetics of protocatechuic acid in mouse and its quantification in human plasma using LC-tandem mass spectrometry. *J Chromatogr B Analyt Technol Biomed Life Sci*, 908, 39–44. doi:10.1016/j.jchromb.2012.09.032.
- Chen, X., Pan, Z., Fang, Z., Lin, W., Wu, S., Yang, F., ... Li, S. (2018). Omega-3 polyunsaturated fatty acid attenuates traumatic brain injury-induced neuronal apoptosis by inducing autophagy through the upregulation of SIRT1-mediated deacetylation of Beclin-1. *J Neuroinflammation*, 15(1), 310. doi:10.1186/s12974-018-1345-8.
- Chiò, A., Benzi, G., Dossena, M., Mutani, R., & Mora, G. (2005). Severely increased risk of amyotrophic lateral sclerosis among Italian professional football players. *Brain*, 128(Pt 3), 472–476. doi:10.1093/brain/awh373.
- Chiò, A., Logroscino, G., Hardiman, O., Swingle, R., Mitchell, D., Beghi, E., ... Eurals Consortium (2009a). Prognostic factors in ALS: A critical review. *Amyotroph Lateral Scler*, 10(5-6), 310–323. doi:10.3109/17482960802566824.
- Chiò, A., Mora, G., Calvo, A., Mazzini, L., Bottacchi, E., Mutani, R., & PARALS (2009). Epidemiology of ALS in Italy: a 10-year prospective population-based study. *Neurology*, 72(8), 725–731. doi:10.1212/01.wnl.0000343008.26874.d1.
- Chiu, I. M., Morimoto, E. T., Goodarzi, H., Liao, J. T., O’Keeffe, S., Phatnani, H. P., ... Maniatis, T. (2013) A neurodegeneration-specific gene-expression signature of

acutely isolated microglia from an amyotrophic lateral sclerosis mouse model. *Cell Rep*, 4 (2), 385–401. doi:10.1016/j.celrep.2013.06.018.

Choi, B. Y., Kim, I. Y., Kim, J. H., Lee, B. E., Lee, S. H., Kho, A. R., ... Suh, S. W. (2016). Decreased cysteine uptake by EAAC1 gene deletion exacerbates neuronal oxidative stress and neuronal death after traumatic brain injury. *Amino acids*, 48(7), 1619–1629. doi:10.1007/s00726-016-2221-4.

Choi, J. R., Kim, J. H., Lee, S., Cho, E. J., & Kim, H. Y. (2020). Protective effects of protocatechuic acid against cognitive impairment in an amyloid beta-induced Alzheimer's disease mouse model. *Food Chem Toxicol*, 144, 111571. doi:10.1016/j.fct.2020.111571.

Cimino, F., Speciale, A., Anwar, S., Canali, R., Ricciardi, E., Virgili, F., ... Saija, A. (2013). Anthocyanins protect human endothelial cells from mild hyperoxia damage through modulation of Nrf2 pathway. *Genes Nutr*, 8(4), 391–399. doi:10.1007/s12263-012-0324-4.

Clarke, B. E., & Patani, R. (2020). The microglial component of amyotrophic lateral sclerosis. *Brain*, 143(12), 3526–3539. doi:10.1093/brain/awaa309.

Clement, A. M., Nguyen, M. D., Roberts, E. A., Garcia, M. L., Boillée, S., Rule, M., ... Cleveland, D. W. (2003). Wild-type nonneuronal cells extend survival of SOD1 mutant motor neurons in ALS mice. *Science*, 302(5642), 113–117. doi:10.1126/science.1086071.

- Clément, T., Lee, J. B., Ichkova, A., Rodriguez-Grande, B., Fournier, M. L., Aussudre, J., ... Badaut, J. (2020). Juvenile mild traumatic brain injury elicits distinct spatiotemporal astrocyte responses. *Glia*, 68(3), 528–542. doi:10.1002/glia.23736.
- Cobley, J. N., Fiorello, M. L., & Bailey, D. M. (2018). 13 reasons why the brain is susceptible to oxidative stress. *Redox Biol*, 15, 490–503. doi:10.1016/j.redox.2018.01.008.
- Conte, V., Uryu, K., Fujimoto, S., Yao, Y., Rokach, J., Longhi, L., ... Praticò, D. (2004). Vitamin E reduces amyloidosis and improves cognitive function in Tg2576 mice following repetitive concussive brain injury. *J Neurochem*, 90(3), 758–764. doi:10.1111/j.1471-4159.2004.02560.x.
- Cook, R. L., Parker, H. M., Donges, C. E., O'Dwyer, N. J., Cheng, H. L., Steinbeck, K. S., ... O'Connor, H. T. (2019). Omega-3 polyunsaturated fatty acids status and cognitive function in young women. *Lipids Health Dis*, 18(1), 194. doi:10.1186/s12944-019-1143-z.
- Cooksley, R., Maguire, E., Lannin, N. A., Unsworth, C. A., Farquhar, M., Galea, C., ... Schmidt, J. (2018). Persistent symptoms and activity changes three months after mild traumatic brain injury. *Aust Occup Ther J*, 65(3), 168–175. doi:10.1111/1440-1630.12457.
- Cornelius, C., Crupi, R., Calabrese, V., Graziano, A., Milone, P., Pennisi, G., ... Cuzzocrea, S. (2013). Traumatic brain injury: Oxidative stress and

neuroprotection. *Antioxid Redox Signal*, 19(8), 836–853.

doi:10.1089/ars.2012.4981.

Corona, J. C., & Tapia, R. (2007). Ca²⁺-permeable AMPA receptors and intracellular Ca²⁺ determine motoneuron vulnerability in rat spinal cord in vivo.

Neuropharmacology, 52(5), 1219–1228. doi:10.1016/j.neuropharm.2006.12.008.

Couratier, P., Hugon, J., Sindou, P., Vallat, J. M., & Dumas, M. (1993). Cell culture evidence for neuronal degeneration in amyotrophic lateral sclerosis being linked to glutamate AMPA/kainate receptors. *Lancet*, 341(8840), 265–268.

doi:10.1016/0140-6736(93)92615-z.

Cova, E., Bongioanni, P., Cereda, C., Metelli, M. R., Salvaneschi, L., Bernuzzi, S., ...

Ceroni, M. (2010). Time course of oxidant markers and antioxidant defenses in subgroups of amyotrophic lateral sclerosis patients. *Neurochem Int*, 56(5), 687–693. doi:10.1016/j.neuint.2010.02.004.

Cruz-Haces, M., Tang, J., Acosta, G., Fernandez, J., & Shi, R. (2017). Pathological correlations between traumatic brain injury and chronic neurodegenerative diseases. *Transl Neurodegener*, 6, 20. doi:10.1186/s40035-017-0088-2.

D'Amico, E., Factor-Litvak, P., Santella, R. M., & Mitsumoto, H. (2013). Clinical perspective on oxidative stress in sporadic amyotrophic lateral sclerosis. *Free Radic Biol Med*, 65, 509–527. doi:10.1016/j.freeradbiomed.2013.06.029.

- Da Ros, M., Deol, H. K., Savard, A., Guo, H., Meiering, E. M., & Gibbings, D. (2021). Wild-type and mutant SOD1 localizes to RNA-rich structures in cells and mice but does not bind RNA. *J Neurochem*, *156*(4), 524–538. doi:10.1111/jnc.15126.
- Dahl, N. A., Danis, E., Balakrishnan, I., Wang, D., Pierce, A., Walker, F. M., ... Vibhakar, R. (2020). Super elongation complex as a targetable dependency in diffuse midline glioma. *Cell Rep*, *31*(1), 107485. doi:10.1016/j.celrep.2020.03.049.
- Damiano, M., Starkov, A. A., Petri, S., Kipiani, K., Kiaei, M., Mattiazzi, M., ... Manfredi, G. (2006). Neural mitochondrial Ca²⁺ capacity impairment precedes the onset of motor symptoms in G93A Cu/Zn-superoxide dismutase mutant mice. *J Neurochem*, *96*(5), 1349–1361. doi:10.1111/j.1471-4159.2006.03619.x.
- Danbolt, N. C., Storm-Mathisen, J., & Kanner, B. I. (1992). An [Na⁺ + K⁺]coupled L-glutamate transporter purified from rat brain is located in glial cell processes. *Neuroscience*, *51*(2), 295–310. doi:10.1016/0306-4522(92)90316-t.
- Danthiir, V., Burns, N. R., Nettelbeck, T., Wilson, C., & Wittert, G. (2011). The older people, omega-3, and cognitive health (EPOCH) trial design and methodology: a randomised, double-blind, controlled trial investigating the effect of long-chain omega-3 fatty acids on cognitive ageing and wellbeing in cognitively healthy older adults. *Nutr J*, *10*, 117. doi:10.1186/1475-2891-10-117.

- Daoud, H., Valdmanis, P. N., Kabashi, E., Dion, P., Dupré, N., Camu, W., ... Rouleau, G. A. (2009). Contribution of TARDBP mutations to sporadic amyotrophic lateral sclerosis. *J Med Genet*, *46*(2), 112–114. doi:10.1136/jmg.2008.062463.
- Dash, P. K., Hergenroeder, G. W., Jeter, C. B., Choi, H. A., Kobori, N., & Moore, A. N. (2016). Traumatic brain injury alters methionine metabolism: Implications for pathophysiology. *Front Syst Neurosci*, *10*, 36. doi:10.3389/fnsys.2016.00036.
- de Ferrars, R. M., Czank, C., Zhang, Q., Botting, N. P., Kroon, P. A., Cassidy, A., & Kay, C. D. (2014). The pharmacokinetics of anthocyanins and their metabolites in humans. *Br J Pharmacol*, *171*(13), 3268–3282. doi:10.1111/bph.12676.
- de Jong, S. W., Huisman, M. H., Sutedja, N. A., van der Kooi, A. J., de Visser, M., Schelhaas, H. J., ... van den Berg, L. H. (2012). Smoking, alcohol consumption, and the risk of amyotrophic lateral sclerosis: a population-based study. *Am J Epidemiol*, *176*(3), 233–239. doi:10.1093/aje/kws015.
- De Vos, K. J., & Hafezparast, M. (2017). Neurobiology of axonal transport defects in motor neuron diseases: Opportunities for translational research? *Neurobiol Dis*, *105*, 283–299. doi:10.1016/j.nbd.2017.02.004.
- Decker, S.L., Strait, J.E., Roberts, A.M., & Ferraracci, J. (2018). Intellectual and neuropsychological assessment of individuals with sensory and physical disabilities and traumatic brain injury. *Contemporary intellectual assessment: Theories, tests, and issues* (4, 662–683). New York: The Guilford Press.

- Deitch, J. S., Alexander, G. M., Bensinger, A., Yang, S., Jiang, J. T., & Heiman-Patterson, T. D. (2014). Phenotype of transgenic mice carrying a very low copy number of the mutant human G93A superoxide dismutase-1 gene associated with amyotrophic lateral sclerosis. *PloS one*, 9(6), e99879. doi:10.1371/journal.pone.0099879.
- Demirbag, R., Yilmaz, R., & Erel, O. (2005). The association of total antioxidant capacity with sex hormones. *Scand Cardiovasc J*, 39(3), 172–176. doi:10.1080/14017430510035862.
- Dewan, M. C., Rattani, A., Gupta, S., Baticulon, R. E., Hung, Y. C., Panchak, M., ... Park, K. B. (2018). Estimating the global incidence of traumatic brain injury. *J Neurosurg*, 1–18. doi:10.3171/2017.10.JNS17352.
- DeWitt, D. S., & Prough, D. S. (2009). Blast-induced brain injury and posttraumatic hypotension and hypoxemia. *J Neurotrauma*, 26(6), 877–887. doi:10.1089/neu.2007.0439.
- Dhillon, N. K., Linaval, N. T., O'Rourke, J., Barmparas, G., Yang, A., Cho, N., ... Ley, E. J. (2020). How repetitive traumatic injury alters long-term brain function. *J Trauma Acute Care Surg*, 89(5), 955–961. doi:10.1097/TA.0000000000002811.
- Di Giacomo, C., Acquaviva, R., Santangelo, R., Sorrenti, V., Vanella, L., Li Volti, G., ... Galvano, F. (2012). Effect of treatment with cyanidin-3-O- β -D-glucoside on rat ischemic/reperfusion brain damage. *Evid Based Complement Alternat Med*, 2012, 285750. doi:10.1155/2012/285750.

- Di Giorgio, F. P., Carrasco, M. A., Siao, M. C., Maniatis, T., & Eggan, K. (2007) Non-cell autonomous effect of glia on motor neurons in an embryonic stem cell-based ALS model. *Nat Neurosci*, *10*(5), 608–614. doi:10.1038/nn1885.
- Diaz-Amarilla, P., Olivera-Bravo, S., Trias, E., Cragolini, A., Martinez-Palma, L., Cassina, P., ... Barbeito, L. (2011) Phenotypically aberrant astrocytes that promote motoneuron damage in a model of inherited amyotrophic lateral sclerosis. *Proc Natl Acad Sci USA*, *108*(44), 18126–18131. doi:10.1073/pnas.1110689108.
- Dixon K. J. (2017). Pathophysiology of traumatic brain injury. *Phys Med Rehabil Clin N Am*, *28*(2), 215–225. doi:10.1016/j.pmr.2016.12.001.
- Dobrovolny, J., Smrcka, M., & Bienertova-Vasku, J. (2018). Therapeutic potential of vitamin E and its derivatives in traumatic brain injury-associated dementia. *Neurol Sci*, *39*(6), 989–998. doi:10.1007/s10072-018-3398-y.
- Dols-Icardo, O., Montal, V., Sirisi, S., López-Pernas, G., Cervera-Carles, L., Querol-Vilaseca, M., ... Clarimón, J. (2020). Motor cortex transcriptome reveals microglial key events in amyotrophic lateral sclerosis. *Neurol Neuroimmunol Neuroinflamm*, *7*(5), e829. doi:10.1212/NXI.0000000000000829.
- Donovan, V., Kim, C., Anugerah, A. K., Coats, J. S., Oyoyo, U., Pardo, A. C., & Obenaus, A. (2014). Repeated mild traumatic brain injury results in long-term white-matter disruption. *J Cereb Blood Flow Metab*, *34*(4), 715–723. doi:10.1038/jcbfm.2014.6.

- Dorsett, C. R., McGuire, J. L., DePasquale, E. A., Gardner, A. E., Floyd, C. L., & McCullumsmith, R. E. (2017). Glutamate neurotransmission in rodent models of traumatic brain injury. *J neurotrauma*, *34*(2), 263–272. doi:10.1089/neu.2015.4373.
- Dringen, R., Pfeiffer, B., & Hamprecht, B. (1999). Synthesis of the antioxidant glutathione in neurons: supply by astrocytes of CysGly as precursor for neuronal glutathione. *J Neurosci*, *19*(2), 562–569. doi:10.1523/JNEUROSCI.19-02-00562.1999.
- Dwivedi, D., Megha, K., Mishra, R., & Mandal, P. K. (2020). Glutathione in brain: Overview of its conformations, functions, biochemical characteristics, quantitation and potential therapeutic role in brain disorders. *Neurochem Res*, *45*(7), 1461–1480. doi:10.1007/s11064-020-03030-1.
- Edwards, G., 3rd, Moreno-Gonzalez, I., & Soto, C. (2017). Amyloid-beta and tau pathology following repetitive mild traumatic brain injury. *Biochem Biophys Res Commun*, *483*(4), 1137–1142. doi:10.1016/j.bbrc.2016.07.123.
- Edwards, G., 3rd, Zhao, J., Dash, P. K., Soto, C., & Moreno-Gonzalez, I. (2020). Traumatic brain injury induces tau aggregation and spreading. *J Neurotrauma*, *37*(1), 80–92. doi:10.1089/neu.2018.6348.
- Eisenbaum, M., Pearson, A., Gratkowski, A., Mouzon, B., Mullan, M., Crawford, F., ... Bachmeier, C. (2021). Influence of traumatic brain injury on extracellular tau

elimination at the blood-brain barrier. *Fluids Barriers CNS*, 18(1), 48.

doi:10.1186/s12987-021-00283-y.

Eker, M. E., Aaby, K., Budic-Leto, I., Brnčić, S. R., El, S. N., Karakaya, S., ... Pascual-

Teresa, S. (2019). A review of factors affecting anthocyanin bioavailability:

Possible implications for the inter-individual variability. *Foods*, 9(1), 2.

doi:10.3390/foods9010002.

Emmerich, T., Abdullah, L., Ojo, J., Mouzon, B., Nguyen, T., Crynen, G., ... Crawford,

F. (2017). Mild TBI results in a long-term decrease in circulating phospholipids in a mouse model of injury. *Neuromolecular Med*, 19(1), 122–135.

doi:10.1007/s12017-016-8436-4.

Evans, T. M., Jaramillo, C. A., Sataranatarajan, K., Watts, L., Sabia, M., Qi, W., & Van

Remmen, H. (2015). The effect of mild traumatic brain injury on peripheral

nervous system pathology in wild-type mice and the G93A mutant mouse model of motor neuron disease. *Neuroscience*, 298, 410–423.

doi:10.1016/j.neuroscience.2015.04.041.

Faden, A. I., & Loane, D. J. (2015). Chronic neurodegeneration after traumatic brain

injury: Alzheimer disease, chronic traumatic encephalopathy, or persistent

neuroinflammation? *Neurotherapeutics*, 12(1), 143–150. doi:10.1007/s13311-

014-0319-5.

- Fan, H., Zhang, K., Shan, L., Kuang, F., Chen, K., Zhu, K., ... Wang, Y. Z. (2016). Reactive astrocytes undergo M1 microglia/macrophages-induced necroptosis in spinal cord injury. *Mol Neurodegener*, *11*, 14. doi:10.1186/s13024-016-0081-8.
- Fehily, B., & Fitzgerald, M. (2017). Repeated mild traumatic brain injury: Potential mechanisms of damage. *Cell transplant*, *26*(7), 1131–1155. doi:10.1177/0963689717714092.
- Felgines, C., Krisa, S., Mauray, A., Besson, C., Lamaison, J. L., Scalbert, A., ... Texier, O. (2010). Radiolabelled cyanidin 3-O-glucoside is poorly absorbed in the mouse. *Br J Nutr*, *103*(12), 1738–1745. doi:10.1017/S0007114510000061.
- Ferrarese, C., Sala, G., Riva, R., Begni, B., Zoia, C., Tremolizzo, L., ... Italian ALS Study Group (2001). Decreased platelet glutamate uptake in patients with amyotrophic lateral sclerosis. *Neurology*, *56*(2), 270–272. doi:10.1212/wnl.56.2.270.
- Fidan, E., Lewis, J., Kline, A. E., Garman, R. H., Alexander, H., Cheng, J. P., ... Bayir, H. (2016). Repetitive mild traumatic brain injury in the developing brain: Effects on long-term functional outcome and neuropathology. *J Neurotrauma*, *33*(7), 641–651. doi:10.1089/neu.2015.3958.
- Flanagan S. R. (2015). Invited commentary on “Centers for disease control and prevention report to congress: Traumatic brain injury in the United States: Epidemiology and rehabilitation.” *Arch Phys Med Rehabil*, *96*(10), 1753–1755. doi: 10.1016/j.apmr.2015.07.001.

- Fleschhut, J., Kratzer, F., Rechkemmer, G., & Kulling, S. E. (2006). Stability and biotransformation of various dietary anthocyanins in vitro. *Eur J Nutr*, *45*(1), 7–18. doi:10.1007/s00394-005-0557-8.
- Foran, E., & Trotti, D. (2009). Glutamate transporters and the excitotoxic path to motor neuron degeneration in amyotrophic lateral sclerosis. *Antioxid Redox Signal*, *11*(7), 1587–1602. doi:10.1089/ars.2009.2444.
- Fornasaro, S., Ziberna, L., Gasperotti, M., Tramer, F., Vrhovšek, U., Mattivi, F., & Passamonti, S. (2016). Determination of cyanidin 3-glucoside in rat brain, liver and kidneys by UPLC/MS-MS and its application to a short-term pharmacokinetic study. *Sci Rep*, *6*, 22815. doi:10.1038/srep22815.
- Franz, C. K., Joshi, D., Daley, E. L., Grant, R. A., Dalamagkas, K., Leung, A., ... Kiskinis, E. (2019). Impact of traumatic brain injury on amyotrophic lateral sclerosis: from bedside to bench. *J Neurophysiol*, *122*(3), 1174–1185. doi:10.1152/jn.00572.2018.
- Frey, L., Lepkin, A., Schickedanz, A., Huber, K., Brown, M. S., & Serkova, N. (2014). ADC mapping and T1-weighted signal changes on post-injury MRI predict seizure susceptibility after experimental traumatic brain injury. *Neurol Res*, *36*(1), 26–37. doi:10.1179/1743132813Y.0000000269.
- Friedman, S. D., Poliakov, A. V., Budech, C., Shaw, D., Breiger, D., Jinguji, T., ... Ojemann, J. G. (2017). GABA alterations in pediatric sport concussion. *Neurology*, *89*(21), 2151–2156. doi:10.1212/WNL.0000000000004666.

- Fujita, M., Wei, E. P., & Povlishock, J. T. (2012). Intensity-and interval-specific repetitive traumatic brain injury can evoke both axonal and microvascular damage. *J Neurotrauma*, *29*(12), 2172–2180. doi:10.1089/neu.2012.2357.
- Gabrieli, D., Schumm, S. N., Vigilante, N. F., & Meaney, D. F. (2021). NMDA receptor alterations after mild traumatic brain injury induce deficits in memory acquisition and recall. *Neural Comput*, *33*(1), 67–95. doi:10.1162/neco_a_01343.
- Gahm, C., Holmin, S., Wiklund, P. N., Brundin, L., & Mathiesen, T. (2006). Neuroprotection by selective inhibition of inducible nitric oxide synthase after experimental brain contusion. *J Neurotrauma*, *23*(9), 1343–1354. doi:10.1089/neu.2006.23.1343.
- Galli, R. L., Bielinski, D. F., Szprengiel, A., Shukitt-Hale, B., & Joseph, J. A. (2006). Blueberry supplemented diet reverses age-related decline in hippocampal HSP70 neuroprotection. *Neurobiol Aging*, *27*(2), 344–350. doi:10.1016/j.neurobiolaging.2005.01.017.
- Gao, H., Han, Z., Bai, R., Huang, S., Ge, X., Chen, F., & Lei, P. (2017). The accumulation of brain injury leads to severe neuropathological and neurobehavioral changes after repetitive mild traumatic brain injury. *Brain Res*, *1657*, 1–8. doi:10.1016/j.brainres.2016.11.028.
- Gardner, R. C., Byers, A. L., Barnes, D. E., Li, Y., Boscardin, J., & Yaffe, K. (2018). Mild TBI and risk of Parkinson disease: A chronic effects of neurotrauma

consortium study. *Neurology*, 90(20), e1771–e1779.

doi:10.1212/WNL.0000000000005522.

Gardner, R. C., & Yaffe, K. (2015). Epidemiology of mild traumatic brain injury and neurodegenerative disease. *Mol Cell Neurosci*, 66(Pt B), 75–80.

doi:10.1016/j.mcn.2015.03.001.

Gavett BE, Stern RA, McKee AC. Chronic traumatic encephalopathy: a potential late effect of sport-related concussive and subconcussive head trauma. (2011). *Clin Sports Med*, 30(1):179-88, xi. doi:10.1016/j.csm.2010.09.007.

George, K. K., Heithoff, B. P., Shandra, O., & Robel, S. (2022). Mild traumatic brain injury/concussion initiates an atypical astrocyte response caused by blood-brain barrier dysfunction. *J neurotrauma*, 39(1-2), 211–226.

doi:10.1089/neu.2021.0204.

Ghasemi, M., & Brown, R. H., Jr (2018). Genetics of Amyotrophic Lateral Sclerosis. *Cold Spring Harb Perspect Med*, 8(5), a024125.

doi:10.1101/cshperspect.a024125.

Gladman, M., & Zinman, L. (2015). The economic impact of amyotrophic lateral sclerosis: a systematic review. *Expert Rev Pharmacoecon Outcomes Res*, 15(3), 439–450. doi:10.1586/14737167.2015.1039941.

Golenia, A., Leśkiewicz, M., Regulska, M., Budziszewska, B., Szczęśny, E., Jagiełła, J., ... Słowik, A. (2014). Catalase activity in blood fractions of patients with

sporadic ALS. *Pharmacol Rep*, 66(4), 704–707.

doi:10.1016/j.pharep.2014.02.021.

Goodrich, G. S., Kabakov, A. Y., Hameed, M. Q., Dhamne, S. C., Rosenberg, P. A., & Rotenberg, A. (2013). Ceftriaxone treatment after traumatic brain injury restores expression of the glutamate transporter, GLT-1, reduces regional gliosis, and reduces post-traumatic seizures in the rat. *J Neurotrauma*, 30(16), 1434–1441. doi:10.1089/neu.2012.2712.

Goss, J. R., Taffe, K. M., Kochanek, P. M., & DeKosky, S. T. (1997). The antioxidant enzymes glutathione peroxidase and catalase increase following traumatic brain injury in the rat. *Exp Neurol*, 146(1), 291–294. doi:10.1006/exnr.1997.6515.

Gowing, G., Philips, T., Van Wijmeersch, B., Audet, J. N., Dewil, M., Van Den Bosch, ... Julien, J. P. (2008). Ablation of proliferating microglia does not affect motor neuron degeneration in amyotrophic lateral sclerosis caused by mutant superoxide dismutase. *J Neurosci*, 28(41), 10234–10244. doi:10.1523/JNEUROSCI.3494-08.2008.

Graber, D. J., Hickey, W. F., & Harris, B. T. Progressive changes in microglia and macrophages in spinal cord and peripheral nerve in the transgenic rat model of amyotrophic lateral sclerosis. (2010). *J Neuroinflamm*, 7:8. doi:10.1186/1742-2094-7-8.

- Graham, N. S., & Sharp, D. J. (2019). Understanding neurodegeneration after traumatic brain injury: from mechanisms to clinical trials in dementia. *J Neurol Neurosurg Psychiatry*, *90*(11), 1221–1233. doi:10.1136/jnnp-2017-317557.
- Gregory, J. M., Livesey, M. R., McDade, K., Selvaraj, B. T., Barton, S. K., Chandran, S., & Smith, C. (2020). Dysregulation of AMPA receptor subunit expression in sporadic ALS post-mortem brain. *J Pathol*, *250*(1), 67–78. doi:10.1002/path.5351.
- Grin'kina, N. M., Li, Y., Haber, M., Sangobowale, M., Nikulina, E., Le'Pre, C., ... Bergold, P. J. (2016). Righting reflex predicts long-term histological and behavioral outcomes in a closed head model of traumatic brain injury. *PLoS One*, *11*(9), e0161053. doi:10.1371/journal.pone.0161053.
- Grovola, M. R., Paleologos, N., Brown, D. P., Tran, N., Wofford, K. L., Harris, J. P., ... Duda, J. E. (2021). Diverse changes in microglia morphology and axonal pathology during the course of 1 year after mild traumatic brain injury in pigs. *Brain Pathol*, *31*(5), e12953. doi:10.1111/bpa.12953.
- Guan, S., Jiang, B., Bao, Y. M., & An, L. J. (2006). Protocatechuic acid suppresses MPP⁺-induced mitochondrial dysfunction and apoptotic cell death in PC12 cells. *Food Chem Toxicol*, *44*(10), 1659–1666. doi:10.1016/j.fct.2006.05.004.
- Guerriero, R. M., Giza, C. C., & Rotenberg, A. (2015). Glutamate and GABA imbalance following traumatic brain injury. *Curr Neurol Neurosci Rep*, *15*(5), 27. doi:10.1007/s11910-015-0545-1.

- Guo, W., Stoklund Dittlau, K., & Van Den Bosch, L. (2020). Axonal transport defects and neurodegeneration: Molecular mechanisms and therapeutic implications. *Semin Cell Dev Biol*, *99*, 133–150. doi:10.1016/j.semcdb.2019.07.010.
- Guo, Y. S., Wu, D. X., Wu, H. R., Wu, S. Y., Yang, C., Li, B., ... Li, C. Y. (2009). Sensory involvement in the SOD1-G93A mouse model of amyotrophic lateral sclerosis. *Exp Mol Med*, *41*(3), 140–150. doi:10.3858/emm.2009.41.3.017.
- Gurney, M. E., Pu, H., Chiu, A. Y., Dal Canto, M. C., Polchow, C. Y., Alexander, D. D., ... Deng, H. X. (1994). Motor neuron degeneration in mice that express a human Cu,Zn superoxide dismutase mutation. *Science*, *264*(5166), 1772–1775. doi:10.1126/science.8209258.
- Guskiewicz, K. M., McCrea, M., Marshall, S. W., Cantu, R. C., Randolph, C., Barr, W., ... Kelly, J. P. (2003). Cumulative effects associated with recurrent concussion in collegiate football players: the NCAA Concussion Study. *JAMA*, *290*(19), 2549–2555. doi:10.1001/jama.290.19.2549.
- Haidet-Phillips, A. M., Hester, M. E., Miranda, C. J., Meyer, K., Braun, L., Frakes, A., ... Kaspar, B. K. (2011). Astrocytes from familial and sporadic ALS patients are toxic to motor neurons. *Nat Biotechnol*, *29*(9), 824–828. doi:10.1038/nbt.1957.
- Haley R. W. (2003). Excess incidence of ALS in young Gulf War veterans. *Neurology*, *61*(6), 750–756. doi:10.1212/wnl.61.6.750.

- Harish, G., Mahadevan, A., Pruthi, N., Sreenivasamurthy, S. K., Puttamallesh, V. N., Keshava Prasad, T. S., ... Srinivas Bharath, M. M. (2015). Characterization of traumatic brain injury in human brains reveals distinct cellular and molecular changes in contusion and pericontusion. *J Neurochem*, *134*(1), 156–172. doi:10.1111/jnc.13082.
- Harvey, C. J., Thimmulappa, R. K., Singh, A., Blake, D. J., Ling, G., Wakabayashi, N., ... Biswal, S. (2009). Nrf2-regulated glutathione recycling independent of biosynthesis is critical for cell survival during oxidative stress. *Free Radic Biol Med*, *46*(4), 443–453. doi:10.1016/j.freeradbiomed.2008.10.040.
- Healy, E. F., Roth-Rodriguez, A., & Toledo, S. (2020). A model for gain of function in superoxide dismutase. *Biochem Biophys Rep*, *21*, 100728. doi:10.1016/j.bbrep.2020.100728.
- Heiman-Patterson, T. D., Deitch, J. S., Blankenhorn, E. P., Erwin, K. L., Perreault, M. J., Alexander, B. K., ... Alexander, G. M. (2005). Background and gender effects on survival in the TgN(SOD1-G93A)1Gur mouse model of ALS. *J Neurol Sci*, *236*(1-2), 1–7. doi:10.1016/j.jns.2005.02.006.
- Hemerková, P., & Vališ, M. (2021). Role of oxidative stress in the pathogenesis of amyotrophic lateral sclerosis: Antioxidant metalloenzymes and therapeutic strategies. *Biomolecules*, *11*(3), 437. doi:10.3390/biom11030437.
- Hensley, K., Floyd, R. A., Gordon, B., Mou, S., Pye, Q. N., Stewart, C., ... Williamson, K. (2002). Temporal patterns of cytokine and apoptosis-related gene expression in

spinal cords of the G93A-SOD1 mouse model of amyotrophic lateral sclerosis. *J Neurochem*, 82(2), 365–374. doi:10.1046/j.1471-4159.2002.00968.x.

Hernández-Camacho, J. D., Bernier, M., López-Lluch, G., & Navas, P. (2018). Coenzyme Q10 supplementation in aging and disease. *Front Physiol*, 9, 44. doi:10.3389/fphys.2018.00044.

Hicdonmez, T., Kanter, M., Tiryaki, M., Parsak, T., & Cobanoglu, S. (2006). Neuroprotective effects of N-acetylcysteine on experimental closed head trauma in rats. *Neurochem Res*, 31(4), 473–481. doi:10.1007/s11064-006-9040-z.

Hiebert, J. B., Shen, Q., Thimmesch, A. R., & Pierce, J. D. (2015). Traumatic brain injury and mitochondrial dysfunction. *Am J Med Sci*, 350(2), 132–138. doi:10.1097/MAJ.0000000000000506.

Hill, C. S., Coleman, M. P., & Menon, D. K. (2016). Traumatic axonal injury: Mechanisms and translational opportunities. *Trends Neurosci*, 39(5), 311–324. doi:10.1016/j.tins.2016.03.002.

Hirrlinger, J., Gutterer, J. M., Kussmaul, L., Hamprecht, B., & Dringen, R. (2000). Microglial cells in culture express a prominent glutathione system for the defense against reactive oxygen species. *Dev Neurosci*, 22(5–6), 384–392. doi:10.1159/000017464.

Hoffer, M. E., Balaban, C., Slade, M. D., Tsao, J. W., & Hoffer, B. (2013). Amelioration of acute sequelae of blast induced mild traumatic brain injury by N-acetyl

cysteine: a double-blind, placebo controlled study. *PLoS one*, 8(1), e54163.

doi:10.1371/journal.pone.0054163.

Honan, C. A., McDonald, S., Gowland, A., Fisher, A., & Randall, R. K. (2015). Deficits in comprehension of speech acts after TBI: The role of theory of mind and executive function. *Brain Lang*, 150, 69–79. doi:10.1016/j.bandl.2015.08.007.

Hoogenboom, W. S., Branch, C. A., & Lipton, M. L. (2019). Animal models of closed-skull, repetitive mild traumatic brain injury. *Pharmacol Ther*, 198, 109–122.

doi:10.1016/j.pharmthera.2019.02.016.

Horiuchi, D., Collins, C. A., Bhat, P., Barkus, R. V., Diantonio, A., & Saxton, W. M. (2007). Control of a kinesin-cargo linkage mechanism by JNK pathway kinases.

Curr Biol, 17(15), 1313–1317. doi:10.1016/j.cub.2007.06.062.

Hornedo-Ortega, R., Álvarez-Fernández, M. A., Cerezo, A. B., Richard, T., Troncoso, A. M., & Garcia-Parrilla, M. C. (2016). Protocatechuic acid: Inhibition of fibril formation, destabilization of preformed fibrils of amyloid- β and α -synuclein, and neuroprotection. *J Agric Food Chem*, 64(41), 7722–7732.

doi:10.1021/acs.jafc.6b03217.

Horner, R. D., Grambow, S. C., Coffman, C. J., Lindquist, J. H., Oddone, E. Z., Allen, K. D., & Kasarskis, E. J. (2008). Amyotrophic lateral sclerosis among 1991 Gulf War veterans: evidence for a time-limited outbreak. *Neuroepidemiology*, 31(1), 28–32. doi:10.1159/000136648.

- Hossain, I., Mohammadian, M., Takala, R., Tenovuo, O., Azurmendi Gil, L., Frantzen, J., ... Posti, J. P. (2020). Admission levels of total tau and β -amyloid isoforms 1-40 and 1-42 in predicting the outcome of mild traumatic brain injury. *Front Neurol*, *11*, 325. doi:10.3389/fneur.2020.00325.
- Hossain, I., Mohammadian, M., Takala, R., Tenovuo, O., Lagerstedt, L., Ala-Seppälä, H., ... Posti, J. P. (2019). Early levels of glial fibrillary acidic protein and neurofilament light protein in predicting the outcome of mild traumatic brain injury. *J Neurotrauma*, *36*(10), 1551–1560. doi:10.1089/neu.2018.5952.
- Huh, J. W., Franklin, M. A., Widing, A. G., & Raghupathi, R. (2006). Regionally distinct patterns of calpain activation and traumatic axonal injury following contusive brain injury in immature rats. *Dev Neurosci*, *28*(4-5), 466–476. doi:10.1159/000094172.
- Ide, T., Tsutsui, H., Ohashi, N., Hayashidani, S., Suematsu, N., Tsuchihashi, M., ... Takeshita, A. (2002). Greater oxidative stress in healthy young men compared with premenopausal women. *Arterioscler Thromb Vasc Biol*, *22*(3), 438–442. doi:10.1161/hq0302.104515.
- Ignowski, E., Winter, A. N., Duval, N., Fleming, H., Wallace, T., Manning, E., ... Linseman, D. A. (2018). The cysteine-rich whey protein supplement, Immunocal®, preserves brain glutathione and improves cognitive, motor, and histopathological indices of traumatic brain injury in a mouse model of controlled

cortical impact. *Free Radic Biol Med*, 124, 328–341.

doi:10.1016/j.freeradbiomed.2018.06.026.

Ikawa, M., Okazawa, H., Tsujikawa, T., Matsunaga, A., Yamamura, O., Mori, T., ...

Yoneda M. (2015). Increased oxidative stress is related to disease severity in the ALS motor cortex. *Neurology*, 84(20), 2033–2039.

doi:10.1212/WNL.0000000000001588.

Ikenaka, K., Katsuno, M., Kawai, K., Ishigaki, S., Tanaka, F., & Sobue, G. (2012).

Disruption of axonal transport in motor neuron diseases. *Int J Mol Sci*, 13(1), 1225–1238. doi:10.3390/ijms13011225.

Ilieva, H., Polymenidou, M., & Cleveland, D. W. (2009). Non-cell autonomous toxicity

in neurodegenerative disorders: ALS and beyond. *J Cell Biol*, 187(6), 761–772.

doi:10.1083/jcb.200908164.

Impellizzeri, D., Campolo, M., Bruschetta, G., Crupi, R., Cordaro, M., Paterniti, I., ...

Esposito, E. (2016). Traumatic brain injury leads to development of Parkinson's disease related pathology in mice. *Front Neurosci*, 10, 458.

doi:10.3389/fnins.2016.00458.

Institute of Medicine (US) Committee on Nutrition, Trauma, and the Brain. (2011).

Antioxidants. Erdman, J. & Pillsbury, L. *Nutrition and traumatic brain injury:*

Improving acute and subacute health outcomes in military personnel. Washington

(DC): National Academies Press (US).

- Ismail, H., Shakkour, Z., Tabet, M., Abdelhady, S., Kobaisi, A., Abedi, R., ... Salameh, J. (2020). Traumatic brain injury: Oxidative stress and novel anti-oxidants such as Mitoquinone and Edaravone. *Antioxidants (Basel)*, *9*(10), 943. doi:10.3390/antiox9100943.
- Iwata, A., Chen, X. H., McIntosh, T. K., Browne, K. D., & Smith, D. H. (2002). Long-term accumulation of amyloid-beta in axons following brain trauma without persistent upregulation of amyloid precursor protein genes. *J Neuropathol Exp Neurol*, *61*(12), 1056–1068. doi:10.1093/jnen/61.12.1056.
- Jassam, Y. N., Izzy, S., Whalen, M., McGavern, D. B., & El Khoury, J. (2017). Neuroimmunology of traumatic brain Injury: Time for a paradigm shift. *Neuron*, *95*(6), 1246–1265. doi:10.1016/j.neuron.2017.07.010.
- Jin, M., Günther, R., Akgün, K., Hermann, A., & Ziemssen, T. (2020). Peripheral proinflammatory Th1/Th17 immune cell shift is linked to disease severity in amyotrophic lateral sclerosis. *Sci Rep*, *10*(1), 5941. doi:10.1038/s41598-020-62756-8.
- Johnson, V. E., Stewart, J. E., Begbie, F. D., Trojanowski, J. Q., Smith, D. H., & Stewart, W. (2013a). Inflammation and white matter degeneration persist for years after a single traumatic brain injury. *Brain*, *136*(Pt 1), 28–42. doi:10.1093/brain/aws322.
- Johnson, V. E., Stewart, W., & Smith, D. H. (2013b). Axonal pathology in traumatic brain injury. *Exp Neurol*, *246*, 35–43. doi:10.1016/j.expneurol.2012.01.013.

- Jong, C. J., Azuma, J., & Schaffer, S. (2012). Mechanism underlying the antioxidant activity of taurine: prevention of mitochondrial oxidant production. *Amino acids*, 42(6), 2223–2232. doi:10.1007/s00726-011-0962-7.
- Jordan, F. L., & Thomas, W. E. (1988). Brain macrophages: questions of origin and interrelationship. *Brain Res*, 13(2), 165-178. doi:10.1016/0165-0173(88)90019-7.
- Kaewmool, C., Kongtawelert, P., Phitak, T., Pothacharoen, P., & Udomruk, S. (2020). Protocatechuic acid inhibits inflammatory responses in LPS-activated BV2 microglia via regulating SIRT1/NF- κ B pathway contributed to the suppression of microglial activation-induced PC12 cell apoptosis. *J Neuroimmunol*, 341, 577164. doi:10.1016/j.jneuroim.2020.577164.
- Kalayci, M., Unal, M. M., Gul, S., Acikgoz, S., Kandemir, N., Hanci, V., ... Acikgoz, B. (2011). Effect of coenzyme Q10 on ischemia and neuronal damage in an experimental traumatic brain-injury model in rats. *BMC Neurosci*, 12, 75. doi:10.1186/1471-2202-12-75.
- Kander, M. C., Cui, Y., & Liu, Z. (2017). Gender difference in oxidative stress: a new look at the mechanisms for cardiovascular diseases. *J Cell Mol Med*, 21(5), 1024–1032. doi:10.1111/jcmm.13038.
- Kang, T. H., Hur, J. Y., Kim, H. B., Ryu, J. H., & Kim, S. Y. (2006). Neuroprotective effects of the cyanidin-3-O-beta-d-glucopyranoside isolated from mulberry fruit against cerebral ischemia. *Neurosci Lett*, 391(3), 122–126. doi:10.1016/j.neulet.2005.08.053.

- Kawahara, Y., & Kwak, S. (2005). Excitotoxicity and ALS: what is unique about the AMPA receptors expressed on spinal motor neurons? *Amyotroph Lateral Scler Other Motor Neuron Disord*, 6(3), 131–144. doi:10.1080/14660820510037872.
- Kawamata, H., & Manfredi, G. (2010). Mitochondrial dysfunction and intracellular calcium dysregulation in ALS. *Mech Ageing Dev*, 131(7-8), 517–526. doi:10.1016/j.mad.2010.05.003.
- Kelsey, N., Hulick, W., Winter, A., Ross, E., & Linseman, D. A. (2011). Neuroprotective effects of anthocyanins on apoptosis induced by mitochondrial oxidative stress. *Nutr Neurosci*, 14(6), 249–259. doi:10.1179/1476830511Y.0000000020.
- Khan, M., Im, Y. B., Shunmugavel, A., Gilg, A. G., Dhindsa, R. K., Singh, A. K., & Singh, I. (2009). Administration of S-nitrosoglutathione after traumatic brain injury protects the neurovascular unit and reduces secondary injury in a rat model of controlled cortical impact. *J Neuroinflammation*, 6, 32. doi:10.1186/1742-2094-6-32.
- Khalil, M., Teunissen, C. E., Otto, M., Piehl, F., Sormani, M. P., Gattringer, T., ... Kuhle, J. (2018). Neurofilaments as biomarkers in neurological disorders. *Nat Rev Neurol*, 14(10), 577–589. doi:10.1038/s41582-018-0058-z.
- Khalili, H., Ahl, R., Cao, Y., Paydar, S., Sjölin, G., Niakan, A., ... Mohseni, S. (2017). Early selenium treatment for traumatic brain injury: Does it improve survival and functional outcome? *Injury*, 48(9), 1922–1926. doi:10.1016/j.injury.2017.07.005.

- Khatri, N., Thakur, M., Pareek, V., Kumar, S., Sharma, S., & Datusalia, A. K. (2018). Oxidative stress: Major threat in traumatic brain injury. *CNS Neurol Disord Drug Targets*, *17*(9), 689–695. doi:10.2174/1871527317666180627120501.
- Kho, A. R., Choi, B. Y., Lee, S. H., Hong, D. K., Lee, S. H., Jeong, J. H., ... Suh, S. W. (2018). Effects of protocatechuic acid (PCA) on global cerebral ischemia-induced hippocampal neuronal death. *Int J Mol Sci*, *19*(5), 1420. doi:10.3390/ijms19051420.
- Khoo, H. E., Azlan, A., Tang, S. T., & Lim, S. M. (2017). Anthocyanidins and anthocyanins: colored pigments as food, pharmaceutical ingredients, and the potential health benefits. *Food Nutr Res*, *61*(1), 1361779. doi:10.1080/16546628.2017.1361779.
- Kim, H. J., Kim, N. C., Wang, Y. D., Scarborough, E. A., Moore, J., Diaz, Z., ... Taylor, J. P. (2013). Mutations in prion-like domains in hnRNPA2B1 and hnRNPA1 cause multisystem proteinopathy and ALS. *Nature*, *495*(7442), 467–473. doi:10.1038/nature11922.
- Kim, K. T., Nam, T. K., Park, Y. S., Kim, Y. B., & Park, S. W. (2011). Neuroprotective effect of anthocyanin on experimental traumatic spinal cord injury. *J Korean Neurosurg Soc*, *49*(4), 205–211. doi:10.3340/jkns.2011.49.4.205.
- Kim, S. M., Chung, M. J., Ha, T. J., Choi, H. N., Jang, S. J., Kim, S. O., ... Park, Y. I. (2012). Neuroprotective effects of black soybean anthocyanins via inactivation of

ASK1-JNK/p38 pathways and mobilization of cellular sialic acids. *Life Sci*, 90(21-22), 874–882. doi:10.1016/j.lfs.2012.04.025.

King, A. E., Woodhouse, A., Kirkcaldie, M. T., & Vickers, J. C. (2016). Excitotoxicity in ALS: Overstimulation, or overreaction? *Exp Neurol*, 275 Pt 1, 162–171. doi:10.1016/j.expneurol.2015.09.019.

Kirby, J., Halligan, E., Baptista, M. J., Allen, S., Heath, P. R., Holden, H., ... Shaw, P. J. (2005). Mutant SOD1 alters the motor neuronal transcriptome: implications for familial ALS. *Brain*, 128(Pt 7), 1686–1706. doi:10.1093/brain/awh503.

Konrad, C., Geburek, A. J., Rist, F., Blumenroth, H., Fischer, B., Husstedt, I., ... Lohmann, H. (2011). Long-term cognitive and emotional consequences of mild traumatic brain injury. *Psychol Med*, 41(6), 1197–1211. doi:10.1017/S0033291710001728.

Koza, L., & Linseman, D. A. (2019). Glutathione precursors shield the brain from trauma. *Neural Regen Res*, 14(10), 1701–1702. doi:10.4103/1673-5374.257520.

Koza, L. A., Winter, A. N., Holsopple, J., Baybayon-Grandgeorge, A. N., Pena, C., Olson, J. R., ... Linseman, D. A. (2020). Protocatechuic acid extends survival, improves motor function, diminishes gliosis, and sustains neuromuscular junctions in the hSOD1G93A mouse model of amyotrophic lateral sclerosis. *Nutrients*, 12(6), 1824. doi:10.3390/nu12061824.

- Kozakiewicz, M., Kornatowski, M., Krzywińska, O., & Kędziora-Kornatowska, K. (2019). Changes in the blood antioxidant defense of advanced age people. *Clin Interv Aging, 14*, 763 - 771.
- Kropat, C., Mueller, D., Boettler, U., Zimmermann, K., Heiss, E. H., Dirsch, V. M., Rogoll, D., ... Marko, D. (2013). Modulation of Nrf2-dependent gene transcription by bilberry anthocyanins in vivo. *Mol Nutr Food Res, 57*(3), 545–550. doi:10.1002/mnfr.201200504.
- Krzysztoforska, K., Mirowska-Guzel, D., & Widy-Tyszkiewicz, E. (2019). Pharmacological effects of protocatechuic acid and its therapeutic potential in neurodegenerative diseases: Review on the basis of in vitro and in vivo studies in rodents and humans. *Nutr Neurosci, 22*(2), 72–82. doi:10.1080/1028415X.2017.1354543.
- Kucur, M., Taner, T., Reza, D., Halil, A., Ercument, Y., Ahmet, B., ... Mehmet Yasar, K. (2005). Superoxide dismutase, catalase, and guanase in traumatic brain injury. *Neurosurg Q, 15*(3), 186-189. doi:10.1097/01.wnq.0000173450.16339.77.
- Kumar, P. R., Essa, M. M., Al-Adawi, S., Dradekh, G., Memon, M. A., Akbar, M., & Manivasagam, T. (2014). Omega-3 Fatty acids could alleviate the risks of traumatic brain injury - a mini review. *J Tradit Complement Med, 4*(2), 89–92. doi:10.4103/2225-4110.130374.

- Kumar, V., Kashav, T., & Hassan, M. I. (2019). Amyotrophic lateral sclerosis: Current therapeutic perspectives. In: Singh S., Joshi N., editors. *Pathology, Prevention and Therapeutics of Neurodegenerative Disease*, Springer; Singapore, 207–224.
- Kwon, H.S., Koh, S.H. (2020). Neuroinflammation in neurodegenerative disorders: the roles of microglia and astrocytes. *Transl Neurodegener* 9, 42.
doi:10.1186/s40035-020-00221-2.
- Kyyriäinen, J., Kajevu, N., Bañuelos, I., Lara, L., Lipponen, A., Balosso, S., ... Pitkänen, A. (2021). Targeting oxidative stress with antioxidant duotherapy after experimental traumatic brain injury. *Int J Mol Sci*, 22(19), 10555.
doi:10.3390/ijms221910555.
- Ladak, A. A., Enam, S. A., & Ibrahim, M. T. (2019). A review of the molecular mechanisms of traumatic brain injury. *World Neurosurg*, 131, 126–132.
doi:10.1016/j.wneu.2019.07.039.
- Lamark, T., & Johansen, T. (2012). Aggrephagy: selective disposal of protein aggregates by macroautophagy. *Int J Cell Biol*, 2012, 736905. doi:10.1155/2012/736905.
- Lawson, L. J., Perry, V. H., & Gordon, S. (1992). Turnover of resident microglia in the normal adult mouse brain. *Neuroscience*, 48(2), 405–415. doi:10.1016/0306-4522(92)90500-2.
- Lazarus, R. C., Buonora, J. E., Jacobowitz, D. M., & Mueller, G. P. (2015). Protein carbonylation after traumatic brain injury: cell specificity, regional susceptibility,

and gender differences. *Free Radic Biol Med*, 78, 89–100.

doi:10.1016/j.freeradbiomed.2014.10.507.

Lee, J., Ryu, H., & Kowall, N. W. (2009). Differential regulation of neuronal and inducible nitric oxide synthase (NOS) in the spinal cord of mutant SOD1 (G93A) ALS mice. *Biochem Biophys Res Commun*, 387(1), 202–206.

doi:10.1016/j.bbrc.2009.07.007.

Lee, J. E., Garber, B., & Zamorski, M. A. (2015). Prospective analysis of premilitary mental health, somatic symptoms, and postdeployment postconcussive symptoms. *Psychosom Med*, 77(9), 1006–1017. doi:10.1097/PSY.0000000000000250.

Lee, K. H., Cha, M., & Lee, B. H. (2020). Neuroprotective effect of antioxidants in the brain. *Int J Mol Sci*, 21(19), 7152. doi:10.3390/ijms21197152.

Lee, M. C., Ting, K. K., Adams, S., Brew, B. J., Chung, R., & Guillemin, G. J. (2010). Characterisation of the expression of NMDA receptors in human astrocytes. *PloS one*, 5(11), e14123. doi:10.1371/journal.pone.0014123.

Lee, S., & Kim, H. J. (2015). Prion-like mechanism in amyotrophic lateral sclerosis: are protein aggregates the key? *Exp Neurobiol*, 24(1), 1–7.

doi:10.5607/en.2015.24.1.1.

Lee, S. H., Choi, B. Y., Lee, S. H., Kho, A. R., Jeong, J. H., Hong, D. K., & Suh, S. W. (2017). Administration of protocatechuic acid reduces traumatic brain injury-induced neuronal death. *Int J Mol Sci*, 18(12), 2510. doi:10.3390/ijms18122510.

- Lehman, E. J., Hein, M. J., Baron, S. L., & Gersic, C. M. (2012). Neurodegenerative causes of death among retired National Football League players. *Neurology*, 79(19), 1970–1974. doi:10.1212/WNL.0b013e31826daf50.
- Lende, A. B., Kshirsagar, A. D., Deshpande, A. D., Muley, M. M., Patil, R. R., Bafna, P. A., & Naik, S. R. (2011). Anti-inflammatory and analgesic activity of protocatechuic acid in rats and mice. *Inflammopharmacology*, 19(5), 255–263. doi:10.1007/s10787-011-0086-4.
- Levin, H. S., & Diaz-Arrastia, R. R. (2015). Diagnosis, prognosis, and clinical management of mild traumatic brain injury. *Lancet Neurol*, 14(5), 506–517. doi:10.1016/S1474-4422(15)00002-2.
- Levin, H. S., Temkin, N. R., Barber, J., Nelson, L. D., Robertson, C., Brennan, J., ... Zafonte, R. (2021). Association of sex and age with mild traumatic brain injury-related symptoms: A TRACK-TBI study. *JAMA Netw Open*, 4(4), e213046. doi:10.1001/jamanetworkopen.2021.3046.
- Li, X., Wang, X., Chen, D., & Chen, S. (2011). Antioxidant activity and mechanism of protocatechuic acid in vitro. *Funct Foods Health Dis*, 1(7). doi:10.31989/ffhd.v1i7.127.
- Liddel, S. A., Guttenplan, K. A., Clarke, L. E., Bennett, F. C., Bohlen, C. J., Schirmer, L., ... Barres, B. A. (2017). Neurotoxic reactive astrocytes are induced by activated microglia. *Nature*, 541 (7638), 481–487. doi:10.1038/nature21029.

- Lifshitz, J., Friberg, H., Neumar, R. W., Raghupathi, R., Welsh, F. A., Janmey, P., ... McIntosh, T. K. (2003). Structural and functional damage sustained by mitochondria after traumatic brain injury in the rat: evidence for differentially sensitive populations in the cortex and hippocampus. *J Cereb Blood Flow Metab*, 23(2), 219–231. doi:10.1097/01.WCB.0000040581.43808.03.
- Lila, M. A., Burton-Freeman, B., Grace, M., & Kalt, W. (2016). Unraveling anthocyanin bioavailability for human health. *Annu Rev Food Sci Technol*, 7, 375–393. doi:10.1146/annurev-food-041715-033346.
- Lindenau, J., Noack, H., Asayama, K., & Wolf, G. (1998). Enhanced cellular glutathione peroxidase immunoreactivity in activated astrocytes and in microglia during excitotoxin induced neurodegeneration. *Glia*, 24(2), 252–256.
- Liu, F., Zhao, F., Wang, W., Sang, J., Jia, L., Li, L., & Lu, F., (2020). Cyanidin-3-O-glucoside inhibits A β 40 fibrillogenesis, disintegrates preformed fibrils, and reduces amyloid cytotoxicity. *Food Funct*, 11(3), 2573–2587. doi:10.1039/c9fo00316a.
- Liu, Y. M., Jiang, B., Bao, Y. M., & An, L. J. Protocatechuic acid inhibits apoptosis by mitochondrial dysfunction in rotenone-induced PC12 cells. (2008). *Toxicol In Vitro*, 22(2), 430–437. doi:10.1016/j.tiv.2007.10.012.
- Lolekha, P., Phanthumchinda, K., & Bhidayasiri, R. (2010). Prevalence and risk factors of Parkinson's disease in retired Thai traditional boxers. *Mov Disord*, 25(12), 1895–1901. doi:10.1002/mds.23210.

- Longinetti, E., & Fang, F. (2019). Epidemiology of amyotrophic lateral sclerosis: an update of recent literature. *Curr Opin Neurol*, 32(5), 771–776.
doi:10.1097/WCO.0000000000000730.
- Lopez-Gonzalez, R., Lu, Y., Gendron, T. F., Karydas, A., Tran, H., Yang, D., Petrucelli, L., ... Gao, F. B. (2016). Poly(GR) in C9ORF72-related ALS/FTD compromises mitochondrial function and increases oxidative stress and DNA damage in iPSC-derived motor neurons. *Neuron*, 92(2), 383–391.
doi:10.1016/j.neuron.2016.09.015.
- Losada-Barreiro, S. & Bravo-Díaz, C. (2017). Free radicals and polyphenols: The redox chemistry of neurodegenerative diseases. *Eur J Med Chem*, 133, 379–402.
doi:10.1016/j.ejmech.2017.03.061.
- Lu, C. H., Petzold, A., Topping, J., Allen, K., Macdonald-Wallis, C., Clarke, J., ... Malaspina, A. (2015). Plasma neurofilament heavy chain levels and disease progression in amyotrophic lateral sclerosis: insights from a longitudinal study. *J Neurol Neurosurg Psychiatry*, 86(5), 565–573. doi:10.1136/jnnp-2014-307672.
- Lukaszuk, J. M., Shokrani, M., Roy, P. G., Hoppensteadt, J., & Umoren, J. (2018). Effects of antigen leukocyte cellular activation test-based diet on inflammation, body composition, and medical symptoms. *Altern Complement Ther*, 24(5), 215–221. doi:10.1089/act.2018.29183.jml.
- Luo, C. L., Li, B. X., Li, Q. Q., Chen, X. P., Sun, Y. X., Bao, H. J., ... Zhao, Z. Q. (2011). Autophagy is involved in traumatic brain injury-induced cell death and

contributes to functional outcome deficits in mice. *Neuroscience*, *184*, 54–63.
doi:10.1016/j.neuroscience.2011.03.021.

Ma, C., Wu, X., Shen, X., Yang, Y., Chen, Z., Sun, X., & Wang, Z. (2019). Sex differences in traumatic brain injury: a multi-dimensional exploration in genes, hormones, cells, individuals, and society. *Chin Neurosurg JI*, *5*, 24.
doi:10.1186/s41016-019-0173-8.

Mackay, G. M., Forrest, C. M., Stoy, N., Christofides, J., Egerton, M., Stone, T. W., & Darlington, L. G. (2006). Tryptophan metabolism and oxidative stress in patients with chronic brain injury. *Eur J Neurol*, *13*(1), 30–42. doi:10.1111/j.1468-1331.2006.01220.x.

Madill, M., McDonagh, K., Ma, J., Vajda, A., McLoughlin, P., O'Brien, T., ... Shen, S. (2017). Amyotrophic lateral sclerosis patient iPSC-derived astrocytes impair autophagy via non-cell autonomous mechanisms. *Mol Brain*, *10* (1), 22.
doi:10.1186/s13041-017-0300-4.

Maigler, K. C., Buhr, T. J., Park, C. S., Miller, S. A., Kozłowski, D. A., & Marr, R. A. (2021). Assessment of the effects of altered amyloid-beta clearance on behavior following repeat closed-head brain injury in amyloid-beta precursor protein humanized mice. *J Neurotrauma*, *38*(5), 665–676. doi:10.1089/neu.2020.6989.

Malik, R., & Wiedau, M. (2020). Therapeutic approaches targeting protein aggregation in amyotrophic lateral sclerosis. *Front Mol Neurosci*, *13*, 98.
doi:10.3389/fnmol.2020.00098.

- Manach, C., Williamson, G., Morand, C., Scalbert, A., & Rémésy, C. (2005). Bioavailability and bioefficacy of polyphenols in humans. I. Review of 97 bioavailability studies. *Am J Clin Nutr*, *81*(1 Suppl), 230S–242S. doi:10.1093/ajcn/81.1.230S.
- Mancuso, R., Oliván, S., Osta, R., & Navarro, X. (2011). Evolution of gait abnormalities in SOD1(G93A) transgenic mice. *Brain Res*, *1406*, 65–73. doi:10.1016/j.brainres.2011.06.033.
- Marcuzzo, S., Zucca, I., Mastropietro, A., de Rosbo, N. K., Cavalcante, P., Tartari, S., ... Bernasconi, P. (2011). Hind limb muscle atrophy precedes cerebral neuronal degeneration in G93A-SOD1 mouse model of amyotrophic lateral sclerosis: a longitudinal MRI study. *Exp Neurol*, *231*(1), 30–37. doi:10.1016/j.expneurol.2011.05.007.
- Marklund, N., Vedung, F., Lubberink, M., Tegner, Y., Johansson, J., Blennow, K., ... Antoni, G. (2021). Tau aggregation and increased neuroinflammation in athletes after sports-related concussions and in traumatic brain injury patients - A PET/MR study. *NeuroImage Clin*, *30*, 102665. doi:10.1016/j.nicl.2021.102665.
- Marshall, S., Bayley, M., McCullagh, S., Velikonja, D., & Berrigan, L. (2012). Clinical practice guidelines for mild traumatic brain injury and persistent symptoms. *Can Fam Physician*, *58*(3), 257–e140.
- Mattioli, R., Francioso, A., Mosca, L., & Silva, P. (2020). Anthocyanins: a comprehensive review of their chemical properties and health effects on

cardiovascular and neurodegenerative diseases. *Molecules*, 25(17), 3809.

doi:10.3390/molecules25173809.

Mauter, A.E.M., Thome, D., Steudel, W.I., Nacimiento, A.C., Yang, Y., & Shohami, E. (2001). Changes in regional energy metabolism after closed head injury in the rat. *J Mol Neurosci*, 16, 33–39. doi:10.1385/JMN:16:1:33.

Maynard, M. E., Underwood, E. L., Redell, J. B., Zhao, J., Kobori, N., Hood, K. N., ... Dash, P. K. (2019). Carnosic acid improves outcome after repetitive mild traumatic brain injury. *J neurotrauma*, 36(13), 2147–2152. doi:10.1089/neu.2018.6155.

Mazzetti, A. P., Fiorile, M. C., Primavera, A., & Lo Bello, M. (2015). Glutathione transferases and neurodegenerative diseases. *Neurochem Int*, 82, 10–18. doi:10.1016/j.neuint.2015.01.008.

McCrea, M., Iverson, G. L., McAllister, T. W., Hammeke, T. A., Powell, M. R., Barr, W. B., & Kelly, J. P. (2009). An integrated review of recovery after mild traumatic brain injury (MTBI): implications for clinical management. *Clin Neuropsychol*, 23(8), 1368–1390. doi:10.1080/13854040903074652.

McCrory, P., Meeuwisse, W. H., Aubry, M., Cantu, B., Dvorák, J., Echemendia, R. J., ... Turner, M. (2013). Consensus statement on concussion in sport: the 4th International Conference on Concussion in Sport held in Zurich, November 2012. *Br J Sports Med*, 47(5), 250–258. doi:10.1136/bjsports-2013-092313.

- McDonald, S. J., O'Brien, W. T., Symons, G. F., Chen, Z., Bain, J., Major, B. P., ... Shultz, S. R. (2021). Prolonged elevation of serum neurofilament light after concussion in male Australian football players. *Biomark Res*, 9(1), 4. doi:10.1186/s40364-020-00256-7.
- McGeer, P. L. & McGeer, E. G. (2002). Inflammatory processes in amyotrophic lateral sclerosis. *Muscle Nerve*, 26(4), 459–470. doi:10.1002/mus.10191.
- McGill, R., Tukey, J. W., & Larsen, W. A. (1978). Variations of box plots. *Am stat*, 32(1), 12-16. doi:10.2307/2683468.
- McKee, A. C., Cantu, R. C., Nowinski, C. J., Hedley-Whyte, E. T., Gavett, B. E., Budson, B. E., ... Stern, R. A. (2009). Chronic traumatic encephalopathy in athletes: Progressive tauopathy after repetitive head injury. *J Neuropathol Exp Neurol*, 68(7), 709–735. doi:10.1097/NEN.0b013e3181a9d503.
- McKee, A. C., & Daneshvar, D. H. (2015). The neuropathology of traumatic brain injury. *Handb Clin Neurol*, 127, 45–66. doi:10.1016/B978-0-444-52892-6.00004-0.
- McNamara, R. K., Jandacek, R., Tso, P., Dwivedi, Y., Ren, X., & Pandey, G. N. (2013). Lower docosahexaenoic acid concentrations in the postmortem prefrontal cortex of adult depressed suicide victims compared with controls without cardiovascular disease. *Psychiatry Res*, 47(9), 1187–1191. doi:10.1016/j.jpsychires.2013.05.007.

- Meissner, F., Molawi, K., & Zychlinsky, A. (2010). Mutant superoxide dismutase 1-induced IL-1 accelerates ALS pathogenesis. *Proc Natl Acad Sci USA*, *107* (29), 13046–13050. doi:10.1073/pnas.1002396107.
- Mejzini, R., Flynn, L. L., Pitout, I. L., Fletcher, S., Wilton, S. D., & Akkari, P. A. (2019). ALS genetics, mechanisms, and therapeutics: Where are we now? *Front Neurosci*, *13*, 1310. doi:10.3389/fnins.2019.01310.
- Metting, Z., Wilczak, N., Rodiger, L. A., Schaaf, J. M., & van der Naalt, J. (2012). GFAP and S100B in the acute phase of mild traumatic brain injury. *Neurology*, *78*(18), 1428–1433. doi:10.1212/WNL.0b013e318253d5c7.
- Mikolić, A., van Klaveren, D., Groeniger, J. O., Wieggers, E., Lingsma, H. F., Zeldovich, M., ... CENTER-TBI Participants and Investigators (2021). Differences between men and women in treatment and outcome after traumatic brain injury. *J neurotrauma*, *38*(2), 235–251. doi:10.1089/neu.2020.7228.
- Milanese, M., Zappettini, S., Onofri, F., Musazzi, L., Tardito, D., Bonifacino, T., ... Bonanno, G. (2011). Abnormal exocytotic release of glutamate in a mouse model of amyotrophic lateral sclerosis. *J Neurochem*, *116*(6), 1028–1042. doi:10.1111/j.1471-4159.2010.07155.x.
- Miller, K. J., Ivins, B. J., & Schwab, K. A. (2013). Self-reported mild TBI and postconcussive symptoms in a peacetime active duty military population: effect of multiple TBI history versus single mild TBI. *J Head Trauma Rehabil*, *28*(1), 31–38. doi:10.1097/HTR.0b013e318255ceae.

- Mills, J. D., Hadley, K., & Bailes, J. E. (2011). Dietary supplementation with the omega-3 fatty acid docosahexaenoic acid in traumatic brain injury. *Neurosurg*, 68(2), 474–481. doi:10.1227/NEU.0b013e3181ff692b.
- Min, S. W., Ryu, S. N., & Kim, D. H. (2010). Anti-inflammatory effects of black rice, cyanidin-3-O-beta-D-glucoside, and its metabolites, cyanidin and protocatechuic acid. *Int Immunopharmacol*, 10(8), 959–966. doi:10.1016/j.intimp.2010.05.009.
- Mitsumoto, H., Santella, R. M., Liu, X., Bogdanov, M., Zipprich, J., Wu, H. C., ... Factor-Litvak, P. (2008). Oxidative stress biomarkers in sporadic ALS. *Amyotroph Lateral Scler*, 9(3), 177–183. doi:10.1080/17482960801933942.
- Moghaddam, O. M., Lahiji, M. N., Hassani, V., & Mozari, S. (2017). Early administration of selenium in patients with acute traumatic brain injury: A randomized double-blinded controlled trial. *Indian J Crit Care Med*, 21(2), 75–79. doi:10.4103/ijccm.IJCCM_391_16.
- Morfini, G. A., Bosco, D. A., Brown, H., Gatto, R., Kaminska, A., Song, Y., ... Brady, S. T. (2013). Inhibition of fast axonal transport by pathogenic SOD1 involves activation of p38 MAP kinase. *PLoS one*, 8(6), e65235. doi:10.1371/journal.pone.0065235.
- Morimoto, N., Nagai, M., Ohta, Y., Miyazaki, K., Kurata, T., Morimoto, M., ... Abe, K. (2007). Increased autophagy in transgenic mice with a G93A mutant SOD1 gene. *Brain Res*, 1167, 112–117. doi:10.1016/j.brainres.2007.06.045.

- Morin, A., Mouzon, B., Ferguson, S., Paris, D., Browning, M., Stewart, W., ... Crawford, F. (2020). Nilvadipine suppresses inflammation via inhibition of P-SYK and restores spatial memory deficits in a mouse model of repetitive mild TBI. *Acta Neuropathol Commun*, 8, 166. doi:10.1186/s40478-020-01045-x.
- Morin, A., Mouzon, B., Ferguson, S., Paris, D., Saltiel, N., Browning, M., ... Crawford, F. (2021). A 3-month-delayed treatment with anatabine improves chronic outcomes in two different models of repetitive mild traumatic brain injury in hTau mice. *Sci Rep*, 11(1), 7900. doi:10.1038/s41598-021-87161-7.
- Morris, D. R., & Levenson, C. W. (2013). Zinc in traumatic brain injury: from neuroprotection to neurotoxicity. *Curr Opin Clin Nutr Metab Care*, 16(6), 708–711. doi:10.1097/MCO.0b013e328364f39c.
- Morris, G., Puri, B. K., Walker, A. J., Berk, M., Walder, K., Bortolasci, C. C., ... Maes, M. (2019). The compensatory antioxidant response system with a focus on neuroprogressive disorders. *Prog Neuropsychopharmacol Biol Psychiatry*, 95, 109708. doi:10.1016/j.pnpbp.2019.109708.
- Mortimer, J. A., van Duijn, C. M., Chandra, V., Fratiglioni, L., Graves, A. B., Heyman, A., ... Rocca, W. A. (1991). Head trauma as a risk factor for Alzheimer's disease: a collaborative re-analysis of case-control studies. EURODEM Risk Factors Research Group. *Int J Epidemiol*, 20 Suppl 2, S28–S35. doi:10.1093/ije/20.supplement_2.s28.

- Mott, T. F., McConnon, M. L., & Rieger, B. P. (2012). Subacute to chronic mild traumatic brain injury. *Am Fam Physician*, *86*(11), 1045–1051.
- Mouzon, B., Chaytow, H., Crynen, G., Bachmeier, C., Stewart, J., Mullan, M., ... Crawford, F. (2012). Repetitive mild traumatic brain injury in a mouse model produces learning and memory deficits accompanied by histological changes. *J Neurotrauma*, *29*(18), 2761–2773. doi:10.1089/neu.2012.2498.
- Mouzon, B. C., Bachmeier, C., Ferro, A., Ojo, J. O., Crynen, G., Acker, C. M., ... Crawford, F. (2014). Chronic neuropathological and neurobehavioral changes in a repetitive mild traumatic brain injury model. *Ann Neurol*, *75*(2), 241–254. doi:10.1002/ana.24064.
- Mouzon, B. C., Bachmeier, C., Ojo, J. O., Acker, C. M., Ferguson, S., Paris, D., ... Crawford, F. (2017). Lifelong behavioral and neuropathological consequences of repetitive mild traumatic brain injury. *Ann Clin Transl Neurol*, *5*(1), 64–80. doi:10.1002/acn3.510.
- Mozaffari, K., Dejam, D., Duong, C., Ding, K., French, A., Ng, E., ... Yang, I. (2021). Systematic review of serum biomarkers in traumatic brain injury. *Cureus*, *13*(8), e17056. doi:10.7759/cureus.17056.
- Müller, K., Oh, K. W., Nordin, A., Panthi, S., Kim, S. H., Nordin, F., ... Andersen, P. M. (2022). De novo mutations in SOD1 are a cause of ALS. *J Neurol Neurosurg Psychiatry*, *93*(2), 201–206. doi:10.1136/jnnp-2021-327520.

- Muralidharan, N., Bhat, T., & Kumari, S. N. (2017). A study on effect of ageing on the levels of total antioxidant and lipid peroxidation. *Int J Contemp Med*, 4(12), 8-10. doi:10.2147/CIA.S201250.
- Murukan, G., & Murugan, K. (2018). Anthocyanin content of teak and its potential therapeutic traits: Some observations. *World J Pharm Res*, 7(9), 977–985.
- Nagai, M., Re, D. B., Nagata, T., Chalazonitis, A., Jessell, T. M., Wichterle, H., & Przedborski, S. (2007). Astrocytes expressing ALS-linked mutated SOD1 release factors selectively toxic to motor neurons. *Nat Neurosci*, 10(5), 615–622. doi:10.1038/nn1876.
- Nakamura, Y., Torikai, K., & Ohgashi, H. A. (2001). A catechol antioxidant protocatechuic acid potentiates inflammatory leukocyte-derived oxidative stress in mouse skin via a tyrosinase bioactivation pathway. *Free Radic Biol Med*, 30(9), 967–978. doi:10.1016/S0891-5849(01)00481-6.
- Namjoshi, D. R., Cheng, W. H., Bashir, A., Wilkinson, A., Stukas, S., Martens, K. M., ... Wellington, C. L. (2017). Defining the biomechanical and biological threshold of murine mild traumatic brain injury using CHIMERA (Closed Head Impact Model of Engineered Rotational Acceleration). *Exp Neurol*, 292, 80–91. doi:10.1016/j.expneurol.2017.03.003.
- Narai, H., Manabe, Y., Nagai, M., Nagano, I., Ohta, Y., Murakami, T., ... Abe, K. (2009). Early detachment of neuromuscular junction proteins in ALS mice with SODG93A mutation. *Neurol Int*, 1(1), e16. doi:10.4081/ni.2009.e16.

- Ng, S. Y., & Lee, A. (2019). Traumatic brain injuries: Pathophysiology and potential therapeutic targets. *Front Cell Neurosci*, *13*, 528. doi:10.3389/fncel.2019.00528
- Niu, X., Zheng, S., Liu, H., & Li, S. (2018). Protective effects of taurine against inflammation, apoptosis, and oxidative stress in brain injury. *Mol Med Rep*, *18*(5), 4516–4522. doi:10.3892/mmr.2018.9465.
- Nonaka, T., Masuda-Suzukake, M., Arai, T., Hasegawa, Y., Akatsu, H., Obi, T., ... Hasegawa, M. (2013). Prion-like properties of pathological TDP-43 aggregates from diseased brains. *Cell Rep*, *4*(1), 124–134. doi:10.1016/j.celrep.2013.06.007.
- O'Keeffe, E., Kelly, E., Liu, Y., Giordano, C., Wallace, E., Hynes, M., ... Campbell, M. (2020). Dynamic blood-brain barrier regulation in mild traumatic brain injury. *J neurotrauma*, *37*(2), 347–356. doi:10.1089/neu.2019.6483.
- Ojo, J. O., Bachmeier, C., Mouzon, B. C., Tzekov, R., Mullan, M., Davies, H., ... Crawford, F. (2015). Ultrastructural changes in the white and gray matter of mice at chronic time points after repeated concussive head injury. *J Neuropathol Exp Neurol*, *74*(10), 1012–1035. doi:10.1097/NEN.0000000000000247.
- Orsini, M., Oliveira, A. B., Nascimento, O. J., Reis, C. H., Leite, M. A., de Souza, J. A., ... Smidt, B. (2015). Amyotrophic lateral sclerosis: New perspectives and update. *Neurol int*, *7*(2), 5885. doi:10.4081/ni.2015.5885.

- Osier, N. D., & Dixon, C. E. (2016). The controlled cortical impact model: Applications, considerations for researchers, and future directions. *Front Neurol*, 7, 134.
doi:10.3389/fneur.2016.00134.
- Oskarsson, B., Gendron, T. F., & Staff, N. P. (2018). Amyotrophic lateral sclerosis: An update for 2018. *Mayo Clin Proc* 93(11), 1617–1628.
doi:10.1016/j.mayocp.2018.04.007.
- Palomo, G. M. & Manfredi, G. (2015). Exploring new pathways of neurodegeneration in ALS: The role of mitochondria quality control. *Brain Res*, 1607, 36–46.
doi:10.1016/j.brainres.2014.09.065.
- Panayiotou, A., Jackson, M., & Crowe, S. F. (2010). A meta-analytic review of the emotional symptoms associated with mild traumatic brain injury. *J Clin Exp Neuropsychol*, 32(5), 463–473. doi:10.1080/13803390903164371.
- Park, C. S., Lee, J. Y., Choi, H. Y., Ju, B. G., Youn, I., & Yune, T. Y. (2019). Protocatechuic acid improves functional recovery after spinal cord injury by attenuating blood-spinal cord barrier disruption and hemorrhage in rats. *Neurochem Int*, 124, 181–192. doi:10.1016/j.neuint.2019.01.013.
- Passamonti, S., Vrhovsek, U., Vanzo, A., & Mattivi, F. (2003). The stomach as a site for anthocyanins absorption from food. *FEBS Lett*, 544(1-3), 210–213.
doi:10.1016/s0014-5793(03)00504-0.

- Patterson, Z. R., & Holahan, M. R. (2012). Understanding the neuroinflammatory response following concussion to develop treatment strategies. *Front Cell Neurosci*, 6, 58. doi:10.3389/fncel.2012.00058.
- Paul, B. D., Sbodio, J. I., & Snyder, S. H. (2018). Cysteine metabolism in neuronal redox homeostasis. *Trends Pharmacol Sci*, 39(5), 513–524. doi:10.1016/j.tips.2018.02.007.
- Pavlovic, D., Pekic, S., Stojanovic, M., & Popovic, V. (2019). Traumatic brain injury: neuropathological, neurocognitive and neurobehavioral sequelae. *Pituitary*, 22(3), 270–282. doi:10.1007/s11102-019-00957-9.
- Pearn, M. L., Niesman, I. R., Egawa, J., Sawada, A., Almenar-Queralt, A., Shah, S. B., ... Head, B. P. (2017). Pathophysiology associated with traumatic brain injury: Current treatments and potential novel therapeutics. *Cell Mol Neurobiol*, 37(4), 571–585. doi:10.1007/s10571-016-0400-1.
- Persson, M., Sandberg, M., Hansson, E., & Rönnbäck, L. (2006). Microglial glutamate uptake is coupled to glutathione synthesis and glutamate release. *Eur J Neurosci*, 24(4), 1063–1070. doi:10.1111/j.1460-9568.2006.04974.x.
- Petraglia, A. L., Plog, B. A., Dayawansa, S., Dashnaw, M. L., Czerniecka, K., Walker, C. T., ... Nedergaard, M. (2014). The pathophysiology underlying repetitive mild traumatic brain injury in a novel mouse model of chronic traumatic encephalopathy. *Surg Neurol Int*, 5(1), 184. doi:10.4103/2152-7806.147566.

- Pham, L., Wright, D. K., O'Brien, W. T., Bain, J., Huang, C., Sun, M., ... McDonald, S. J. (2021). Behavioral, axonal, and proteomic alterations following repeated mild traumatic brain injury: Novel insights using a clinically relevant rat model. *Neurobiol Dis*, *148*, 105151. doi:10.1016/j.nbd.2020.105151.
- Pickles, S., Destroismaisons, L., Peyrard, S. L., Cadot, S., Rouleau, G. A., Brown, R. H., ... Vande Velde, C. (2013). Mitochondrial damage revealed by immunoselection for ALS-linked misfolded SOD1. *Hum Mol Genet*, *22*(19), 3947–3959. doi:10.1093/hmg/ddt249.
- Pickles, S., Semmler, S., Broom, H. R., Destroismaisons, L., Legroux, L., Arbour, N., ... Vande Velde, C. (2016). ALS-linked misfolded SOD1 species have divergent impacts on mitochondria. *Acta Neuropathol. Commun*, *4*(1), 43. doi:10.1186/s40478-016-0313-8.
- Pierce, A. M., Witt, D. A., Donson, A. M., Gilani, A., Sanford, B., Sill, M., ... Griesinger, A. M. (2019). Establishment of patient-derived orthotopic xenograft model of 1q+ posterior fossa group A ependymoma. *Neuro Oncol*, *21*(12), 1540–1551. doi:10.1093/neuonc/noz116.
- Pierce, J. D., Shen, Q., Peltzer, J., Thimmesch, A., & Hiebert, J. B. (2017). A pilot study exploring the effects of ubiquinol on brain genomics after traumatic brain injury. *Nurs Outlook*, *65*(5S), S44–S52. doi:10.1016/j.outlook.2017.06.012.
- Pisoschi, A. M., & Pop, A. (2015). The role of antioxidants in the chemistry of oxidative stress: A review. *Eur J Med Chem*, *97*, 55–74. doi:10.1016/j.ejmech.2015.04.040.

- Ponsford, J., Cameron, P., Fitzgerald, M., Grant, M., Mikocka-Walus, A., & Schönberger, M. (2012). Predictors of postconcussive symptoms 3 months after mild traumatic brain injury. *Neuropsychology, 26*(3), 304–313. doi:10.1037/a0027888.
- Pooley, A. E., Benjamin, R. C., Sreedhar, S., Eagle, A. L., Robison, A. J., Mazei-Robison, M. S., ... Jordan, C. L. (2018). Sex differences in the traumatic stress response: the role of adult gonadal hormones. *Biol Sex Differ, 9*(1), 32. doi:10.1186/s13293-018-0192-8.
- Popescu, C., Anghelescu, A., Daia, C., & Onose, G. (2015). Actual data on epidemiological evolution and prevention endeavours regarding traumatic brain injury. *J Med Life, 8*(3), 272–277.
- Potter, D. W., & Tran, T. B. (1993). Apparent rates of glutathione turnover in rat tissues. *Toxicol Appl Pharmacol, 120*(2), 186–192. doi:10.1006/taap.1993.1102.
- Prince, C., & Bruhns, M. E. (2017). Evaluation and treatment of mild traumatic brain injury: The role of neuropsychology. *Brain Sci, 7*(8), 105. doi:10.3390/brainsci7080105.
- Prins, M. L., Alexander, D., Giza, C. C., & Hovda, D. A. (2013). Repeated mild traumatic brain injury: mechanisms of cerebral vulnerability. *J neurotrauma, 30*(1), 30–38. doi:10.1089/neu.2012.2399.

- Pronto-Laborinho, A., Pinto, S., Gromicho, M., Pereira, M., Swash, M., & de Carvalho, M. (2019). Interleukin-6 and amyotrophic lateral sclerosis. *J Neurol Sci*, 398, 50–53. doi:10.1016/j.jns.2019.01.026.
- Protter, D., & Parker, R. (2016). Principles and properties of stress granules. *Trends Cell Biol*, 26(9), 668–679. doi:10.1016/j.tcb.2016.05.004.
- Pu, H., Guo, Y., Zhang, W., Huang, L., Wang, G., Liou, A. K., ... Gao, Y. (2013). Omega-3 polyunsaturated fatty acid supplementation improves neurologic recovery and attenuates white matter injury after experimental traumatic brain injury. *J Cereb Blood Flow Metab*, 33(9), 1474–1484. doi:10.1038/jcbfm.2013.108.
- Pu, H., Jiang, X., Wei, Z., Hong, D., Hassan, S., Zhang, W., ... Chen, J. (2017). Repetitive and prolonged omega-3 fatty acid treatment after traumatic brain injury enhances long-term tissue restoration and cognitive recovery. *Cell transplant*, 26(4), 555–569. doi:10.3727/096368916X693842.
- Ramírez-Jarquín, U. N., Rojas, F., van Zundert, B., & Tapia, R. (2017). Chronic infusion of SOD1 (G93A) astrocyte-secreted factors induces spinal motoneuron degeneration and neuromuscular dysfunction in healthy rats. *J Cell Physiol*, 232(10), 2610–2615. doi:10.1002/jcp.25827.
- Ramlackhansingh, A. F., Brooks, D. J., Greenwood, R. J., Bose, S. K., Turkheimer, F. E., Kinnunen, K. M., ... Sharp, D. J. (2011). Inflammation after trauma: microglial

activation and traumatic brain injury. *Ann Neurol*, 70(3), 374–383.

doi:10.1002/ana.22455.

Razmkon, A., Sadidi, A., Sherafat-Kazemzadeh, E., Mehrafshan, A., Jamali, M., Malekpour, B., & Saghafinia, M. (2011). Administration of vitamin C and vitamin E in severe head injury: a randomized double-blind controlled trial. *Clin Neurosurg*, 58, 133–137. doi:10.1227/neu.0b013e3182279a8f.

Reed, T. T., Owen, J., Pierce, W. M., Sebastian, A., Sullivan, P. G., & Butterfield, D. A. (2009). Proteomic identification of nitrated brain proteins in traumatic brain-injured rats treated postinjury with gamma-glutamylcysteine ethyl ester: insights into the role of elevation of glutathione as a potential therapeutic strategy for traumatic brain injury. *J Neurosci Res*, 87(2), 408–417. doi:10.1002/jnr.21872.

Richards, D., Morren, J. A., & Pioro, E. P. (2020). Time to diagnosis and factors affecting diagnostic delay in amyotrophic lateral sclerosis. *J Neurol Sci*, 417, 117054. doi:10.1016/j.jns.2020.117054.

Robinson, S., Berglass, J. B., Denson, J. L., Berkner, J., Anstine, C. V., Winer, J. L., ... Jantzie, L. L. (2017). Microstructural and microglial changes after repetitive mild traumatic brain injury in mice. *J Neurosci Res*, 95(4), 1025–1035. doi:10.1002/jnr.23848.

Rosen, D. R., Siddique, T., Patterson, D., Figlewicz, D. A., Sapp, P., Hentati, A., ... Deng, H. X. (1993). Mutations in Cu/Zn superoxide dismutase gene are

associated with familial amyotrophic lateral sclerosis. *Nature*, 362(6415), 59–62.
doi:10.1038/362059a0.

Ross, E. K., Gray, J. J., Winter, A. N., & Linseman, D. A. (2012). Immunocal® and preservation of glutathione as a novel neuroprotective strategy for degenerative disorders of the nervous system. *Recent Pat CNS Drug Discov*, 7(3), 230–235.
doi:10.2174/157488912803252014.

Ross, E. K., Winter, A. N., Wilkins, H. M., Sumner, W. A., Duval, N., Patterson, D., & Linseman, D. A. (2014). A cystine-rich whey supplement (Immunocal®) delays disease onset and prevents spinal cord glutathione depletion in the hSOD1G93A mouse model of amyotrophic lateral sclerosis. *Antioxidants (Basel)*, 3(4), 843–865. doi:10.3390/antiox3040843.

Rudnick, N. D., Griffey, C. J., Guarnieri, P., Gerbino, V., Wang, X., Piersaint, J. A., ... Maniatis, T. (2017). Distinct roles for motor neuron autophagy early and late in the SOD1^{G93A} mouse model of ALS. *Proc Natl Acad Sci USA*, 114(39), E8294–E8303. doi:10.1073/pnas.1704294114.

Ruszkiewicz, J. A., Miranda-Vizueté, A., Tinkov, A. A., Skalnaya, M. G., Skalny, A. V., Tsatsakis, A., & Aschner, M. (2019). Sex-specific differences in redox homeostasis in brain norm and disease. *J Mol Neurosci*, 67(2), 312–342.
doi:10.1007/s12031-018-1241-9.

- Rutland-Brown, W., Langlois, J. A., Thomas, K. E., & Xi, Y. L. (2006). Incidence of traumatic brain injury in the United States, 2003. *J Head Trauma Rehabil*, *21*(6), 544–548. doi:10.1097/00001199-200611000-00009.
- Sacson, R. A., Bunton-Stasyshyn, R. K., Fisher, E. M., & Fratta, P. (2013). Is SOD1 loss of function involved in amyotrophic lateral sclerosis? *Brain*, *136*(Pt 8), 2342–2358. doi:10.1093/brain/awt097.
- Sandoval-Ramírez, B. A., Catalán, Ú., Fernández-Castillejo, S., Pedret, A., Llauradó, E., & Solà, R. (2020). Cyanidin-3-glucoside as a possible biomarker of anthocyanin-rich berry intake in body fluids of healthy humans: a systematic review of clinical trials. *Nutr Rev*, *78*(7), 597–610. doi:10.1093/nutrit/nuz083.
- Sandsmark, D. K., Bashir, A., Wellington, C. L., & Diaz-Arrastia, R. (2019). Cerebral microvascular injury: A potentially treatable endophenotype of traumatic brain injury-induced neurodegeneration. *Neuron*, *103*(3), 367–379. doi:10.1016/j.neuron.2019.06.002.
- Sargsyan, S. A., Blackburn, D. J., Barber, S. C., Monk, P. N., & Shaw, P. J. (2009). Mutant SOD1 G93A microglia have an inflammatory phenotype and elevated production of MCP-1. *Neuroreport*, *20*(16), 1450–1455. doi:10.1097/WNR.0b013e328331e8fa.
- Sarlette, A., Krampfl, K., Grothe, C., Neuhoff, N. v., Dengler, R., & Petri, S. (2008). Nuclear erythroid 2-related factor 2-antioxidative response element signaling pathway in motor cortex and spinal cord in amyotrophic lateral sclerosis. *J*

Neuropathol Exp Neurol, 67(11), 1055–1062.

doi:10.1097/NEN.0b013e31818b4906.

Sasaki, S., & Iwata, M. (2007). Mitochondrial alterations in the spinal cord of patients with sporadic amyotrophic lateral sclerosis. *J Neuropathol Exp Neurol*, 66(1), 10–16. doi:10.1097/nen.0b013e31802c396b.

Scarmeas, N., Shih, T., Stern, Y., Ottman, R., & Rowland, L. P. (2002). Premorbid weight, body mass, and varsity athletics in ALS. *Neurology*, 59(5), 773–775. doi:10.1212/wnl.59.5.773.

Schaffer, S., & Kim, H. W. (2018). Effects and mechanisms of taurine as a therapeutic agent. *Biomol Ther*, 26(3), 225–241. doi:10.4062/biomolther.2017.251.

Schmidt, S., Kwee, L. C., Allen, K. D., & Oddone, E. Z. (2010). Association of ALS with head injury, cigarette smoking and APOE genotypes. *J Neurol Sci*, 291(1-2), 22–29. doi:10.1016/j.jns.2010.01.011.

Schwab, N., Grenier, K., & Hazrati, L. N. (2019a). DNA repair deficiency and senescence in concussed professional athletes involved in contact sports. *Acta Neuropathol Commun*, 7(1), 182. doi:10.1186/s40478-019-0822-3.

Schwab, N., Tator, C., & Hazrati, L. N. (2019b). DNA damage as a marker of brain damage in individuals with history of concussions. *Lab Invest*, 99(7), 1008–1018. doi:10.1038/s41374-019-0199-8.

- Seeram, N. P., Bourquin, L. D., & Nair, M. G. (2001a). Degradation products of cyanidin glycosides from tart cherries and their bioactivities. *J Agric Food Chem*, *49*(10), 4924–4929. doi:10.1021/jf0107508.
- Seeram, N. P., Momin, R. A., Nair, M. G., & Bourquin, L. D. (2001b). Cyclooxygenase inhibitory and antioxidant cyanidin glycosides in cherries and berries. *Phytomedicine*, *8*(5), 362–369. doi:10.1078/0944-7113-00053.
- Seifert, J. (2007). Incidence and economic burden of injuries in the United States. *J Epidemiol Community Health*, *61*(10), 926. doi:10.1136/jech.2007.059717.
- Seki, Y., Kimura, M., Mizutani, N., Fujita, M., Aimi, Y., & Suzuki, Y. (2005). Cerebrospinal fluid taurine after traumatic brain injury. *Neurochem Res*, *30*(1), 123–128. doi:10.1007/s11064-004-9693-4.
- Semaming, Y., Sripetchwandee, J., Sa-Nguanmoo, P., Pintana, H., Pannangpetch, P., Chattipakorn, N., & Chattipakorn, S. C. (2015). Protocatechuic acid protects brain mitochondrial function in streptozotocin-induced diabetic rats. *Appl Physiol Nutr Metab*, *40*(10), 1078–1081. doi:10.1139/apnm-2015-0158.
- Sen, I., Nalini, A., Joshi, N. B., & Joshi, P. G. (2005). Cerebrospinal fluid from amyotrophic lateral sclerosis patients preferentially elevates intracellular calcium and toxicity in motor neurons via AMPA/kainate receptor. *J Neurol Sci*, *235*(1-2), 45–54. doi:10.1016/j.jns.2005.03.049.

- Seo, J. S., Baek, I. S., Leem, Y. H., Kim, T. K., Cho, Y., Lee, S. M., ... Han, P. L. (2011). SK-PC-B70M alleviates neurologic symptoms in G93A-SOD1 amyotrophic lateral sclerosis mice. *Brain Res*, *1368*, 299–307. doi:10.1016/j.brainres.2010.10.048.
- Serkova, N. J., Renner, B., Larsen, B. A., Stoldt, C. R., Hasebroock, K. M., Bradshaw-Pierce, E. L., ... Thurman, J. M. (2010). Renal inflammation: targeted iron oxide nanoparticles for molecular MR imaging in mice. *Radiology*, *255*(2), 517–526. doi:10.1148/radiol.09091134.
- Shafiee, M., Ahmadnezhad, M., Tayefi, M., Arekhi, S., Vatanparast, H., Esmaeili, H., ... Ghayour-Mobarhan, M. (2018). Depression and anxiety symptoms are associated with prooxidant-antioxidant balance: A population-based study. *J Affect Disord*, *238*, 491–498. doi:10.1016/j.jad.2018.05.079.
- Shahim, P., Blennow, K., Zetterberg, H., Tegner, Y. (2017a). Mild traumatic brain injury is associated with increased levels of axonal injury biomarkers in blood. *Br J Sports Med*, *51*, A6-A7. doi:10.1136/bjsports-2016-097270.15.
- Shahim, P., Politis, A., van der Merwe, A., Moore, B., Chou, Y. Y., Pham, D. L., ... Chan, L. (2020). Neurofilament light as a biomarker in traumatic brain injury. *Neurology*, *95*(6), e610–e622. doi:10.1212/WNL.00000000000009983.
- Shahim, P., Zetterberg, H., Tegner, Y., & Blennow, K. (2017b). Serum neurofilament light as a biomarker for mild traumatic brain injury in contact sports. *Neurology*, *88*(19), 1788–1794. doi:10.1212/WNL.00000000000003912.

- Shahrokhi, N., Haddad, M. K., Joukar, S., Shabani, M., Keshavarzi, Z., & Shahozehi, B. (2012). Neuroprotective antioxidant effect of sex steroid hormones in traumatic brain injury. *Pak J Pharm Sci*, *25*(1), 219–225.
- Shan, X., Vocadlo, D., & Krieger, C. (2009). Mislocalization of TDP-43 in the G93A mutant SOD1 transgenic mouse model of ALS. *Neurosci Lett*, *458*(2), 70–74. doi:10.1016/j.neulet.2009.04.031.
- Shandra, O., Winemiller, A. R., Heithoff, B. P., Munoz-Ballester, C., George, K. K., Benko, M. J., ... Robel, S. (2019). Repetitive diffuse mild traumatic brain injury causes an atypical astrocyte response and spontaneous recurrent seizures. *J neurosci*, *39*(10), 1944–1963. doi:10.1523/JNEUROSCI.1067-18.2018.
- Shang, Y., & Huang, E. J. (2016). Mechanisms of FUS mutations in familial amyotrophic lateral sclerosis. *Brain Res*, *1647*, 65–78. doi:10.1016/j.brainres.2016.03.036.
- Sharma, S., Kumar, A., Choudhary, A., Sharma, S., Khurana, L., Sharma, N., ... Bisht, A. (2020). Neuroprotective role of oral vitamin D supplementation on consciousness and inflammatory biomarkers in determining severity outcome in acute traumatic brain injury patients: A double-blind randomized clinical trial. *Clin Drug Investig*, *40*(4), 327–334. doi:10.1007/s40261-020-00896-5.
- Shih, A. Y., Erb, H., Sun, X., Toda, S., Kalivas, P. W., & Murphy, T. H. (2006). Cystine/glutamate exchange modulates glutathione supply for neuroprotection from oxidative stress and cell proliferation. *J Neurosci*, *26*(41), 10514–10523. doi:10.1523/JNEUROSCI.3178-06.2006.

- Shlosberg, D., Benifla, M., Kaufer, D., & Friedman, A. (2010). Blood-brain barrier breakdown as a therapeutic target in traumatic brain injury. *Nat Rev Neurol*, *6*(7), 393–403. doi:10.1038/nrneurol.2010.74.
- Shreenath, A. P., Ameer, M. A., & Dooley, J. (2021). Selenium deficiency. *StatPearls*. Treasure Island: StatPearls Publishing.
- Shukitt-Hale, B., Kelly, M. E., Bielinski, D. F., & Fisher, D. R. (2016). Tart cherry extracts reduce inflammatory and oxidative stress signaling in microglial cells. *Antioxidants (Basel)*, *5*(4), 33. doi:10.3390/antiox5040033.
- Singh, S., Swarnkar, S., Goswami, P., Nath, C. (2011). Astrocytes and microglia: Responses to pathological conditions. *Int J Neurosci*, *121*(11), 589–597. doi:10.3109/00207454.2011.598981.
- Solovyev, N., Drobyshev, E., Blume, B., & Michalke, B. (2021). Selenium at the neural barriers: A review. *Front Neurosci*, *15*, 630016. doi:10.3389/fnins.2021.630016.
- Song, Y., Cui, T., Xie, N., Zhang, X., Qian, Z., & Liu, J. (2014). Protocatechuic acid improves cognitive deficits and attenuates amyloid deposits, inflammatory response in aged A β PP/PS1 double transgenic mice. *Int Immunopharmacol*, *20*(1), 276–281. doi:10.1016/j.intimp.2014.03.006.
- Soo, K. Y., Farg, M., & Atkin, J. D. (2011). Molecular motor proteins and amyotrophic lateral sclerosis. *Int J Mol Sci*, *12*(12), 9057–9082. doi:10.3390/ijms12129057.

- Sorokina, E. G., Semenova, Z. B., Reutov, V. P., Arsenieva, E. N., Karaseva, O. V., Fisenko, A. P., ... Pinelis, V. G. (2021). Brain biomarkers in children after mild and severe traumatic brain injury. *Acta Neurochir Suppl*, *131*, 103–107. doi:10.1007/978-3-030-59436-7_22.
- Stefanatos, R., & Sanz, A. (2018). The role of mitochondrial ROS in the aging brain. *FEBS Lett*, *592*(5), 743–758. doi:10.1002/1873-3468.12902.
- Stifani N. (2014). Motor neurons and the generation of spinal motor neuron diversity. *Front Cell Neurosci*, *8*, 293. doi:10.3389/fncel.2014.00293.
- Styrke, J., Sojka, P., Björnstig, U., Bylund, P. O., & Stålnacke, B. M. (2013). Sex-differences in symptoms, disability, and life satisfaction three years after mild traumatic brain injury: a population-based cohort study. *J Rehabil Med*, *45*(8), 749–757. doi:10.2340/16501977-1215.
- Su, Y., Fan, W., Ma, Z., Wen, X., Wang, W., Wu, Q., & Huang, H. (2014). Taurine improves functional and histological outcomes and reduces inflammation in traumatic brain injury. *Neuroscience*, *266*, 56–65. doi:10.1016/j.neuroscience.2014.02.006.
- Subash, S., Essa, M. M., Al-Asmi, A., Al-Adawi, S., Vaishnav, R., & Guillemin, G. J. (2015a). Effect of dietary supplementation of dates in Alzheimer's disease APPsw/2576 transgenic mice on oxidative stress and antioxidant status. *Nutr, Neurosci*, *18*(6), 281–288. doi:10.1179/1476830514Y.0000000134.

- Subash, S., Essa, M. M., Braidy, N., Awlad-Thani, K., Vaishnav, R., Al-Adawi, ...
Guillemin, G. J. (2015b). Diet rich in date palm fruits improves memory, learning and reduces beta amyloid in transgenic mouse model of Alzheimer's disease. *J Ayurveda Integr Med*, 6(2), 111–120. doi:10.4103/0975-9476.159073.
- Sulhan, S., Lyon, K. A., Shapiro, L. A., & Huang, J. H. (2020). Neuroinflammation and blood-brain barrier disruption following traumatic brain injury: Pathophysiology and potential therapeutic targets. *J Neurosci Res*; 98(1), 19–28.
doi:10.1002/jnr.24331.
- Sun, Y., Bai, L., Niu, X., Wang, Z., Yin, B., Bai, G., ... Zhang, M. (2019). Elevated serum levels of inflammation-related cytokines in mild traumatic brain injury are associated with cognitive performance. *Front neurol*, 10, 1120.
doi:10.3389/fneur.2019.01120.
- Sutedja, N. A., Veldink, J. H., Fischer, K., Kromhout, H., Heederik, D., Huisman, M. H., ... van den Berg, L. H. (2009). Exposure to chemicals and metals and risk of amyotrophic lateral sclerosis: a systematic review. *Amyotroph Lateral Scler*, 10(5-6), 302–309. doi:10.3109/17482960802455416.
- Suzuki, H., & Matsuoka, M. (2013). The JNK/c-Jun signaling axis contributes to the TDP-43-induced cell death. *Mol Cell Biochem*, 372(1-2), 241–248.
doi:10.1007/s11010-012-1465-x.

- Suzuki, N., Akiyama, T., Warita, H., & Aoki, M. (2020). Omics approach to axonal dysfunction of motor neurons in amyotrophic lateral sclerosis (ALS). *Front Neurosci*, *14*, 194. doi:10.3389/fnins.2020.00194.
- Synofzik, M., Fernández-Santiago, R., Maetzler, W., Schöls, L., & Andersen, P. M. (2010). The human G93A SOD1 phenotype closely resembles sporadic amyotrophic lateral sclerosis. *J Neurol Neurosurg Psychiatry*, *81*(7), 764–767. doi:10.1136/jnnp.2009.181719.
- Tan, J., Li, Y., Hou, D. X., & Wu, S. (2019). The effects and mechanisms of cyanidin-3-glucoside and its phenolic metabolites in maintaining intestinal integrity. *Antioxidants (Basel)*, *8*(10), 479. doi:10.3390/antiox8100479.
- Tan, W., Pasinelli, P., & Trotti, D. (2014). Role of mitochondria in mutant SOD1 linked amyotrophic lateral sclerosis. *Biochim Biophys Acta*, *1842*(8), 1295–1301. doi:10.1016/j.bbadis.2014.02.009.
- Tan, Y. L., Yuan, Y., & Tian, L. (2020). Microglial regional heterogeneity and its role in the brain. *Mol Psychiatry*, *25*(2), 351–367. doi:10.1038/s41380-019-0609-8.
- Tarozzi, A., Morroni, F., Hrelia, S., Angeloni, C., Marchesi, A., Cantelli-Forti, G., & Hrelia, P. (2007). Neuroprotective effects of anthocyanins and their in vivo metabolites in SH-SY5Y cells. *Neurosci Lett*, *424*(1), 36–40. doi:10.1016/j.neulet.2007.07.017.

- Tateno, M., Sadakata, H., Tanaka, M., Itohara, S., Shin, R. M., Miura, M., ... Takahashi, R. (2004). Calcium-permeable AMPA receptors promote misfolding of mutant SOD1 protein and development of amyotrophic lateral sclerosis in a transgenic mouse model. *Hum Mol Genet*, *13*(19), 2183–2196. doi:10.1093/hmg/ddh246.
- Tefera, T. W., Steyn, F. J., Ngo, S. T., & Borges, K. (2021). CNS glucose metabolism in Amyotrophic Lateral Sclerosis: A therapeutic target? *Cell Biosci*, *11*(1), 14. doi:10.1186/s13578-020-00511-2.
- Theadom, A., Starkey, N., Barker-Collo, S., Jones, K., Ameratunga, S., Feigin, V., & BIONIC4you Research Group (2018). Population-based cohort study of the impacts of mild traumatic brain injury in adults four years post-injury. *PloS one*, *13*(1), e0191655. doi:10.1371/journal.pone.0191655.
- Thomas, E. V., Fenton, W. A., McGrath, J., & Horwich, A. L. (2017). Transfer of pathogenic and nonpathogenic cytosolic proteins between spinal cord motor neurons in vivo in chimeric mice. *Proc Natl Acad Sci U S A*, *114*(15), E3139–E3148. doi:10.1073/pnas.1701465114.
- Tiwari, A., & Hayward, L. J. (2005). Mutant SOD1 instability: implications for toxicity in amyotrophic lateral sclerosis. *Neurodegener Dis*, *2*(3-4), 115–127. doi:10.1159/000089616.
- Tokuda, E., Okawa, E., Watanabe, S., Ono, S., & Marklund, S. L. (2013). Dysregulation of intracellular copper homeostasis is common to transgenic mice expressing

human mutant superoxide dismutase-1s regardless of their copper-binding abilities. *Neurobiol Dis*, 54, 308–319. doi:10.1016/j.nbd.2013.01.001.

Topal, N. B., Hakyemez, B., Erdogan, C., Bulut, M., Koksal, O., Akkose, S., ... Korfali, E. (2008). MR imaging in the detection of diffuse axonal injury with mild traumatic brain injury. *Neurol Res*, 30(9), 974–978.
doi:10.1179/016164108X323799.

Tortelli, R., Zecca, C., Piccininni, M., Benmahamed, S., Dell'Abate, M. T., Barulli, M., ... Logroscino, G. (2020). Plasma inflammatory cytokines are elevated in ALS. *Front Neurol*, 11, 552295. doi:10.3389/fneur.2020.552295.

Traber M. G. (2014). Vitamin E inadequacy in humans: Causes and consequences, advances in nutrition. *Adv Food Nutr Res*, 5(5), 503–514.
doi:10.3945/an.114.006254.

Tripathi, P., Rodriguez-Muela, N., Klim, J. R., de Boer, A. S., Agrawal, S., Sandoe, J., ... Zhou, Q. (2017). Reactive astrocytes promote ALS-like degeneration and intracellular protein aggregation in human motor neurons by disrupting autophagy through TGF- β 1. *Stem Cell Rep*, 9(2), 667–680.
doi:10.1016/j.stemcr.2017.06.008.

Tsai, S. J. & Yin, M. C. (2012). Anti-glycative and anti-inflammatory effects of protocatechuic acid in brain of mice treated by D-galactose. *Food Chem Toxicol*, 50(9), 3198–3205. doi:10.1016/j.fct.2012.05.056.

- Tsuda, T., Horio, F., & Osawa, T. (1999). Absorption and metabolism of cyanidin 3-O-beta-D-glucoside in rats. *FEBS Lett*, *449*(2-3), 179–182. doi:10.1016/s0014-5793(99)00407-x.
- Tyurin, V. A., Tyurina, Y. Y., Borisenko, G. G., Sokolova, T. V., Ritov, V. B., Quinn, P. J., ... Kagan, V. E. (2000). Oxidative stress following traumatic brain injury in rats: quantitation of biomarkers and detection of free radical intermediates. *J neurochem*, *75*(5), 2178–2189. doi:10.1046/j.1471-4159.2000.0752178.x.
- Tyzack, G. E., Hall, C. E., Sibley, C. R., Cymes, T., Forostyak, S., Carlino, G., ... Lakatos, A. (2017). A neuroprotective astrocyte state is induced by neuronal signal EphB1 but fails in ALS models. *Nat Commun*, *8*(1), 1164. doi:10.1038/s41467-017-01283-z.
- Underwood, E. L., Redell, J. B., Maynard, M. E., Kobori, N., Hylin, M. J., Hood, K. N., ... Dash, P. K. (2022). Metformin reduces repeat mild concussive injury pathophysiology. *eNeuro*, *9*(1), ENEURO.0421-21.2021. doi:10.1523/ENEURO.0421-21.2021.
- Vagnozzi, R., Marmarou, A., Tavazzi, B., Signoretti, S., Di Pierro, D., del Bolgia, F., ... Lazzarino, G. (1999). Changes of cerebral energy metabolism and lipid peroxidation in rats leading to mitochondrial dysfunction after diffuse brain injury. *J Neurotrauma*, *16*(10), 903–913. doi:10.1089/neu.1999.16.903.
- Vahdat, M., Hosseini, S. A., Soltani, F., Cheraghian, B., & Namjoonia, M. (2021). The effects of Taurine supplementation on inflammatory markers and clinical

outcomes in patients with traumatic brain injury: a double-blind randomized controlled trial. *Nutr J*, 20(1), 53. doi:10.1186/s12937-021-00712-6.

Valentine, J. S., Doucette, P. A., & Zittin Potter, S. (2005). Copper-zinc superoxide dismutase and amyotrophic lateral sclerosis. *Annu Rev Biochem*, 74, 563–593. doi:10.1146/annurev.biochem.72.121801.161647.

Van Den Bosch, L., Van Damme, P., Bogaert, E., & Robberecht, W. (2006). The role of excitotoxicity in the pathogenesis of amyotrophic lateral sclerosis. *Biochim Biophys Acta*, 1762(11-12), 1068–1082. doi:10.1016/j.bbadis.2006.05.002.

Vargas, M. R., Pehar, M., Cassina, P., Beckman, J. S., & Barbeito, L. (2006). Increased glutathione biosynthesis by Nrf2 activation in astrocytes prevents p75NTR-dependent motor neuron apoptosis. *J Neurochem*, 97(3), 687–696. doi:10.1111/j.1471-4159.2006.03742.x.

Vina, J., Gambini, J., Lopez-Grueso, R., Abdelaziz, K. M., Jove, M., & Borras, C. (2011). Females live longer than males: Role of oxidative stress. *Curr Pharm Des*, 17(36), 3959–3965. doi:10.2174/138161211798764942.

Vitaglione, P., Donnarumma, G., Napolitano, A., Galvano, F., Gallo, A., Scalfi, L., & Fogliano, V. (2007). Protocatechuic acid is the major human metabolite of cyanidin-glucosides. *J Nutr*, 137(9), 2043–2048. doi:10.1093/jn/137.9.2043.

von Reyn, C. R., Spaethling, J. M., Mesfin, M. N., Ma, M., Neumar, R. W., Smith, D. H., ... Meaney, D. F. (2009). Calpain mediates proteolysis of the voltage-gated

sodium channel alpha-subunit. *J Neurosci*, 29(33), 10350–10356.

doi:10.1523/JNEUROSCI.2339-09.2009.

Voormolen, D. C., Haagsma, J. A., Polinder, S., Maas, A., Steyerberg, E. W., Vuleković, P., ... von Steinbuechel, N. (2019). Post-concussion symptoms in complicated vs. uncomplicated mild traumatic brain injury patients at three and six months post-injury: Results from the CENTER-TBI study. *J Clin Med*, 8(11), 1921.

doi:10.3390/jcm8111921.

Vyas, P., Kalidindi, S., Chibrikova, L., Igamberdiev, A. U., & Weber, J. T. (2013).

Chemical analysis and effect of blueberry and lingonberry fruits and leaves against glutamate-mediated excitotoxicity. *J Agric Food Chem*, 61(32), 7769–7776. doi:10.1021/jf401158a.

Wagner, A.K., Bayir, H., Ren, D., Puccio, A., Zafonte, R. D., & Kochanek, P. M. (2004).

Relationships between cerebrospinal fluid markers of excitotoxicity, ischemia, and oxidative damage after severe TBI: The impact of gender, age, and hypothermia. *J Neurotrauma*, 21(2), 125-136.

doi:10.1089/089771504322778596.

Walczak, J., Dębska-Vielhaber, G., Vielhaber, S., Szymański, J., Charzyńska, A.,

Duszyński, J., and Szczepanowska, J. (2019). Distinction of sporadic and familial forms of ALS based on mitochondrial characteristics. *FASEB J*, 33(3), 4388–4403. doi:10.1096/fj.201801843R.

- Wäljas, M., Lange, R. T., Hakulinen, U., Huhtala, H., Dastidar, P., Hartikainen, K., ... Iverson, G. L. (2014). Biopsychosocial outcome after uncomplicated mild traumatic brain injury. *J Neurotrauma*, *31*(1), 108–124. doi:10.1089/neu.2013.2941.
- Wang, C. Q., Ye, Y., Chen, F., Han, W. C., Sun, J. M., Lu, X., ... Liao, L. C. (2017). Posttraumatic administration of a sub-anesthetic dose of ketamine exerts neuroprotection via attenuating inflammation and autophagy. *Neuroscience*, *343*, 30–38. doi:10.1016/j.neuroscience.2016.11.029.
- Wang, G., Zhang, Y. P., Gao, Z., Shields, L., Li, F., Chu, T., ... Cai, J. (2018). Pathophysiological and behavioral deficits in developing mice following rotational acceleration-deceleration traumatic brain injury. *Dis Model Mech*, *11*(1), dmm030387. doi:10.1242/dmm.030387.
- Wang, H., Li, S., Zhang, G., Wu, H., & Chang, X. (2019). Potential therapeutic effects of cyanidin-3-O-glucoside on rheumatoid arthritis by relieving inhibition of CD38+ NK cells on Treg cell differentiation. *Arthritis Res Ther*, *21*(1), 220. doi:10.1186/s13075-019-2001-0.
- Wang, K. K., Moghieb, A., Yang, Z., & Zhang, Z. (2013). Systems biomarkers as acute diagnostics and chronic monitoring tools for traumatic brain injury. *SPIE Defense, Security, and Sensing*, *872300*. doi:10.1117/12.2020030.

- Wang, Q., Fan, W., Cai, Y., Wu, Q., Mo, L., Huang, Z., & Huang, H. (2016). Protective effects of taurine in traumatic brain injury via mitochondria and cerebral blood flow. *Amino acids*, *48*(9), 2169–2177. doi:10.1007/s00726-016-2244-x.
- Wang, R., Yang, B., & Zhang, D. (2011). Activation of interferon signaling pathways in spinal cord astrocytes from an ALS mouse model. *Glia*, *59*(6), 946–958. doi:10.1002/glia.21167.
- Wang, Z., Bai, Z., Qin, X., & Cheng, Y. (2019). Aberrations in oxidative stress markers in amyotrophic lateral sclerosis: A systematic review and meta-analysis. *Oxid Med Cell Longev*, *2019*, 1712323. doi:10.1155/2019/1712323.
- Webster, K. M., Wright, D. K., Sun, M., Semple, B. D., Ozturk, E., Stein, D. G., ... Shultz, S. R. (2015). Progesterone treatment reduces neuroinflammation, oxidative stress and brain damage and improves long-term outcomes in a rat model of repeated mild traumatic brain injury. *J Neuroinflammation*, *12*, 238. doi:10.1186/s12974-015-0457-7.
- Weiduschat, N., Mao, X., Hupf, J., Armstrong, N., Kang, G., Lange, D. J., ... Shungu, D. C. (2014). Motor cortex glutathione deficit in ALS measured in vivo with the J-editing technique. *Neurosci Lett*, *570*, 102–107. doi:10.1016/j.neulet.2014.04.020.
- Weisskopf, M. G., Morozova, N., O'Reilly, E. J., McCullough, M. L., Calle, E. E., Thun, M. J., & Ascherio, A. (2009). Prospective study of chemical exposures and amyotrophic lateral sclerosis. *J Neurol Neurosurg Psychiatry*, *80*(5), 558–561. doi:10.1136/jnnp.2008.156976.

- Weydt, P., Hong, S., Kliot, M., & Möller, T. (2003). Assessing disease onset and progression in the SOD1 mouse model of ALS. *NeuroReport*, *14*(7), 1051–1054. doi:10.1097/00001756-200305230-00029.
- Wickham, H. (2016). *ggplot2: Elegant graphics for data analysis*. New York: Springer-Verlag.
- Wilke, B. C., Vidailhet, M., Favier, A., Guillemin, C., Ducros, V., Arnaud, J., & Richard, M. J. (1992). Selenium, glutathione peroxidase (GSH-Px) and lipid peroxidation products before and after selenium supplementation. *Clin Chim Acta*, *207*(1-2), 137–142. doi:10.1016/0009-8981(92)90157-1.
- Winter, A. N., & Bickford, P. C. (2019). Anthocyanins and their metabolites as therapeutic agents for neurodegenerative disease. *Antioxidants (Basel)*, *8*(9), 333. doi:10.3390/antiox8090333.
- Winter, A. N., Brenner, M. C., Punessen, N., Snodgrass, M., Byars, C., Arora, Y., & Linseman, D. A. (2017a). Comparison of the neuroprotective and anti-inflammatory effects of the anthocyanin metabolites, protocatechuic acid and 4-hydroxybenzoic acid. *Oxid Med Cell Longev*, *2017*, 6297080. doi:10.1155/2017/6297080.
- Winter, A. N., Ross, E. K., Daliparthi, V., Sumner, W. A., Kirchhof, D. M., Manning, E., ... Linseman, D. A. (2017b). A cystine-rich whey supplement (Immunocal®) provides neuroprotection from diverse oxidative stress-inducing agents in vitro by

preserving cellular glutathione. *Ox Med and Cellular Longev*, 2017, 3103272.
doi:10.1155/2017/3103272.

Winter, A. N., Ross, E. K., Khatter, S., Miller, K., & Linseman, D. A. (2017c). Chemical basis for the disparate neuroprotective effects of the anthocyanins, callistephin and kuromanin, against nitrosative stress. *Free Radic Biol Med*, 103, 23–34.
doi:10.1016/j.freeradbiomed.2016.12.012.

Winter, A. N., Ross, E. K., Wilkins, H. M., Stankiewicz, T. R., Wallace, T., Miller, K., & Linseman, D. A. (2018). An anthocyanin-enriched extract from strawberries delays disease onset and extends survival in the hSOD1G93A mouse model of amyotrophic lateral sclerosis. *Nutr Neurosci*, 21(6), 414–426.
doi:10.1080/1028415X.2017.1297023.

Witkowski, E. D., Gao, Y., Gavszyk, A. F., Maor, I., DeWalt, G. J., Eldred, W. D., ... Davison, I. G. (2019). Rapid changes in synaptic strength after mild traumatic brain injury. *Front Cell Neurosci*, 13, 166. doi:10.3389/fncel.2019.00166

Wolozin, B., & Apicco, D. (2015). RNA binding proteins and the genesis of neurodegenerative diseases. *Adv Exp Med Biol*, 822, 11–15. doi:10.1007/978-3-319-08927-0_3.

Wolozin, B., & Ivanov, P. (2019). Stress granules and neurodegeneration. *Nat Rev Neurosci*, 20(11), 649–666. doi:10.1038/s41583-019-0222-5.

- Wootz, H., Enjin, A., Wallén-Mackenzie, A., Lindholm, D., & Kullander, K. (2010). Reduced VGLUT2 expression increases motor neuron viability in Sod1(G93A) mice. *Neurobiol Dis*, 37(1), 58–66. doi:10.1016/j.nbd.2009.09.006.
- Wright, D. K., Liu, S., van der Poel, C., McDonald, S. J., Brady, R. D., Taylor, L., ... Shultz, S. R. (2017). Traumatic brain injury results in cellular, structural and functional changes resembling motor neuron disease. *Cereb Cortex*, 27(9), 4503–4515. doi:10.1093/cercor/bhw254.
- Wu, A., Ying, Z., & Gomez-Pinilla, F. (2010). Vitamin E protects against oxidative damage and learning disability after mild traumatic brain injury in rats. *Neurorehabil Neural Repair*, 24(3), 290–298. doi:10.1177/1545968309348318.
- Wu, T., Fang, X., Xu, J., Jiang, Y., Cao, F., & Zhao, L. (2020). Synergistic effects of ginkgolide B and protocatechuic acid on the treatment of Parkinson's disease. *Molecules*, 25(17), 3976. doi:10.3390/molecules25173976.
- Xiao, Q., Zhao, W., Beers, D. R., Yen, A. A., Xie, W., Henkel, J. S., & Appel, S. H. Mutant SOD1(G93A) microglia are more neurotoxic relative to wild-type microglia. *J Neurochem*, 102(6), 2008–2019. doi:10.1111/j.1471-4159.2007.04677.x.
- Xiong, Y., Mahmood, A., & Chopp, M. (2013). Animal models of traumatic brain injury. *Nat Rev Neurosci*, 14(2), 128–142. doi:10.1038/nrn3407.

- Xiong, Y., Mahmood, A., & Chopp, M. (2018). Current understanding of neuroinflammation after traumatic brain injury and cell-based therapeutic opportunities. *Chin J Traumatol*, *21*(3), 137–151. doi:10.1016/j.cjtee.2018.02.003.
- Xiong, Y., Shie, F. S., Zhang, J., Lee, C. P., & Ho, Y. S. (2004). The protective role of cellular glutathione peroxidase against trauma-induced mitochondrial dysfunction in the mouse brain. *J Stroke Cerebrovasc Dis*, *13*(3), 129–137. doi:10.1016/j.jstrokecerebrovasdis.2004.05.001.
- Xu, X., Cowan, M., Beraldo, F., Schranz, A., McCunn, P., Geremia, N., ... Brown, A. (2021). Repetitive mild traumatic brain injury in mice triggers a slowly developing cascade of long-term and persistent behavioral deficits and pathological changes. *Acta Neuropathologica Commun*, *9*, 60 (2021). doi:10.1186/s40478-021-01161-2.
- Yamanaka, K., Boillee, S., Roberts, E. A., Garcia, M. L., McAlonis-Downes, M., Mikse, O. R., ... Goldstein, L. S. (2008). Mutant SOD1 in cell types other than motor neurons and oligodendrocytes accelerates onset of disease in ALS mice. *Proc Natl Acad Sci USA*, *105*(21), 7594–7599. doi:10.1073/pnas.0802556105.
- Yamanaka, K., & Komine, O. (2018). The multi-dimensional roles of astrocytes in ALS. *Neurosci Res*, *126*, 31–38. doi:10.1016/j.neures.2017.09.011.

- Yasen, A. L., Smith, J., & Christie, A. D. (2018). Glutamate and GABA concentrations following mild traumatic brain injury: a pilot study. *J Neurophysiol*, *120*(3), 1318–1322. doi:10.1152/jn.00896.2017.
- Yates, N. J., Lydiard, S., Fehily, B., Weir, G., Chin, A., Bartlett, C. A., ... & Fitzgerald, M. (2017). Repeated mild traumatic brain injury in female rats increases lipid peroxidation in neurons. *Exp Brain Res*, *235*(7), 2133–2149. doi:10.1007/s00221-017-4958-8.
- Yeiser, E. C., Vanlandingham, J. W., & Levenson, C. W. (2002). Moderate zinc deficiency increases cell death after brain injury in the rat. *Nutr Neurosci*, *5*(5), 345–352. doi:10.1080/1028415021000033811.
- Yi, J. H., & Hazell, A. S. (2006). Excitotoxic mechanisms and the role of astrocytic glutamate transporters in traumatic brain injury. *Neurochem Int*, *48*(5), 394–403. doi:10.1016/j.neuint.2005.12.001.
- Yin, T. C., Voorhees, J. R., Genova, R. M., Davis, K. C., Madison, A. M., Britt, J. K., ... Pieper, A. A. (2016). Acute axonal degeneration drives development of cognitive, motor, and visual deficits after blast-mediated traumatic brain injury in mice. *eNeuro*, *3*(5), 220–236. doi:10.1523/ENEURO.0220-16.2016.
- Yoshihara, T., Ishigaki, S., Yamamoto, M., Liang, Y., Niwa, J., Takeuchi, H., ... Sobue, G. (2002). Differential expression of inflammation- and apoptosis-related genes in spinal cords of a mutant SOD1 transgenic mouse model of familial amyotrophic

lateral sclerosis. *J Neurochem*, 80(1), 158–167. doi:10.1046/j.0022-3042.2001.00683.x.

Youdim, K. A., Martin, A., & Joseph, J. A. (2000). Incorporation of the elderberry anthocyanins by endothelial cells increases protection against oxidative stress. *Free Radic Biol Med*, 29(1), 51–60. doi:10.1016/s0891-5849(00)00329-4.

Zafra-Stone, S., Yasmin, T., Bagchi, M., Chatterjee, A., Vinson, J. A., & Bagchi, D. (2007). Berry anthocyanins as novel antioxidants in human health and disease prevention. *Mol Nutr Food Res*, 51(6), 675–683. doi:10.1002/mnfr.200700002.

Zaghloul, N., Patel, H., Codipilly, C., Marambaud, P., Dewey, S., Frattini, S., ... Ahmed, M. (2014). Overexpression of extracellular superoxide dismutase protects against brain injury induced by chronic hypoxia. *PloS one*, 9(9), e108168. doi:10.1371/journal.pone.0108168.

Zeineddine, R., Farrarwell, N. E., Lambert-Smith, I. A., & Yerbury, J. J. (2017). Addition of exogenous SOD1 aggregates causes TDP-43 mislocalisation and aggregation. *Cell Stress Chaperones*, 22(6), 893–902. doi:10.1007/s12192-017-0804-y.

Zeng, X. J., Li, P., Ning, Y. L., Zhao, Y., Peng, Y., Yang, N., ... Zhou, Y.G. (2018). Impaired autophagic flux is associated with the severity of trauma and the role of A2AR in brain cells after traumatic brain injury. *Cell Death Dis*, 9(252). doi:10.1038/s41419-018-0316-4.

- Zeng, Z., Zhang, Y., Jiang, W., He, L., & Qu, H. (2020). Modulation of autophagy in traumatic brain injury. *J Cell Physiol*, 235(3), 1973–1985. doi:10.1002/jcp.29173.
- Zhang, E., Wan, X., Yang, L., Wang, D., Chen, Z., Chen, Y., ... Fan, Z. (2020). Omega-3 polyunsaturated fatty acids alleviate traumatic brain injury by regulating the glymphatic pathway in mice. *Front Neurol*, 11, 707. doi:10.3389/fneur.2020.00707.
- Zhang, H. N., An, C. N., Zhang, H. N., & Pu, X. P. (2010). Protocatechuic acid inhibits neurotoxicity induced by MPTP in vivo. *Neurosci Lett*, 474(2), 99–103. doi:10.1016/j.neulet.2010.03.016.
- Zhang, K., Johnson, B., Pennell, D., Ray, W., Sebastianelli, W., & Slobounov, S. (2010). Are functional deficits in concussed individuals consistent with white matter structural alterations: combined FMRI & DTI study. *Exp Brain Res*, 204(1), 57–70. doi:10.1007/s00221-010-2294-3.
- Zhang, L., Rzigalinski, B. A., Ellis, E. F., & Satin, L. S. (1996). Reduction of voltage-dependent Mg²⁺ blockade of NMDA current in mechanically injured neurons. *Science*, 274(5294), 1921–1923. doi:10.1126/science.274.5294.1921.
- Zhang, Y. J., Wu, L., Zhang, Q. L., Li, J., Yin, F. X., & Yuan, Y. (2011). Pharmacokinetics of phenolic compounds of Danshen extract in rat blood and brain by microdialysis sampling. *J Ethnopharmacol*, 136(1), 129–136. doi:10.1016/j.jep.2011.04.023.

- Zhang, Z., Li, G., Szeto, S. S. W., Chong, C. M., Quan, Q., Huang, C., ... Chu, I. K. (2015). Examining the neuroprotective effects of protocatechuic acid and chrysin on in vitro and in vivo models of Parkinson disease. *Free Radi. Biol Med*, 84, 331–343. doi:10.1016/j.freeradbiomed.2015.02.030.
- Zhao, W., Beers, D. R., Henkel, J. S., Zhang, W., Urushitani, M., Julien, J. P., & Appel, S. H. (2010). Extracellular mutant SOD1 induces microglial-mediated motoneuron injury. *Glia*, 58(2), 231–243. doi:10.1002/glia.20919.
- Zheng, J., Xiong, H., Li, Q., He, L., Weng, H., Ling, W., & Wang, D. (2019). Protocatechuic acid from chicory is bioavailable and undergoes partial glucuronidation and sulfation in healthy humans. *Food Sci Nutr*, 7(9), 3071–3080. doi:10.1002/fsn3.1168.

APPENDICES

Appendix A: Abbreviations

Δ : change

#: number

3-NT: 3-nitrotyrosine

4-HNE: 4-hydroxynonenal

8-oxo-dG: 8-oxo-2'-deoxyguanosine

A β : amyloid- β

Ach: acetylcholine

AD: Alzheimer's disease

ADC: apparent diffusion coefficient

ALS: amyotrophic lateral sclerosis

AMPA: α -amino-3-hydroxy-5-methyl-4-isoxazole propionic acid

APP: amyloid precursor protein

ATP: adenosine 5'-triphosphate

BBB: blood brain barrier

BDNF: brain-derived neurotrophic factor

BTx: alpha-bungarotoxin

C9orf72: chromosome 9 open reading frame 72

Ca²⁺: calcium ion

CAT: catalase

CCI: controlled cortical impact

CD38: cluster of differentiation 38

CHIMERA: closed-head impact model of engineered rotational acceleration

CNS: central nervous system

Coq10: coenzyme-q10

CTE: chronic traumatic encephalopathy

COX-1: cyclooxygenase-1

COX-2: cyclooxygenase-2

EAAC1: excitatory amino acid carrier type 1

EAAT: excitatory amino acid transporter

ELISA: enzyme-linked immunosorbent assay

ETC: electron transport chain

FDA: Food and Drug Administration

FUS: fused in sarcoma

G93A: untreated hSOD1^{G93A} control mice

G93A + PCA: 100mg/kg PCA treated hSOD1^{G93A} mice

GABA: γ -aminobutyric acid

GCEE: γ -glutamylcysteine ethyl ester

GFAP: glial fibrillary acidic protein

Glu: glutamate

GPx: glutathione peroxidase

GR: glutathione reductase

GSH: glutathione

GSNO: S-nitrosoglutathione

GSSG: oxidized glutathione/ glutathione disulfide

hnRNP A1/2 heterogeneous nuclear ribonucleoproteins A1/A2

hSOD1^{G93A}: human mutant SOD-1 with a glycine to alanine substitution at position 93

IACUC: Institutional Animal Care and Use Committee

Iba-1: ionized calcium-binding adapter molecule 1

ICAL: Immunocal®

IFN- γ : interferon- γ

IHC: immunohistochemical

IL: interleukin

iNOS: inducible NO synthase

IQR: interquartile range

LPS: lipopolysaccharide

MDA: malondialdehyde

Mg⁺: magnesium ion

MRI: magnetic resonance imaging

MSQ: medical symptom questionnaire

mTBI: mild traumatic brain injury

Na⁺: sodium ion

NAC: N-acetylcysteine

NAch: nicotinic acetylcholine

NF: neurofilament

NF κ B: nuclear factor- κ B

NfL: neurofilament light chain protein

NK: natural killer

NMDA: N-methyl-D-aspartic acid

NMJ: neuromuscular junction

NO: nitric oxide

Nrf2-Keap1: nuclear factor erythroid 2-related factor 2–Kelch-like erythroid cell-derived protein with CNC homology [ECH]-associated protein 1

O⁻: free radical oxygen

O₂: oxygen

OCT: optimal cutting temperature

O.D.: optical density

PaGE: paw grip endurance

PBS: phosphate buffered saline

PCA: protocatechuic acid

PD: Parkinson's disease

P. Tau: phosphorylated tau

PUFA: polyunsaturated fatty acid

PVGav1: piebald virol glaxo

rmTBI: repetitive mild traumatic brain injury

rmmTBI: repetitive mild-moderate traumatic brain injury

rTBI: repetitive traumatic brain injury

S100 β : S100 calcium-binding protein β

SAM: S-adenosylmethionine

SHAM: sham surgery

SOD: superoxide dismutase

SOD-1: Cu, Zn-superoxide dismutase-1

RBCs: red blood cells

ROS: reactive oxygen species

ROS/RNS: reactive oxygen species/ reactive nitrogen species

RNS: reactive nitrogen species

TBI: traumatic brain injury

TDP-43: TAR DNA-binding protein-43

TNF- α : tumor necrosis factor- α

Txn: thioredoxin

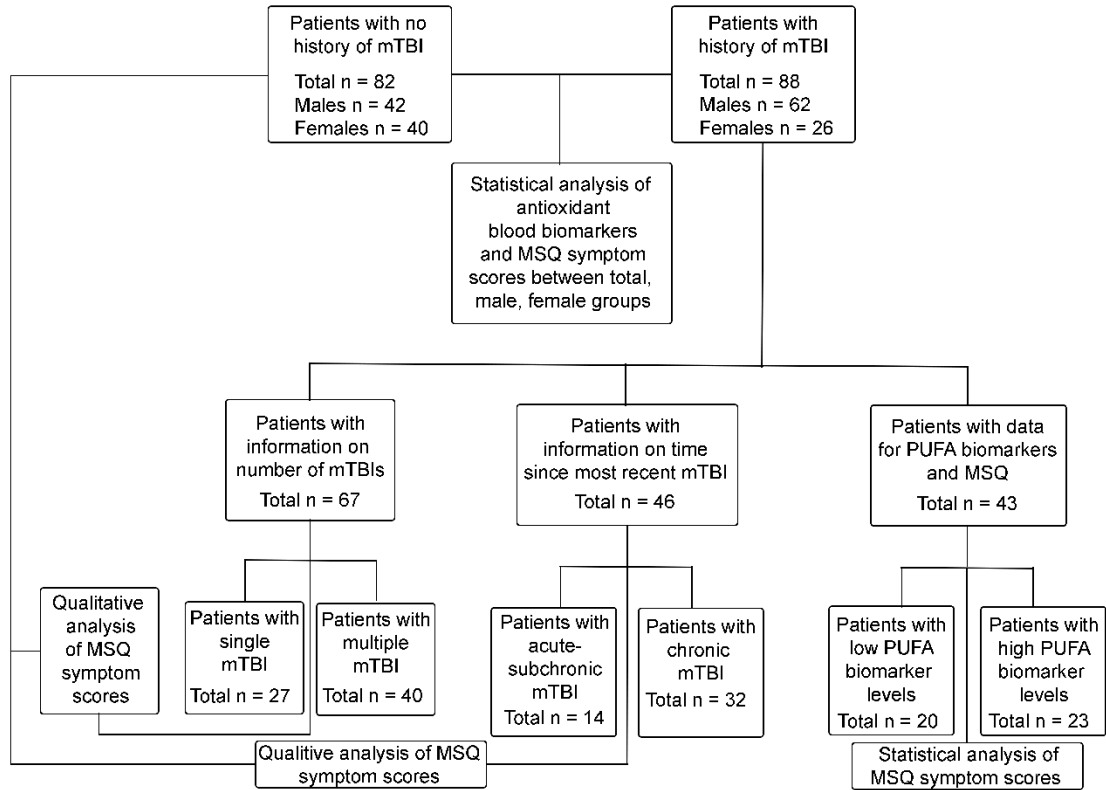
US: United States

VACHT: vesicular acetylcholine transporter

WBCs: white blood cells

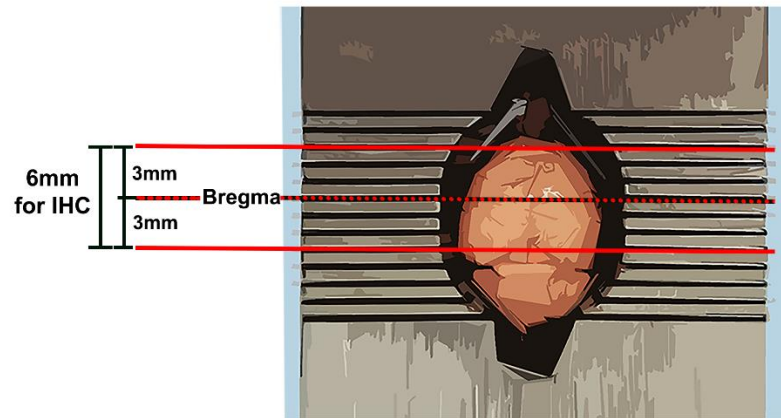
WT: wild-type

Appendix B: Supplementary Figures

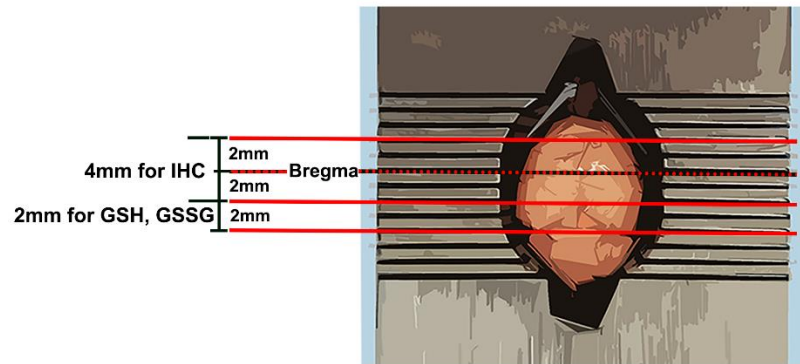


Supplemental Figure 1 Retrospective Study Analyses and Patient Flow Diagram from Chapter Two. Demographic, antioxidant blood biomarker, and medical symptom questionnaire (MSQ) data collected from 170 patients admitted to a sports medicine clinic between 11/2017 - 9/2020 prior to treatment were retrospectively analyzed. Patients with active cancer at the time of visit were excluded. A total of 88 patients, including 62 males and 26 females, had at least one mild traumatic brain injury (mTBI) in their lifetime and were considered to have a history of TBI. The remaining 82 patients, consisting of 42 males and 40 females, had no history of mTBI. Blood biomarkers and MSQ emotional, energy, head, and cognitive symptoms were statistically analyzed between total, male, and female patients with versus without history of mTBI. Patients with a history of mTBI were further categorized. A total of 27 patients reported sustaining a single mTBI, 40 sustained multiple mTBIs, and 21 patients did not report this information and were not included in analyses. Of the 88 history of mTBI patients, 14 patients presented to the clinic within 1 year of their most recent mTBI, termed as acute-subchronic mTBI patients, and 32 patients presented to the clinic greater than 1 year since their most recent TBI, termed chronic mTBI patients. A total of 42 patients did not report this information and were not included in analyses of these populations. A qualitative heatmap analysis of the significant or trending significantly different MSQ symptoms between total, male, and female patients with versus without history of mTBI was performed between no history of mTBI patients, single, and multiple mTBI patients and also between no history of mTBI patients, acute, and chronic mTBI patients. Finally, 43 history of mTBI patients with complete polyunsaturated fatty acid biomarker data (PUFA; linoleic acid and alpha-linolenic acid in plasma and total omega-3, total omega-6, and docosahexaenoic acid in red blood cells) and MSQ data were divided according to high versus low PUFA levels and MSQ emotional, energy, head, and cognitive symptoms were statistically analyzed between these groups.

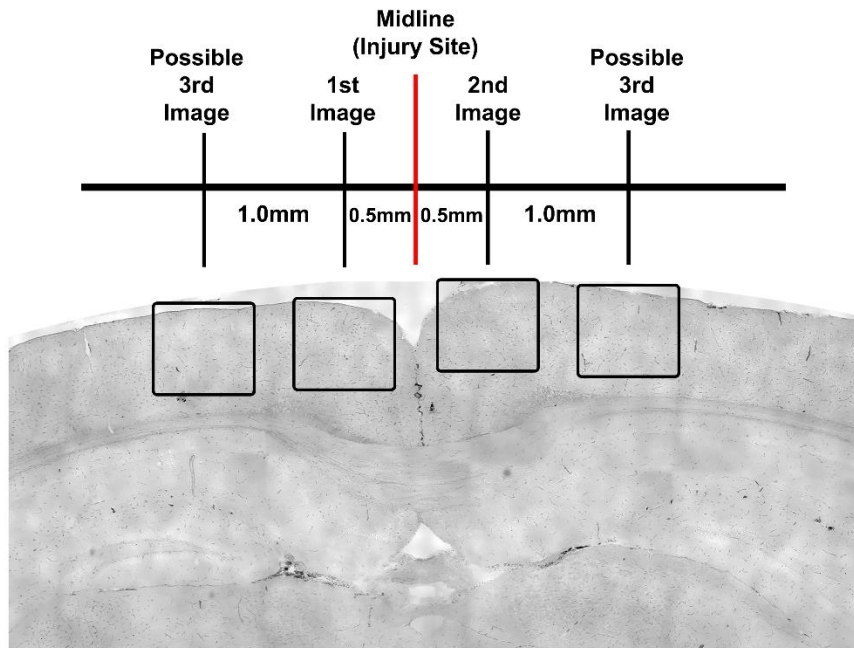
A



B



Supplemental Figure 2 Representative Brain Sectioning for Analysis from Mice Subjected to Repetitive Mild-Traumatic Brain Injury (rmTBI) and Repetitive Mild-Moderate TBI (rmmTBI) Performed in Chapter Three. Representative drawings of brain in 1mm cut stainless steel matrices are displayed with sectioning shown using red lines and annotations denoting brain section sizes in mm used for analyses. For all sham, untreated TBI, and Immunocal®-treated TBI mice subjected to rmTBI at 2 weeks (n=9 mice per group), 2 months (n=9 mice per group), and 6 months (n=5 mice per group) following the last mTBI (**A**), bregma was determined (shown by red and black dotted line) and a 6mm section was taken, which was 3mm posterior and anterior to bregma, and subjected to immunohistochemical (IHC) staining for GFAP and IBA-1 for analysis of astrocytes and microglia in cortex, respectively. For all sham, untreated TBI, and Immunocal®-treated TBI mice subjected to rmmTBI at 72 hours (n =5-7 mice per group) following the last mmTBI (**B**), bregma was determined (shown by red and black dotted line) and a 4mm section was taken, which was 2mm posterior and anterior to bregma, and subjected to IHC staining for GFAP and IBA-1 for analysis of astrocytes and microglia in cortex, respectively. Another 2mm section was taken, posterior to the section taken for IHC staining, and used for determination of brain GSH and GSSG. All analyses are described in the methods section.



Supplemental Figure 3 Representative Fluorescent Imaging Locations of Cortex Stained for Either Iba-1 or GFAP from Mice Subjected to Repetitive Mild-Traumatic Brain Injury (rmTBI) and Repetitive Mild-Moderate TBI (rmmTBI) Performed in Chapter Three. A 20X image of cortex was taken by a blinded researcher in both the left and right hemisphere approximately 0.5mm out from midline (the injury site) but avoiding the longitudinal fissure. An additional third image was taken approximately 1.5mm from the midline in either the left or right hemisphere for a total of 3 images per section.

Appendix C: Supplementary Tables

Supplemental Table 1. Biomarkers That Were Not Significantly or Trending Significantly Different Between Total Patients Without Versus with a History of mTBI From Chapter Two. Biomarkers that were not significantly or trending significantly different ($p > 0.10$) between groups are displayed as mean \pm SEM and analyzed using the Mann Whitney U-Test. Abbreviations: WBC, white blood cell; RBC, red blood cell.

Biomarker	Patients without history of mTBI (n = 82)	Patients with history of mTBI (n = 88)	p-value
Arachidonic acid Serum (%)	n = 65 13.65 \pm 0.55	n = 64 13.17 \pm 0.48	0.550
β-Carotene Serum (mg/L)	n = 80 0.37 \pm 0.03	n = 87 0.34 \pm 0.03	0.520
Coenzyme-q10 Serum (mg/mL)	n = 80 1.51 \pm 0.12	n = 87 1.24 \pm 0.06	0.247
Cysteine Serum (nmol/mL)	n = 37 22.25 \pm 2.13	n = 48 20.64 \pm 1.64	0.642
Docosahexaenoic acid Serum (%)	n = 65 6.23 \pm 0.32	n = 64 6.19 \pm 0.28	0.884
Eicosapentaenoic acid Serum (%)	n = 65 0.59 \pm 0.06	n = 64 0.62 \pm 0.07	1.00
Linoleic acid Serum (%)	n = 65 6.18 \pm 0.30	n = 64 5.83 \pm 0.35	0.268
Lipid peroxides Serum (nmol/mL)	n = 81 1.47 \pm 0.06	n = 88 1.47 \pm 0.06	0.834
Total omega-3 Serum (%)	n = 65 7.85 \pm 0.39	n = 64 7.97 \pm 0.38	0.756
Total omega-6 Serum (%)	n = 65 24.27 \pm 0.89	n = 64 23.05 \pm 0.83	0.408
Vitamin B12 Serum (pg/mL)	n = 69 828.41 \pm 59.10	n = 64 968.22 \pm 70.88	0.173
Vitamin C Serum (mg/dL)	n = 37 0.49 \pm 0.04	n = 48 0.51 \pm 0.04	0.660
25-Hydroxyvitamin D Serum (ng/mL)	n = 69 38.77 \pm 2.17	n = 64 38.34 \pm 1.95	0.896
Alpha-linolenic Plasma (μ mol/L)	n = 81 31.53 \pm 1.62	n = 88 27.55 \pm 1.15	0.134
Arachidonic acid Plasma (μ mol/L)	n = 81 307.90 \pm 11.06	n = 88 285.14 \pm 9.50	0.182
Cystine Plasma (μ mol/L)	n = 76 9.61 \pm 0.78	n = 85 8.71 \pm 0.86	0.262

Docosahexaenoic acid Plasma ($\mu\text{mol/L}$)	n = 81 92.93 \pm 4.26	n = 88 85.99 \pm 3.88	0.240
Eicosapentaenoic acid Plasma ($\mu\text{mol/L}$)	n = 81 44.27 \pm 4.28	n = 88 43.43 \pm 3.91	0.791
Methionine Plasma ($\mu\text{mol/L}$)	n = 77 25.29 \pm 0.73	n = 87 25.54 \pm 0.62	0.603
8-Hydroxy-2-deoxyguanosine Plasma (ng/mg creatine)	n = 78 3.71 \pm 0.25	n = 85 3.47 \pm 0.24	0.254
Eicosapentaenoic acid RBC (%)	n = 37 0.59 \pm 0.06	n = 48 0.51 \pm 0.05	0.231
Total omega-6 RBC (%)	n = 37 26.31 \pm 0.83	n = 48 23.99 \pm 0.86	0.117
Alpha tocopherol WBC (pg/MM)	n = 37 173.44 \pm 20.62	n = 48 156.84 \pm 18.01	0.506
Coenzyme-q10 WBC (pg/MM)	n = 37 80.20 \pm 5.79	n = 48 82.46 \pm 6.39	0.951
Cysteine WBC (pg/MM)	n = 37 166.87 \pm 24.09	n = 48 152.00 \pm 17.02	0.929
Vitamin C WBC (pg/MM)	n = 37 1.78 \pm 0.26	n = 48 1.74 \pm 0.18	0.787
Selenium Whole Blood (ppm)	n = 81 0.21 \pm 0.01	n = 86 0.20 \pm 0.00	0.477

Supplementary Table 2 Impact Parameters and Procedural Details for Repetitive Mild-Traumatic Brain Injury (rmTBI) and Repetitive Mild-Moderate TBI (rmmTBI) From Chapter Three.

	rmTBI	rmmTBI
Site of Impact	Midline at bregma	Midline at bregma
Pre-Injury Procedure Following Anesthesia Induction	<ol style="list-style-type: none"> 1. Head shaved 2. Site of impact indicated with sharpie 	<ol style="list-style-type: none"> 1. Head shaved 2. Site of impact indicated with sharpie 3. Concave 3 mm metallic disk affixed at the reference point using a small drop of tissue adhesive
Number of Impacts	5	3
Time Between Impacts (hours)	48	48
Impact Probe Diameter (mm)	5	5
Velocity of Impact (m/s)	5	5.5
Depth of Impact (mm)	1	2
Dwell Time (ms)	200	200

Appendix D: List of Published Manuscripts and Abstracts

Manuscripts

Content from Chapter One sections 1.3.3, 1.4.1, and 1.4.2 titled “Glutathione, GSH Precursor, and GSH Enzymatic Antioxidant Depletion Following Mild TBI”, “Glutathione Precursors as Treatment Options for Mild TBI”, and “Immunocal® as a Potential GSH Precursor Supplement for Mild TBI”, respectively, is published in *Neural Regeneration Research*.

Koza, L. and Linseman, DA (2019). Glutathione precursors shield the brain from trauma. *Neural Regen Res*, 14 (10)1701-1702. doi:10.4103/1673-5374.257520.

Chapter Two titled “Significant and Sex-Specific Antioxidant Biomarker Depletion in Patients with Mild Traumatic Brain Injury” is in preparation for submission to *Annals of Clinical and Translational Neurology* (Koza, L. A., Bishop, M., Grossberg, A. N., Prusmack, C., & Linseman, D. A.).

Chapter Three titled “Immunocal® Prevents Gliosis in Mouse Models of Repetitive Mild-Moderate Traumatic Brain Injury” is in preparation for submission to *Journal of Clinical Investigation* (Koza, L. A., Pena, C., Russell, M., Smith, A. C., Molnar, J., Devine, M., Serkova, N. J., & Linseman, D. A.).

Chapter Four titled “Protocatechuic Acid Extends Survival, Improves Motor Function, Diminishes Gliosis, and Sustains Neuromuscular Junctions in the hSOD1G93A Mouse Model of Amyotrophic Lateral Sclerosis” is published in *Nutrients*.

Koza, L. A., Winter, A. N., Holsopple, J., Baybayon-Grandgeorge, A. N., Pena, C., Olson, J. R., Mazzarino, R. C., Patterson, D., & Linseman, D. A. (2020). Protocatechuic Acid Extends Survival, Improves Motor Function, Diminishes Gliosis, and Sustains Neuromuscular Junctions in the hSOD1G93A Mouse Model of Amyotrophic Lateral Sclerosis. *Nutrients*, 12(6), 1824. doi:10.3390/nu12061824.

Abstracts

Koza, L. A., Bishop, M., Grossberg, A. N., Prusmack, C., Linseman, D. A.

Significant and sex-specific antioxidant biomarker depletion in patients with mild traumatic brain injury. Society for Free Radical Biology and Medicine. Virtual, November 16, 2021.

Koza, L. A., Pena, C., Russell, M., Smith, A. C., Molnar, J., Devine, M., Serkova, N.

J., & Linseman, D. A. Immunocal® prevents gliosis in mouse models of repetitive mild-moderate traumatic brain injury. The 10th Annual Traumatic Brain Injury Conference. Virtual, November 2, 2020.

Koza, L. A., Winter, A. N., Holsopple, J., Pena, C., Aviso, A., Linseman, D. A.

Protocatechuic acid significantly extends survival, improves motor function, and displays neuroprotective and anti-inflammatory therapeutic benefits in the G93A mutant hSOD1 mouse model of amyotrophic lateral sclerosis.

Northeast Amyotrophic Lateral Sclerosis Consortium®. Clearwater, FL.

October 1, 2019.

Koza, L. A., Winter, A. N., Holsopple, J., Pena, C., Aviso, A., Linseman, D. A.

Protocatechuic acid preserves neuromuscular junctions, diminishes gliosis, and extends survival in the G93A mutant hSOD1 mouse model of amyotrophic lateral sclerosis. Neurodegenerative Diseases: New Insights and

Therapeutic Opportunities. Keystone, CO. June 18, 2019.